

**APPENDIX A**

**BENCH-SCALE AND PILOT SCALE CONTROL STUDIES**

**APPENDIX A****BENCH-SCALE AND PILOT-SCALE CONTROL STUDIES**

MARCOR has conducted other laboratory studies with the ACT reagents organic contaminants, including PAHs, PCBs, and Dioxins/Furans. Dioxin/Furans are principle hazardous constituents contained in the New York/New Jersey Harbor sediments. The dioxins/furan control was conducted concurrently with the BREP subcontracted Bench-Scale Study. Other studies were conducted previously. A brief summary of these control studies is presented below.

**A.1 PAH Bench and PAH/PCB Pilot-Scale Studies****A.1.1 PAH Bench-Scale Study**

MARCOR conducted bench-scale study on Manufactured Gas Plant (MGP) wastes excavated from a client facility in Philadelphia, Pennsylvania. The purpose of this study was to determine the effectiveness of ACT reagent compounds to treat elevated concentrations of PAHs. A total of two (2) waste samples were collected by MARCOR and submitted to MVA, Inc.(MVA) for analysis. MVA was tasked to identify the chemical composition of the test samples and to determine, if possible, differences in leach test results. Test methods included Two-Step Laser Desorption Mass Spectroscopy ( $\mu\text{L}^2\text{MS}$ ) and Infrared Microspectroscopy (IR).

Results of analysis for "control" samples not treated with ACT reagent compounds report a mixture of aromatic and aliphatic compounds (MVA, 1995a), which is representative of the contaminant nature of raw, untreated waste from the MGP site. Those samples treated with ACT reagent compounds on the other hand, report an "intense carbonyl ( $-\text{C}=\text{O}$ ) band at  $\sim 1750\text{ cm}^{-1}$ " at the expense of "aromatic absorption features." The resulting carbonyl compounds in treated samples were identified as a spectral match for palm oil, a complex assemblage of ester compounds, mainly

lanoline, stearin and palmitin. These data suggest that the aromatic PAH compounds present in untreated samples were oxidized to form ester-structured compounds during the ACT treatment process (MVA, 1995a).

#### **A.1.2 PAH/PCB Pilot-Scale Study**

Upon concurrence that ACT can effectively reduce toxic organic compounds to innocuous carbonyl compounds in Bench-Scale studies, MARCOR then conducted an on-site pilot-study at the above referenced MGP site. Selected samples were collected and submitted by MARCOR to MVA for microanalysis of the composition and leachability properties of the test material. Samples treated with a specific formulation of ACT reagent compounds were analyzed using Solvent Extraction, Transmission Electron Microscopy, (TEM), Scanning Electron Microscopy (SEM), Gas Chromatography (GC),  $\mu\text{L}^2\text{MS}$ , IR, and Bulk Carbon analysis. Results of analysis indicate that while total carbon concentrations in all samples remained relatively constant, the concentration of solvent extractable organic carbon was decreased by 50-75%. Organic breakdown products during the ACT process included carbonyl compounds (primarily esters and phthalates) and carbonates.

MVA also reported that the results for a "control" experiment utilizing a specific formulation of ACT reagent compounds and a 16 PAH standard solution indicate that total PAH concentrations were reduced by 50-85% from initial concentrations in the solvent extracts. Greatest organic contaminant reduction was noted in the higher mass PAH compounds. MVA stated further that the ACT treatment process chemically degrades, and can mineralize PAH compounds (MVA, 1995b).

A "control" experiment utilizing ACT reagent compounds and a 6 PCB standard solution was also completed by MVA. Results of this experiment indicated that PCBs (Aroclor 1242) were degraded, and that PCB breakdown products were created. Additional investigation is required to determine the extent of chemical breakdown and the nature of these resultant breakdown products (MVA, 1995b).

## A.2 Dioxins/Furans Bench-Scale Study

MARCOR subcontracted MVA to perform a control study to determine the potential effectiveness of ACT reagent compounds on the reduction of dioxin/furan contaminated soil. Dioxin/furans were chosen as a test subject due to the elevated concentrations of these compounds in New York/New Jersey Harbor sediments. This study was performed concurrently with the BREP Bench-Scale Study.

A total of two (2) controlled experiments were performed. In the first experiment, a single furan compound (2,4,8-trichlorodibenzofuran [2,4,8-TCDF]) test solution comprised of the furan and methylene chloride was slurried with distilled deionized water and an aluminum oxide substrate; this mixture served as a "control" sample. A second sample was similarly prepared with ACT reagent mixture (SWT-25) added for chemical reduction purposes. This second mixture served as the "reactive" sample. Both the control and reactive samples were then contained into 5ml reactor vials and placed into a water bath heated to approximately 35°C for a period of 36 hours. To facilitate chemical reaction activity and to prevent settling, the samples were periodically ultrasonicated.

At the end of the test period, the samples were permitted to rest undisturbed for a period of one hour. Samples of the Methylene Chloride/Furan compound solution were extracted from the sample vials, smeared onto a heated aluminum sample platter and placed under a fume hood for evaporation. The resultant sediment residue was analyzed by  $\mu\text{L}^2\text{MS}$ . A portion of residual sediment was also removed from each vial and placed on aluminum foil. Wet residue samples were placed under a fume hood to dry. Dry encrusted residue was then mounted onto a sample platter for  $\mu\text{L}^2\text{MS}$  analysis.

The second experiment consisted of a lesser volume of a 17 Dioxin/Furan compound solution slurry mixed as presented above into "control" and "reactive" samples. The test samples were placed into microvials lowered into a water bath heated to approximately 30°C for analysis. The test period lasted for 24 hours. At the conclusion of the 24 hour test period, the samples were then handled

according to the procedures presented above.

Solid microbial residues collected from all reaction vessels were analyzed for the presences of carbonates. The carbonate test was completed by adding an aqueous solution of 10% hydrochloric acid (HCL) to the collected residues. The residues were observed for off-gassing of carbon dioxide.

Although a clean extract of the Methylene Chloride and single Furan compound solution was not possible due to expansion of the substrate into overlying solution, review of  $\mu\text{L}^2\text{MS}$  data indicates that "the reduction in concentration of 2,4,8-TCDF must be larger than 40% and it may be much more than this."

The results for the dioxin/furan experiment were more difficult to interpret due to the presence of PAH contaminants in the test sample. However, because the dioxin/furan residues tested positive for carbonates (microbial residues for the "control" sample did not test positive for carbonates), this suggests "that the furans and dioxins in the test mixture may have been chemically degraded and mineralized" (MVA, 1996).

**Report of Results: MVA1342**

**Job No. EV-00701-002**

**Prepared for:**

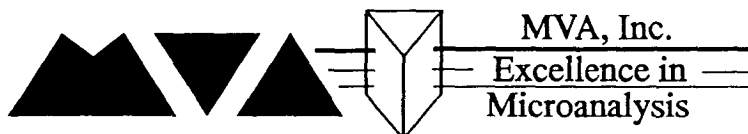
**Ms. Karen Hartley  
Marcor of Pennsylvania, Inc.  
540 Trestle Place  
Downington, PA 19335**

**Prepared by:**

**John P. Bradley  
MVA, Inc.  
5500 Oakbrook Parkway, Suite 200  
Norcross, GA 30093**

**31 May 1995**

D:PROJECTS\1342-RP053195



5500 Oakbrook Parkway #200  
Norcross, Georgia 30093  
404-662-8509

## Report of Results: MVA1342

Job No. EV-00701-002

### Introduction

This report describes MVA's characterization of two (2) hydrocarbon contaminated soil samples that were received on May 5, 1995. The samples identified as from the PECO pilot demonstration were labelled "Control Soil" and SM1 respectively. The purpose of our characterization was to investigate the overall compositions of the organic fractions and, if possible, provide an explanation for the significantly different leach test results obtained from the samples. We employed a combination of infrared (IR) microspectroscopy and two step laser desorption mass spectroscopy ( $\mu\text{L}^2\text{MS}$ ) to analyze the samples.

### Experimental Procedures

The samples were in the form of a grey-black granular soil mix. For IR microspectroscopy, approximately 0.5 gm of each sample was placed in a test tube along with 5 mls of chloroform. The mixture was agitated, then 5 ml of water was added, and the mixture was vigorously agitated again. When the chloroform layer had settled out, a micro pipette was used to remove about 0.1 ml from the chloroform layer. The aliquot was dispersed onto a silver chloride substrate and allowed to dry, leaving an organic residue. This residue was analyzed by transmission IR microspectroscopy over the wavelength range 800 - 4000  $\text{m}^{-1}$ .

Both "neat" (as received) and chloroform extracted samples were prepared for  $\mu\text{L}^2\text{MS}$  analyses. For the neat powder samples preparation involved grinding each of the powders until the mean grain size was  $<150 \mu\text{m}$ . This fine powder was then dried and pressed onto a roughened aluminum sample mount. The purpose of grinding is to produce samples with approximately equivalent surface areas when analyzed by the laser microprobe, and so allow the most accurate comparison of the relative concentrations of the organic phase between the samples. Solvent extracts were made by taking  $\sim 0.085 \text{ mg}$  each of the finely powdered samples and adding 0.4 ml of chloroform solvent. The solvent was evaporated onto a clean quartz sample mount heated to  $70^\circ\text{C}$ . On evaporation of the solvent a dark yellow-brown residue was left.

For all samples a  $10.6 \mu\text{m}$  CO<sub>2</sub> laser beam was used to desorb material from the sample in a spot  $40 \mu\text{m}$  in diameter, the resulting plume of desorbed material was then photoionized at 266 nm by a frequency quadrupled Nd:YAG laser beam. To compensate for spatial inhomogeneities in the samples, 300 shot moving averages were taken. The laser photoionization energy was  $\sim 500 \mu\text{J}/\text{pulse}$  in an unfocused beam of cross sectional area  $1 \text{ mm}^2$ . Under these conditions the peaks observed in the spectra represent the parent ion molecular species present in the sample, i.e., there is little to no fragmentation associated with the ionization process.

### Results

Figure 1 shows an IR spectrum of the chloroform extracted organic fraction of the control soil. The absorption band structure is consistent with a mixture of aromatic and aliphatic compounds. Although aliphatic C-H stretching at  $\sim 2850 \text{ cm}^{-1}$  is the dominant feature of the spectrum, aliphatic compounds are not necessarily more abundant than aromatics. Figure 2 shows an IR spectrum from treated sample. Note the almost complete loss of aromatic absorption features together with the appearance

of an intense carbonyl ( $\text{-C=O}$ ) absorption band at  $\sim 1750 \text{ cm}^{-1}$ . For comparison, IR spectra from both samples are plotted together in Figure 3.

The spectrum from the treated sample was compared via computer with a data base containing IR spectra of over 50,000 organic compounds. The treated sample was spectrally matched with a reference spectrum for palm oil, which consists mainly of the esters palmitin ( $\text{C}_{51}, \text{H}_{98}, \text{O}_6$ ), stearin, and lanolin.

Laser desorption mass spectra of both samples are compared in Figure 5. The untreated sample shows a very strong distribution of polycyclic aromatic hydrocarbons (PAHs) with a mass range extending from 100 amu to beyond 450 amu (Fig. 5a). The most prominent PAHs observed include pyrene (202 amu;  $\text{C}_{16}\text{H}_{10}$ ), chrysene (228 amu;  $\text{C}_{18}\text{H}_{12}$ ) and dibenzopyrene (252 amu;  $\text{C}_{20}\text{H}_{12}$ ). Extensive alkylation of all parent PAH skeletons is observed, with alkylation series extending beyond 6-alkyl observed for nearly all the prominent PAH skeletons. The treated sample, a similar distribution of PAH species is observed although at a greatly reduced concentration (Figs. 5b, 7-9). The decrease of the signal varies between individual PAHs as can be observed from the expanded spectra, (Figs. 7-9) with the total integrated signal being  $\sim 0.6$  times that of the untreated sample.

## Discussion

Infrared (IR) microspectroscopy demonstrates that there is a fundamental difference in the molecular composition of the treated and untreated samples. Whereas the concentrated sample is clearly dominated by aliphatic and aromatic compounds, the treated sample displays intense carbonyl ( $\text{-C=O}$ ) absorption and an overall spectra features consistent with esters. The spectral match to that of palm oil supports the notion that esters are the dominant organic phases in the treated sample. Since the strength of the aromatic absorption bands has decreased in proportion to the increase in carbonyl band intensity, it appears that much of the aromatic material in the untreated sample was oxidized to esters.

The  $\mu\text{L}^2\text{MS}$  results support the above interpretation of the IR spectra. The overall concentration of polyaromatics has been decreased  $\sim 17$  times (Fig. 5). Though the mass envelopes are similar for both samples, there are several notable differences. In the treated sample, the lower mass PAHs (below 230 amu) appear to be more prominent whilst at the higher mass PAHs (greater than 300 amu) appear depleted. Additionally the alkylated/unalkylated PAH ratio in the treated sample is lower on average than that of the untreated sample, with 1-alkyl and 2-alkyl substituents being the most abundant in the treated sample as compared to 3-alkyl and 4-alkyl substituents for the untreated sample. There are no prominent odd mass peaks observed in either sample and there appear to be species that are unique to either sample.

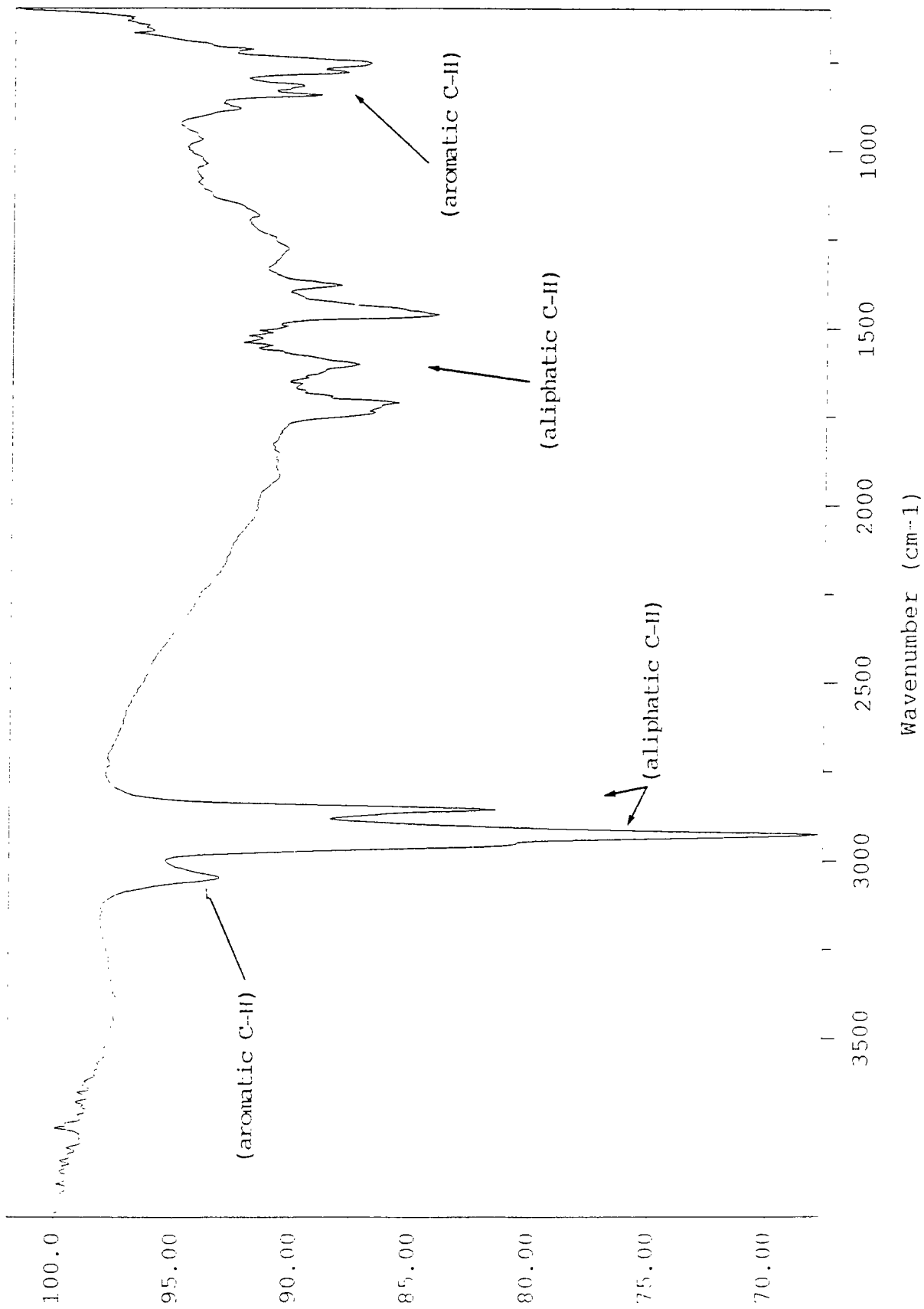


Figure 1. IR spectrum of chloroform extract from untreated PECO control soil.

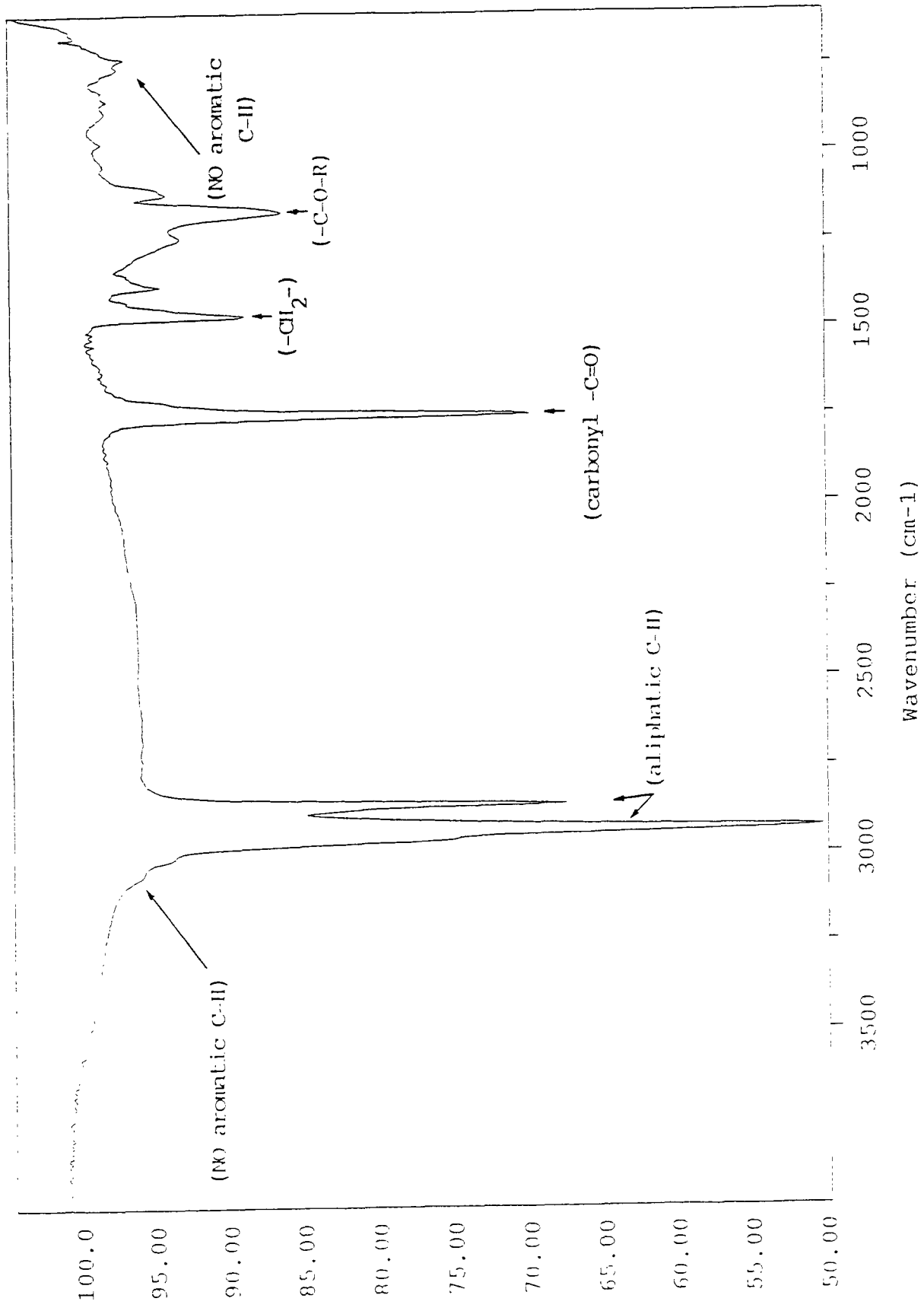


Figure 2. IR spectrum of chloroform extract from treated PECO soil mix, design 1.

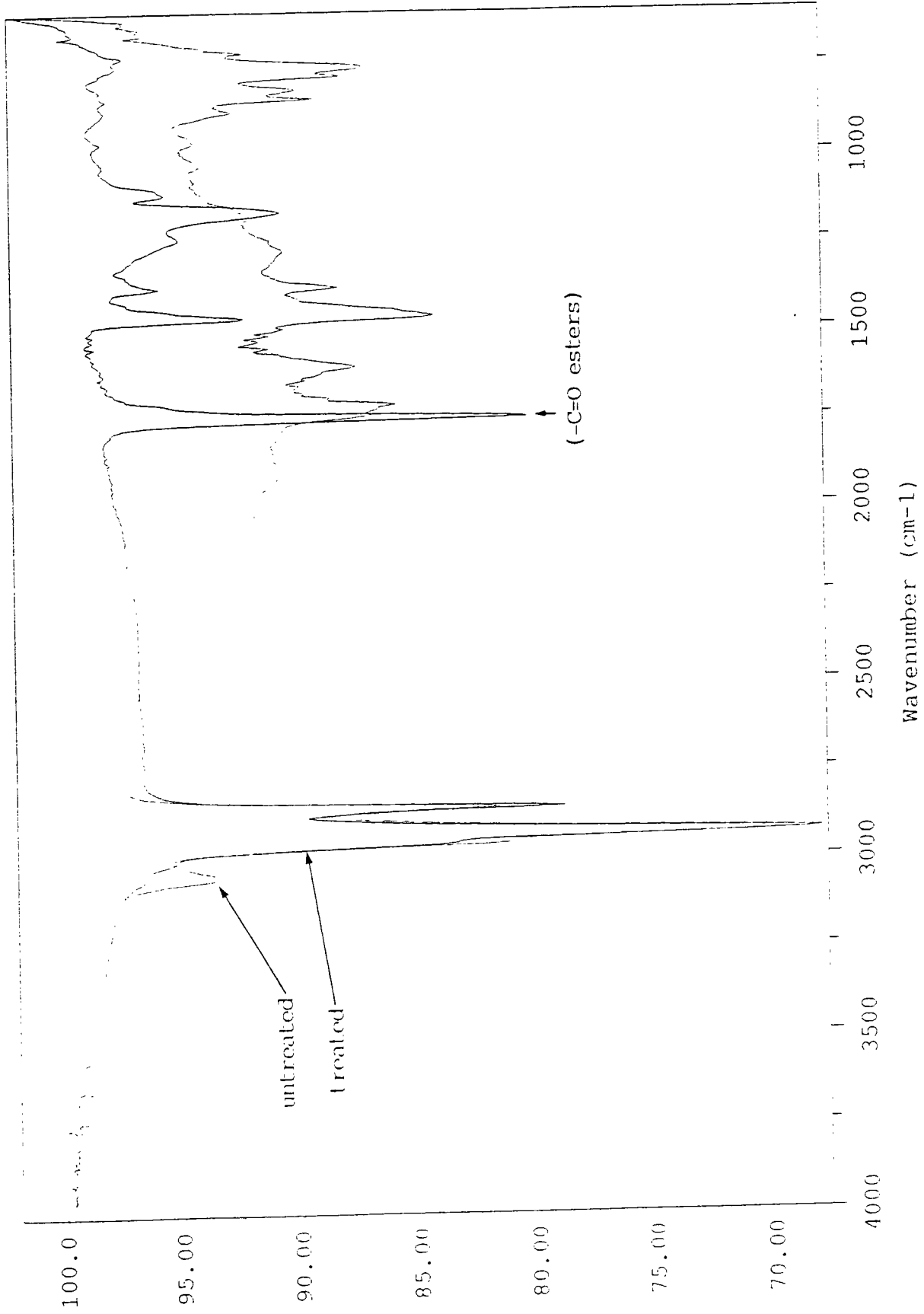


Figure 3. IR spectra of untreated and treated soils.

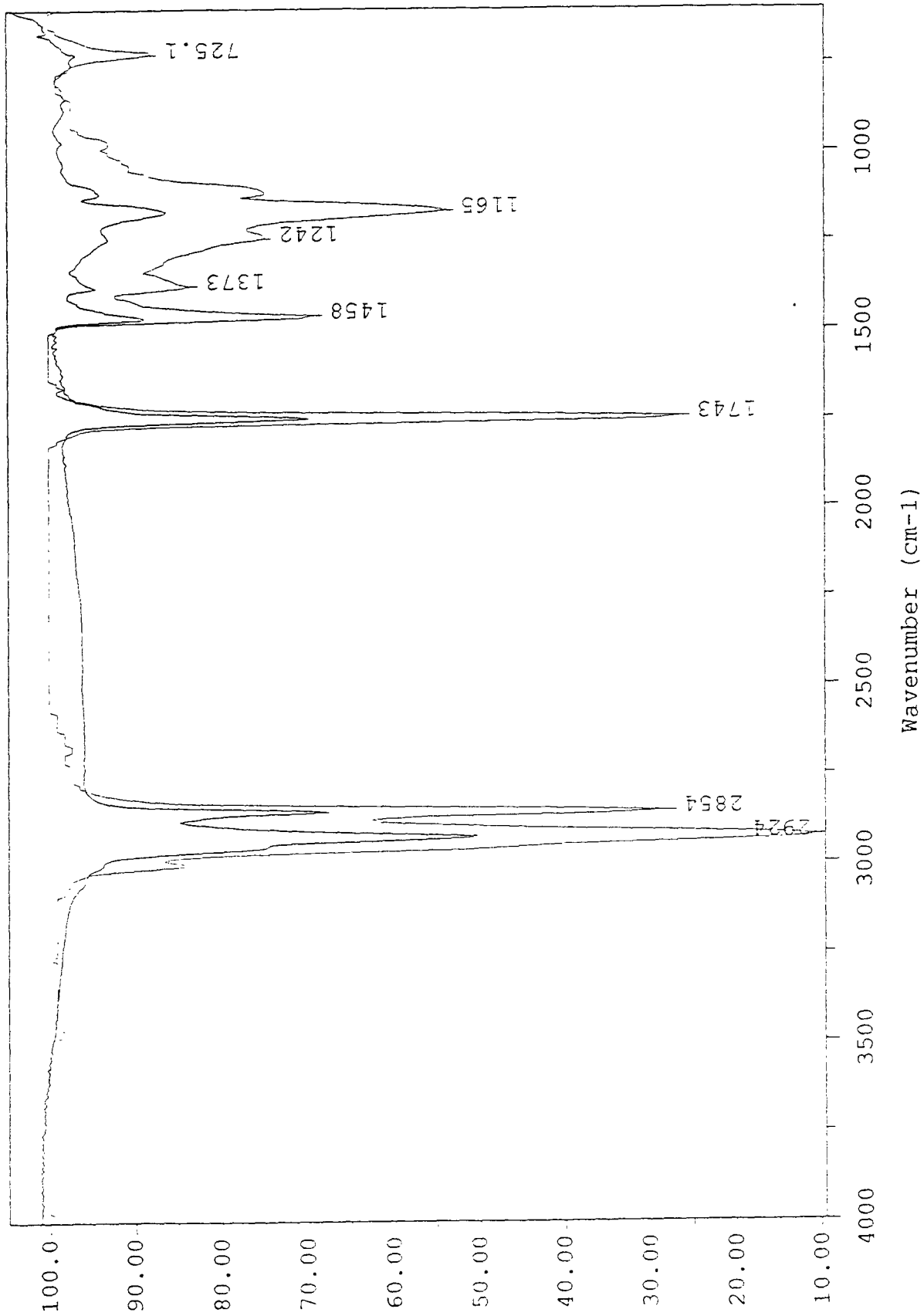


Figure 4. IR spectrum of treated PECO soil mix compare with spectrum of palm oil.

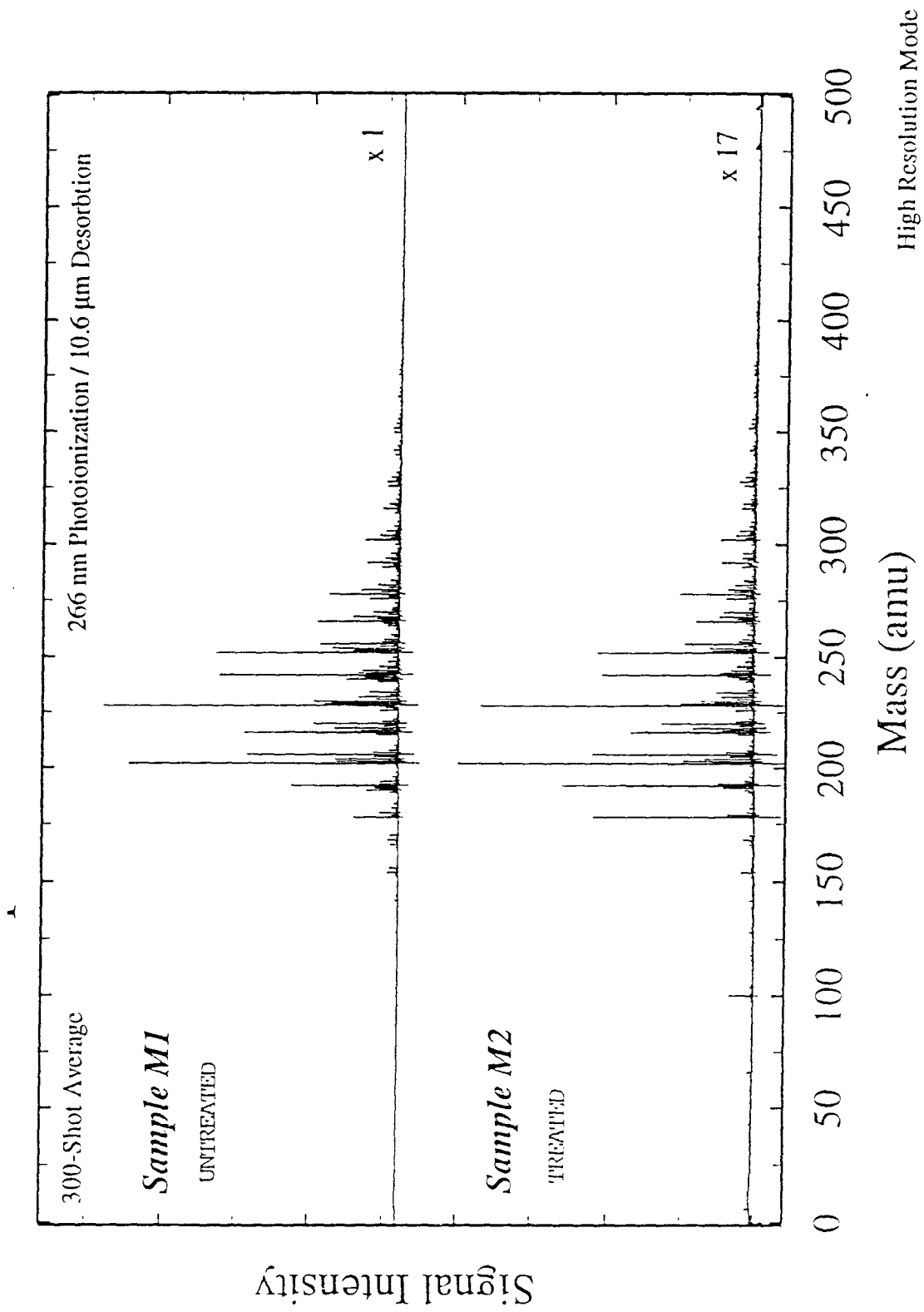


Figure 5.  $\mu\text{L}^2\text{MS}$  spectra of untreated control soil (upper) and treated soil (lower).

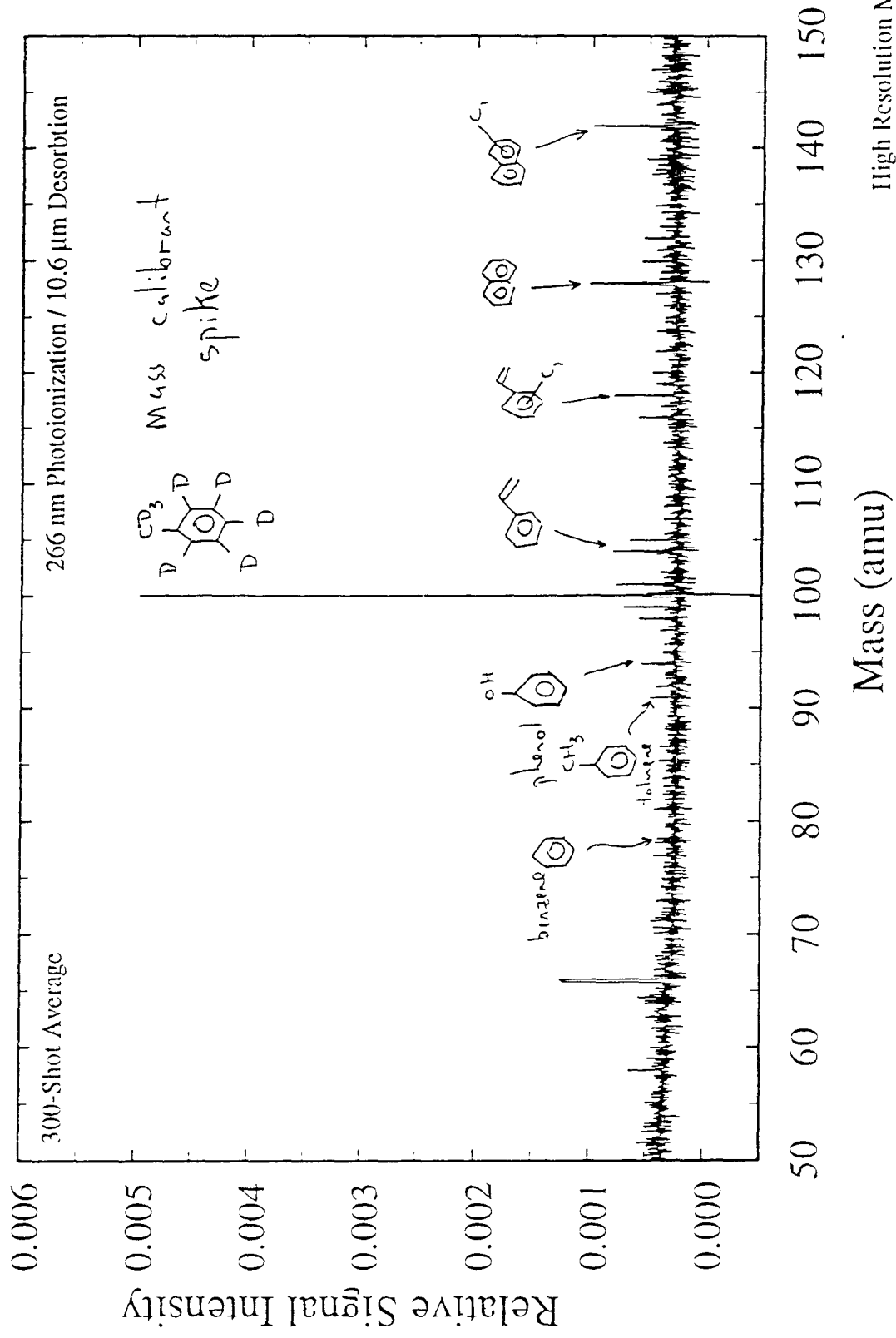


Figure 6.  $\mu\text{L}^2\text{MS}$  spectrum (expanded 8 trace) of 50-150 amu region.

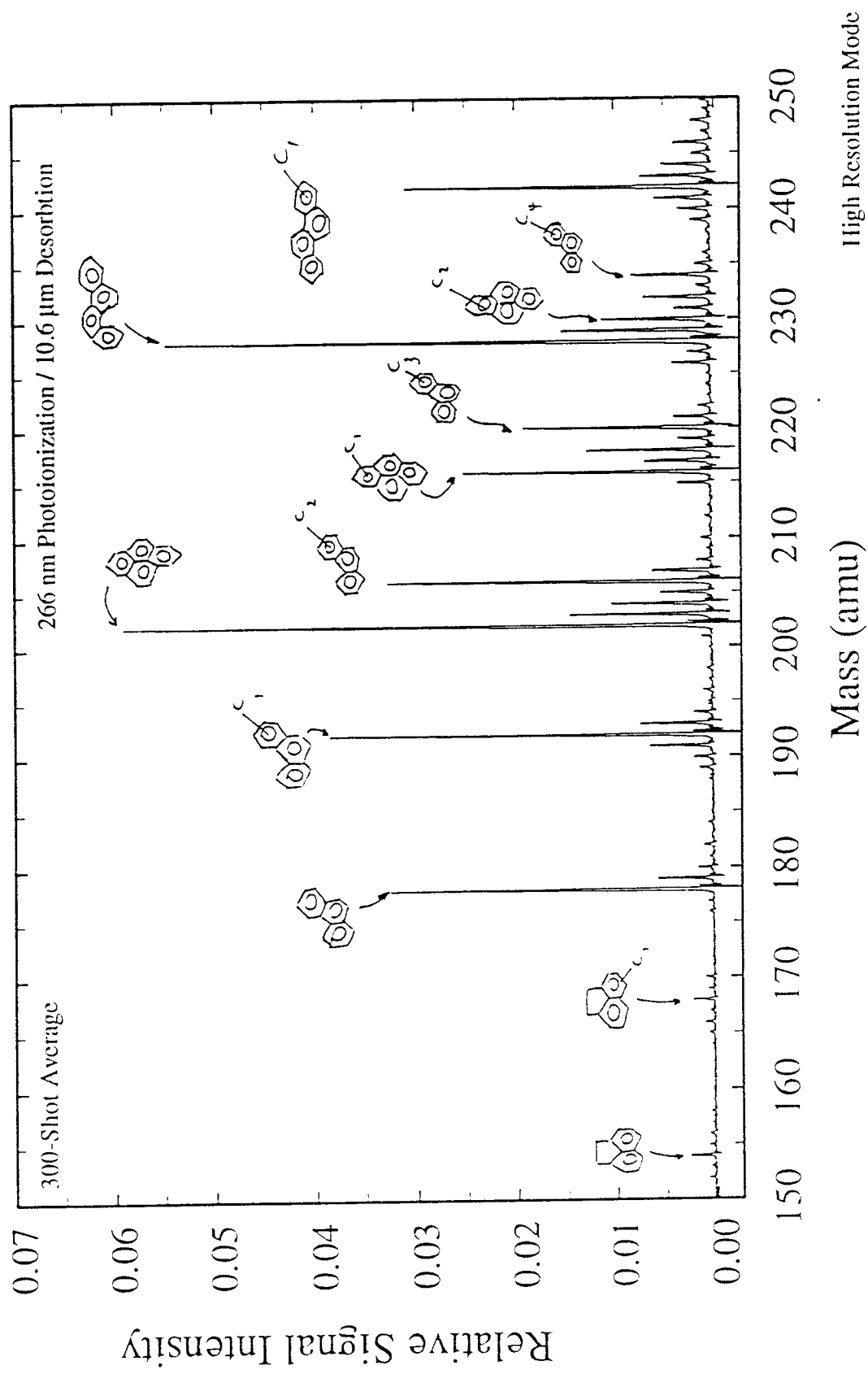
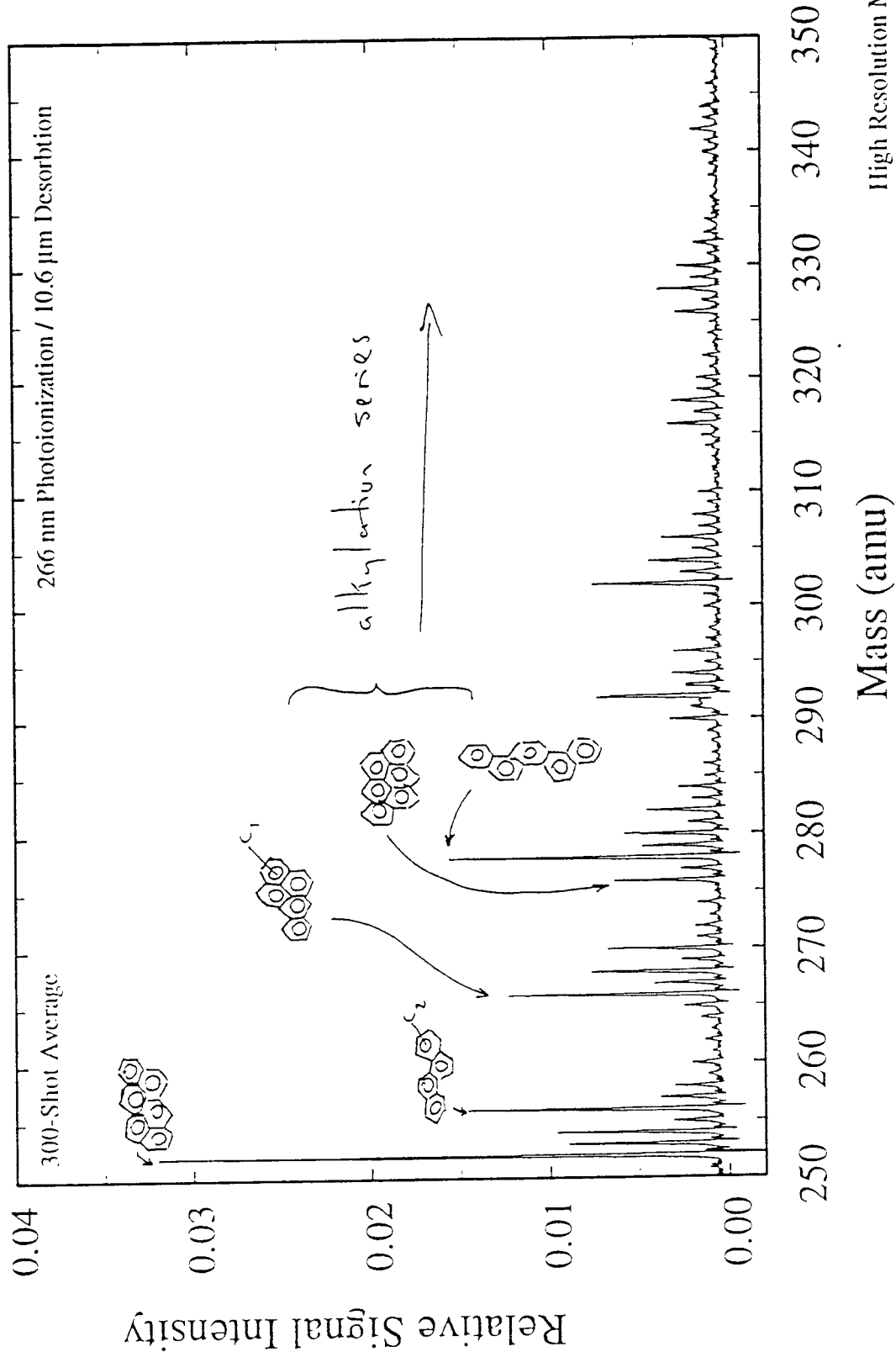


Figure 7.  $\mu\text{L}^2\text{MS}$  spectrum (expanded trace) of 150-250 amu region.



**Figure 8.**  $\mu\text{L}^2\text{MS}$  spectrum (expanded trace) of 250-350 amu region.

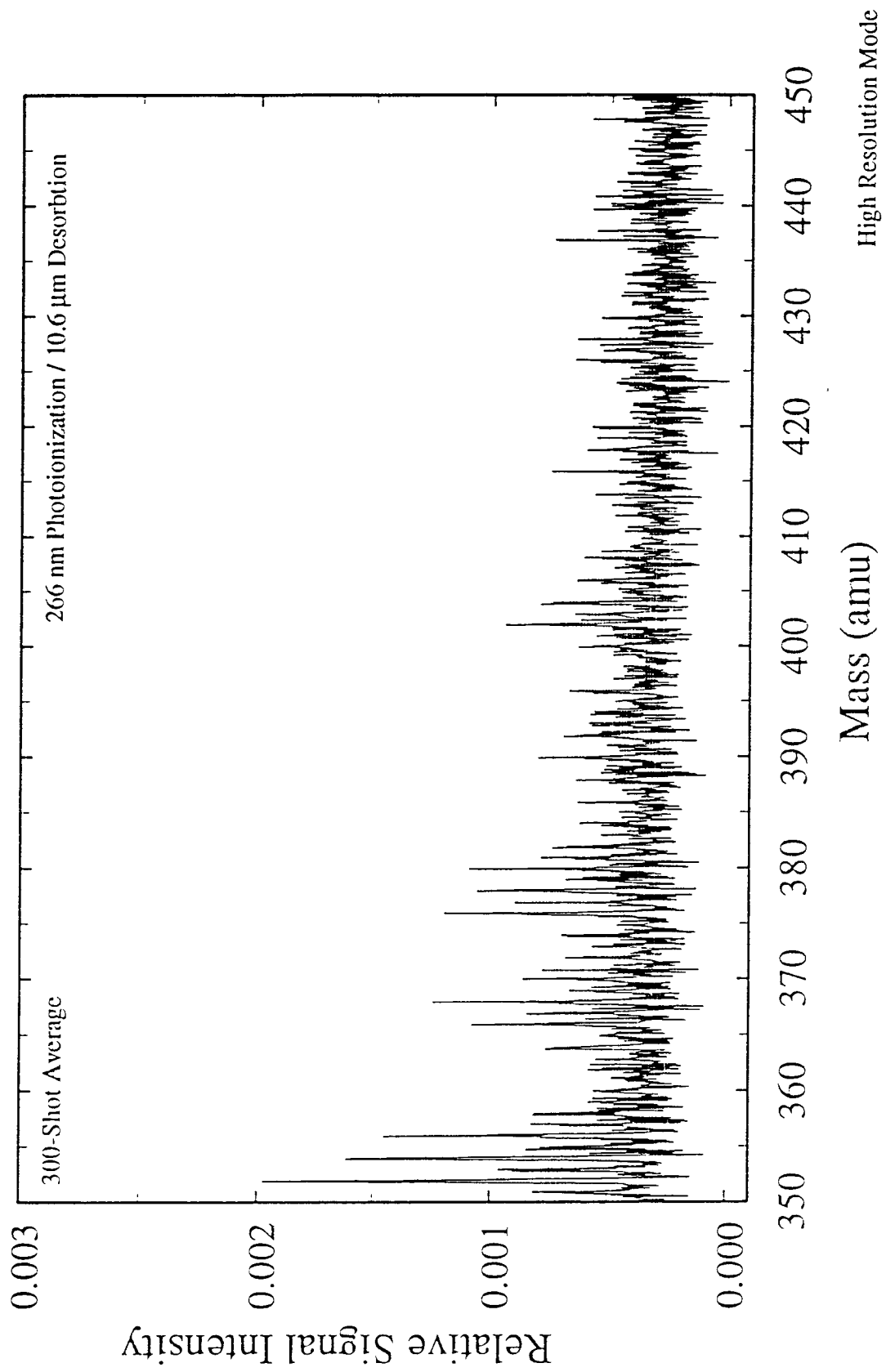


Figure 9.  $\mu\text{L}^2\text{MS}$  spectrum (expanded trace) of 350-450 amu region.

28 Springdale Road  
Cherry Hill, New Jersey 08003  
(609) 751-1122 • (215) 923-2068  
Fax: (609) 751-0824

2925 Richmond Avenue  
Houston, Texas 77098  
(713) 520-1495  
Fax: (713) 523-7107

**Analysis Request and  
Chain-of-Custody**

2324 Vernsdale Road  
Rock Hill, South Carolina 29730  
(803) 324-5310  
Fax: (803) 324-3982

Client: MARCOK of PENNA, INC

Project: PECO: ACT PILOT DEMO

AnalytikEM Contact: JOHN BRADLEY

LAB I.D. NO.	FIELD SAMPLE I.D. NO.	DATE	USE 24 HR. CLOCK TIME	MATRIX	40 ml vials					950 ml Org. Pres.					ANALYSIS REQUESTED PARAMETERS
					Unpres. ml	HNO <sub>3</sub> ml	H <sub>2</sub> SO <sub>4</sub> ml	H <sub>2</sub> SO <sub>4</sub> ml	H <sub>2</sub> SO <sub>4</sub> ml	Unpres. ml	HNO <sub>3</sub> ml	H <sub>2</sub> SO <sub>4</sub> ml	H <sub>2</sub> SO <sub>4</sub> ml	NH <sub>4</sub> OH ml	
	<u>SMA</u>	<u>4/27/95</u>		<u>solid</u>											<u>IR Microspectroscopy</u>
	<u>CONTROL SOIL</u>	<u>4/27/95</u>		<u>SOIL</u>											<u>films</u>
															<u>Run both tests on</u>
															<u>each sample</u>

I. Field Measurements: \_\_\_\_\_  
 Data Sheets: Y N  
 Filtered: Y Not Required

II. Field Conditions/Comments: \_\_\_\_\_

III. Special Instructions: reference Purchase Order # 3998  
 (Detection Limits, Data Package, etc.)

2. Chain of Custody

Seal No. \_\_\_\_\_

<b>Relinquished By:</b> <u>[Signature]</u>	<b>Received By:</b> _____
Print Name: <u>KAREN VIVIO HARREY</u>	Print Name: _____
Signature: _____	Signature: _____
Print Name: _____	Print Name: _____

Date/Time (use 24 hr. clock): 5/4/95 17:15

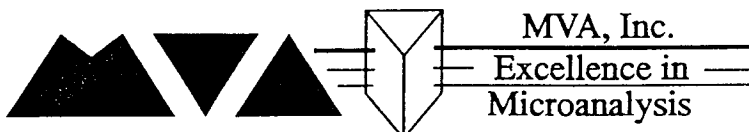
**Final Report**

**Microanalysis of PECO Soils and Sludges**

**Prepared by:**

**John P. Bradley, Ph.D.  
MVA, Inc.  
5500 Oakbrook Parkway, Suite 200  
Norcross, GA 30093**

**02 November 1995**



**5500 Oakbrook Parkway #200  
Norcross, Georgia 30093  
404-662-8509**

## Abstract

PECO soils and sludges treated with the ACT formulation (HWT27) were examined using bulk carbon analysis, solvent extraction, scanning electron microscopy (SEM), transmission electron microscopy (TEM), infrared microspectroscopy, microprobe two-step laser desorption mass spectroscopy ( $\mu\text{L}^2\text{MS}$ ), and gas chromatography (GC). During treatment with ACT, *total* carbon in the soils and sludge remained approximately constant but solvent extractable *organic* carbon fell by 50-75%. Carbonyl compounds (e.g. esters, phthalates) and carbonates formed as reaction byproducts, and PAHs fell by 50-85%. The greatest PAH reductions were among the higher-mass PAHs. SEM x-ray mapping and TEM electron energy-loss spectroscopy (EELS) suggest that ACT "mineralized" a significant fraction of the organic carbon in the soils and sludges.

A "control" experiment was carried out using only ACT powder and a 16 PAH standard solution (Supelco 4-8905M). PAHs were reduced up to 75% in solvent extracts from the experiment and breakdown products were detected in solid residues, confirming for the first time that **ACT chemically degrades PAHs**. Breakdown products were conspicuously absent in solvent extracts from the experiment, suggesting that ACT traps some organics in solid residues such that they are resistant to environmental leaching. Carbonates were formed which confirms that **ACT can mineralize PAHs**. (Mineralization explains why *solvent extractable* organic carbon levels were lower in the treated PECO soils and sludges.)

A "control" experiment was carried out using only ACT powder and a 6 PCB standard solution (Aroclor 1242). PCBs were chemically degraded and breakdown products were identified. The extent of PCB degradation by ACT and the nature of the breakdown products require further study.

## Table of Contents

	Page No.
Chapter 1..... Introduction	1
Chapter 2..... Total Carbon Analyses	2
Chapter 3..... Imaging X-ray mapping using automated scanning electron microscope	9
Chapter 4..... Transmission electron microscopy investigation of clays and carbonates	45
Chapter 5..... Infrared (IR) microspectroscopy	68
Chapter 6..... Microprobe two-step laser desorption mass spectroscopy 6:1 Analysis of PECO soils and sludges 6:2 Control Experiment A: Effect of ACT on PAHs 6:3 Control Experiment B: Effect of ACT on PCBs	77
Chapter 7..... Gas Chromatography	96
Appendix I..... Report of Results: MVA1342 Microanalysis of PECO soils	106

# Chapter 1

## Introduction

This summary document describes our microanalytical characterization of untreated and treated PECO soils and sludges. The study follows our initial exploratory study of PECO soil (Appendix I), in which we used infrared (IR) microspectroscopy and microprobe two-step laser desorption mass spectrometry ( $\mu\text{L}^2\text{MS}$ ) to study the fate of polyaromatic hydrocarbons (PAH's) in PECO soil which had been treated with the Advanced Chemical Treatment (ACT). This initial study suggested that the ACT treatment had resulted in (1) a decrease in the overall levels of PAHs in the soil and, (2) an increase in the abundance of "ester-like" compounds containing carbonyl functional groups. However, the study was limited in scope; solvent extractions were non-aggressive, only two microanalytical techniques (IR and  $\mu\text{L}^2\text{MS}$ ) were employed, and only two samples (one untreated and one treated) were examined.

In this study, we examine multiple soil and sludge samples from the PECO site using a broader range of analytical methods. These methods include aggressive solvent extraction, total (bulk) carbon analyses, scanning electron microscopy (SEM) with x-ray mapping, analytical transmission electron microscopy (AEM), microprobe two-step laser desorption mass spectrometry ( $\mu\text{L}^2\text{MS}$ ), infrared (IR) microspectroscopy, and gas chromatography (GC).

Mass balance with respect to bulk organic and inorganic carbon in the samples before and after treatment with ACT is evaluated. Physical properties (e.g. mineralogy, grain size, texture, carbon petrography) are determined using SEM. The roles of inorganic components (e.g. carbonates and clays) in the ACT treatment are assessed using TEM, while changes in the organic content of the samples are monitored using GC and  $\mu\text{L}^2\text{MS}$ .

Also included in this report are the results of two control experiments in which standard mixtures of PAHs and PCBs were added to HWT27 powder and allowed to react under carefully controlled conditions. **These control experiments provide groundtruth testing of the efficacy of the ACT formulation in the treatment of soils and/or sludges contaminated with PAHs and PCBs.**

For simplicity, results from each microanalytical technique are presented within separate Chapters. At the beginning of each Chapter, an explanation is provided for employing a particular technique and, at the end of the Chapter, a summary of results is provided. Chapter 2 addresses carbon mass balance, with quantitative data on total carbon, carbon as carbonate, and total organic carbon in untreated and treated soils and sludges. Chapter 3 describes the physical characteristics (plus compositional trends) in soils and sludges as measured using (SEM) backscattered electron imaging and X-ray mapping. Electron energy-loss spectroscopy (EELS) of carbon compounds (carbonates, coal, other organic matter) and transmission electron microscopy (TEM) of clays are presented in Chapter 4. Infrared (IR) data from both organic and inorganic components of the samples are presented in Chapter 5. The final two Chapters deal exclusively with organic microanalysis using microprobe two-step laser desorption mass spectrometry ( $\mu\text{L}^2\text{MS}$ ) (Chapter 6) and gas chromatography (GC) (Chapter 7). Chapter 6 includes two very important control experiments in which the ACT formulation (HWT27) was tested on PAH and PCB standards.

## Chapter 2

### Total Carbon Analyses

The purpose of measuring total carbon content of treated and untreated soil and sludge was to evaluate mass balance and determine whether loss by volatilization (vaporization) was significant during the HWT treatment.

The analyses were performed at Galbraith Laboratories, Inc. Total carbon was measured by combustion (at 1050°C in oxygen) using a LECO CHN 1000 furnace. Inorganic carbon (as carbonate) was measured by acid hydrolysis and coulometric titration. Total organic carbon was derived simply by subtracting inorganic carbon from total carbon. Table 2:1 below summarizes the results of the C analyses. The actual Galbraith data sheets and analytical protocols are included in the following pages (pp. 4 through 8).

Table 2:1

#### Carbon Abundances

1	2	3	4
Sample #	Total Carbon	Inorganic Carbon <sup>a</sup>	Organic <sup>b</sup>
M1 (untreated soil)	11.41	0.061	11.35
M2A (treated soil, aged 125 days)	6.67	0.90	5.77
M3 (Treated sludge)	5.6 5.48 <sup>c</sup>	0.22 0.0897 <sup>c</sup> 0.1134 0.2096 0.1515 0.2058	
M4 (Untreated sludge)	8.25 8.49	0.022	

<sup>a</sup>. Carbonate calculated as carbon

<sup>b</sup>. Total carbon less inorganic carbon

<sup>c</sup>. Multiple entries indicate multiple analyses

Summary of total carbon analyses

As expected, most of the carbon in the PECO soils and sludges is organic (compare Table 2:1, columns 2 and 4). Assuming that 25-30% by weight of IWT27 was added during the treatment (column 1), there appears to be *approximate* mass balance for total carbon between untreated and treated samples, **i.e. reduction in PAHs and other organic compounds as a result of the ACT treatment cannot be explained simply by loss through volatilization.**

Note also that the treated soil (M2A) contains almost an order of magnitude more carbonate (0.9 wt. %, column 2) than the treated sludge (~0.17 wt. % on average), which is consistent with our observation that the treated soil showed a much more vigorous reaction when 10% HCl solution was administered. (Administration of a 10% HCl solution is the standard field testing procedure for the presence of carbonates). In terms of PAH reduction, the treated sludge yielded better (GC/MS) results than the treated soil. It is unclear what inference (if any) can be drawn from the observation that the sample containing the least amount of carbonate yielded the best PAH reduction. Futhermore, milligram quantities were analyzed for bulk carbon even though it was clear that the soil and sludge were not optimally mixed in the pug mill during treatment with ACT.



# GALBRAITH LABORATORIES, INC.

*Accuracy with speed - since 1950*

## LABORATORY REPORT

John Bradley  
MVA Incorporated  
5500/200 Oakbrook Parkway  
Norcross GA 30093

Sample Received: 08/23/95  
Report Date: 08/25/95  
Purchase Order #: 0904

SAMPLE ID	LAB ID	ANALYSIS	RESULTS	
M-3	M-3582	Total Carbon	5.60	%
			5.48	%
		Carbonate calculated as Carbon	0.22	%
M-4	M-3583	Total Carbon	8.25	%
			8.49	%
		Carbonate calculated as Carbon	0.022	%

CB:le



# GALBRAITH LABORATORIES, INC.

*Accuracy with speed - since 1950*

## LABORATORY REPORT

John Bradley  
MVA Inc  
5500/200 Oakbrook Parkway  
Norcross GA 30093

Sample Received: 08/29/95  
Report Date: 09/01/95

SAMPLE ID	LAB ID	ANALYSIS	RESULTS	
M1	M-4374	Carbon	11.41	%
		Carbonate	0.061	%
		Calculated as Carbon		
M2A	M-4375	Carbon	6.67	%
		Carbonate	0.90	%
		Calculated as Carbon		

AL:wp



# GALBRAITH LABORATORIES, INC.

*Accuracy with speed - since 1950*

## LABORATORY REPORT

John Bradley  
MVA Incorporated  
5500/200 Oakbrook Parkway  
Norcross GA 30093

Reanalysis Request: 08/28/95  
Previous Lab I.D.: M-3582  
Report Date: 08/30/95

SAMPLE ID	LAB ID	ANALYSIS	RESULTS	
M-3	M-4092	Carbonate calculated as Carbon	0.0897 0.1134 0.2096 0.1515 0.2058	% % % % %

Note: Sample appears to be non-homogeneous. Also there is an indication that Sulfide may be present which contaminates the scrubber.

CBM:le



# GALBRAITH LABORATORIES, INC.

*Accuracy with speed - since 1950*

## Galbraith Laboratories, Inc.

### Method Summary

Procedure #: ME-11 Rev 0      Analyte: CHN      Range: See \*

Title: Carbon, Hydrogen, and Nitrogen by Leco CHN 1000 Determinator

Effective Date: 12/16/94      Superseded:

Procedure: Weigh 10 to 100 mg of sample into a tin capsule to the nearest 0.001 mg. Seal.  
Alternate A - for difficult-to-combust samples - add tin powder or V<sub>2</sub>O<sub>5</sub>.

Instrument: Leco CHN 1000 Determinator

Calibration: Acetanilide (5-70 mg)

Control: s-1483 Cyclohexanone-2,4-dinitrophenylhydrazone ; % C:H:N 51.79: 5.07: 20.14; s-2483 Acetanilide % C:H:N 71.09: 6.72: 10.36; s-3483 Acetanilide % C:H:N 71.09: 6.71: 10.36; s-6483 EDTA % C:H:N 41.10: 5.52: 9.59; s-0606 Carbon Powder % C 100.00  
One every ten samples

Precision and Accuracy:	RSD	RE
s-3483 (H)	2.03 %	0.19 %

Determination: Combustion at 1050 °C in constant O<sub>2</sub> stream ; Infrared absorption for CO<sub>2</sub>, H<sub>2</sub>O ; Thermal conductivity of sampled gas stream for N<sub>2</sub> (reduced nitrogen oxides). Quantitation limit is 0.5 %.  
Method detection limit is 0.3 %.

Calculations: Microprocessor calculates response factors and results from sample weights manually entered.

References: Leco Manual 200-370

Other procedures: ME-2, ME-7

\*Comments: Range C: 0.5-100%    H: 0.5-15%    N: 0.5-50%



# GALBRAITH LABORATORIES, INC.

Accuracy with speed - since 1950

## Galbraith Laboratories, Inc. Method Summary

Procedure#: E 6-5 Rev 3      Analyte: CO<sub>3</sub>      Range: 0.05-3 mg C

Effective Date:      10/12/93      Superseded:

Title:      Coulometric Determination of Inorganic Carbon

Procedure:      Weigh spl to contain greater than 1 mg CO<sub>3</sub>-C if possible

Decomposition: Acid hydrolysis

Instrument:      Carbon Dioxide Coulometer Model #5010  
(Coulometrics, Inc.)

Calibration:      Absolute measurement in coulombs, internal conversion to  $\mu\text{g C}$  - no routine calibration required

Control:      k-1006 Calcium carbonate (12.01% as C)

Sample Intro.:      Generation of CO<sub>2</sub> with acid digestion (H<sub>2</sub>SO<sub>4</sub>); N<sub>2</sub> carrier gas

Determination:      CO<sub>2</sub> converted to acid by ethanolamine, automatic titration with coulometric generation of base. Colorimetric monitor. Range 0.05-3 mg C.

Interferences:      H<sub>2</sub>S; SO<sub>2</sub>; HCl; Cl<sub>2</sub> (use aqueous scrubber) Dry Ag scrubber may be used.

Calculations:      % C = Readout( $\mu\text{g C}$ ) - blank( $\mu\text{g C}$ ) / spl wt(mg) x 10

References:      Microchemical Journal 22; 567-573 (1977).  
Analyst, 96; (1971), 37-46.  
ASTM D-1756.

Other Procedures:      E 6 series

## Chapter 3

### Imaging and X-ray mapping using an automated scanning electron microscope

The purpose of (backscattered electron) imaging and x-ray mapping was to determine the bulk textural, morphological, and chemical characteristics of treated and untreated soil and sludge samples; i.e. establish what the soils and sludges actually look like and what they are composed of.

Polished thick-flat specimens of treated and untreated PECO soil and sludge were prepared by embedding representative samples in epoxy and then polishing the cured epoxy discs on successively finer abrasive substrates. After a final polish using 0.05  $\mu\text{m}$  gamma alumina, a conductive carbon coating was applied to the surfaces of the samples. Figures 3:1 through 3:34 are backscattered electron images together with corresponding x-ray energy-dispersive maps which show the distribution of carbon (C), oxygen (O), aluminum (Al), silicon (Si), calcium (Ca), and iron (Fe).

Figures 3:1 through 3:7 show an untreated PECO soil sample (M1). A large area backscattered electron image is shown (Fig. 3:1), followed by higher magnification images and x-ray maps (Figs. 3:2 - 3:7). The soil consists of agglomerates of micrometer-sized mineral grains held together by carbon-rich matrix (e.g. Fig. 3:2), presumably organic matter (see also Figs. 3:4 - 3:7). Figures 3:6 and 3:7 best depict the distribution of (organic) C throughout the matrices of an agglomerate. (Note the strong C signal from the epoxy embedding medium). Individual coal fragments which contain minor sulfur are also present (see Figs. 3:2 & 3:6).

Figures 3:8 through 3:18 show a treated PECO soil sample (M2). A large area backscattered electron image is shown in Figure 3:8. Note there appears to have been a significant decrease in the soil grain size between untreated and treated soils, possibly as a result of mixing in the pug mill (cf. Figs. 3:1 & 3:8). However, the most important observation in the treated soil concerns the C-rich matrix. The ACT treatment has resulted in infiltration of the organic matrix with Ca-rich material (cf. Figs 3:10 & 3:11, 3:12, 3:13 & 3:14, 3:15 & 3:16 and especially Figs. 3:17 & 3:18).

Figures 3:19 through 3:25 show the untreated PECO sludge (M4). The sludge consists primarily of 1-50  $\mu\text{m}$  diameter fly-ash spheres embedded in what is assumed to be organic matrix (Figs. 3:19 & 3:20). Figures 3:26 through 3:33 show the treated PECO sludge (M3). Note that, as with the treated soil, a Ca-rich phase has infiltrated the organic-rich matrices of the agglomerates of sludge grains. TEM brightfield imaging, energy-dispersive x-ray analyses, and electron energy-loss spectroscopy (EELS) establish that this Ca-rich phase is calcium carbonate (see pp. 45 - 49).

Summary of x-ray mapping and other SEM observations

The PECO soils and sludges consists of agglomerates of mineral grains (in the soils) and fly-ash (in the sludges) embedded in carbon-rich organic matter.

Coal fragments are present in both materials. **The major finding of the SEM study is that a significant fraction of the carbon-rich organic matter in the treated soils and sludges has been mineralized by conversion into Ca-rich carbonate.** The mineralization reaction is most succinctly illustrated in Figures 3:33 and 3:34 where the matrix is clearly C-rich (and essentially Ca-free) in the untreated sludge (Fig. 3:33) and Ca-rich (and C and O-rich) in the treated sludge (Fig. 3:34).

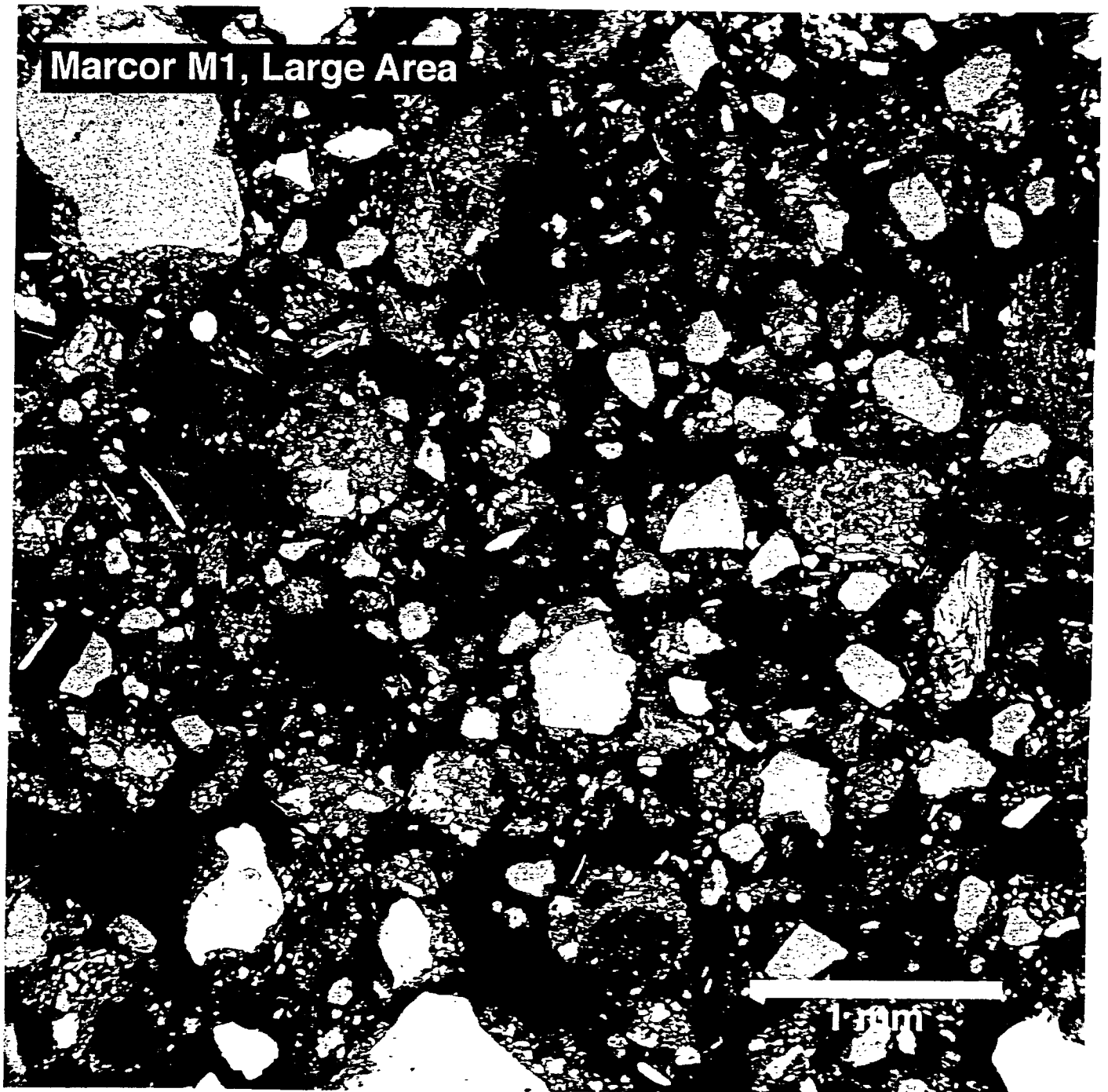


**Figure 3:1.** Large area (~5 X 5 mm) backscattered electron image of polished thick-flat specimen of untreated PECO soil.

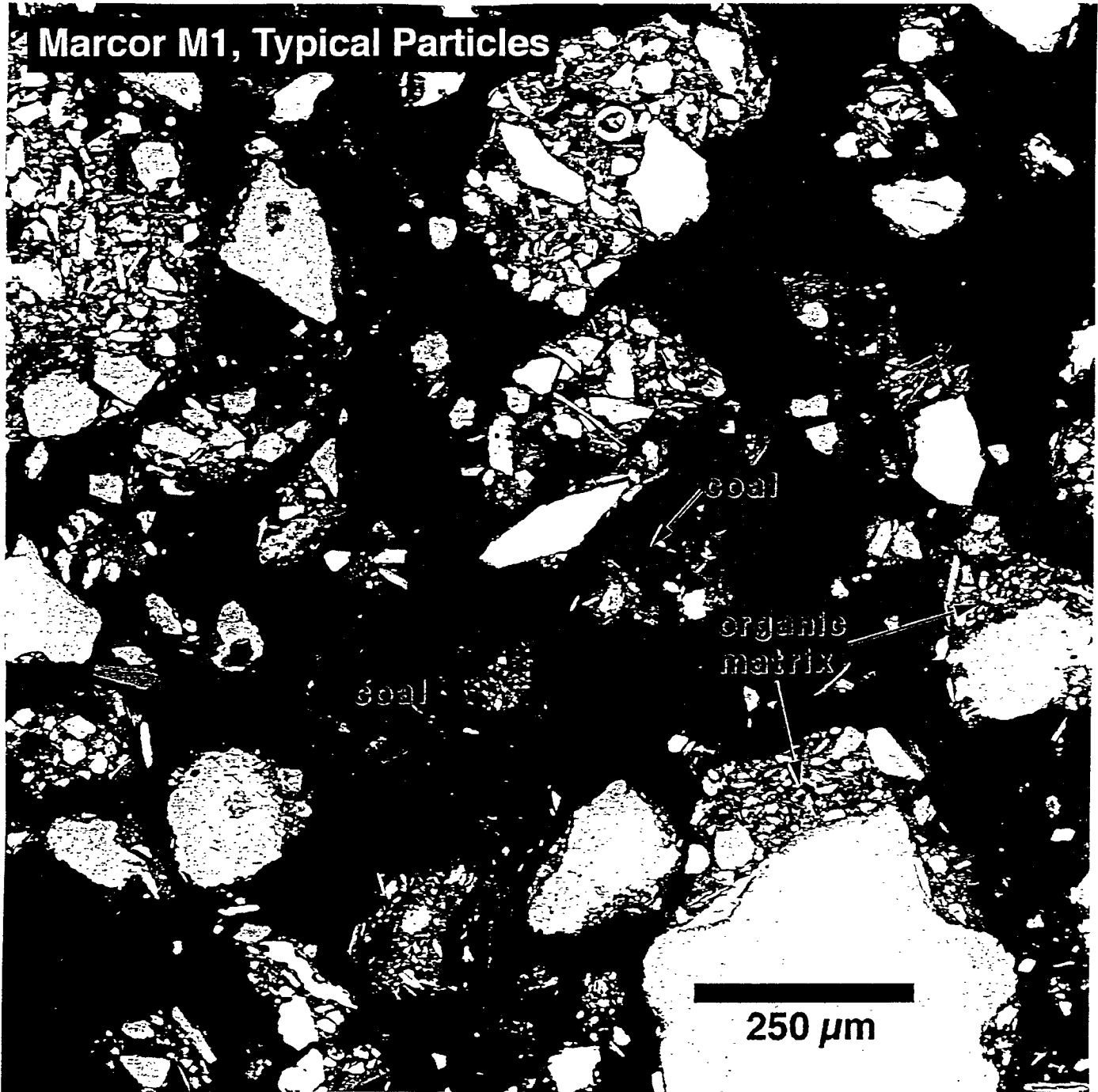


**Figure 3:2.** High-magnification backscattered electron image of untreated PECO soil showing typical soil constituents. Note that organic material forms the matrix which binds together polycrystalline agglomerates of grains (see also Fig. 3.3 overleaf).

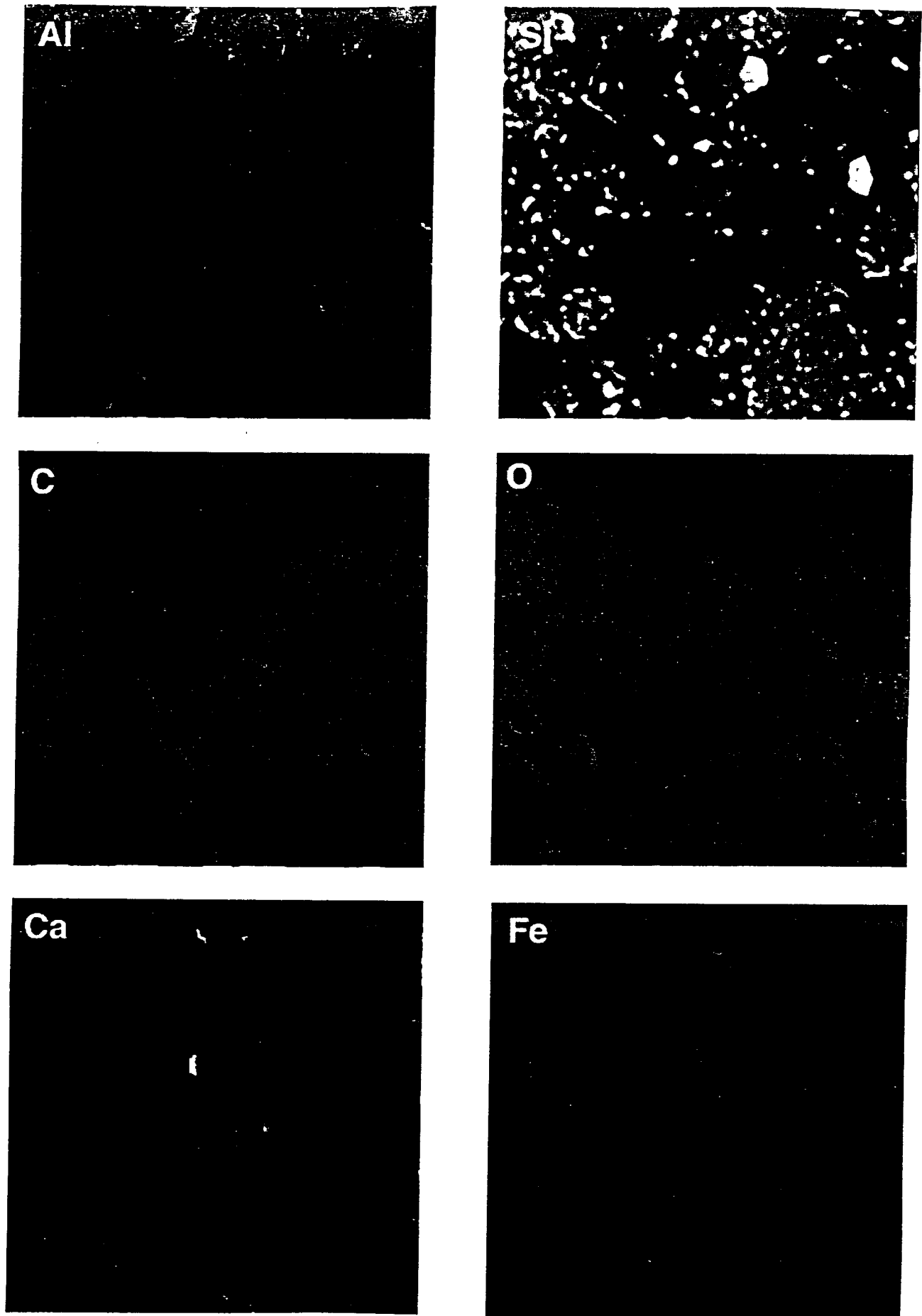


**Figure 3:3.** X-ray compositional maps (corresponding to field-of-view in Fig. 3:2) showing the distribution of Al, Si, C, O, Ca, and Fe in untreated PECO soil.

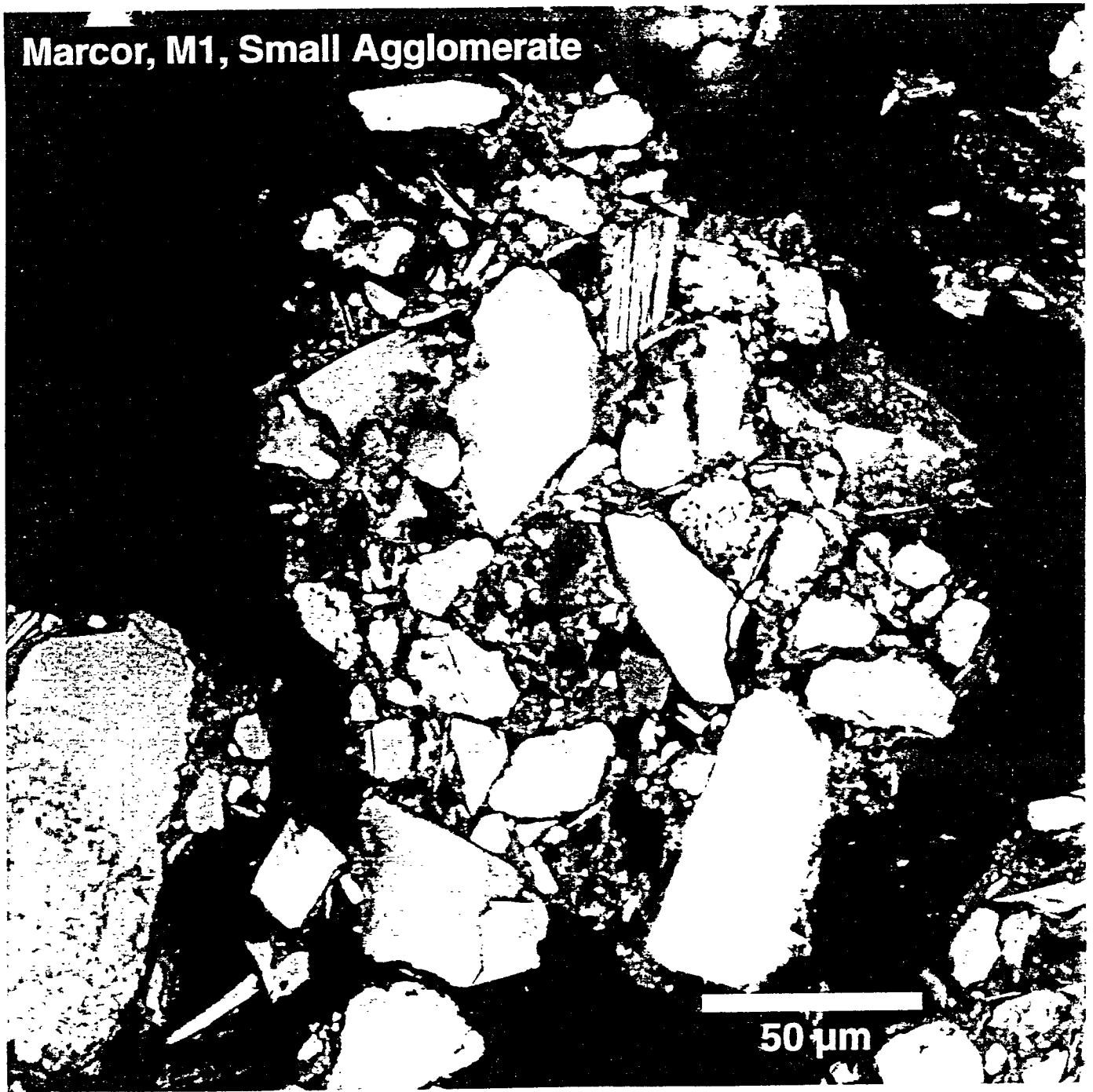


**Figure 3:4.** Backscattered electron image of a small agglomerate in untreated PECO soil (see also Fig. 3:5 overleaf).

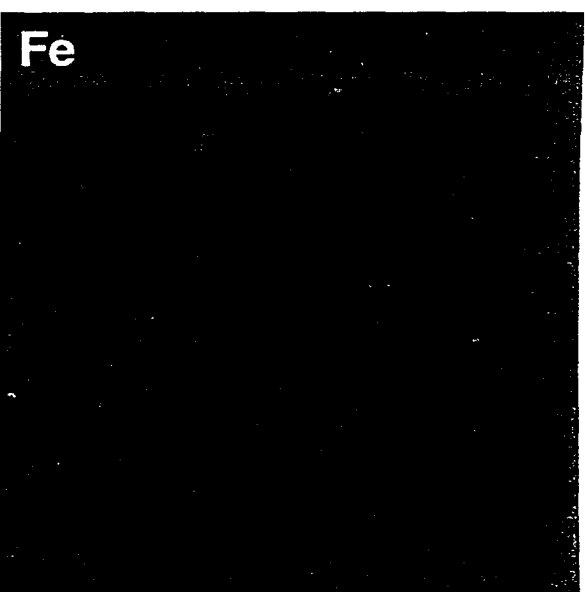
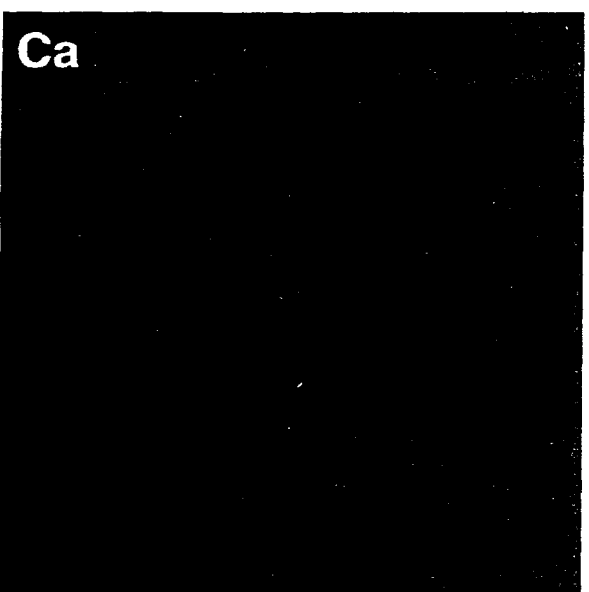
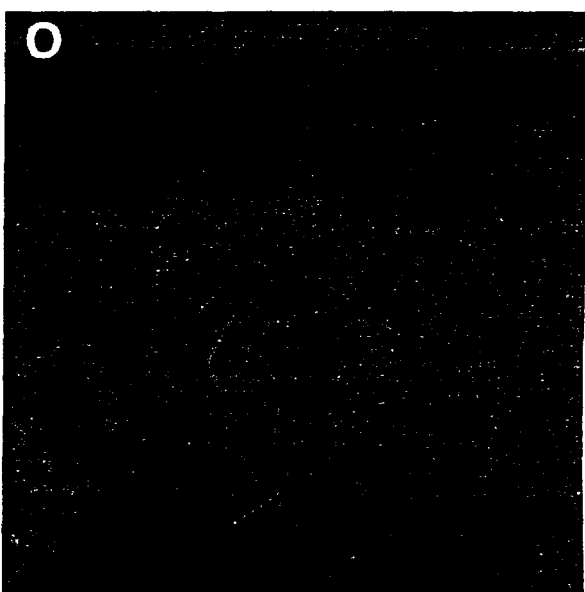
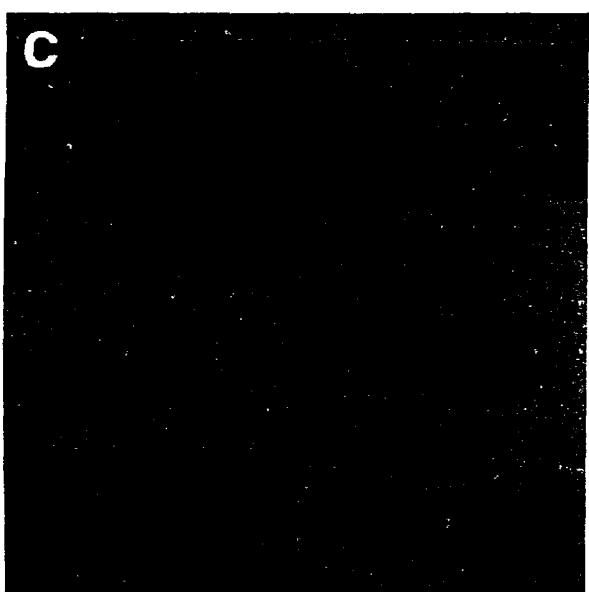
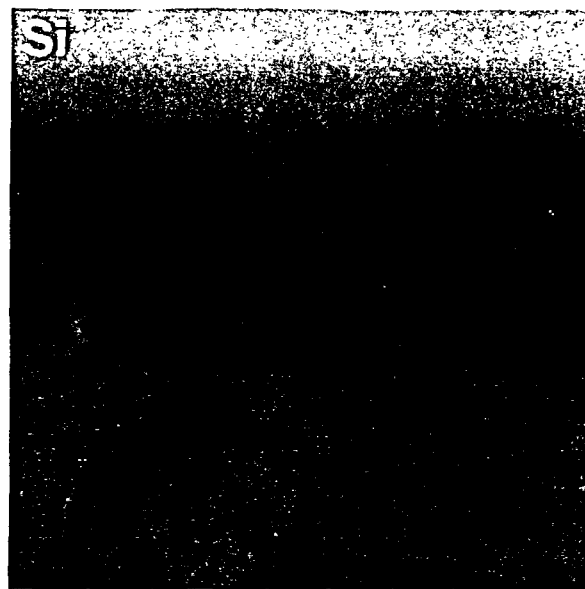
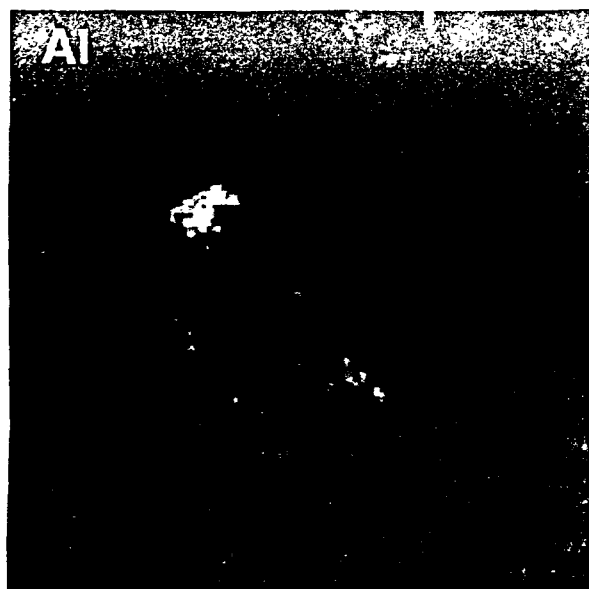


**Figure 3:5.** X-ray compositional maps (corresponding to field-of-view in Fig. 3:4) showing distribution of Al, Si, C, O, Ca, and Fe in a small agglomerate particle in untreated PECO soil.

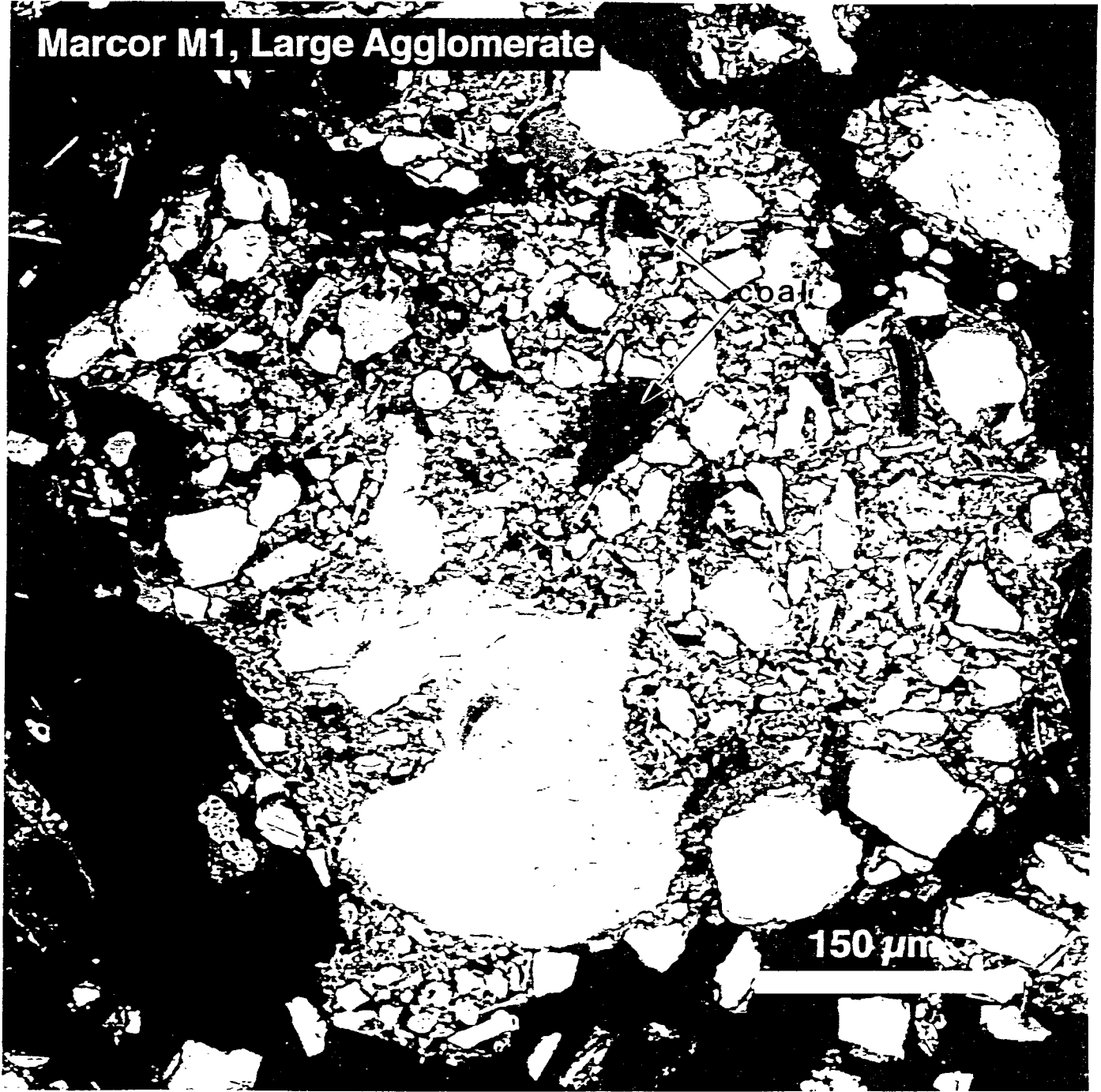


Figure 3:6. Backscattered electron image of a large agglomerate in untreated PECO soil (see also Fig. 3:7 overleaf).

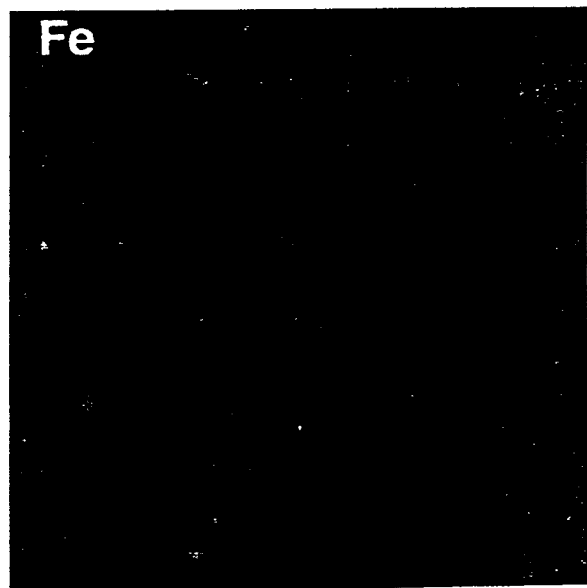
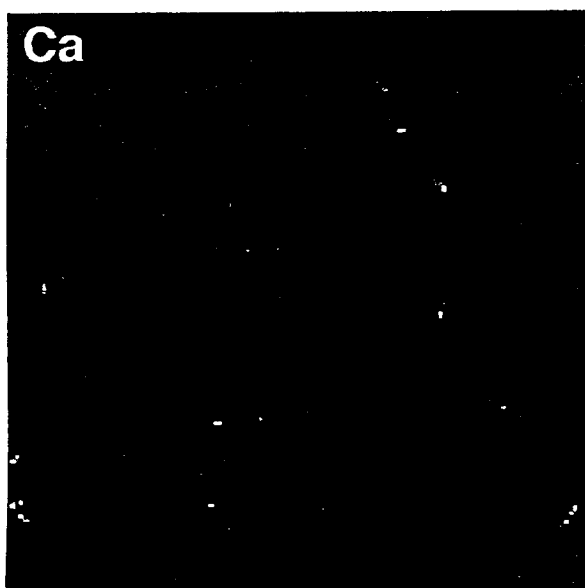
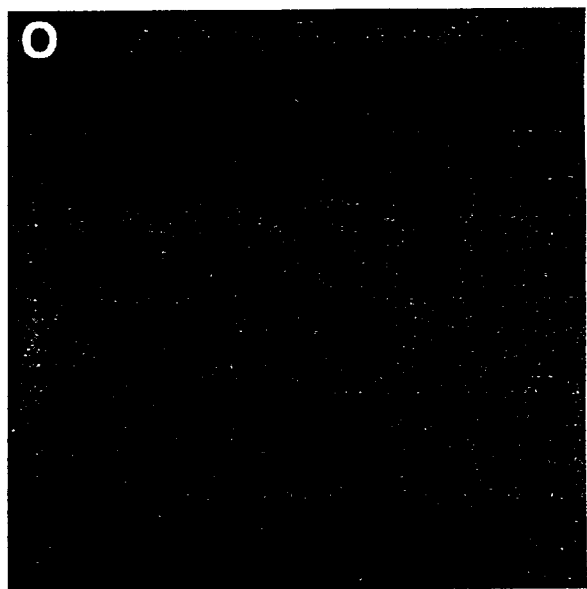
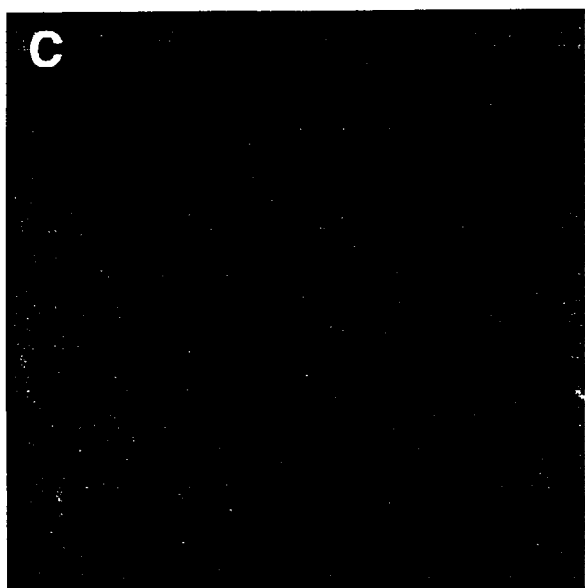
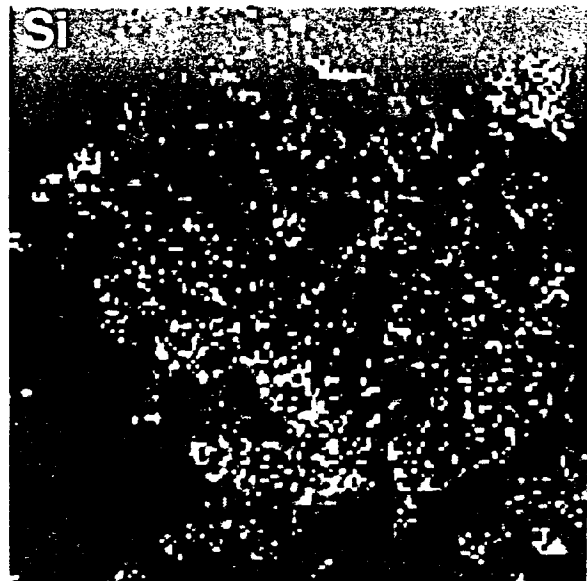
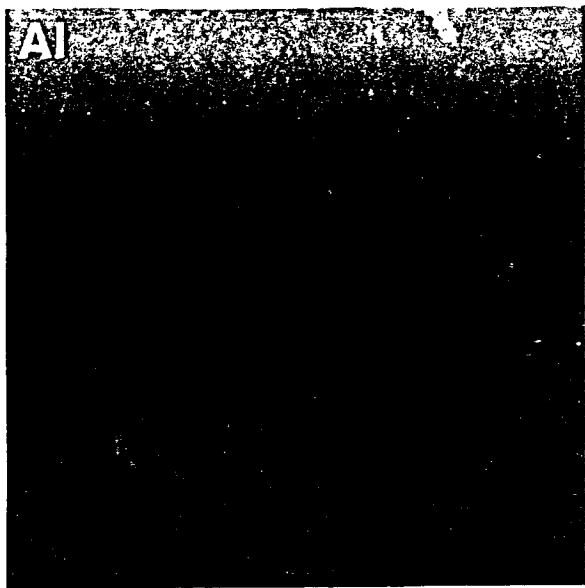


Figure 3:7. X-ray compositional maps (corresponding to field-of-view in Fig. 3:6) showing distribution of Al, Si, C, O, Ca, and Fe in a large agglomerate of untreated PECO soil.

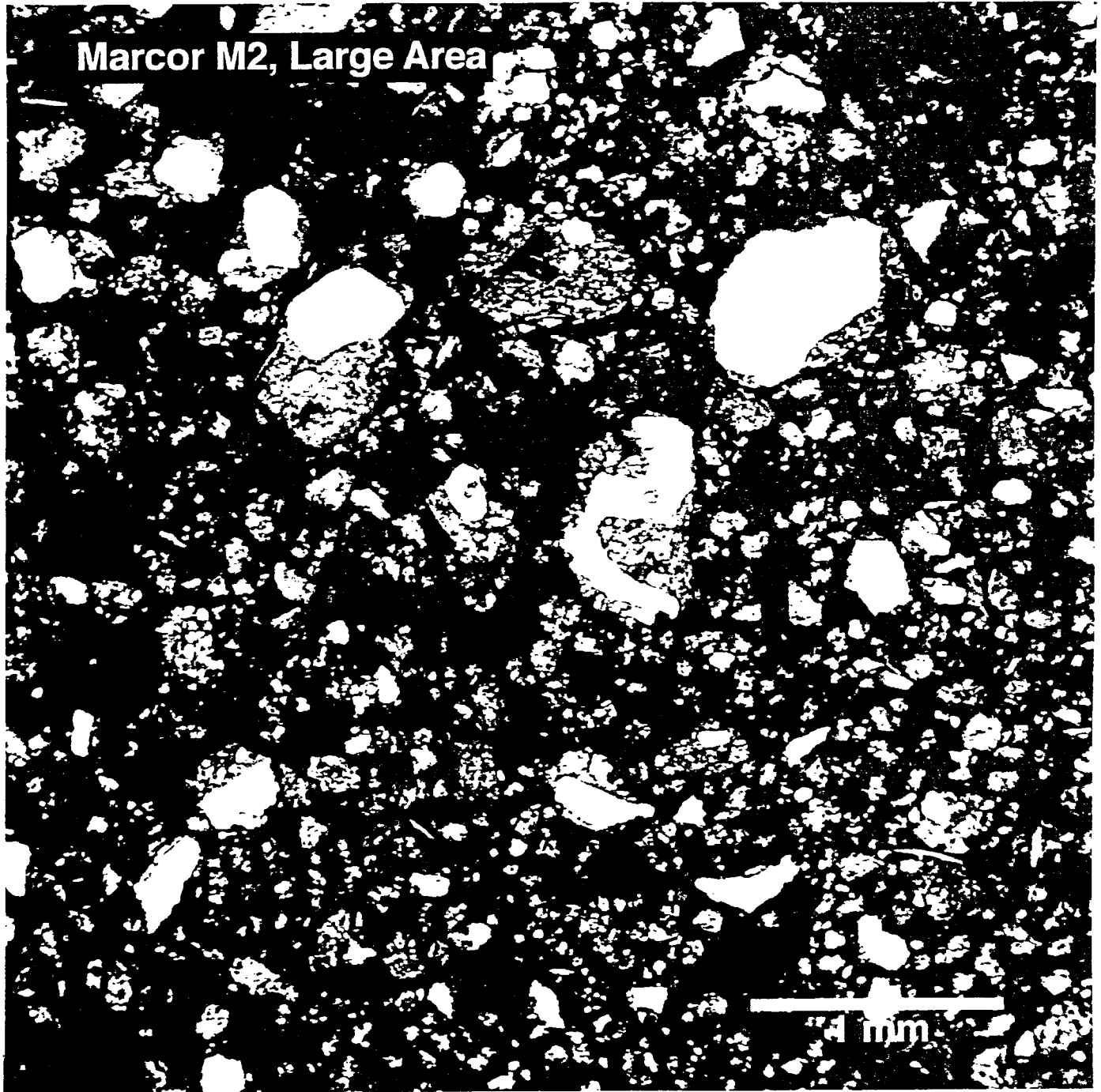


Figure 3:8. Large area (~5 X 5 mm) backscattered electron image of a polished thick-flat specimen of treated PECO soil.

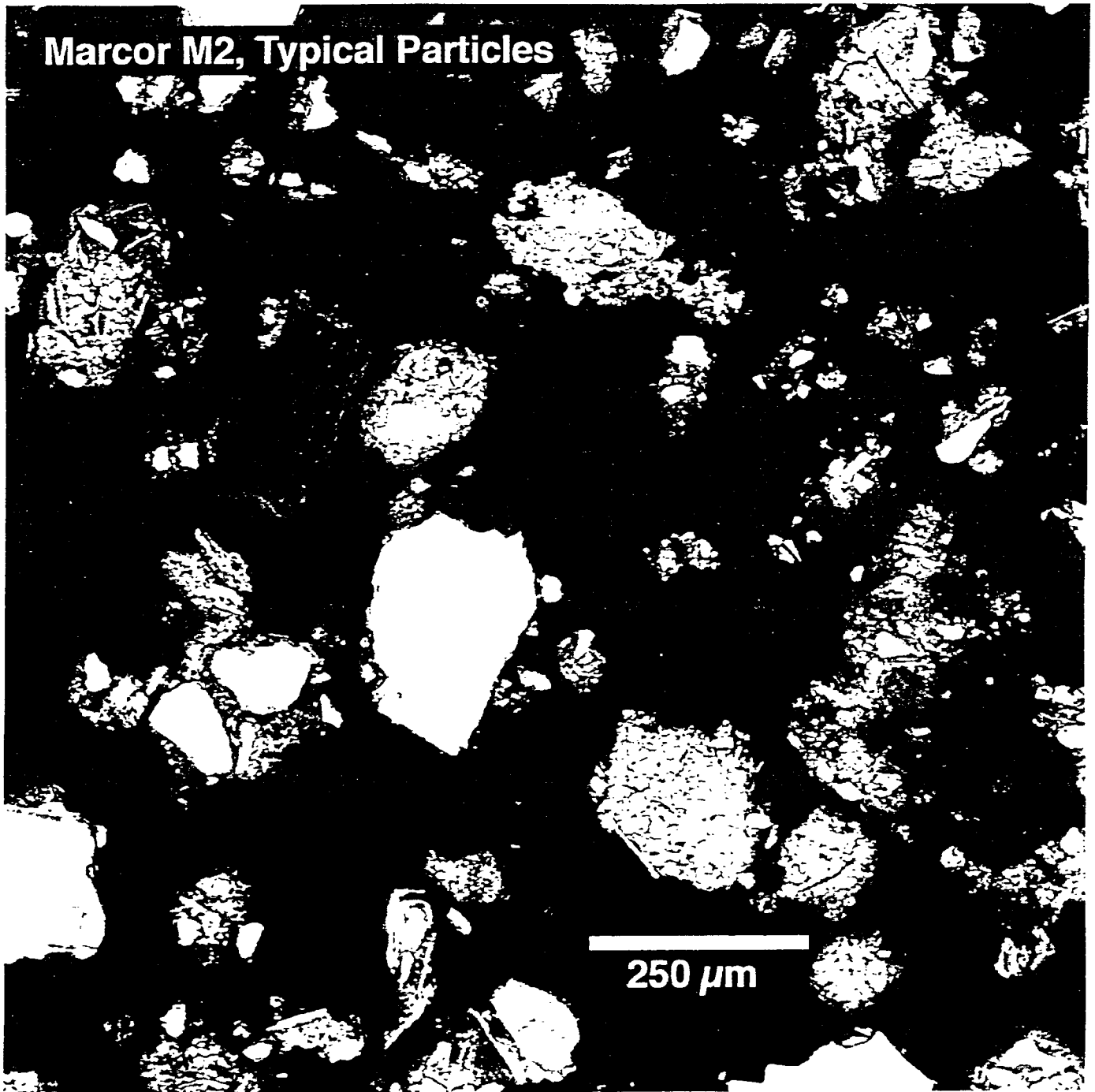


Figure 3:9. High-magnification backscattered electron image of treated PECO soil showing typical soil constituents (see also Fig. 3:10 overleaf).

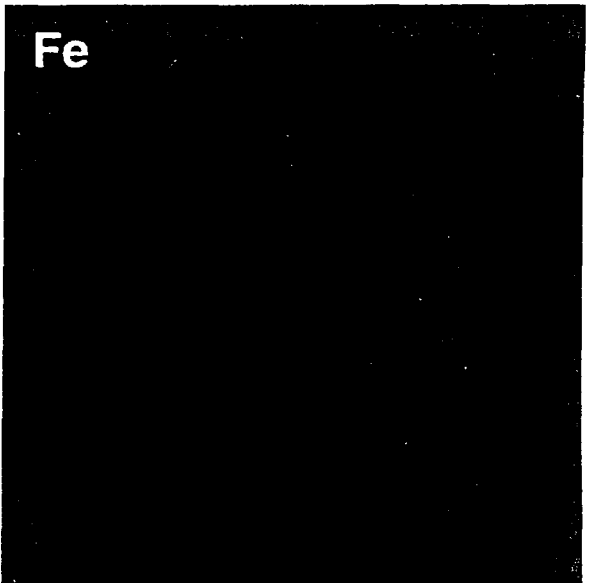
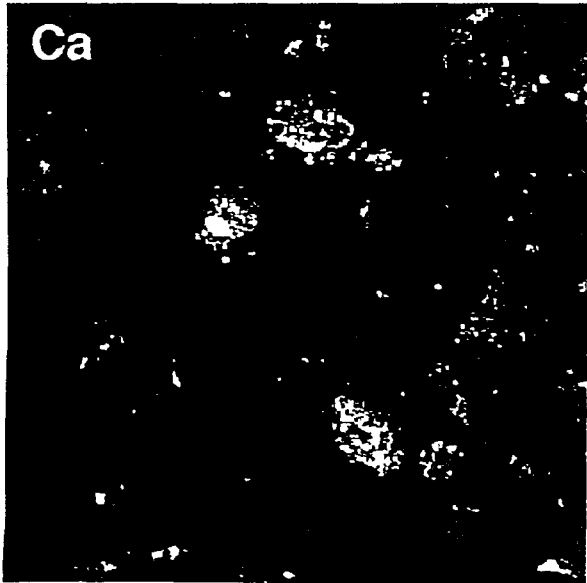
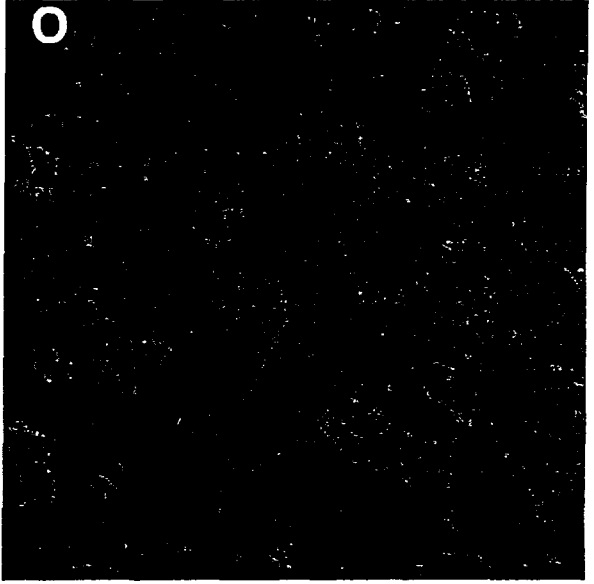
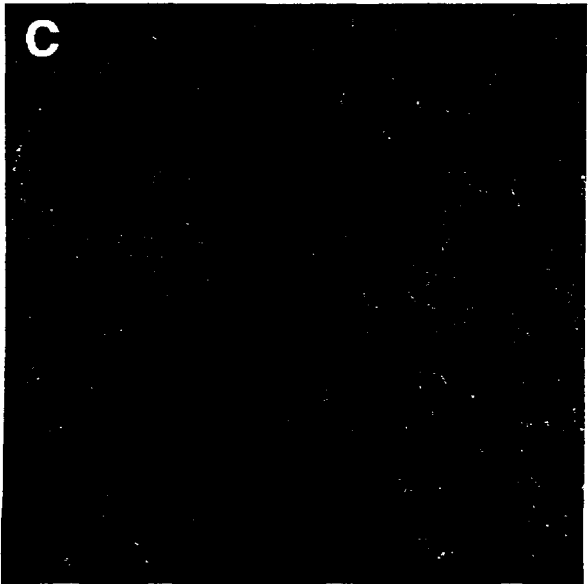
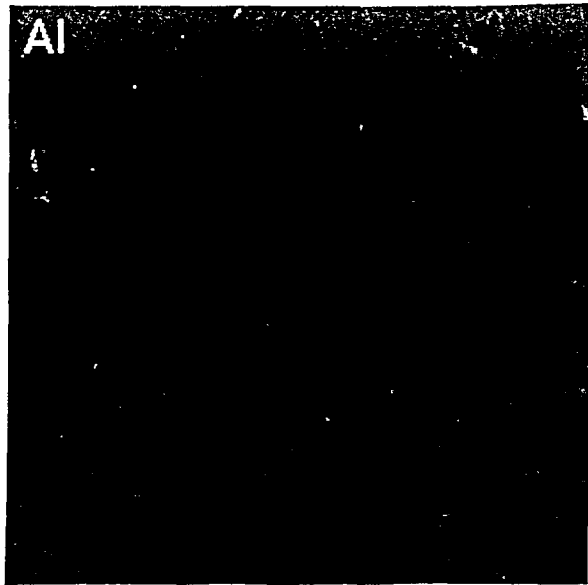


Figure 3:10. X-ray compositional maps (corresponding to field-of-view in Fig. 3:9) showing distribution of Al, Si, C, O, Ca, and Fe in treated PECO soil.

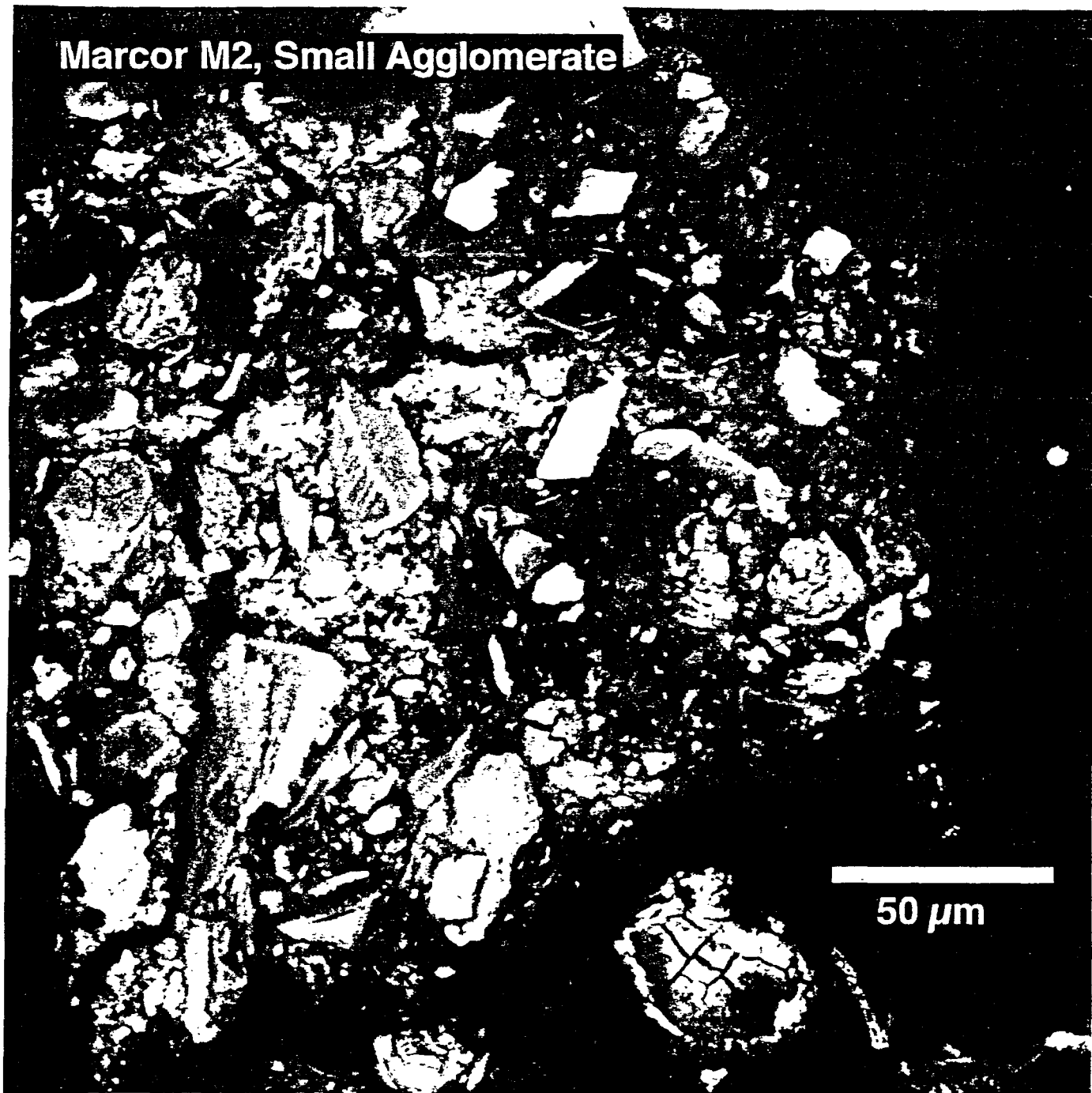
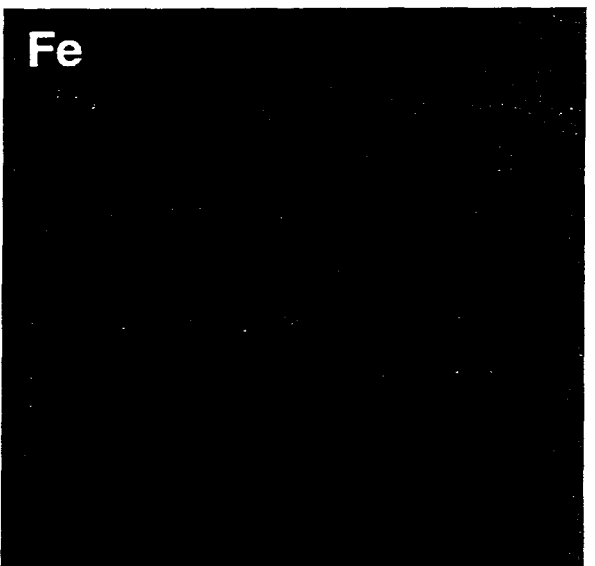
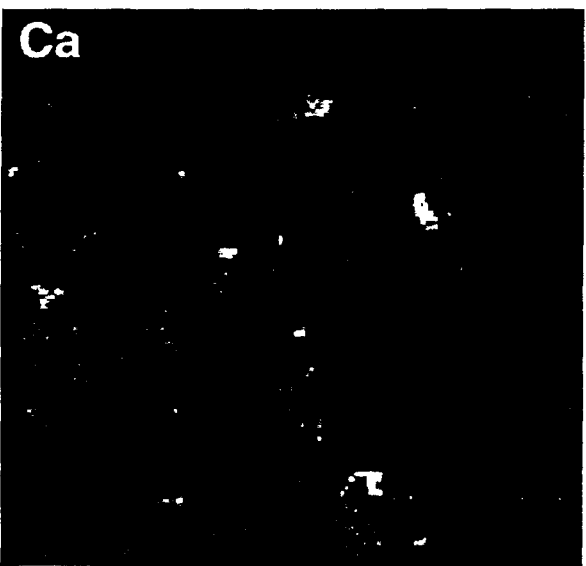
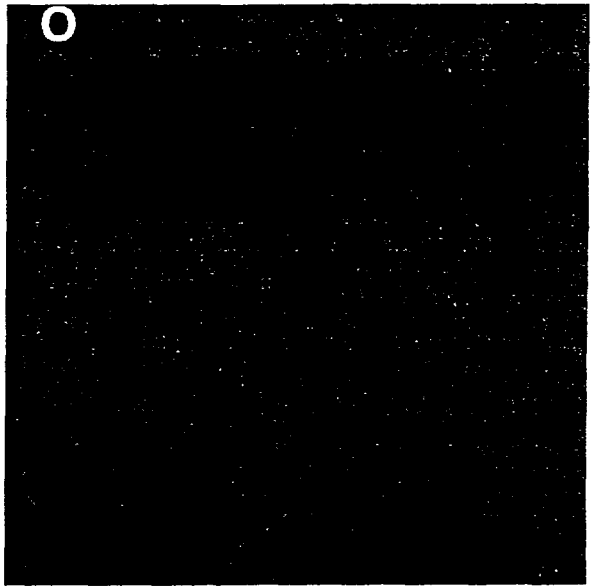
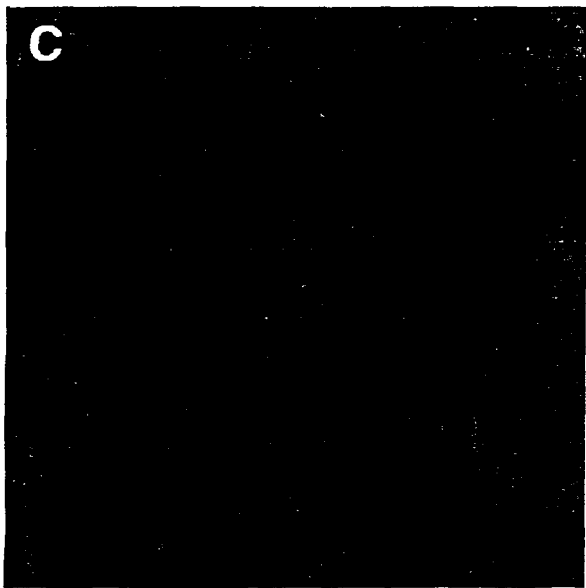
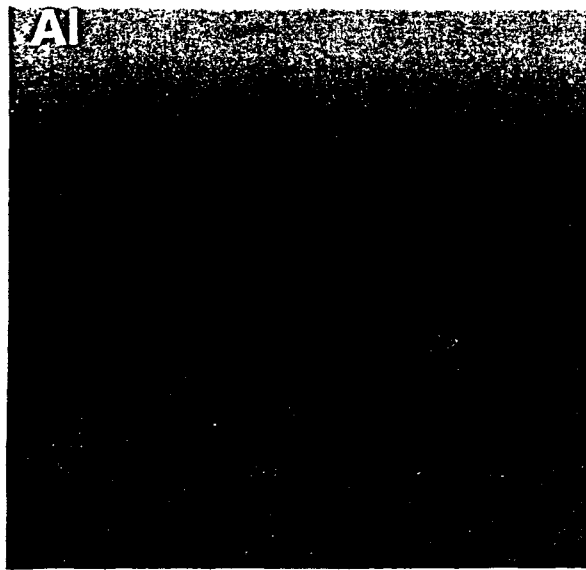


Figure 3:11. Backscattered electron image of a small agglomerate in treated PECO soil (see also Fig. 3:12 overleaf).



**Figure 3:12.** X-ray compositional maps (corresponding to field-of-view in Fig. 3:11) showing distribution of Al, Si, C, O, Ca, and Fe in small agglomerate in treated PECO soil. Note that whereas (organic) C is the major matrix constituent of agglomerates in the untreated soil (see Figs. 3:4 through 3:7), this Figure shows that a Ca-rich phase (Ca carbonate) has replaced/infiltrated the organic carbon.

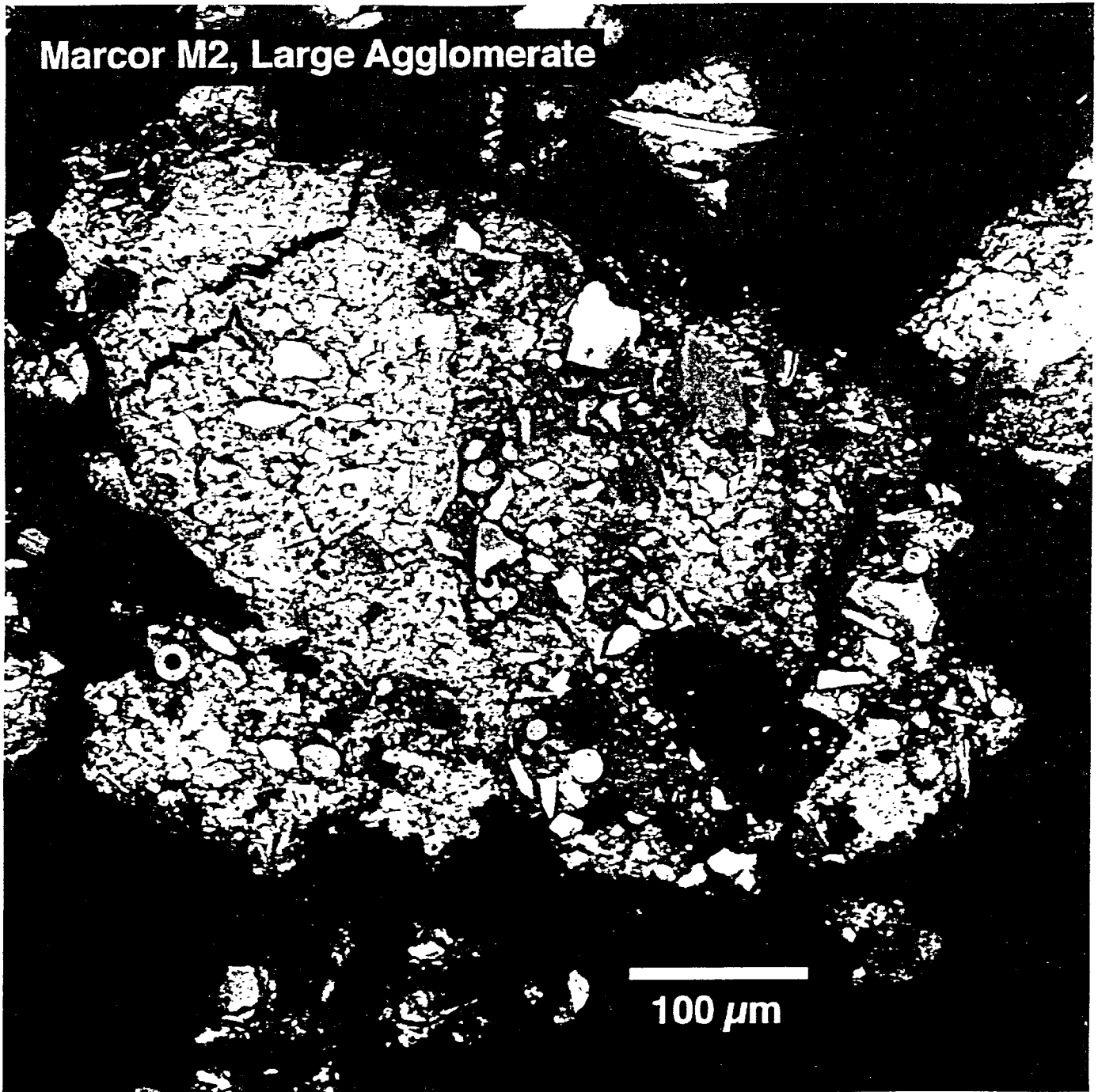
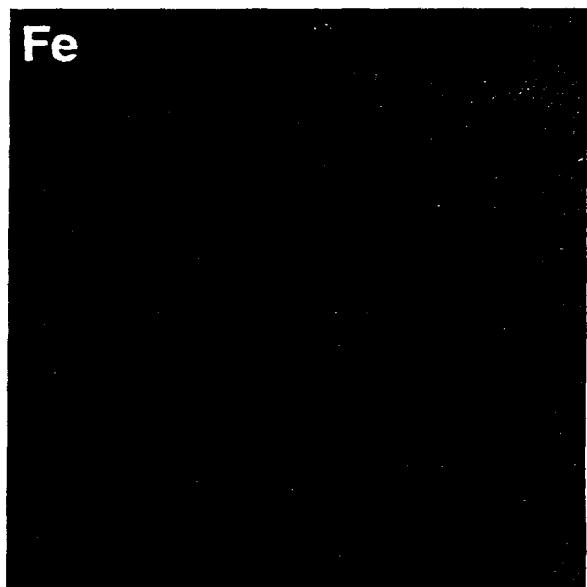
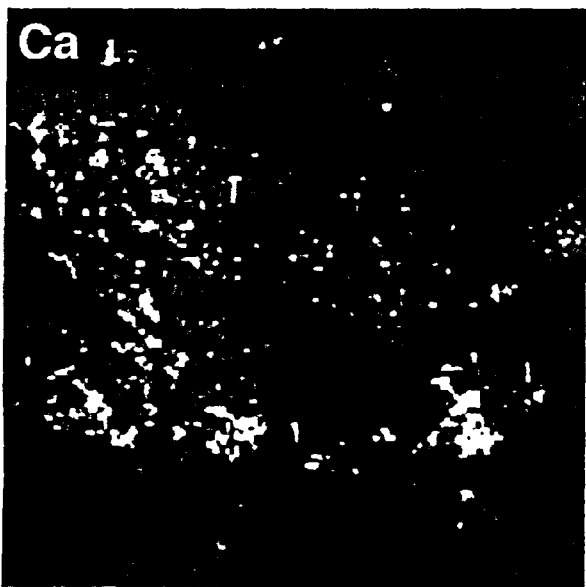
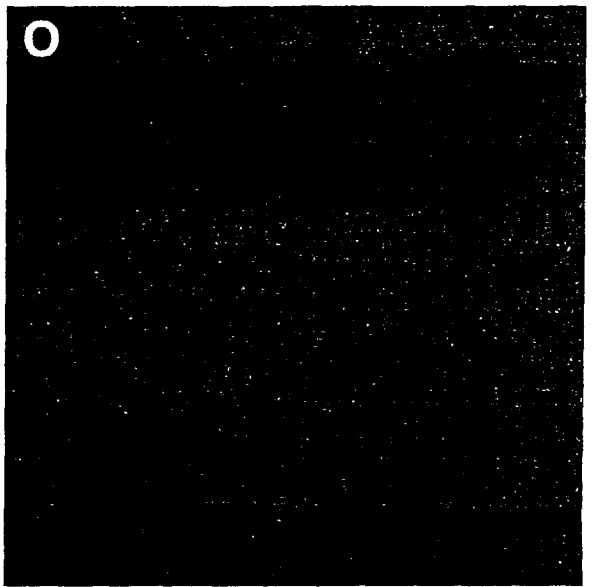
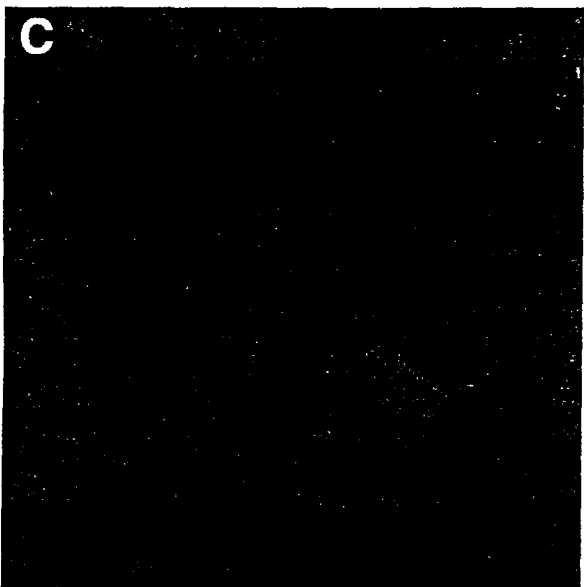
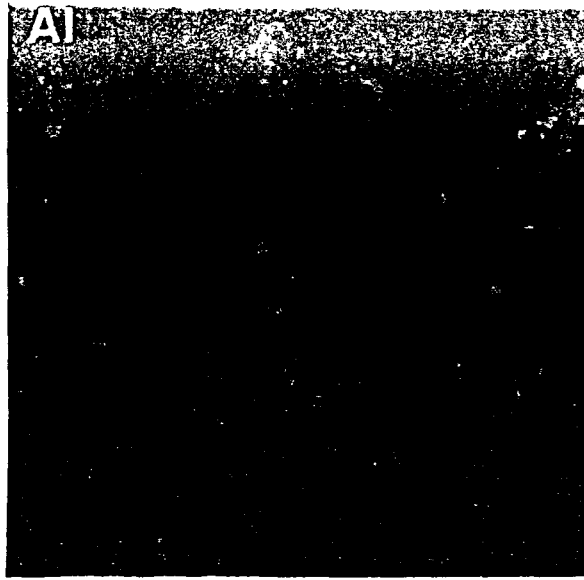
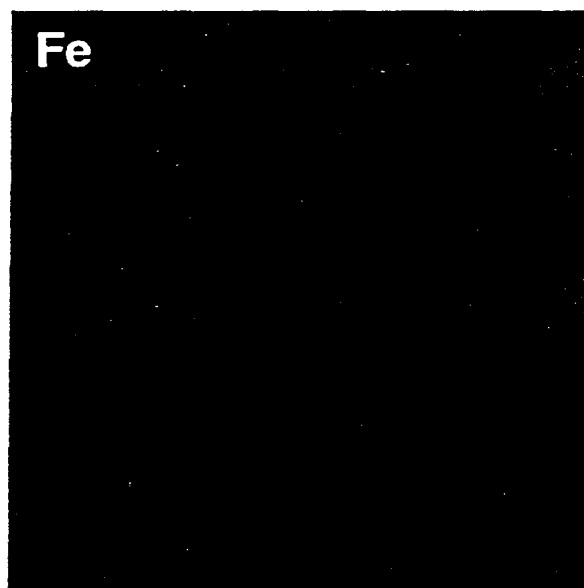
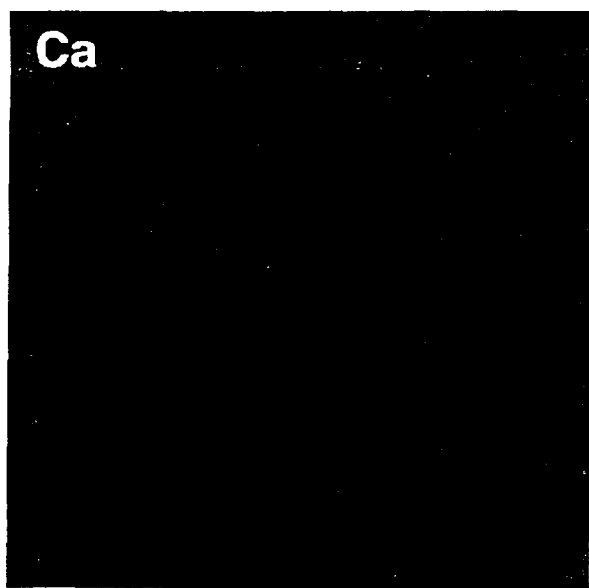
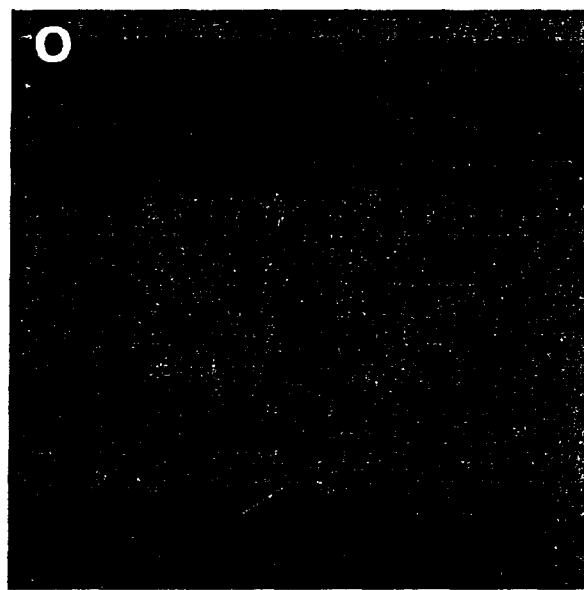
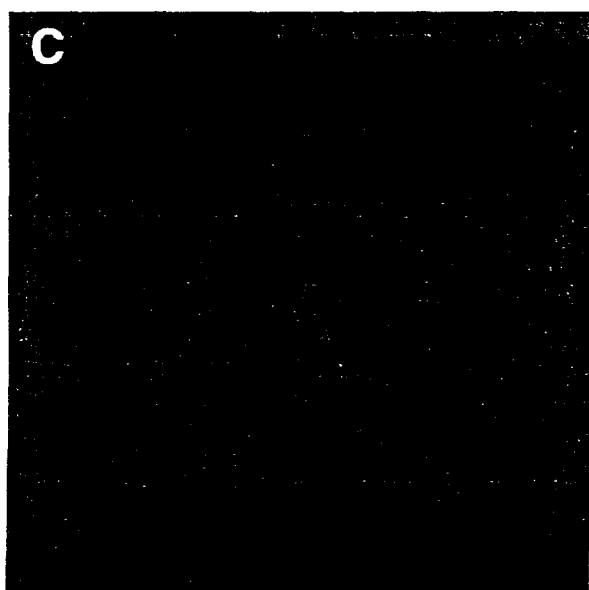
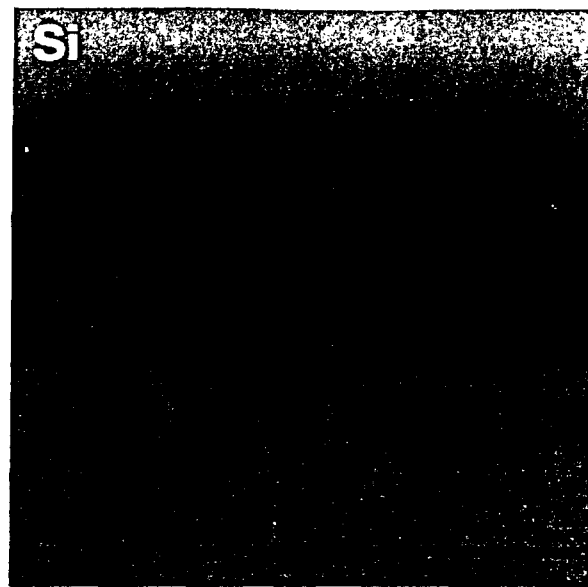
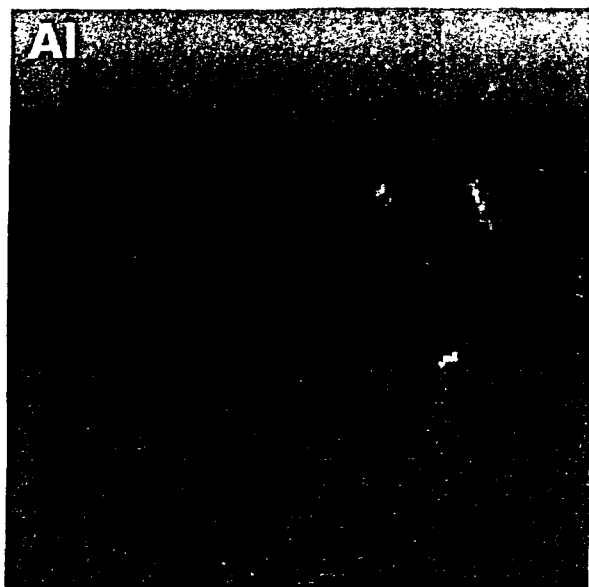


Figure 3:13. Backscattered electron image of a large agglomerate particle in treated PECO soil (see also Fig. 3:14 overleaf).



**Figure 3:14.** X-ray compositional maps (corresponding to the field-of-view in Fig. 3:13) showing distribution of Al, Si, C, O, Ca, and Fe in large agglomerate in treated PECO soil. Note the infiltration of Ca-rich carbonate into the organic matrix of the agglomerate.



**Figure 3:16.** X-ray compositional maps (corresponding to field-of-view in Fig. 3:15) showing distribution of Al, Si, C, O, Ca and Fe in the groundmass agglomerate in treated PECO soil.

**Marcor M2, Agglomerate Groundmass 2**

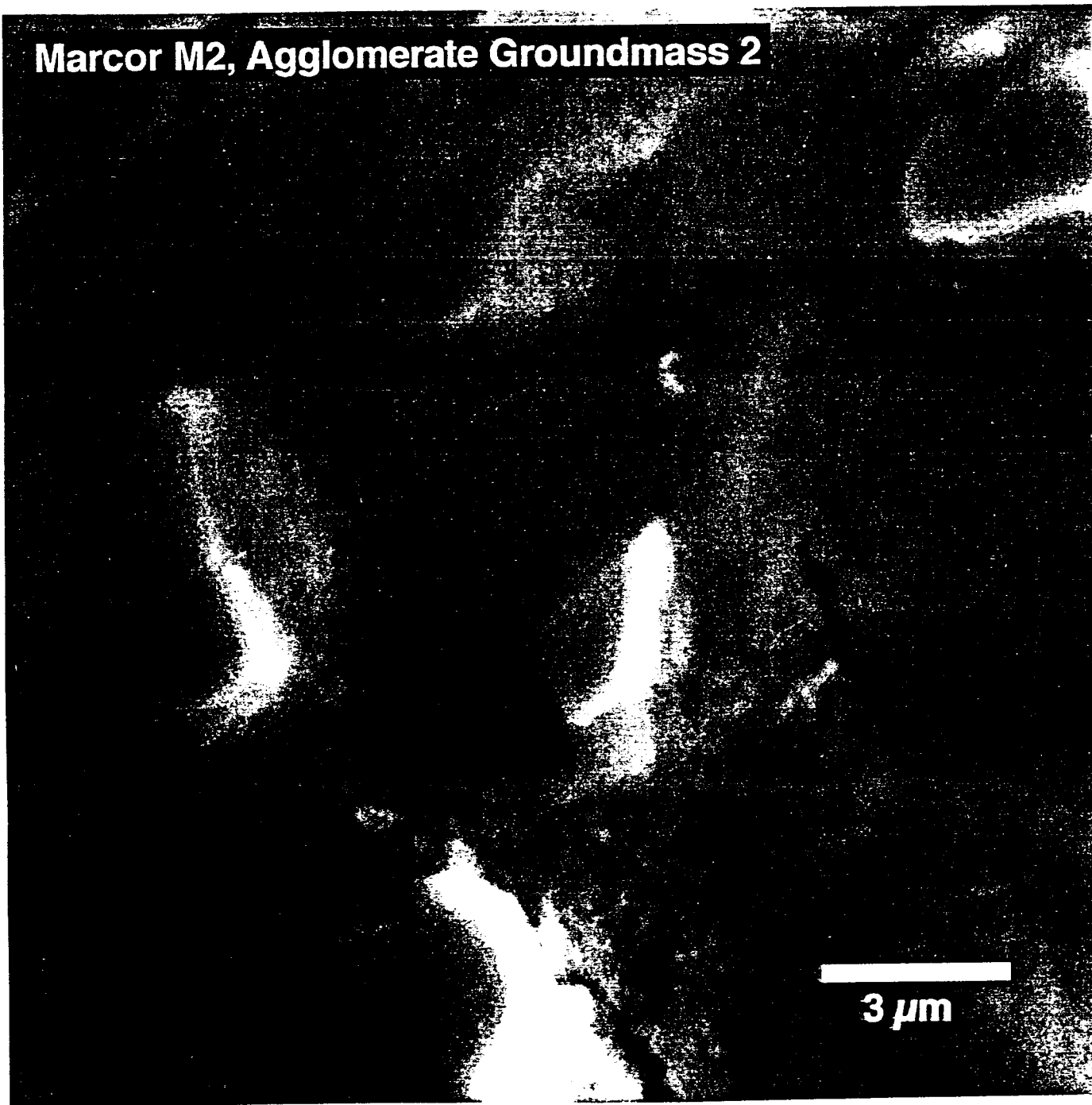


**Figure 3:15.** High-magnification backscattered electron image of the ultrafine-grained groundmass (matrix) of an agglomerate particle in treated PECO soil. Euhedral inclusions are mineral grains (See also Fig. 3:16 overleaf).

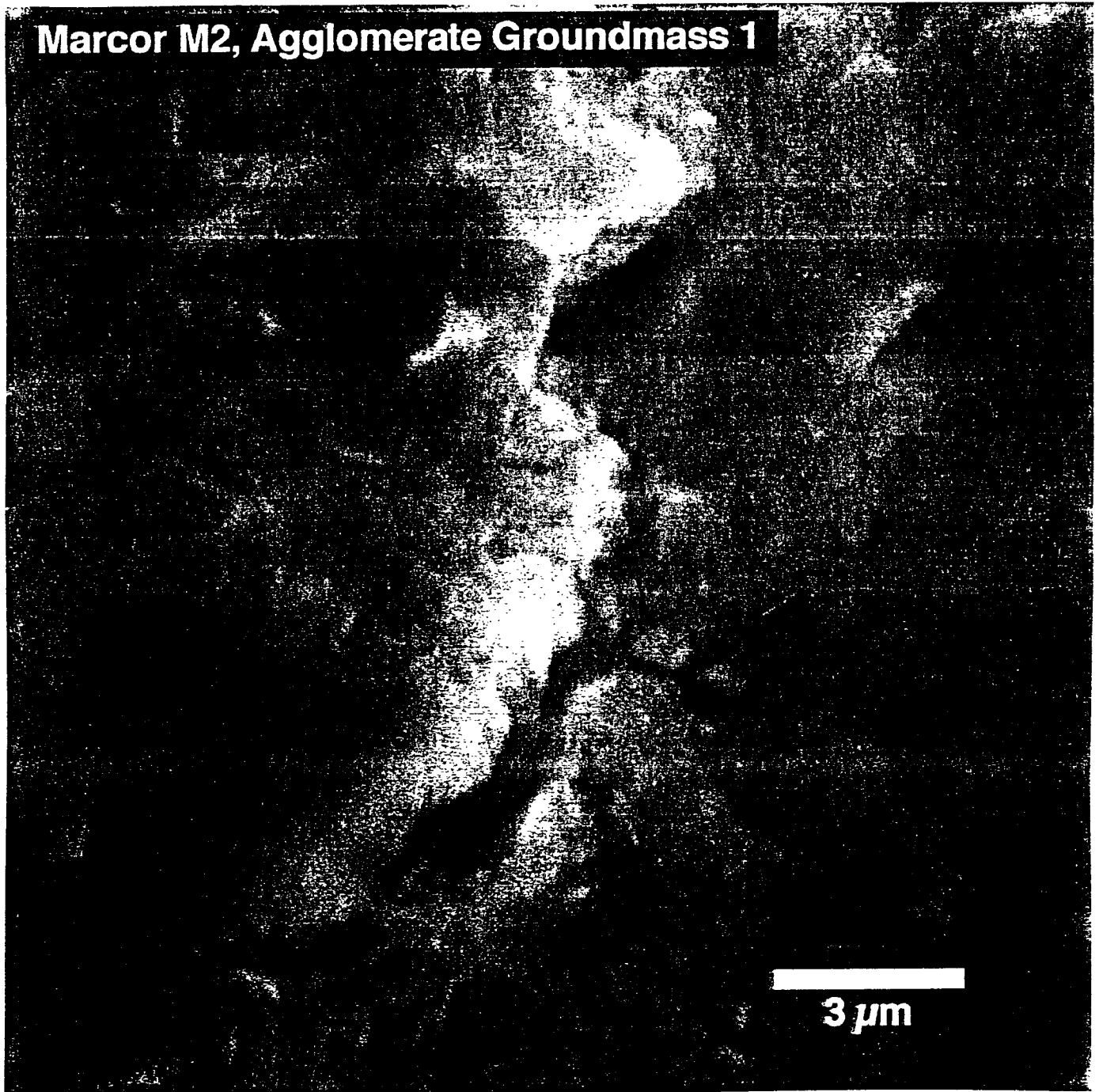


**Figure 3:17.** Backscattered electron image of groundmass in agglomerate in treated PECO soil (see also Fig. 3:18 overleaf).

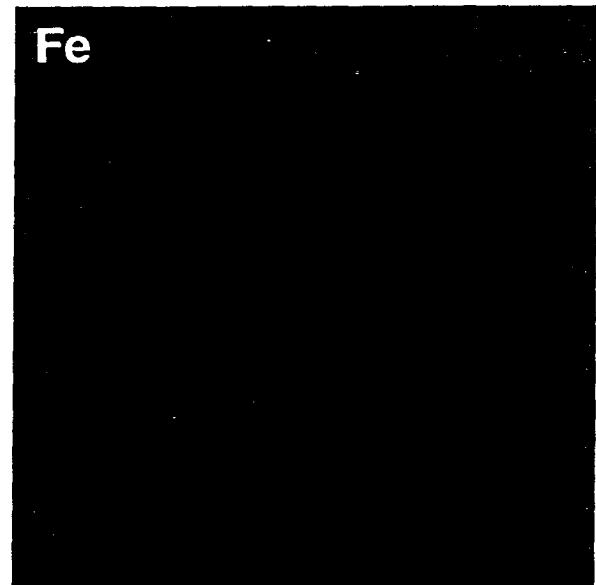
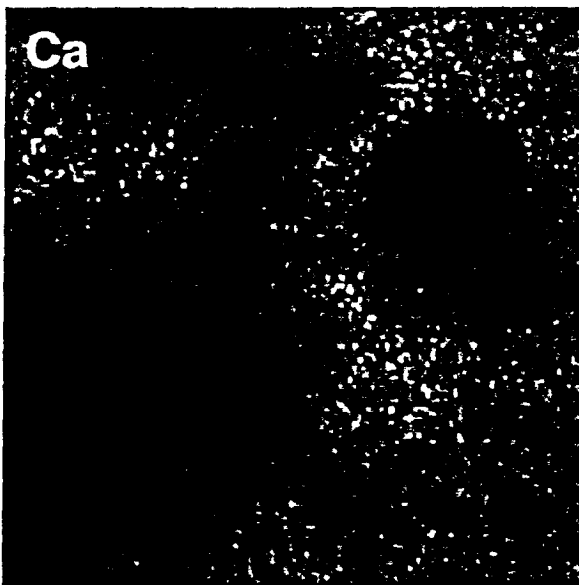
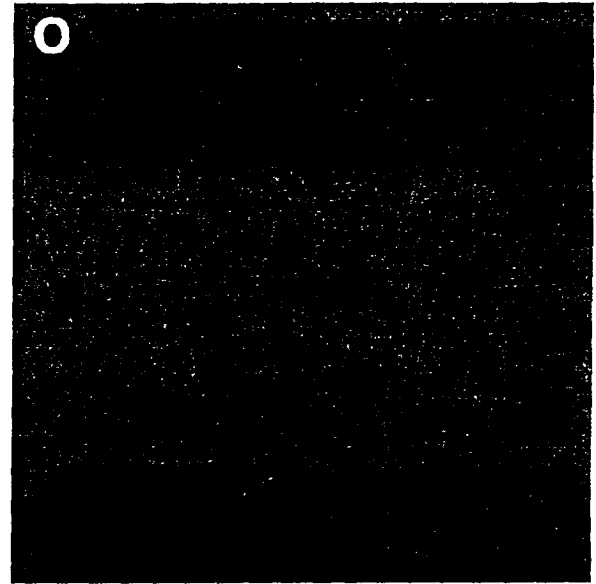
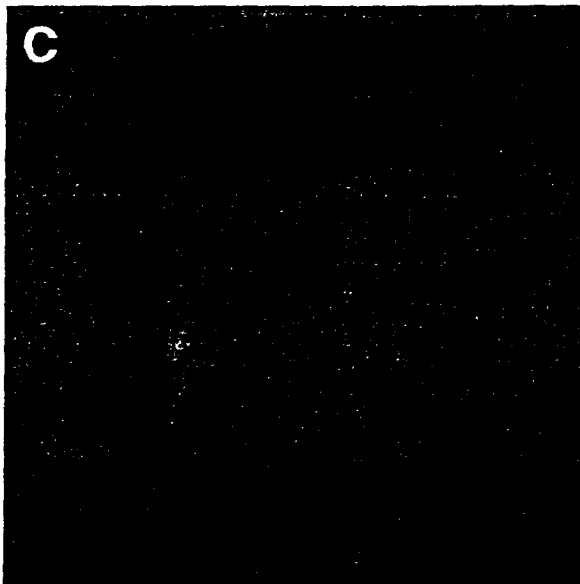
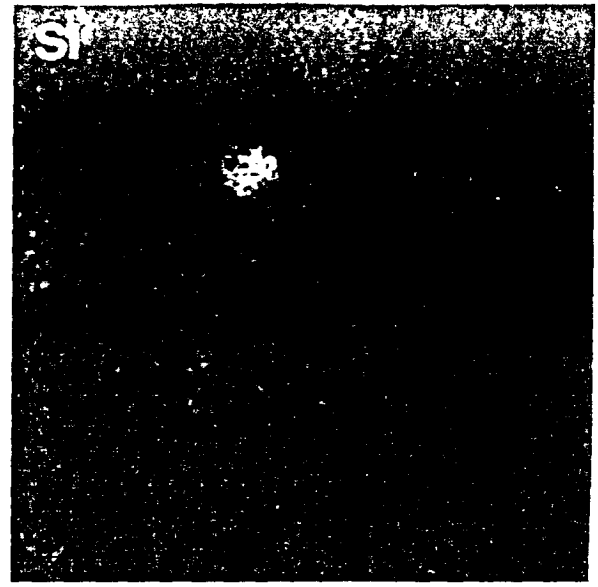
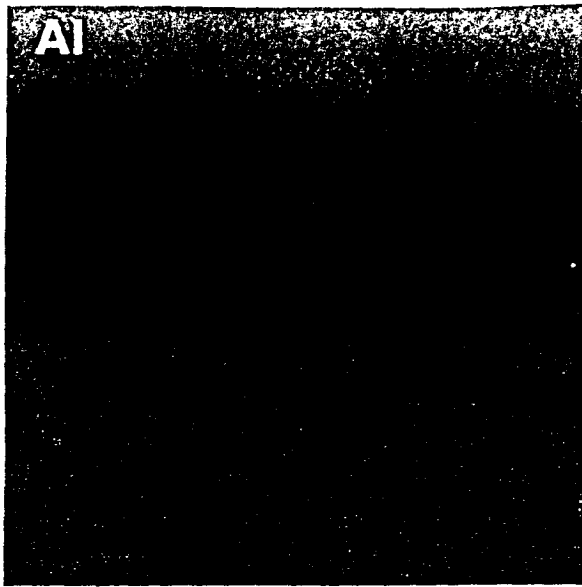
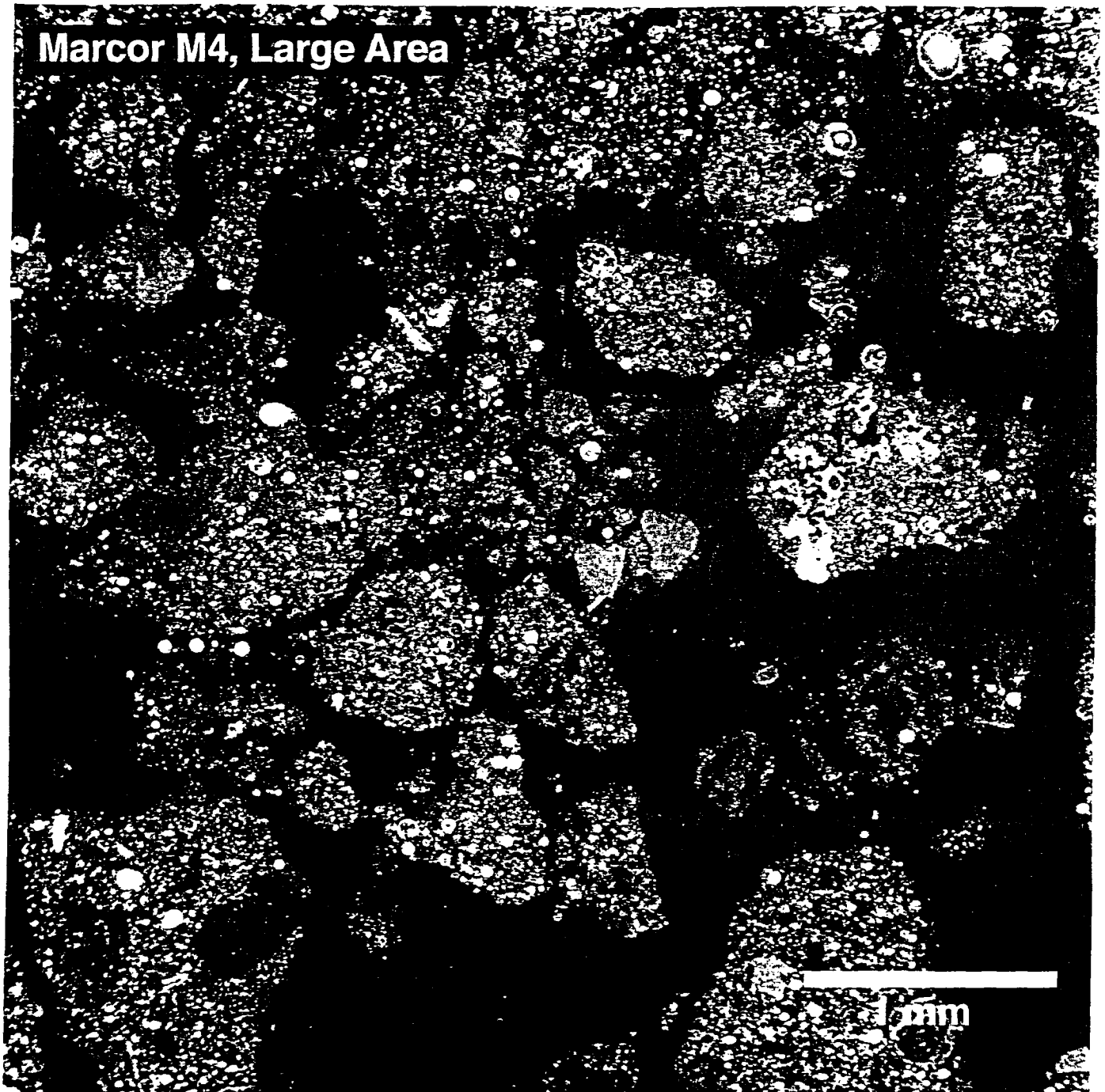
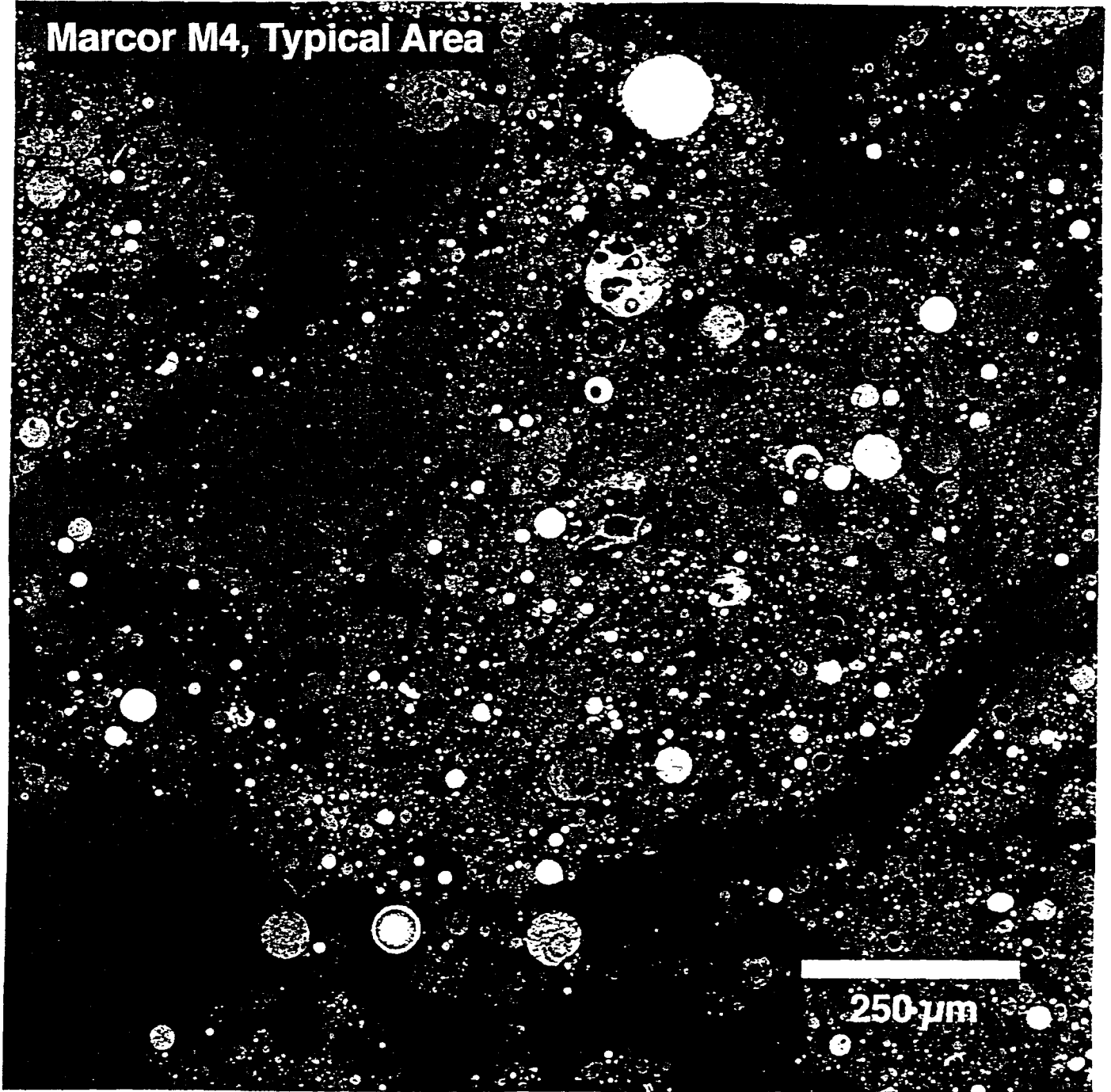


Figure 3:18. X-ray compositional maps (corresponding to field-of-view in Fig. 3:17) showing distribution of Al, Si, C, O, Ca and Fe in groundmass of agglomerate.



**Figure 3:19.** Large area (~5 X 5 mm) field-of-view (backscattered electron image) of polished thick-flat specimen of untreated PECO sludge. In contrast to PECO soil (see Fig. 3:8), the sludge consists predominantly of spherical fly ash embedded in organic carbon.



**Figure 3:20.** Higher magnification image (corresponding to field-of-view in Fig. 3:19) showing typical material in untreated PECO sludge (see also Fig 3:21 overleaf).

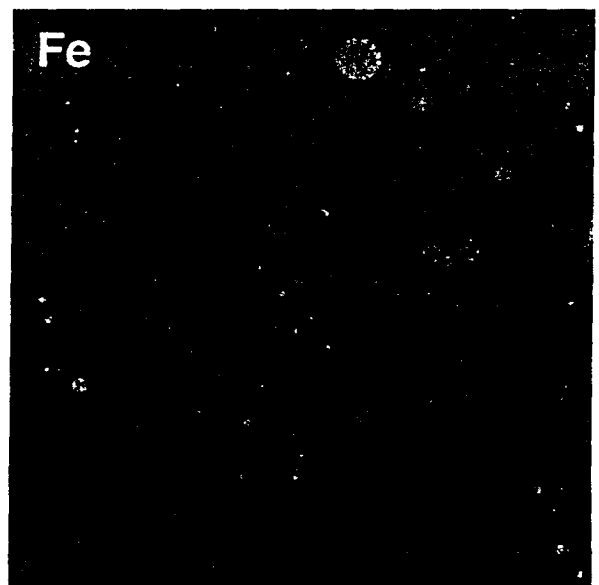
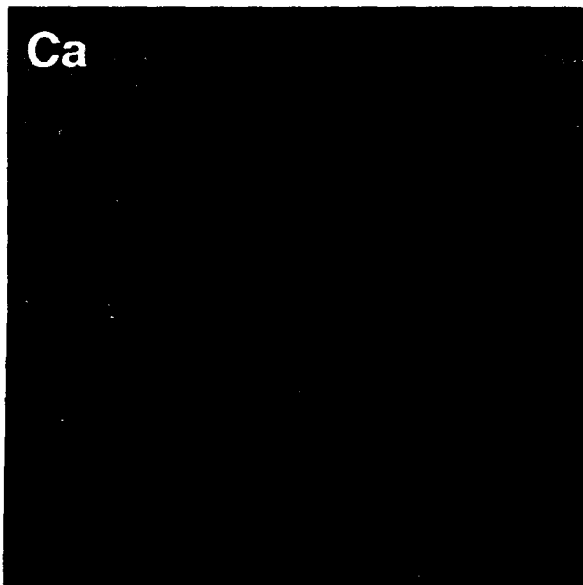
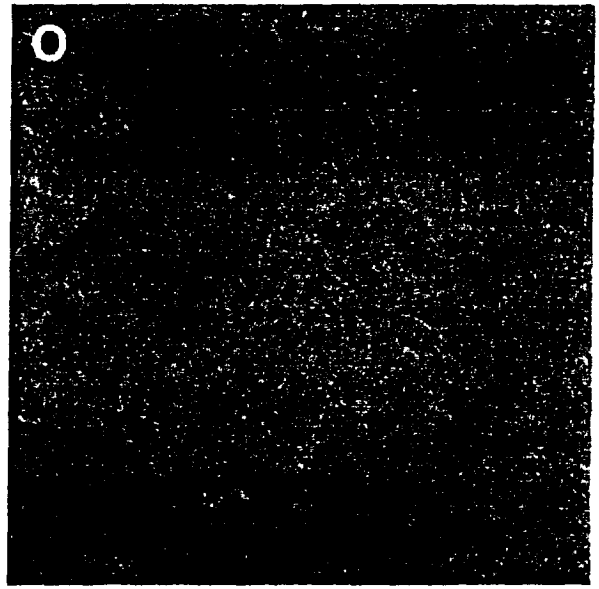
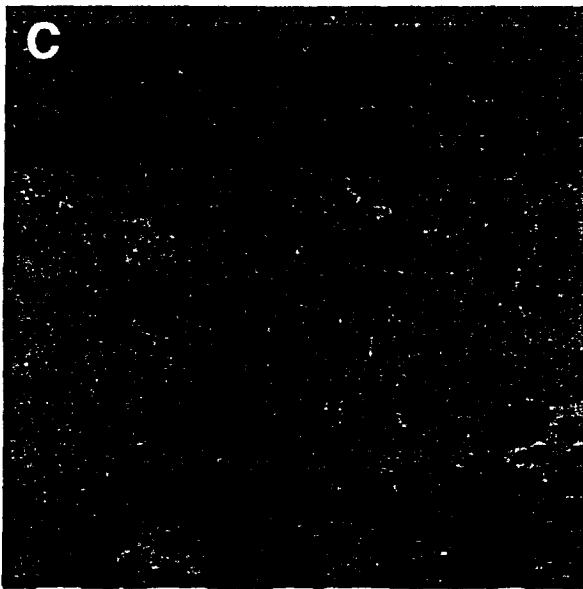
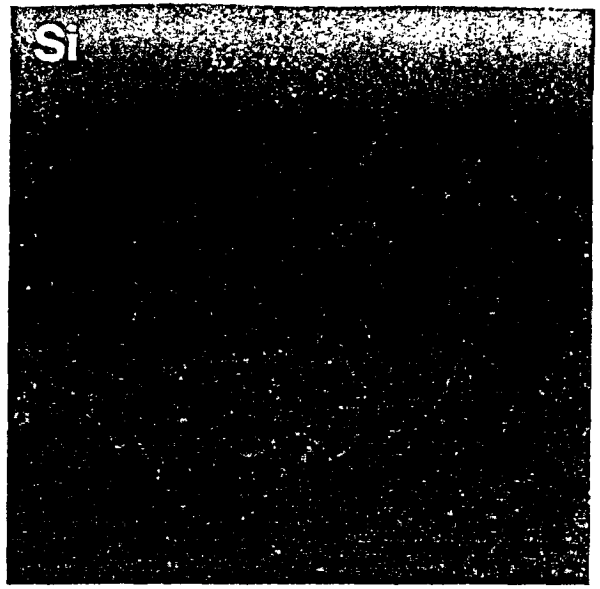
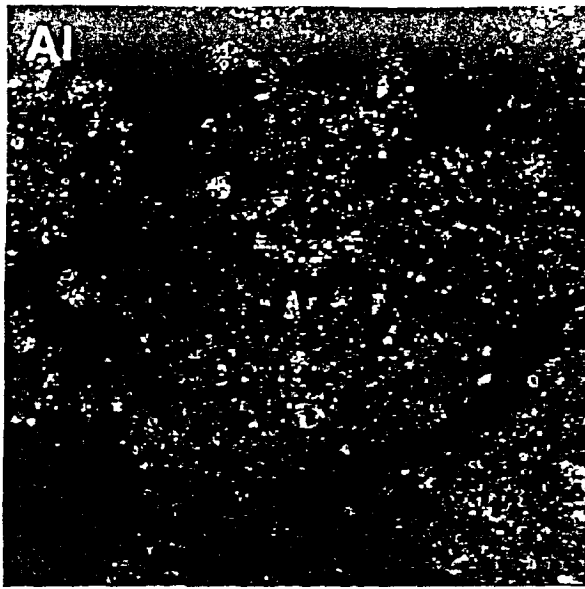


Figure 3:21. X-ray compositional maps showing distribution of Al, Si, C, O, Ca and Fe in untreated PECO sludge.

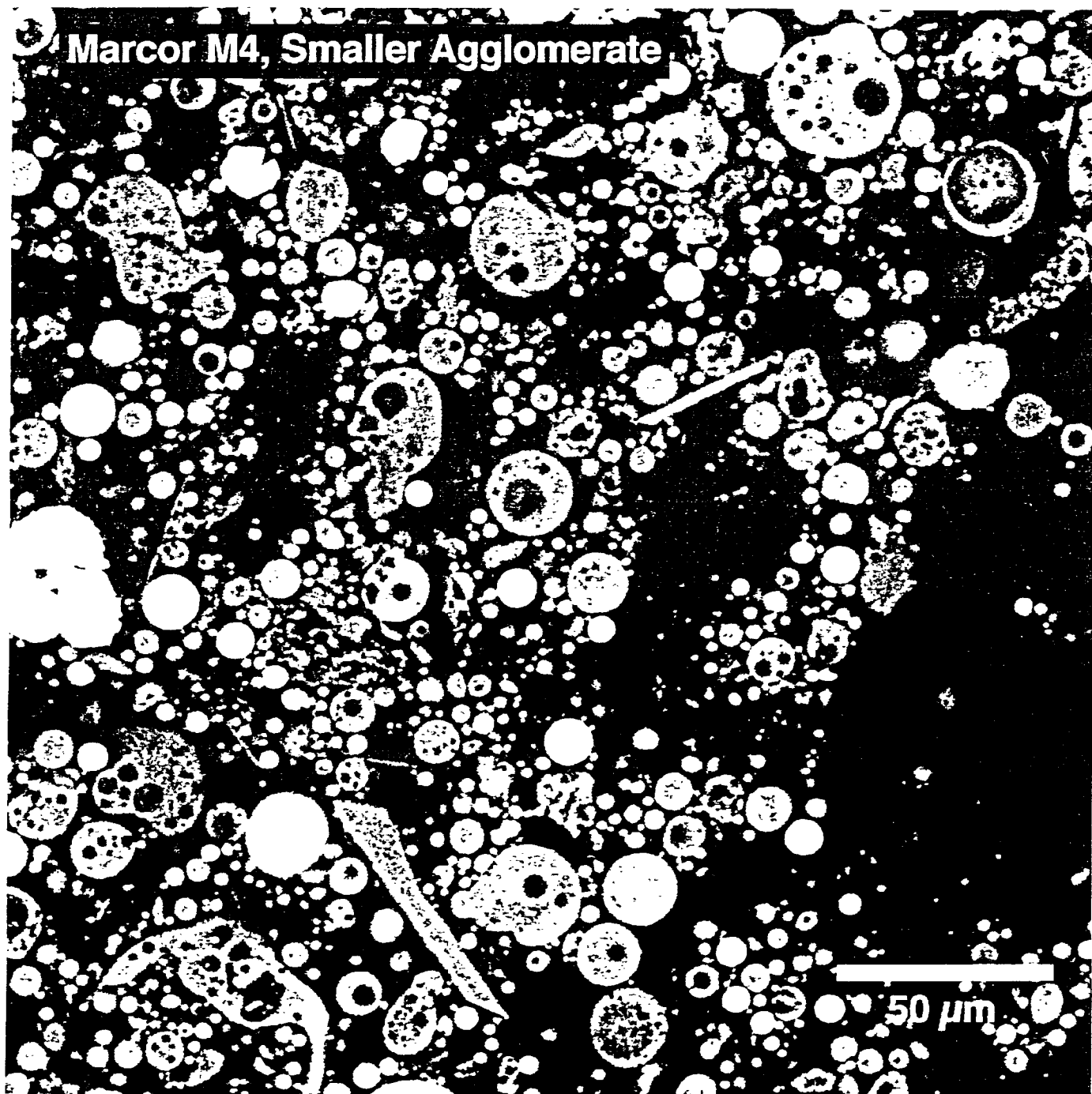
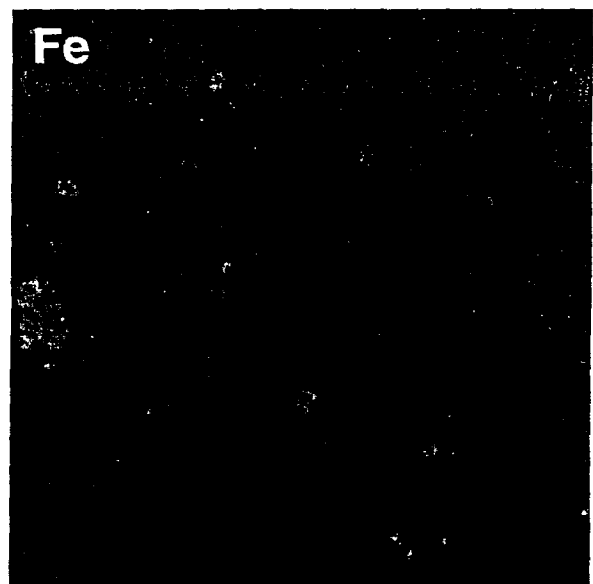
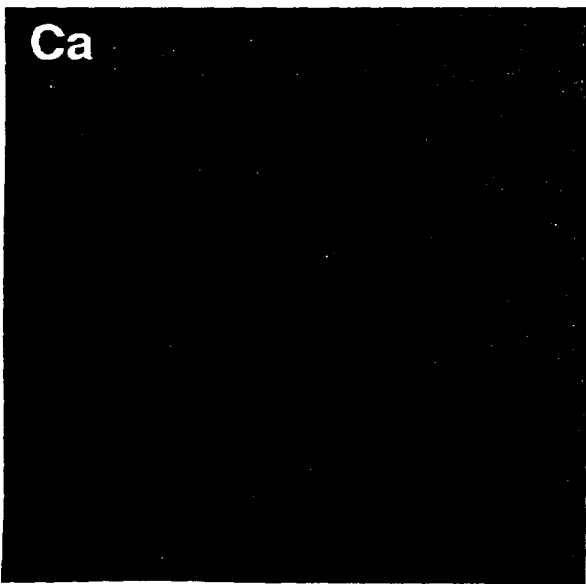
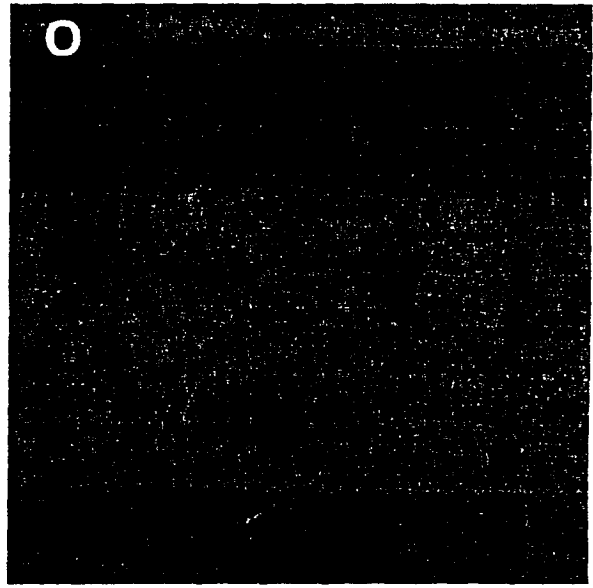
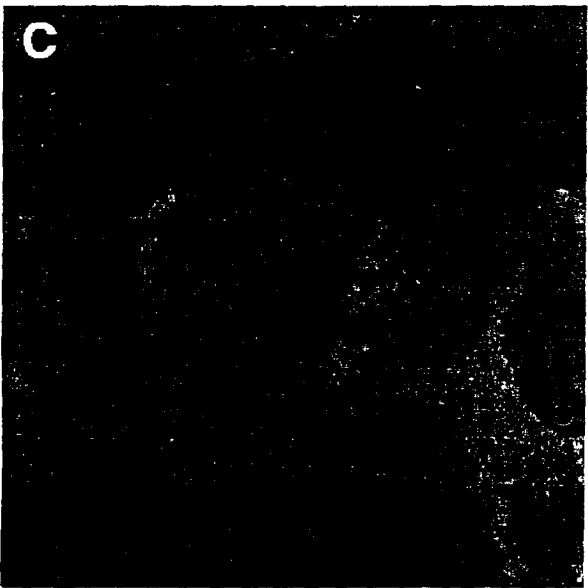


Figure 3:22. Backscattered electron image of small agglomerate particle in untreated PECO sludge (see also Fig. 3:23 overleaf).



**Figure 3:23.** X-ray compositional maps (corresponding to field-of-view in Fig. 3:22) showing distribution of Al, Si, C, O, Ca and Fe in small agglomerate in small untreated sludge agglomerate.

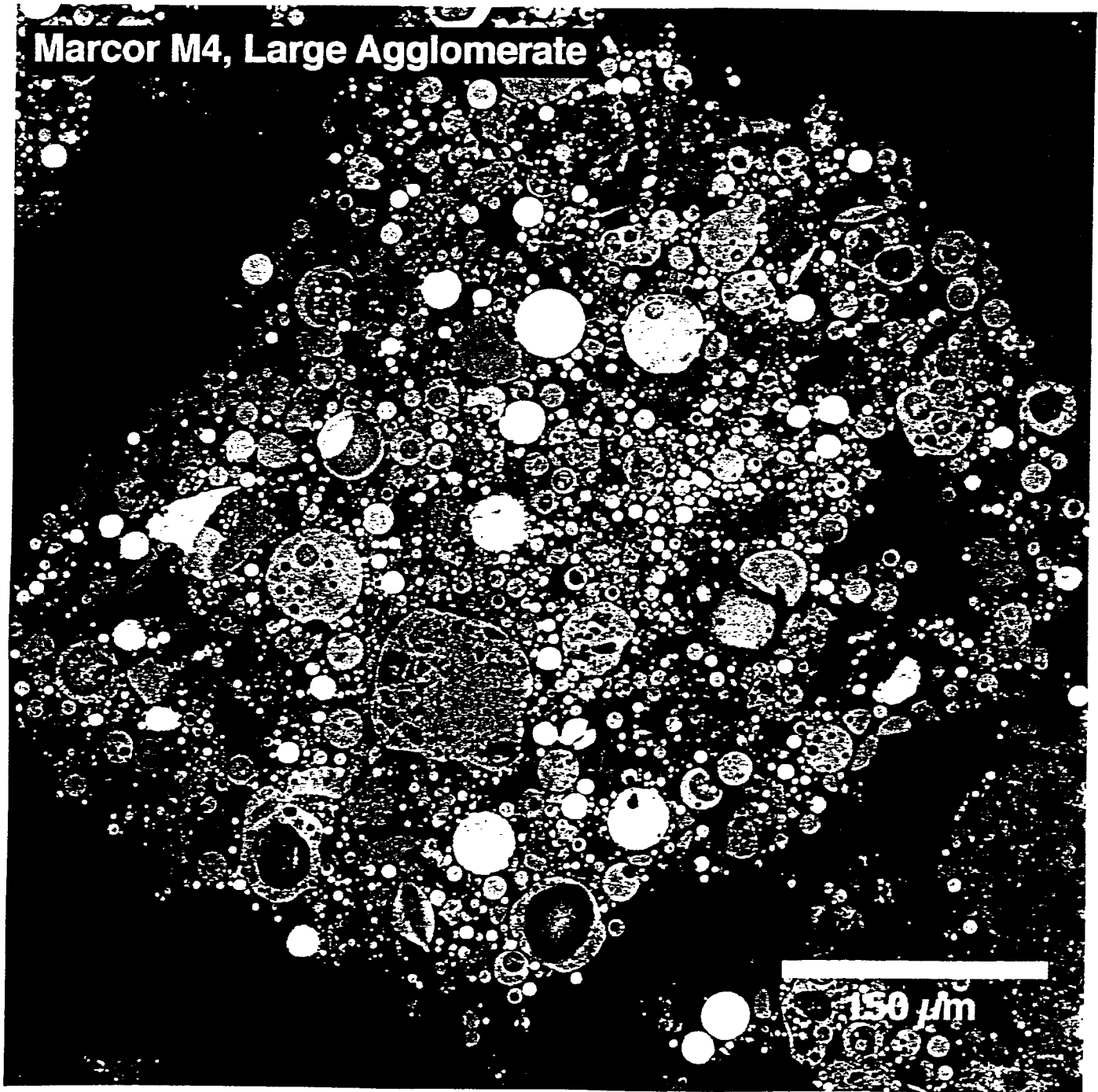
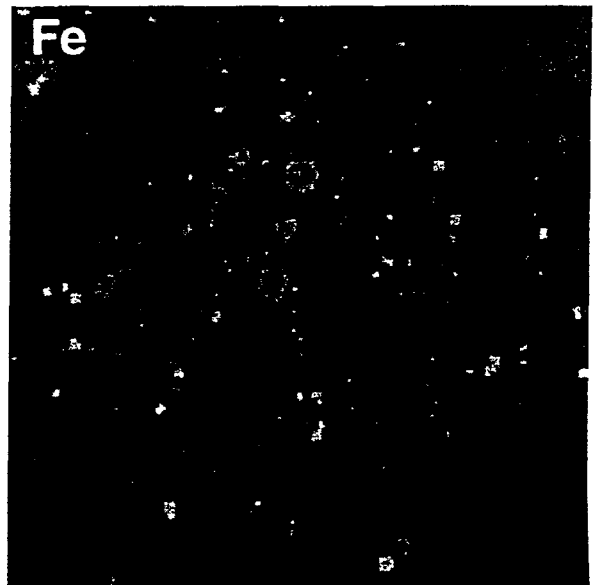
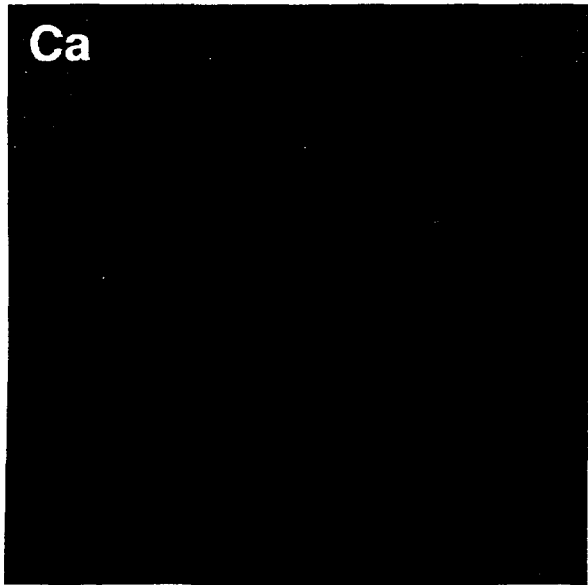
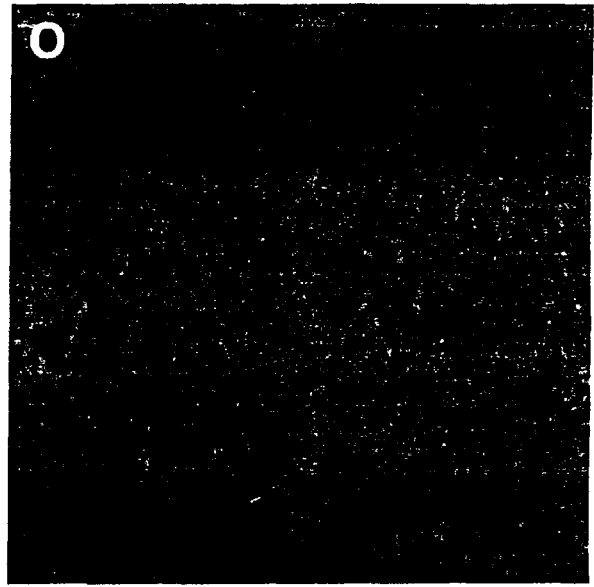
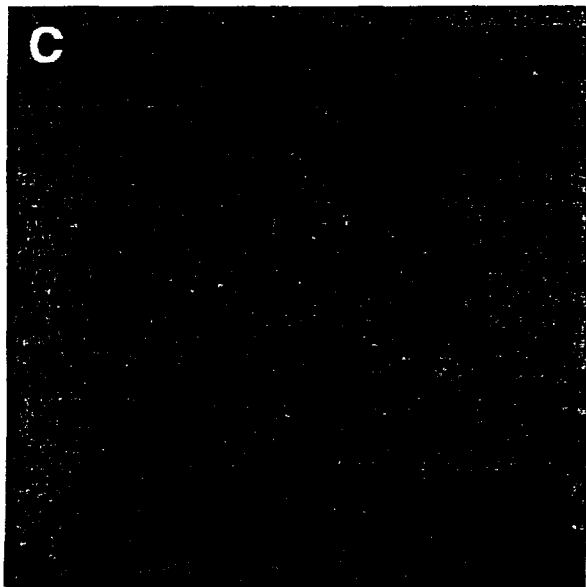
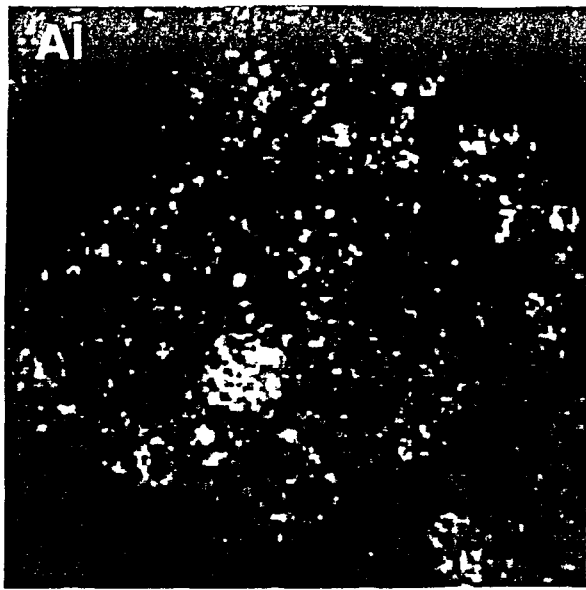
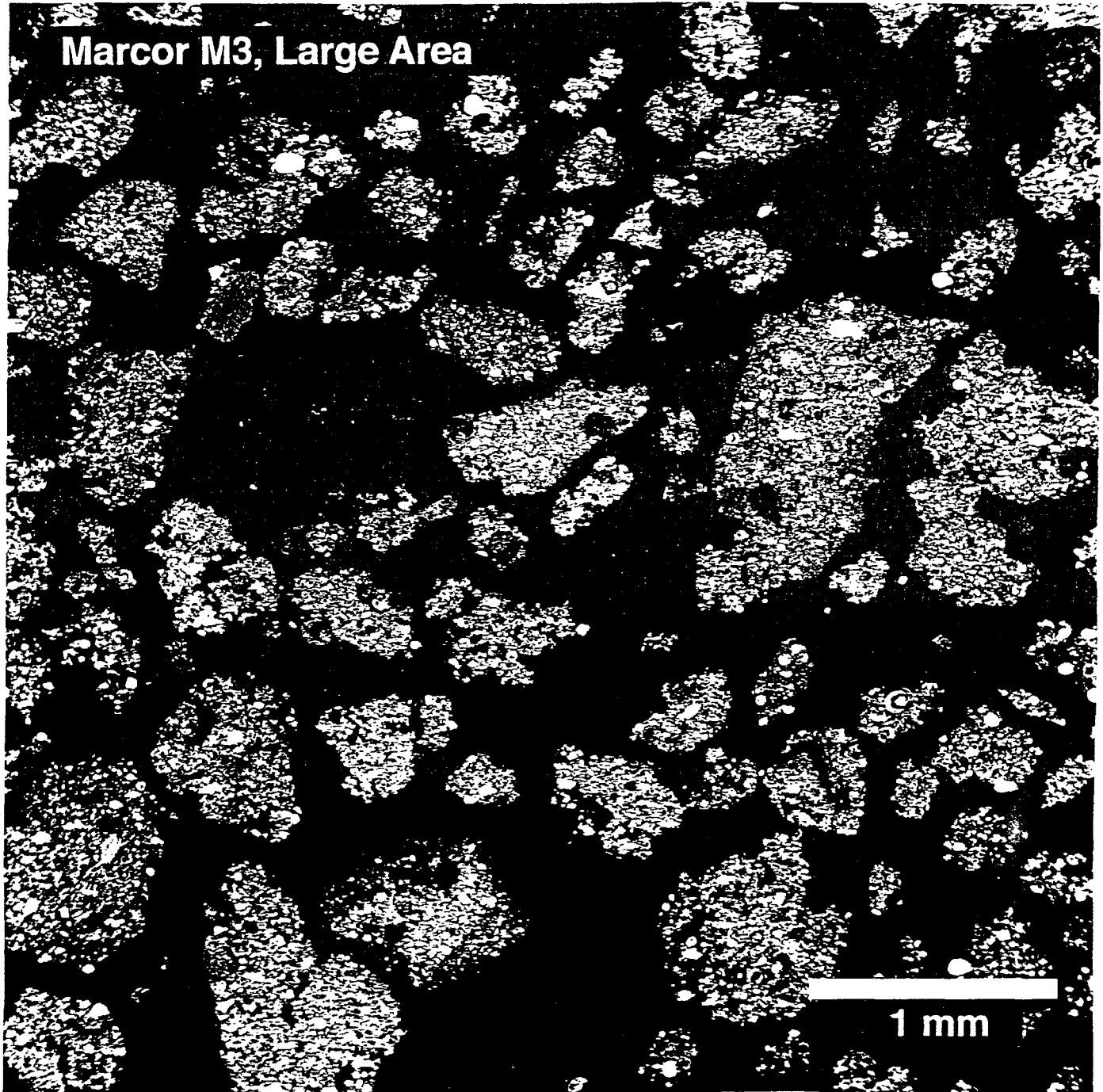


Figure 3:24. Backscattered electron image of large agglomerate particle in untreated PECO sludge (see also Fig. 3:25 overleaf).



**Figure 3:25.** X-ray compositional maps (corresponding to field-of-view in Fig. 3:24) showing distribution of Al, Si, C, O, Ca and Fe in large agglomerate in untreated PECO sludge.



**Figure 3:26.** Large area (~5 X 5 mm) field-of-view (backscattered electron image) of polished thick-flat specimen of treated PECO sludge.

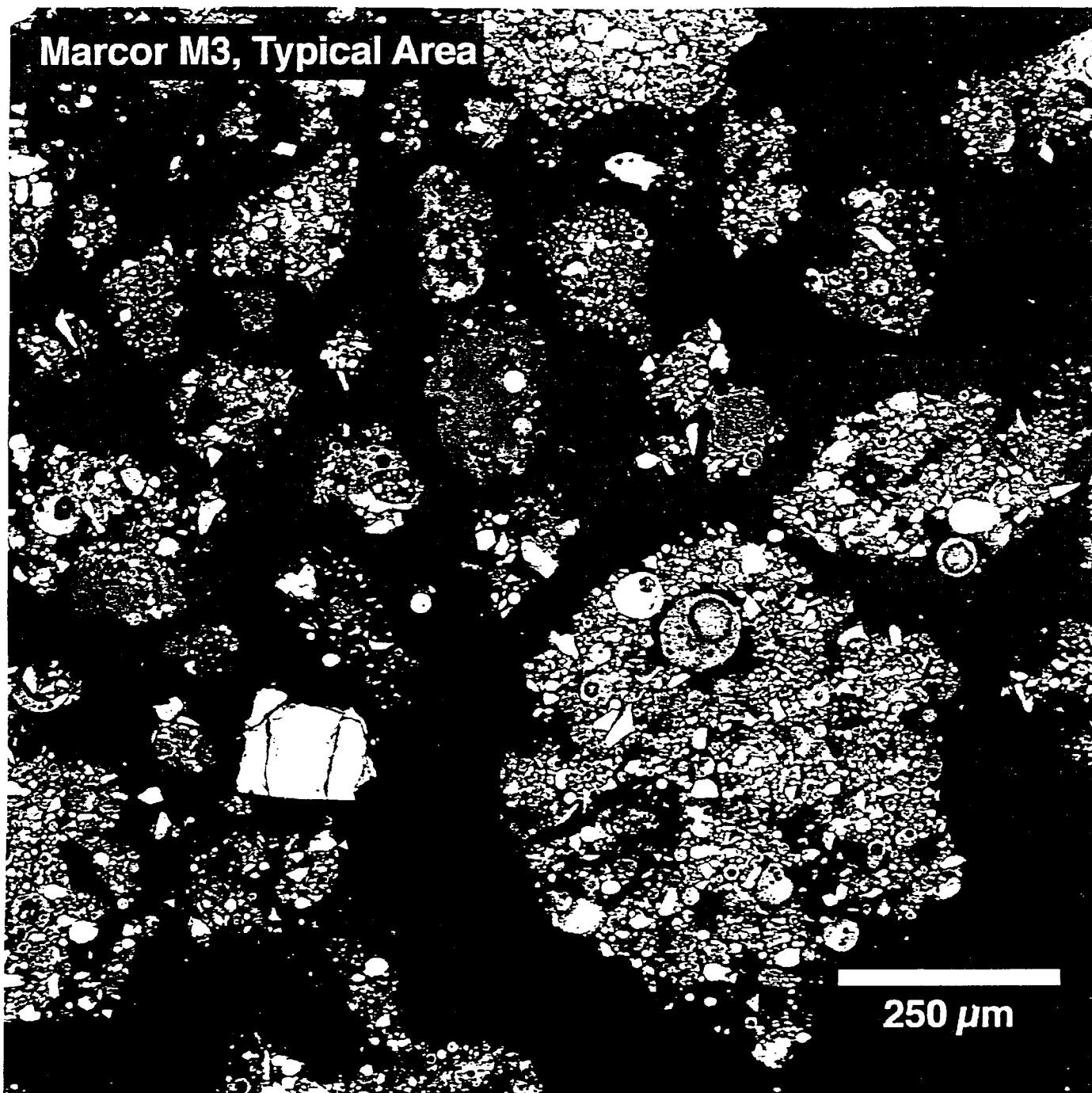
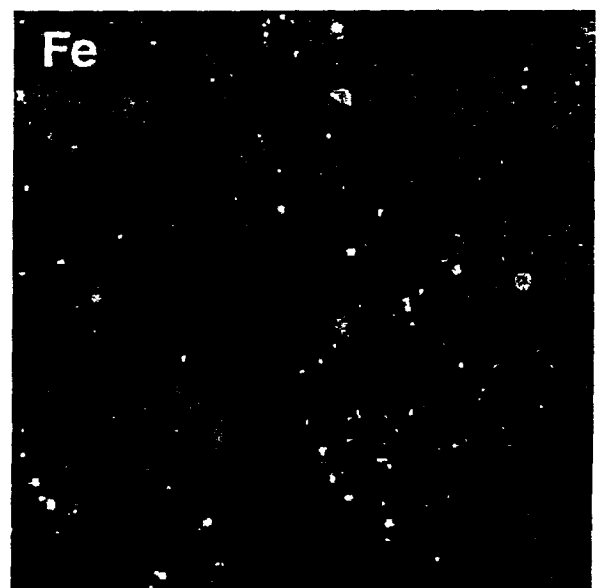
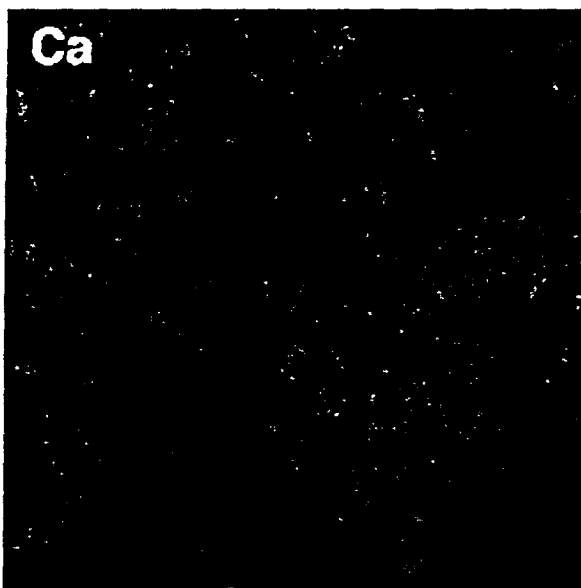
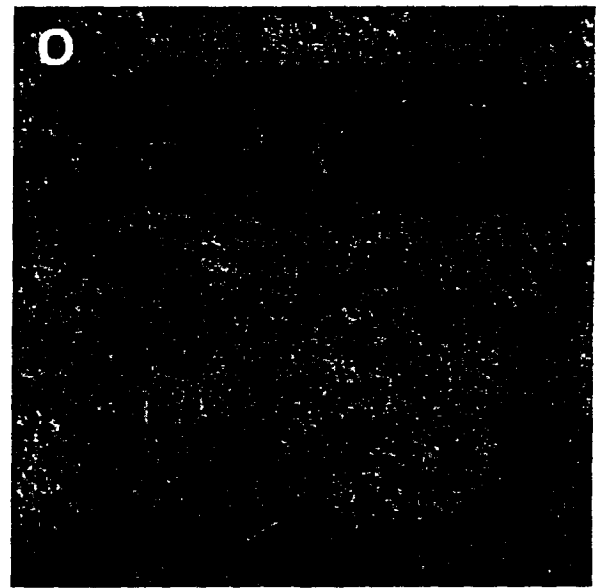
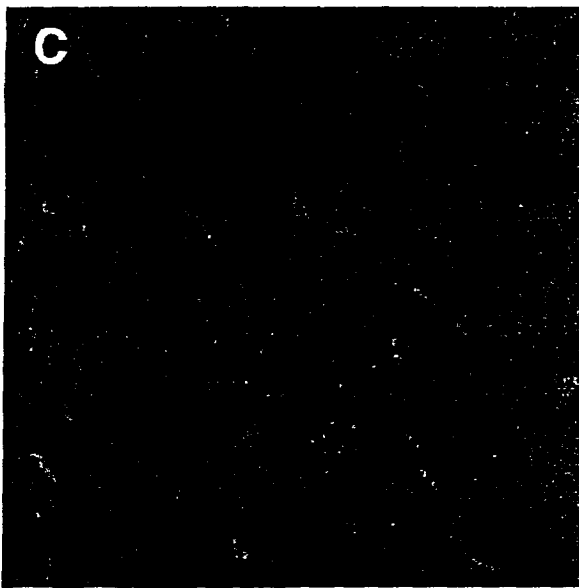
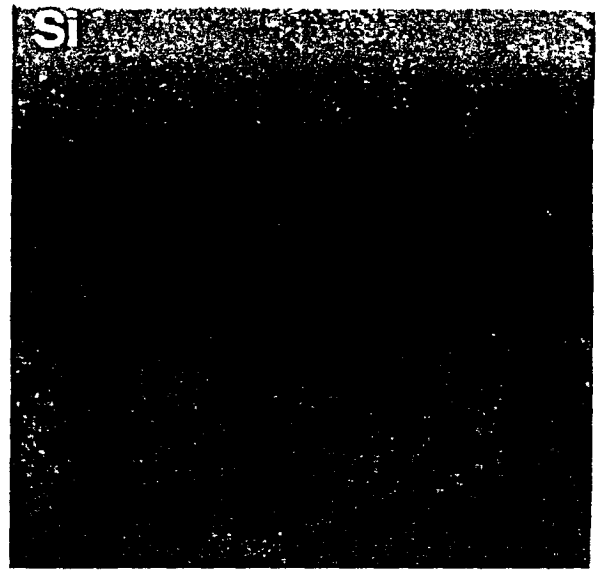
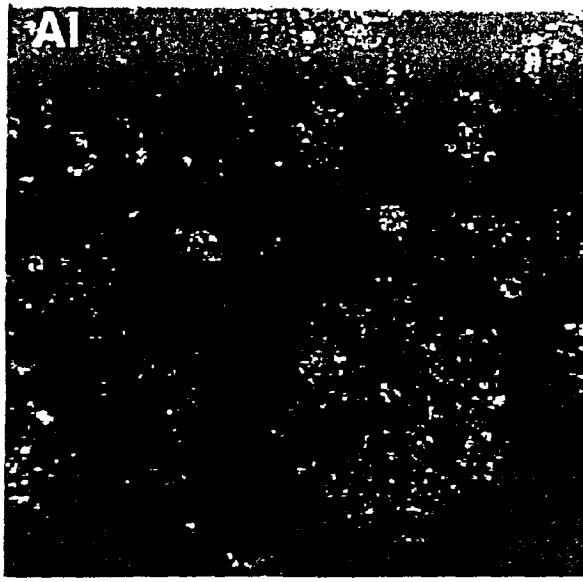


Figure 3:27. Backscattered electron image of typical constituents of treated PECO sludge (see also Figure 3:28 overleaf).



**Figure 3:28.** X-ray compositional maps (corresponding to field-of-view in Fig. 3:27) showing distribution of Al, Si, C, O, Ca and Fe in treated PECO sludge. Note the penetration of Ca (as carbonate) into the organic matrices of individual sludge agglomerates.

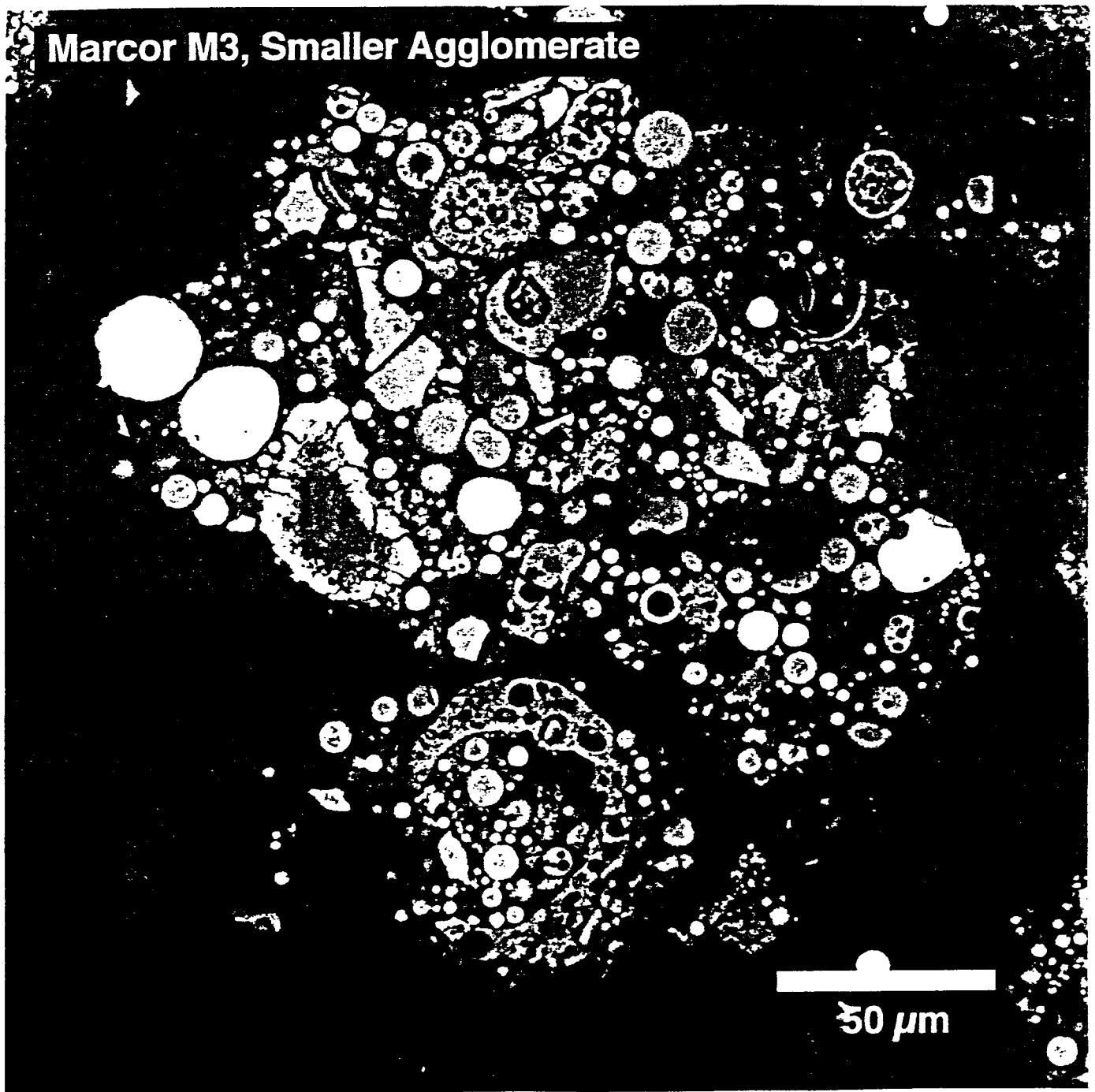


Figure 3:29. Backscattered electron image of a small agglomerate particle in treated PECO sludge (see also Fig. 3:30 overleaf).

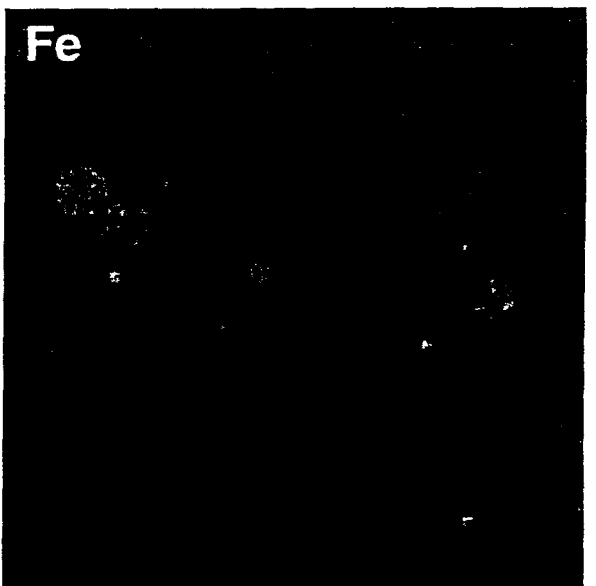
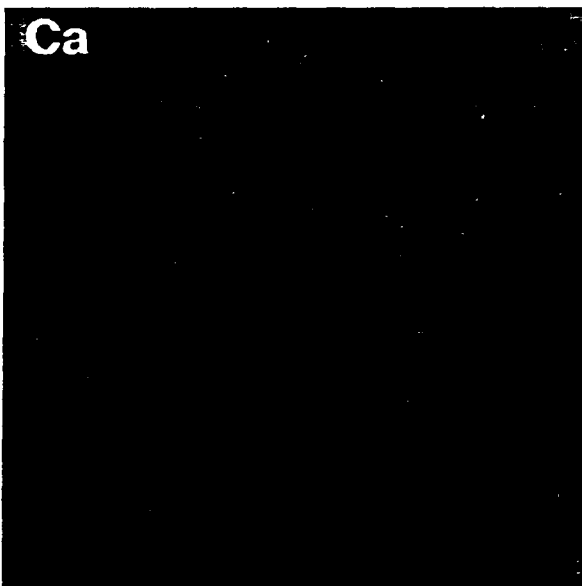
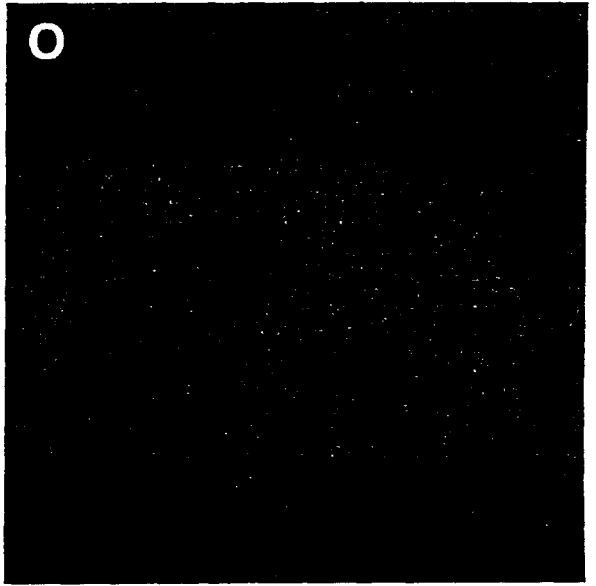
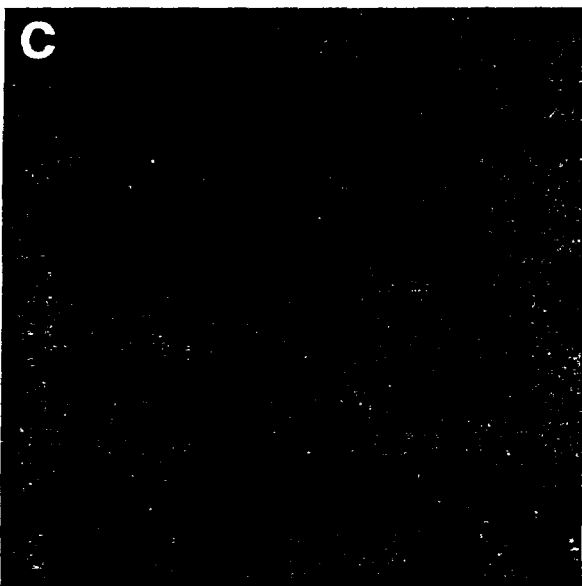
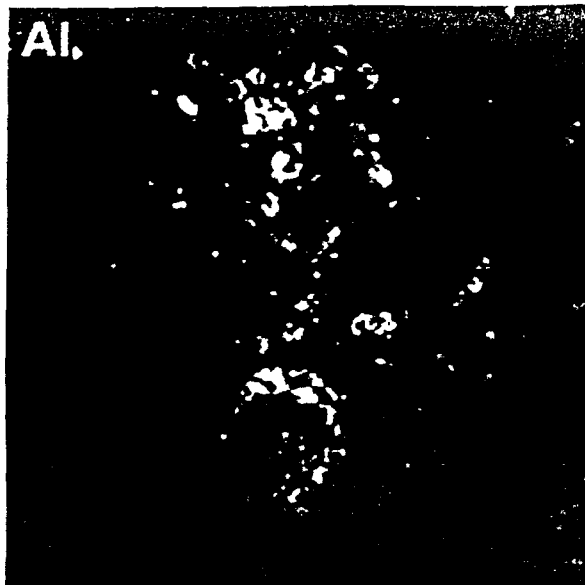
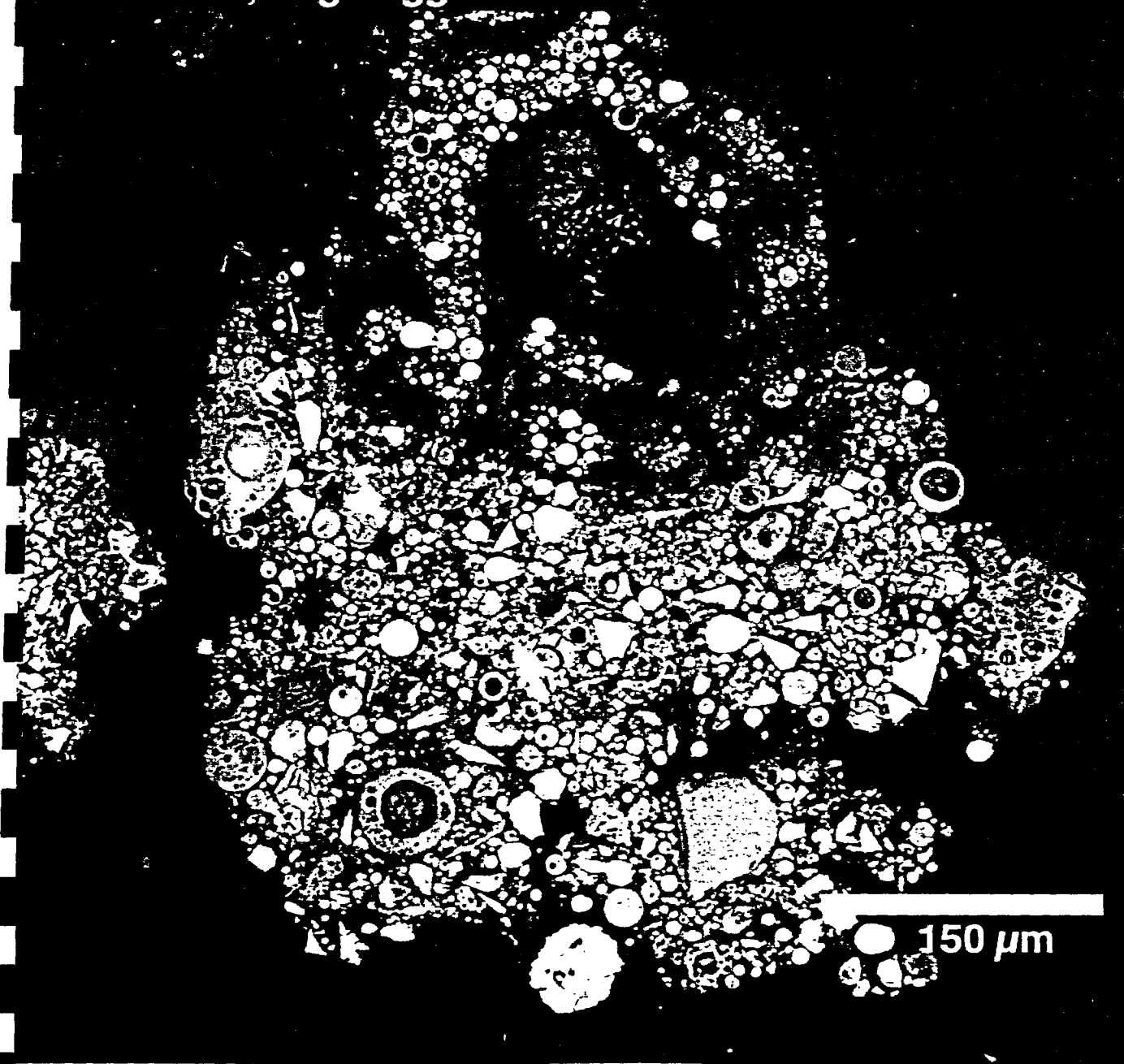


Figure 3:30. X-ray compositional maps (corresponding to field-of-view in Fig. 3:29) showing distribution of Al, Si, C, O, Ca and Fe in treated PECO sludge.

**Marcor M3, Large Agglomerate**



**Figure 3:31.** Backscattered electron image of large agglomerate particle in treated PECO sludge (see also Fig. 3:32 overleaf).

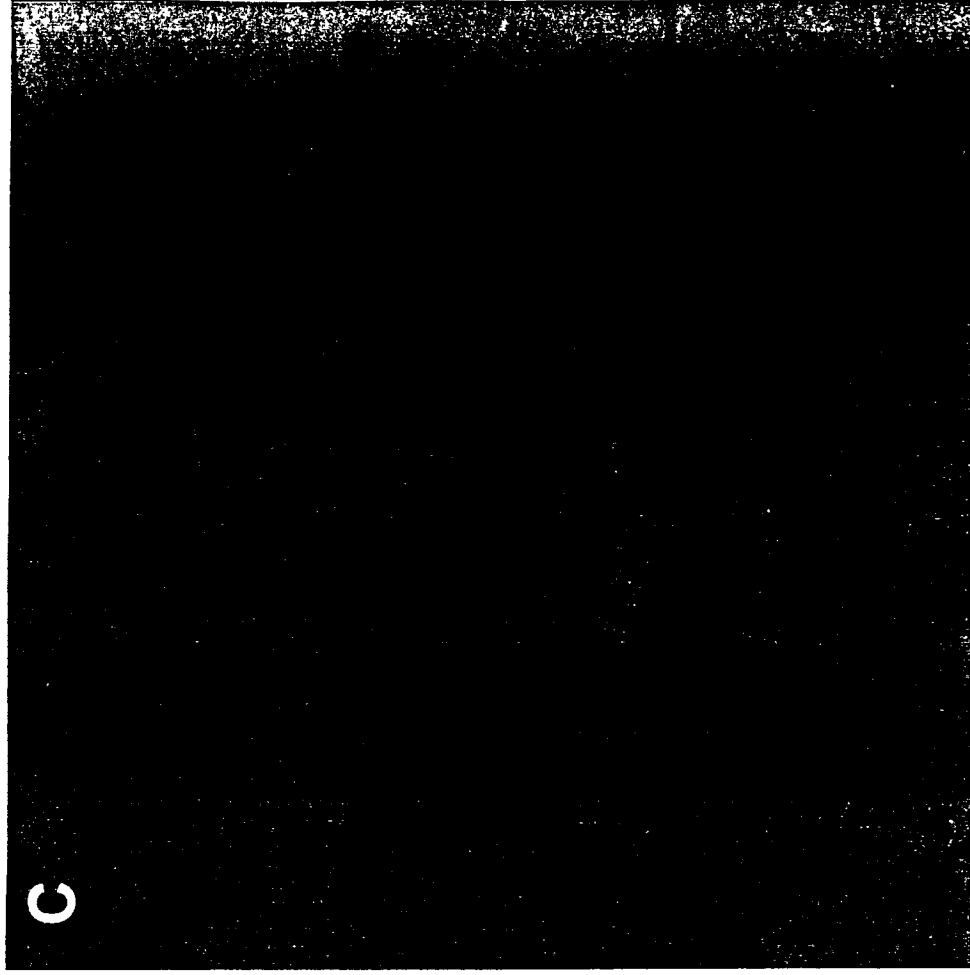
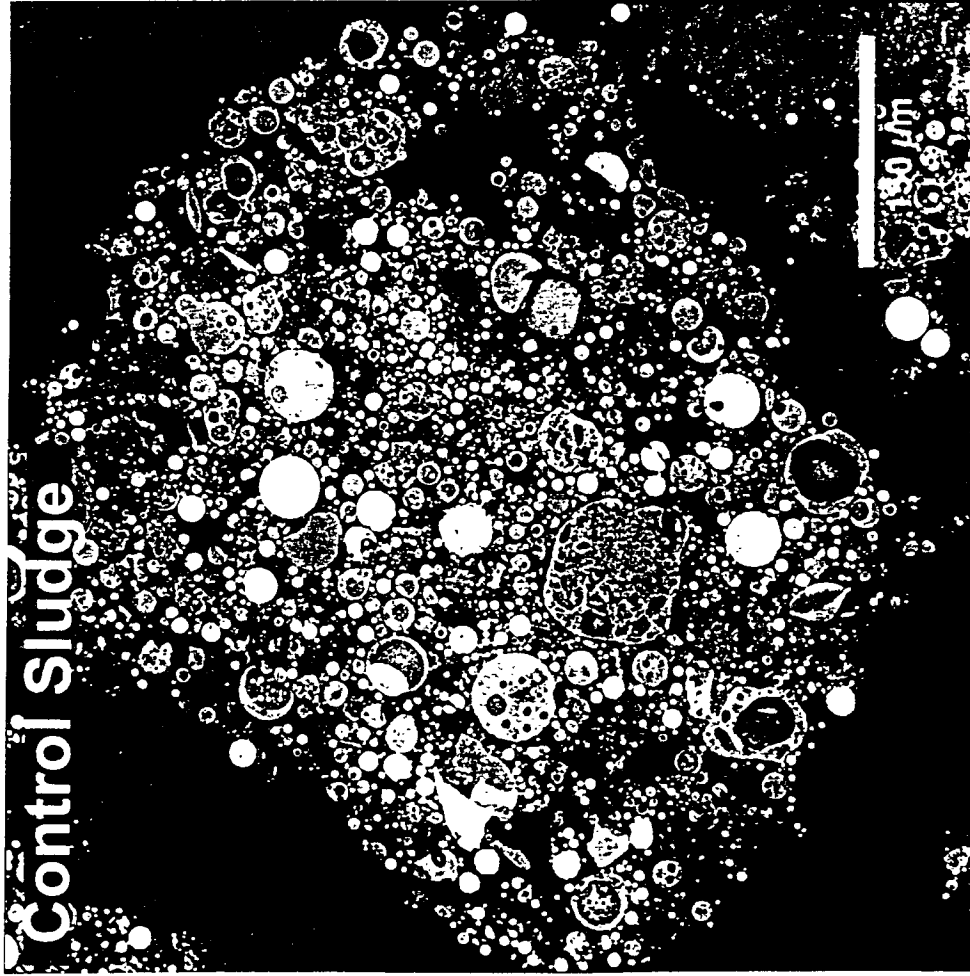


Figure 3-33. Summary overview of SEM findings with respect to untreated PECO sludge. Sludge consists predominantly of agglomerates of fly-ash particles (backscattered electron image, left) held together by organic matter (carbon x-ray map, right).

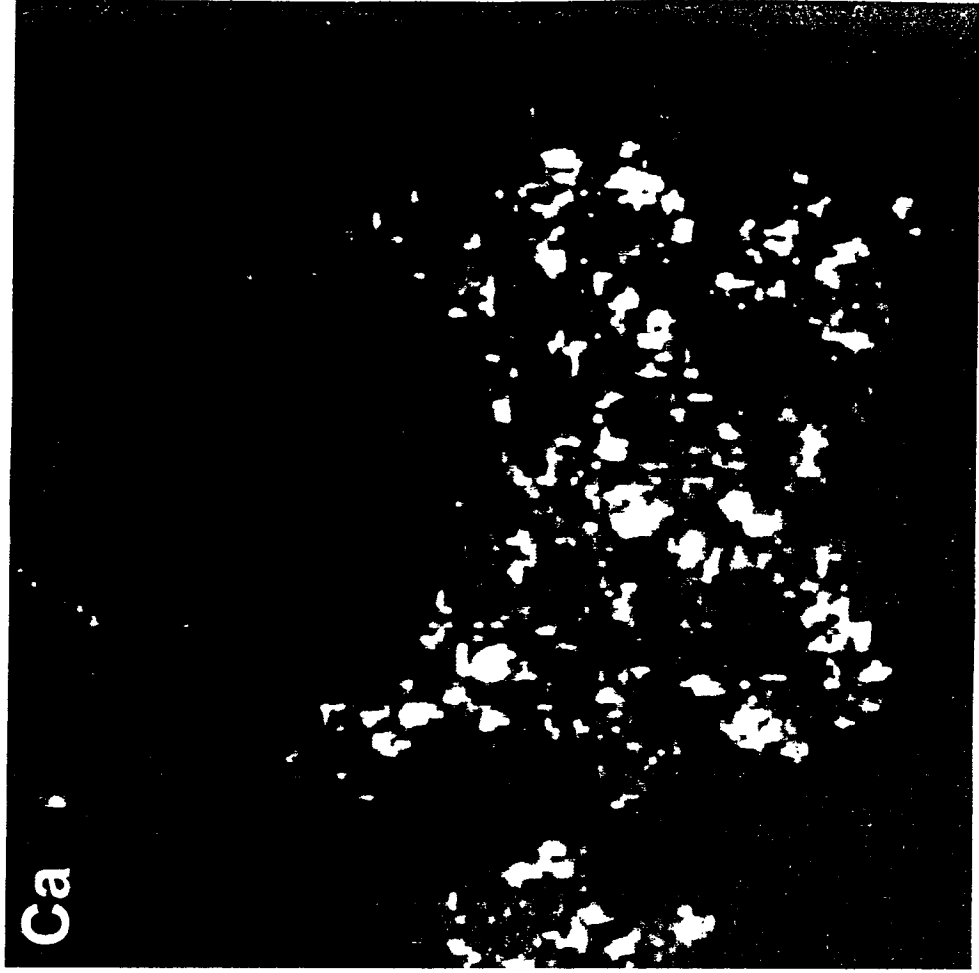
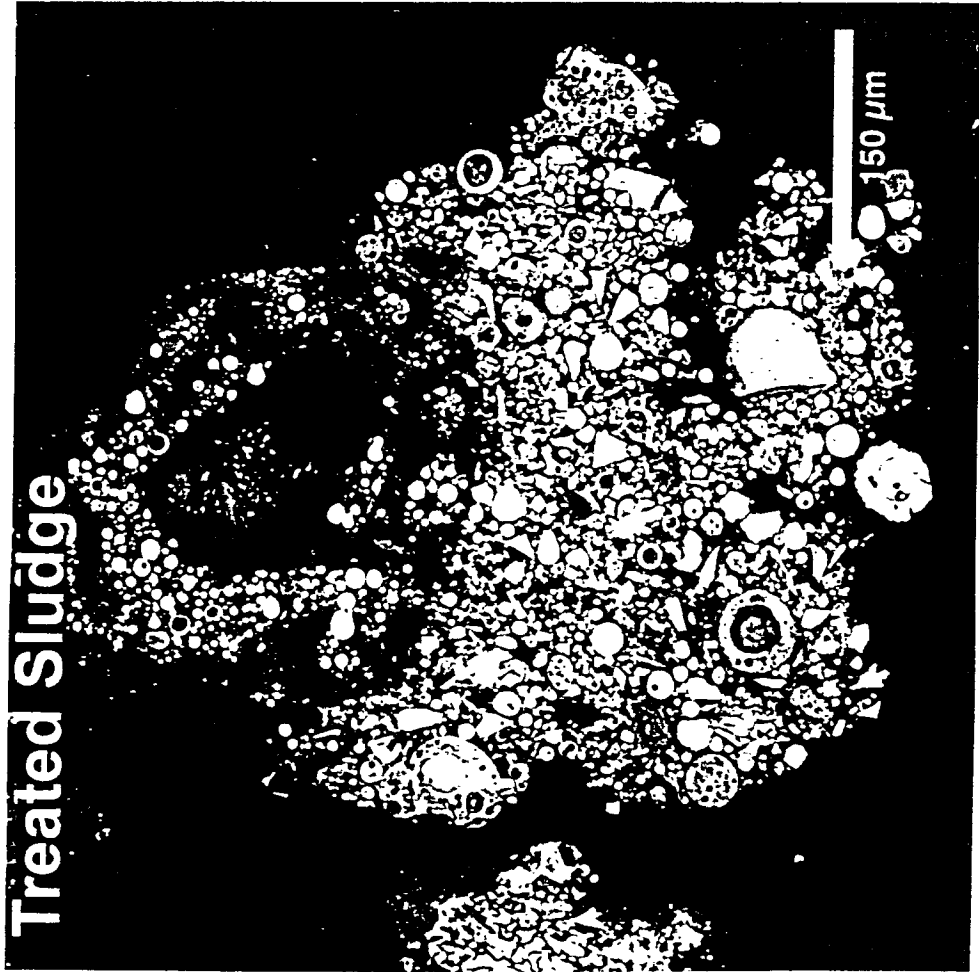


Figure 3:34. Summary overview of SEM findings with respect to treated PECO sludge. The organic matrix has been partially replaced (mineralized) by Ca carbonate (cf. Figs. 3:33 & 3:34).

## Chapter 4

### Transmission electron microscopy investigation of clays and carbonates

The purpose of transmission electron microscopy was (a) to establish the identity of the Ca-rich mineral that has infiltrated (mineralized) the organic matter in treated soil and sludge samples (see Chapter 3), and (b) to evaluate the role of clays in the treatment process.

Random aliquots of untreated and treated soils (M1 & M2A) and untreated and treated sludges (M4 & M3) were embedded in low viscosity epoxy. Electron transparent thin sections (~80 nm thick) were prepared using ultramicrotomy. The thin sections were analyzed using thin-window energy-dispersive x-ray spectrometry (EDX) and parallel electron energy-loss spectrometry (PEELS). Clays in the treated and untreated PECO soils and HWT27 formulation were studied. Clays in PECO sludge were not examined, but the mineralogy of the Ca-rich mineral was determined from examination of (treated) sludge.

#### The Ca-rich mineral.

A sample of **treated sludge** (M3) was dispersed in ethanol and fine particles were deposited on a holey carbon thin film for TEM analysis. Euhedral calcium-rich crystals were observed intimately mixed with the organic carbon (Fig. 4:1). Identification of calcium carbonate was established using EDX and PEELS (Fig. 4:2). In carbonates, the carbon-K edge (at ~284 eV) exhibits a distinctive structure and PEELS spectra from the Ca-rich crystals in the treated sludge clearly show the edge structure characteristic of carbonates (Fig. 4:3). PEELS was also employed to examine the various forms of carbon in the soil and sludge. Figure 4:3 illustrates that each of the important carriers of carbon can be recognized using PEELS.

#### Clays

Brightfield imaging, lattice-fringe imaging, electron diffraction, and EDX were used to examine the clays in all samples. In the **untreated soil** (M1), abundant clay minerals are present, largely as surface coatings on other soil grains (e.g. quartz and glassy slag particles (Figs. 4:4 - 4:7). Two major clay morphologies are observed, *feathery* and *platy*. These clay types are intimately intergrown, with the feathery type most abundant. Electron diffraction patterns and lattice fringe images show that the feathery clays have a basal lattice spacing of ~1 nm (Fig. 4:8). This basal spacing, combined with the crystal morphology are characteristic of smectite-group minerals. Smectite minerals are similar to micas except that their interlayer cations are exchangeable, and the interlayer can expand or contract depending on the humidity and type of interlayer ion (smectite minerals typically have basal spacings of 1.2-1.6 nm in air, but in the high vacuum of the TEM, the interlayer collapses and the basal spacing is ~1 nm). The smectite in the untreated soil occurs in intergrowths with finely disseminated Fe-oxide/hydroxide (Fig. 4:9). EDX analyses indicate that the smectite is aluminum-rich and magnesium-poor, which corresponds closely to the composition of the mineral beidellite  $[A \sim 0.5Al_2(Si, Al)_4O_{10}(OH)_2 \cdot XH_2O]$ , where A is the interlayer cation (mostly K), and X is the interlayer water (Fig. 4:10). The other major clay in the untreated soil is a platy variety which contains significant Mg and Fe. Most of the platy grains show 1.4 nm spacings in high-resolution TEM images and in electron diffraction patterns, however, several grains show coherent intergrowths of 1.4 nm and 1.0 nm layers

(Fig. 4:11). We interpret the 1.4 nm phase as a Mg-rich chlorite intergrown with a mica/illite mineral (which corresponds to the 1.0 nm spacings observed) (Figs. 4:11 & 4:12).

In addition to the clays, a minor Fe-rich phase is present in the untreated soil (Fig. 4:13 and Fig 4:14). Electron diffraction data show only two diffuse spacings of 0.25 and 0.15 nm, which are consistent with poorly-crystalline Fe-oxide/hydroxides such as ferrihydrite.

Two samples of the **treated soil**, M2 and M2A (A = soil aged for 125 days) were examined using TEM. Low magnification TEM images show that the clays occur as coatings on soil grains (Figs. 4:15 & 4:16). Both platy and feathery morphologies of clay are present in the treated soils. Electron diffraction data, high-resolution images, and EDX analyses confirm that the feathery clay is an aluminous smectite with a 1 nm basal spacing (Figs. 4:17 & 4:18). The platy clay mineral is an intergrowth of 1.4 nm layers and 1.0 nm layers, which is consistent with an intergrowth of chlorite with mica/illite (Figs. 4:19 & 4:20). The fine-grained, poorly crystalline, Fe-rich phases observed in the untreated soil are also present in the treated soil (Figs. 4:21 & 4:22). To summarize, clays in the treated soil are on the whole similar to those in the untreated soil.

Clay is also present in the **ACT formulation (HWT27)**. The clay is a fine-grained smectite with characteristic 1.0 nm basal spacings and feathery morphology (Figs. 4:23 & 4:24). EDX analyses show that the smectite is essentially the Al-rich beidellite end member, with no associated Fe-oxide/hydroxide (Fig 4:25). Smectite is a major component the swelling clay bentonite. We conclude that the smectite is organophillic clay, a component of the ACT formulation

#### Summary of TEM observations

Electron energy-loss spectroscopy (EELS) of the treated sludge sample confirms that **calcium carbonate is a major mineralization byproduct of PAH breakdown during ACT treatment**. TEM examination of the untreated and treated PECO soils (M1 & M2A) shows that a similar suite of clays are present before and after treatment with HWT27. **From this limited study, there is no compelling evidence of formation of significant quantities of new "neo" clays or a direct clay role in PAH breakdown during the ACT treatment.** On the other hand, the question of formation of "neoclays" and their possible role(s) in degrading PAHs requires further study. (Infrared results *hint* at a possible role for clays in PAH breakdown reaction(s) (see Figure 57, Page 76)). Since the treated PECO sludge yielded the most favorable results with respect to PAH breakdown, untreated and treated sludges should be included in any future study of clays.

3752

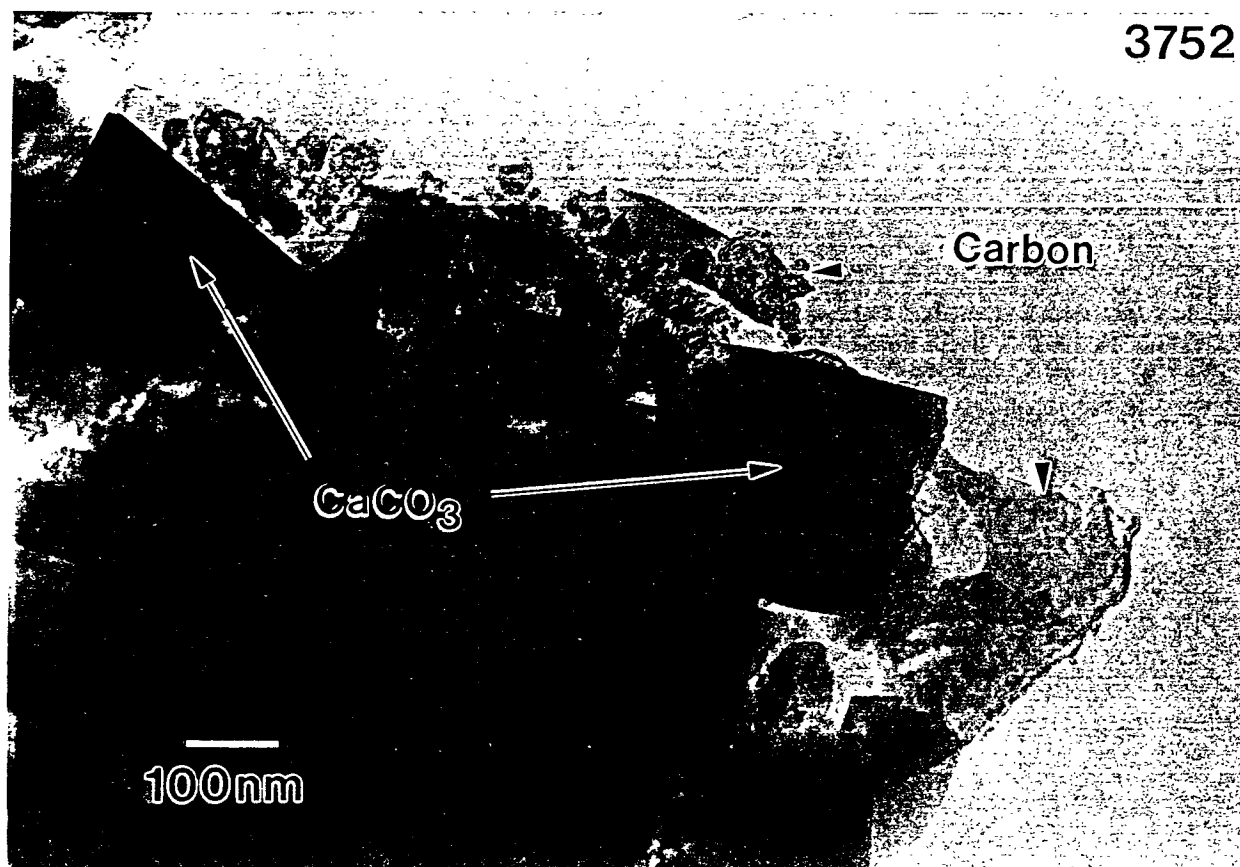
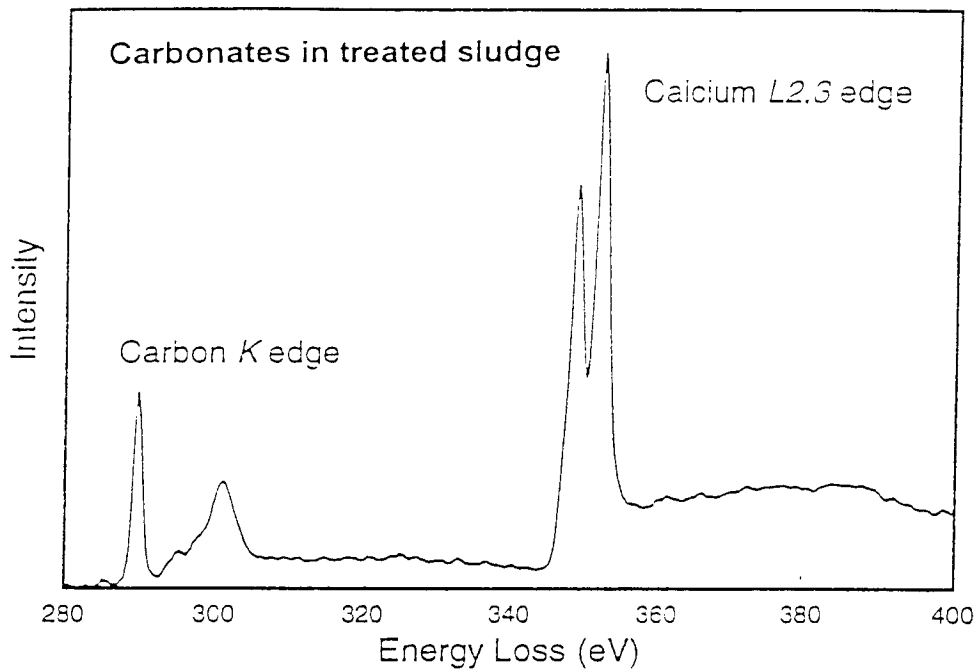
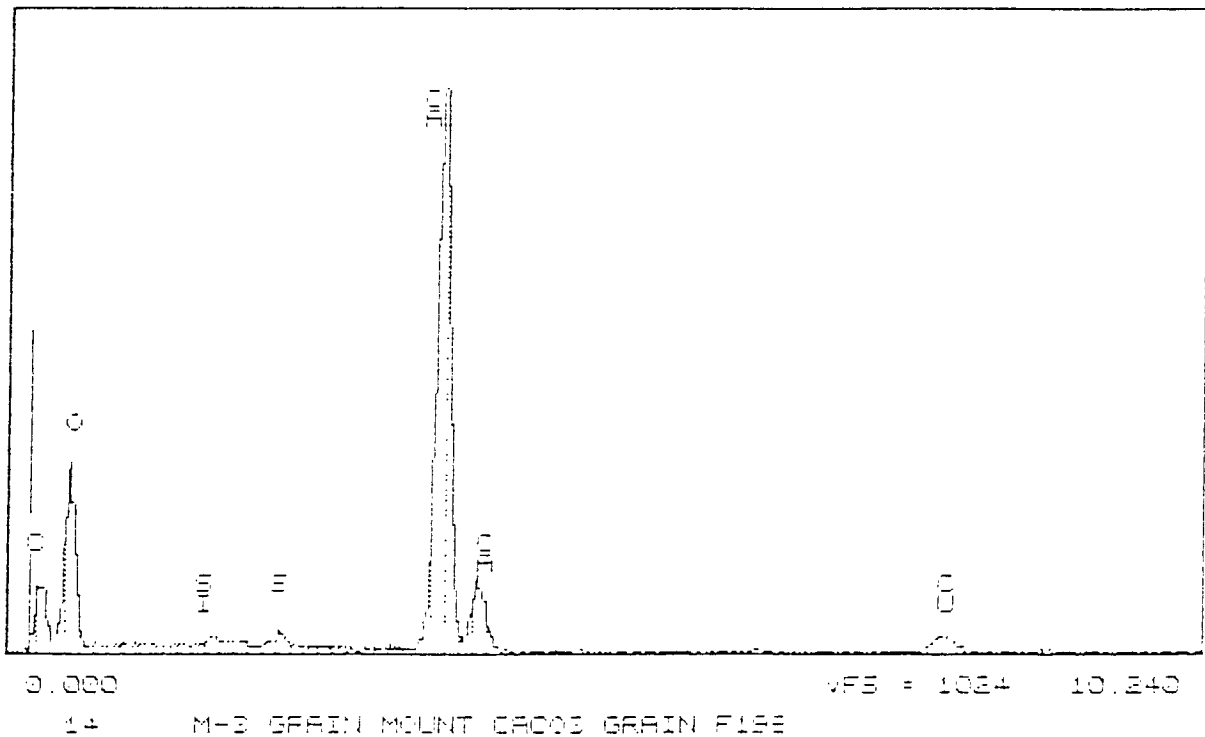


Figure 4:1. Brightfield transmission electron micrograph of organic carbon and euhedral calcium carbonate crystals in matrix of treated sludge agglomerate.



**Figure 4:2. (a)** Electron energy-loss carbon-K and calcium-L core scattering edges from euhedral Ca-rich crystals similar to those in Figure 4:1. The characteristic structure of the carbon-K edge is a “fingerprint” for carbonates (see also Fig. 4:3).

Cursor: 0.000keV = 0      ROI    (15) 0.000: 0.000



**Figure 4:2. (b)** Energy-dispersive x-ray spectrum for carbonate crystal.

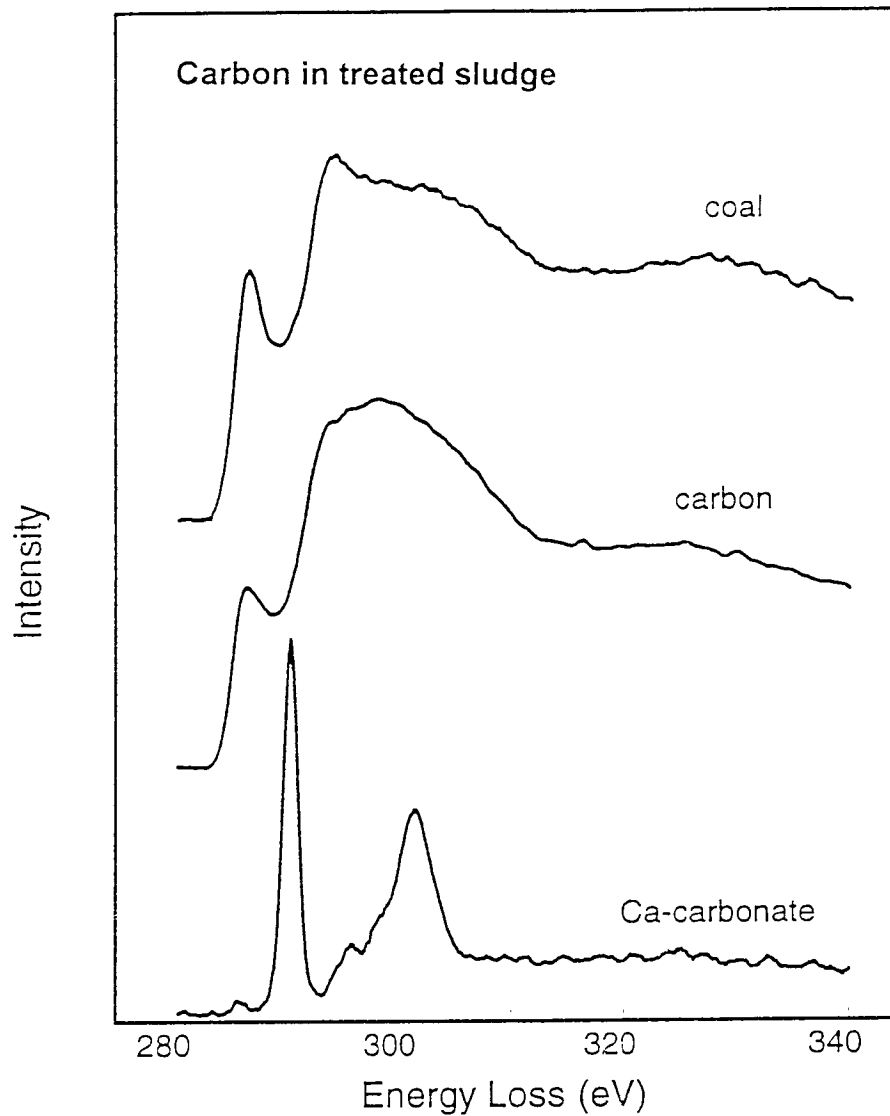


**Figure 4:3.** Electron energy-loss core scattering edges from carbonaceous particles in treated PECO sludge, coal, (organic) carbon, and calcium carbonate.



Figure 4:4. Brightfield electron micrograph of surface coating of clay on a slag particle in untreated soil (M1).

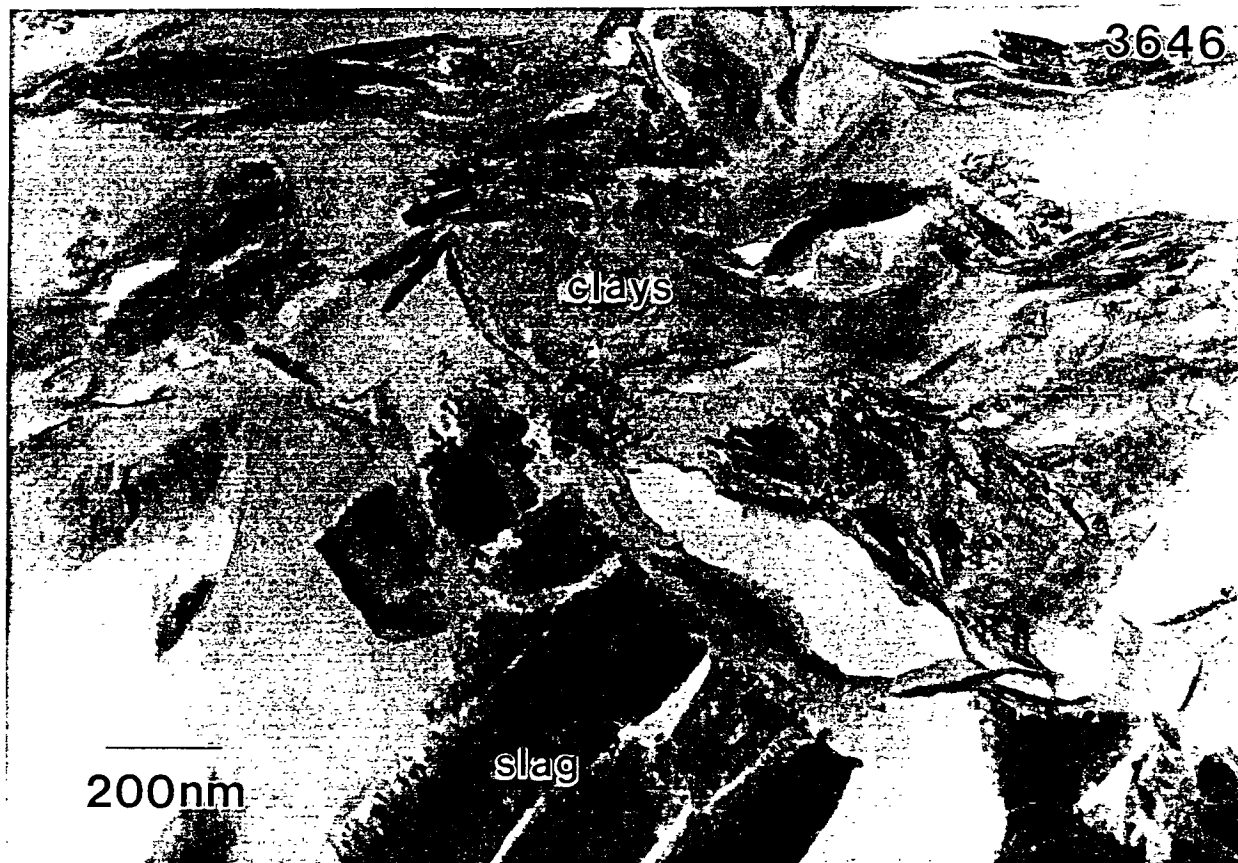


Figure 4:5. Brightfield electron micrograph of surface of surface coating of clay on slag particle in untreated soil (M1).

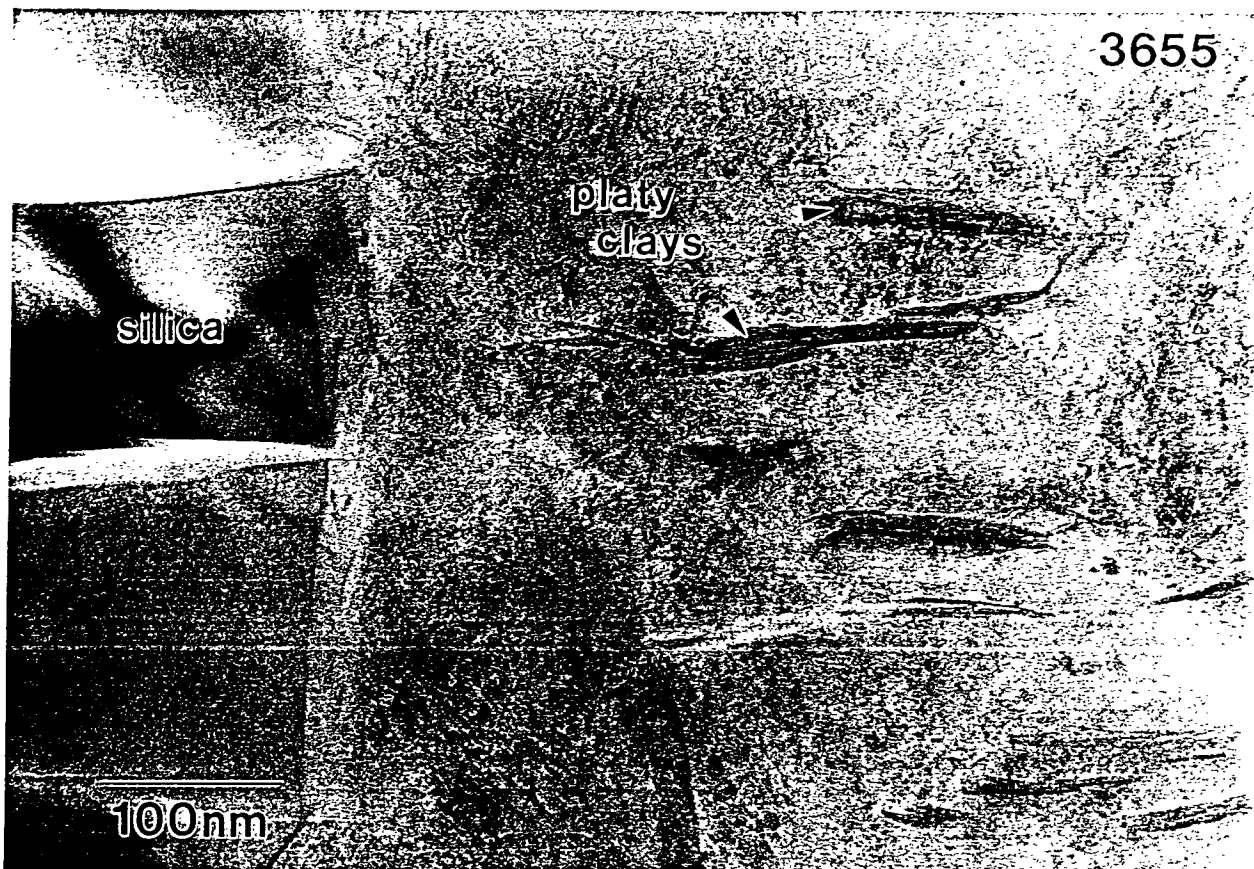


Figure 4:6. Brightfield electron micrograph of platy clays in untreated soil (M1).

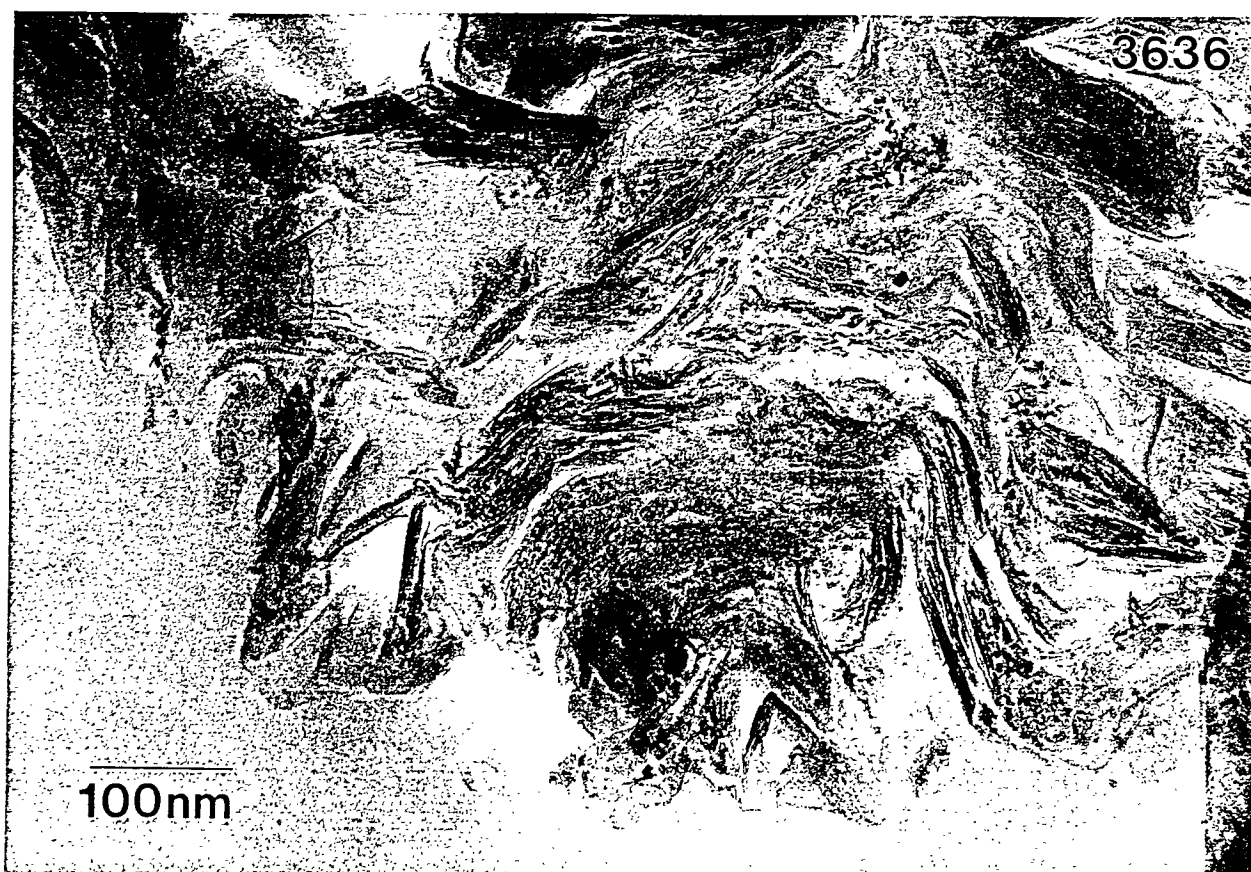
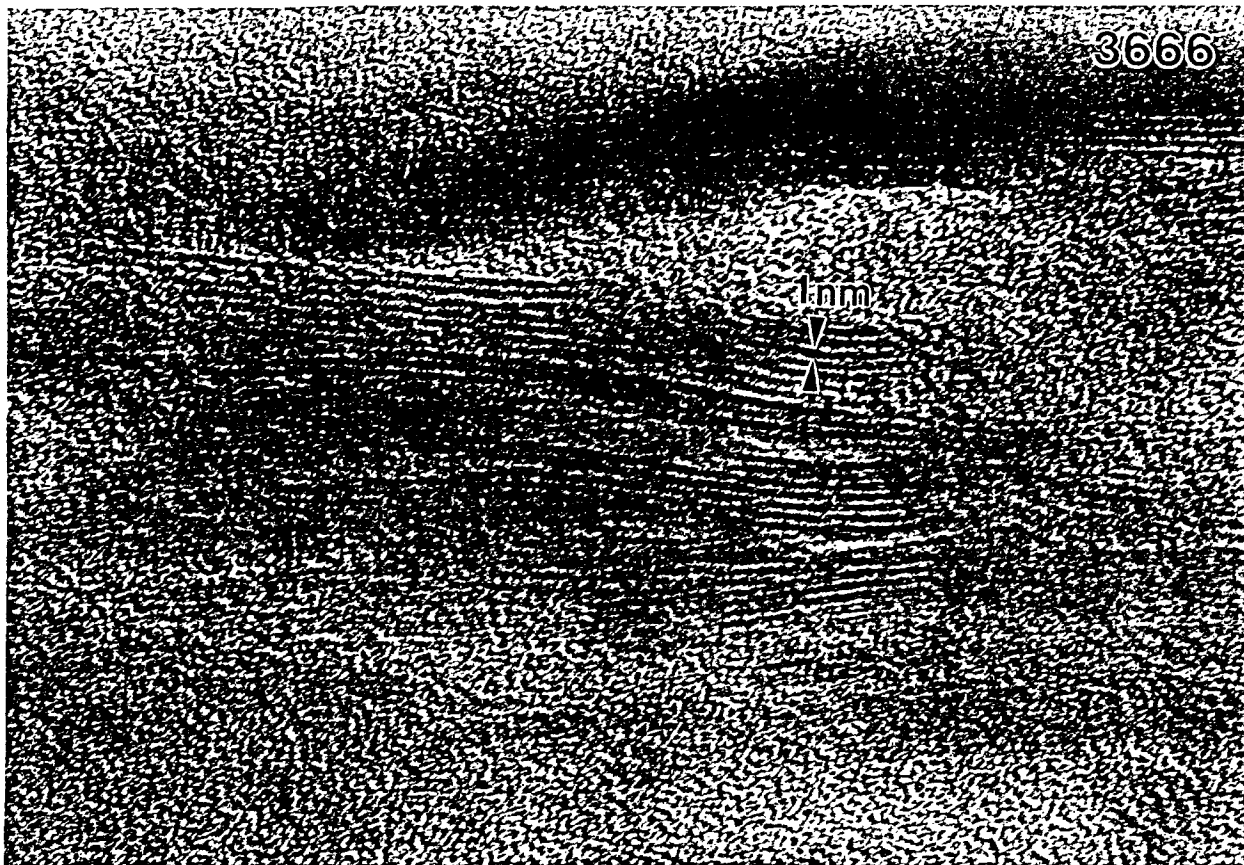
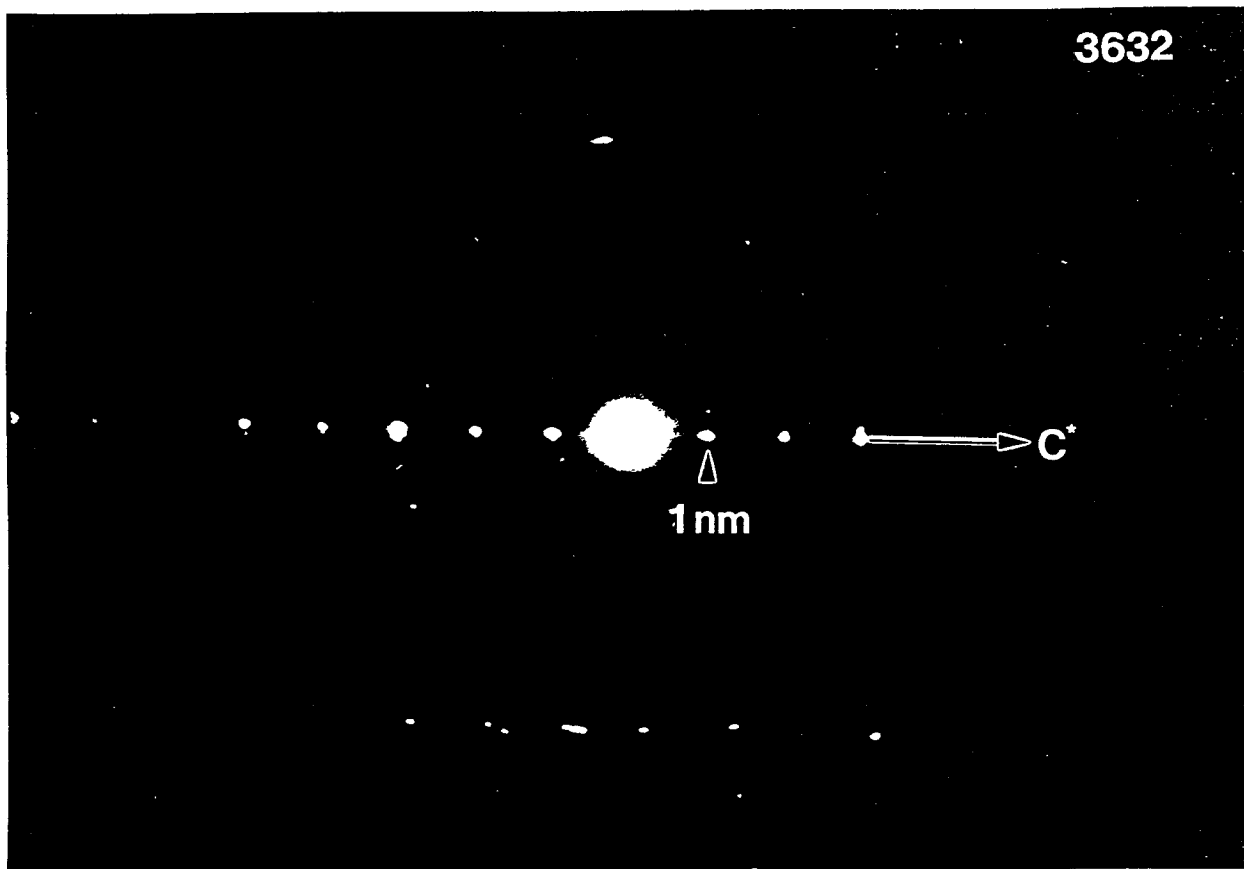


Figure 4:7. Brightfield electron micrograph of feathery clay in untreated soil (M1).



**Figure 4:8. (a)** High-resolution lattice fringe image of feathery clay in untreated soil which exhibits a 1 nanometer (nm) basal lattice spacing.



**Figure 4:8. (b)** Corresponding selected area electron diffraction pattern. This clay is probably smectite.

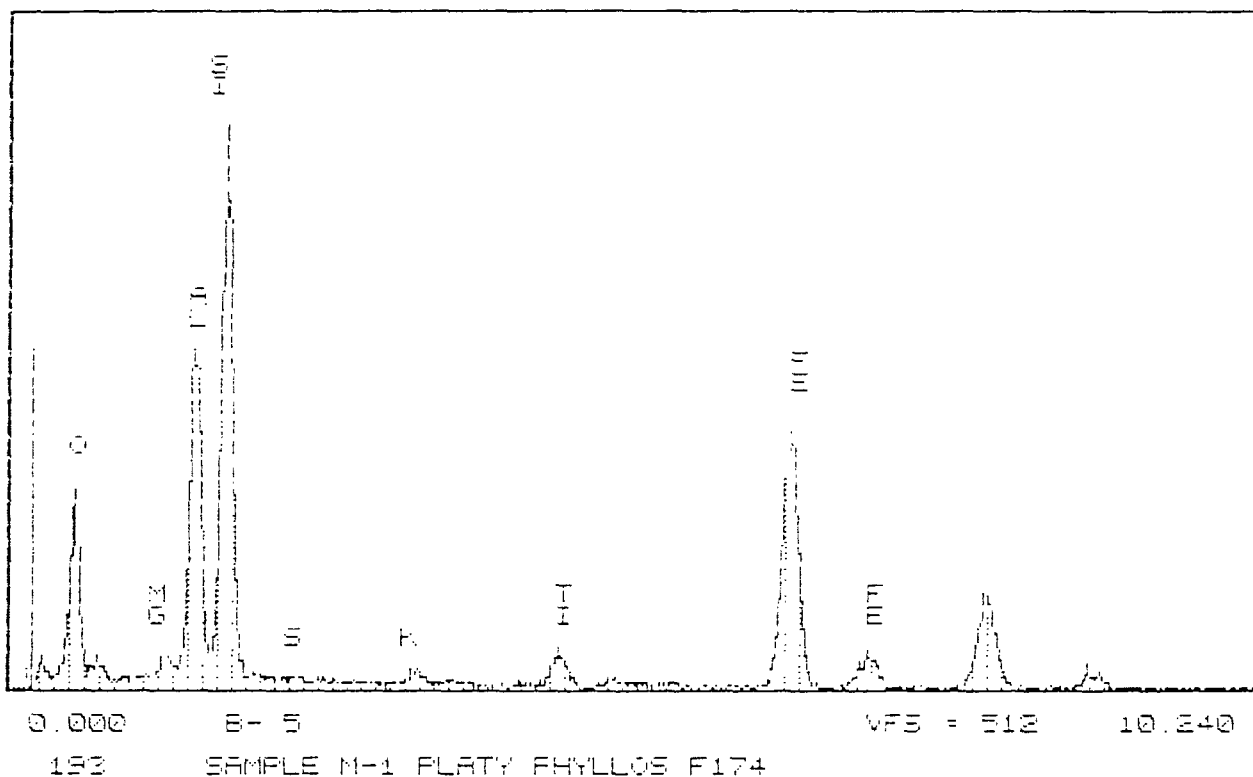


Figure 4:9. Brightfield electron micrograph of clay intergrown with Fe oxide (or hydroxides) in untreated soil (M1).

SERIES 11

FRI 18-AUG-88 17:14

Cursor: 0.000keV = 0



**Figure 4:10.** Energy-dispersive x-ray spectrum from feathery smectite clay in untreated PECO soil (M1).

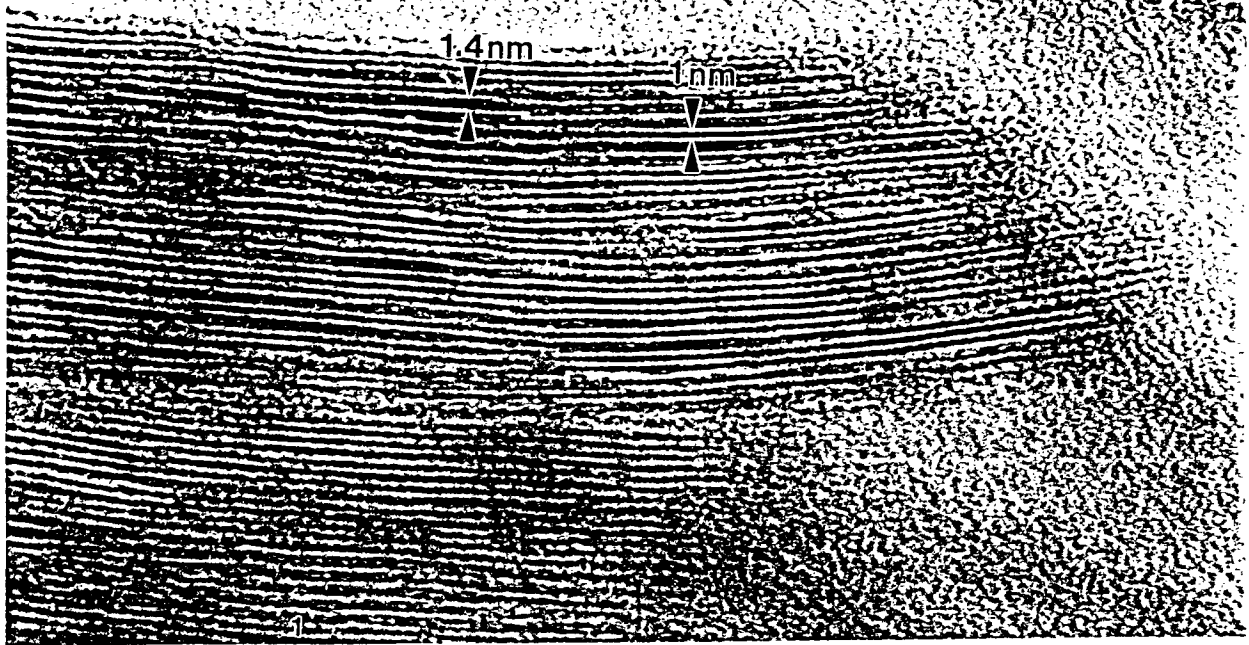


**Figure 4:11. (a)** High-resolution lattice fringe image of platy clay in untreated PECO soil (M1). Note the clay is an intergrowth of two clays with 1 and 1.4 nm basal spacings respectively.

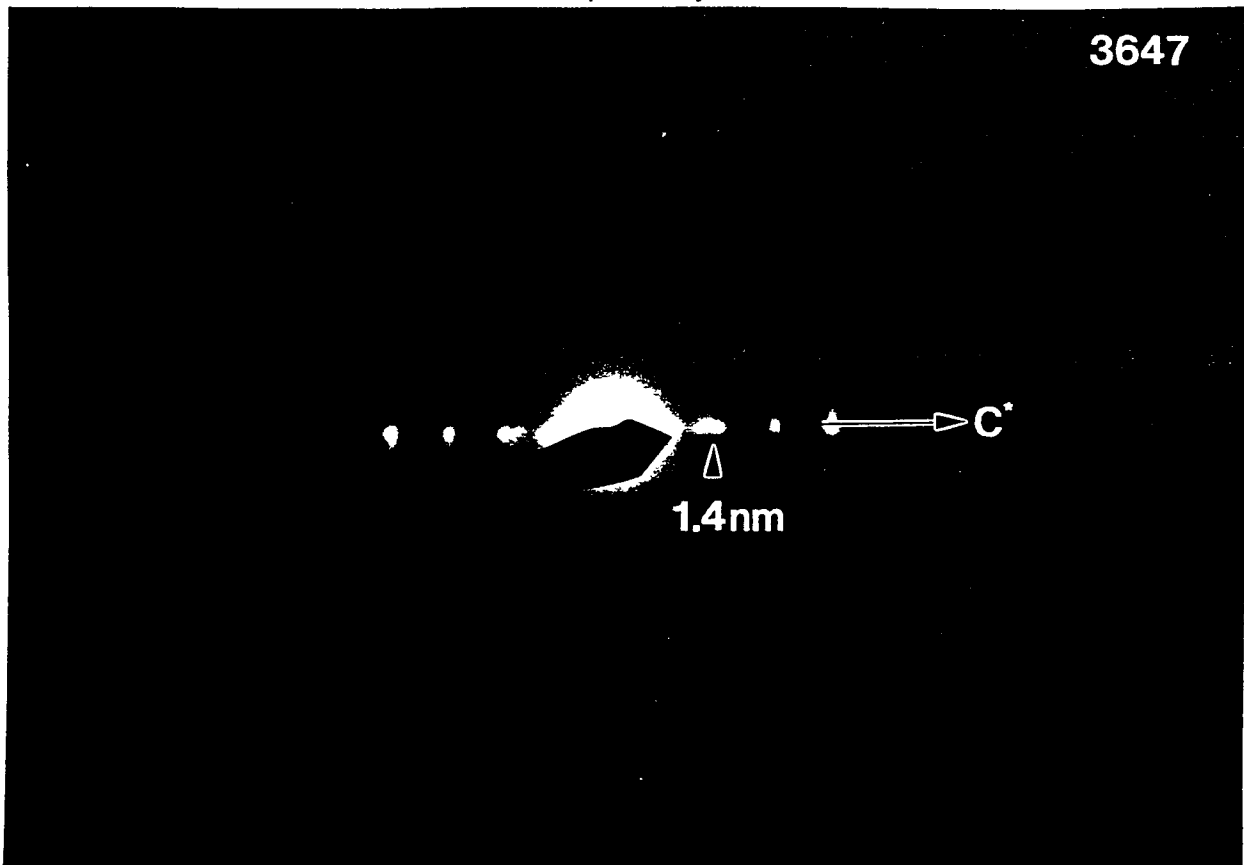


**Figure 4:11. (b)** Corresponding selected area electron diffraction pattern. The 1.4 nm clay is probably chlorite and the 1 nm clay mica/illite.

MVA INC.

FRI 25-AUG-85 10:17

Cursor: 0.000keV = 0

ROI (15) 0.020: 0.000

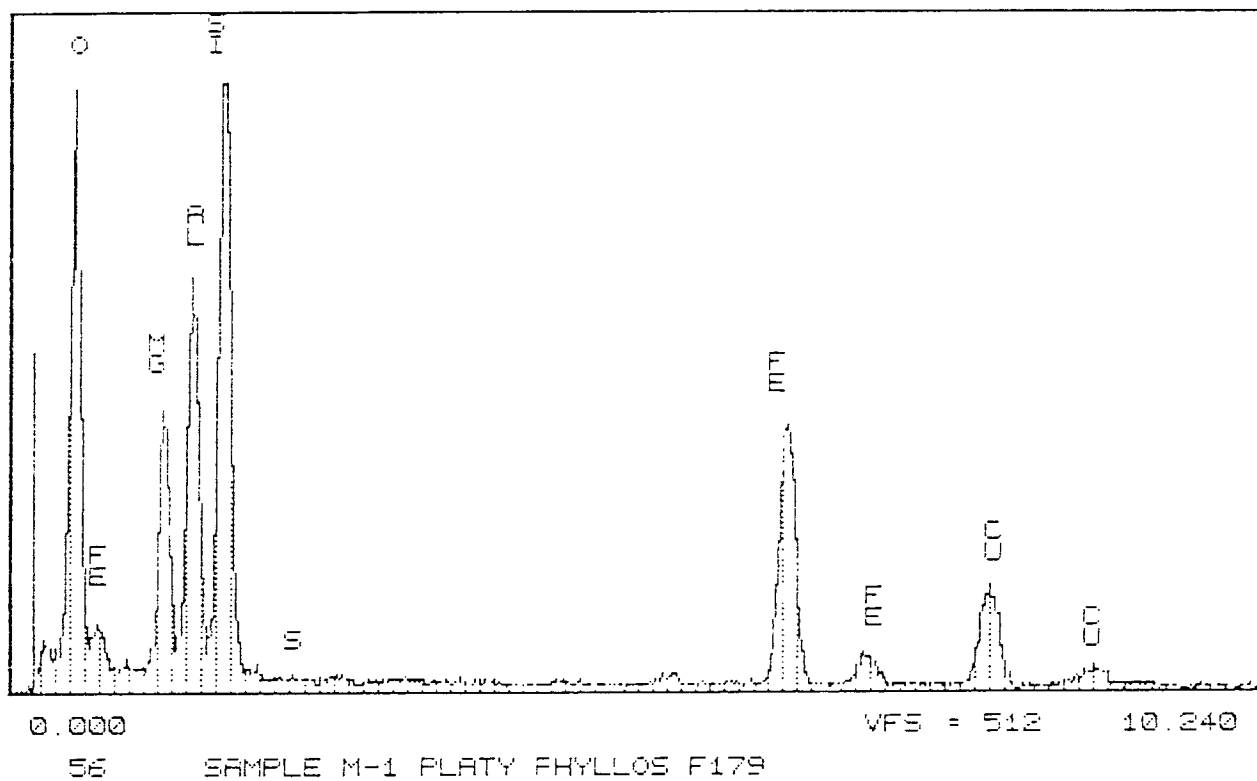


**Figure 4:12.** Energy-dispersive x-ray spectrum from mixed layer clays (shown in Fig. 4:11).

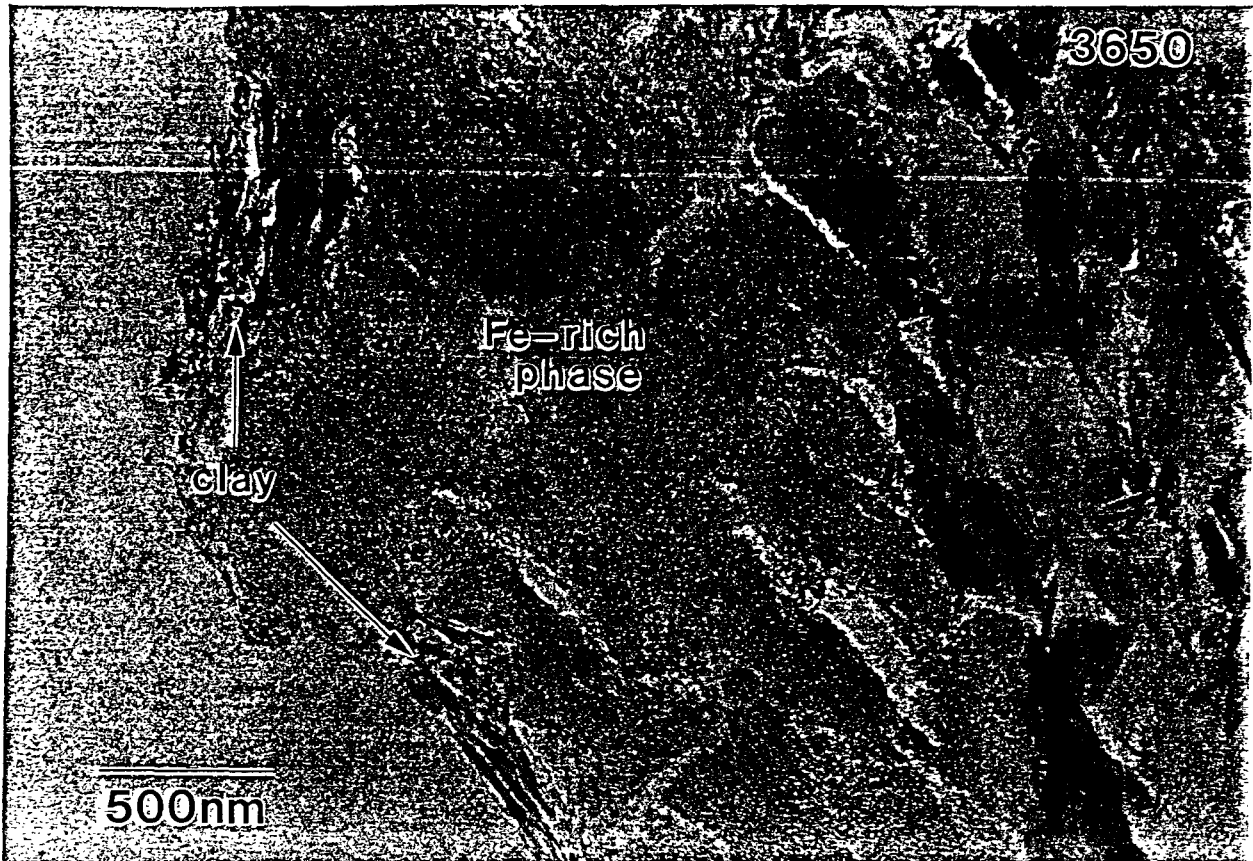


**Figure 4:13.** Poorly crystallized Fe-rich phase common in untreated PECO soil (M1). This mineral is possibly an Fe-oxide/hydroxide such as ferrihydrite.

SERIES II  
Cursor: @ 000keV = @

FRI 18-AUG-85 17:25

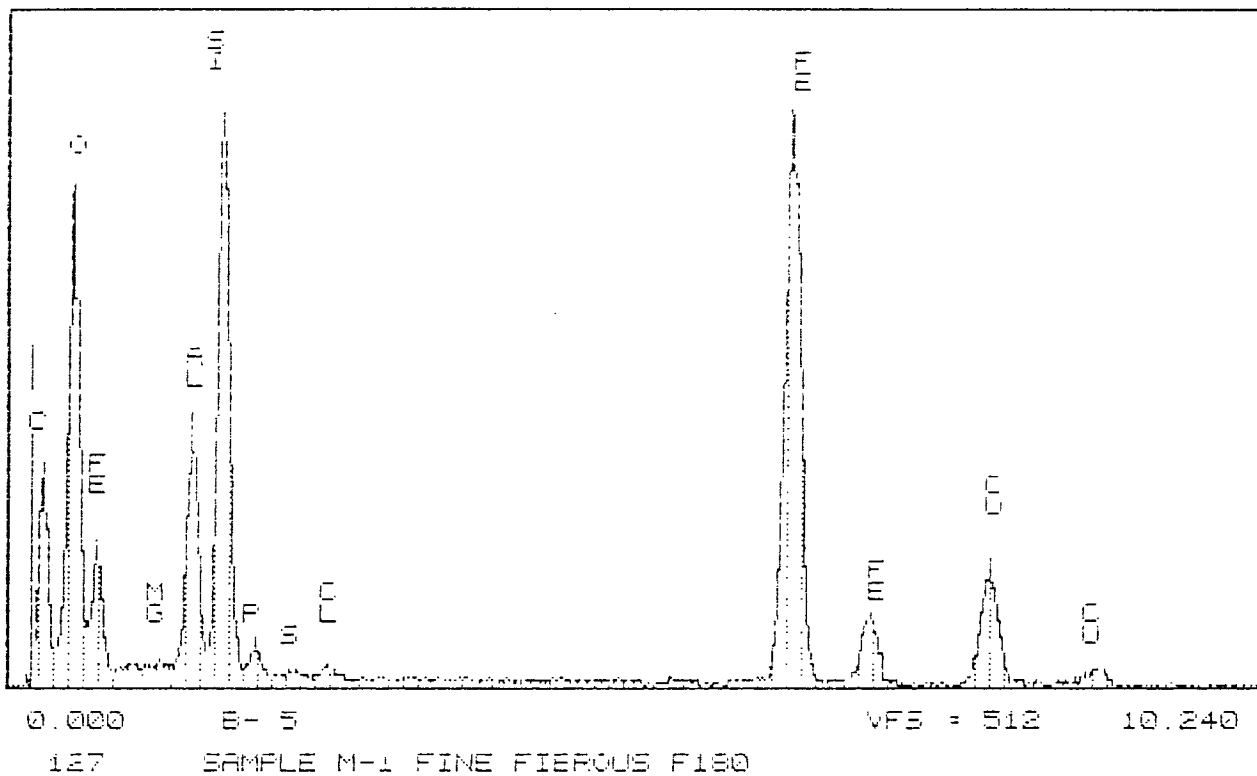


**Figure 4:14.** Energy-dispersive x-ray spectrum from poorly crystallized Fe-rich phase (shown in Fig. 4:13).

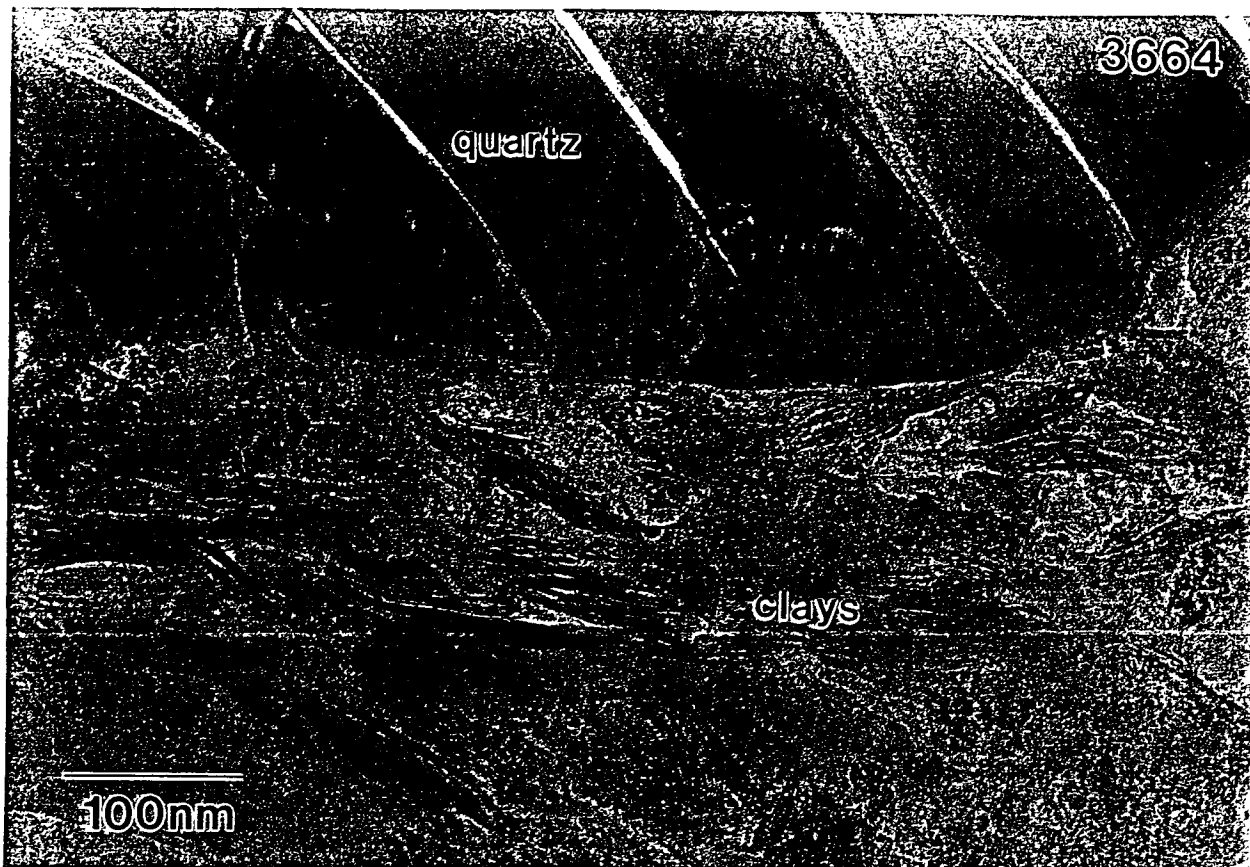


Figure 4:15. Brightfield electron micrograph of surface coating of clay on quartz grain in treated PECO soil (M2A).

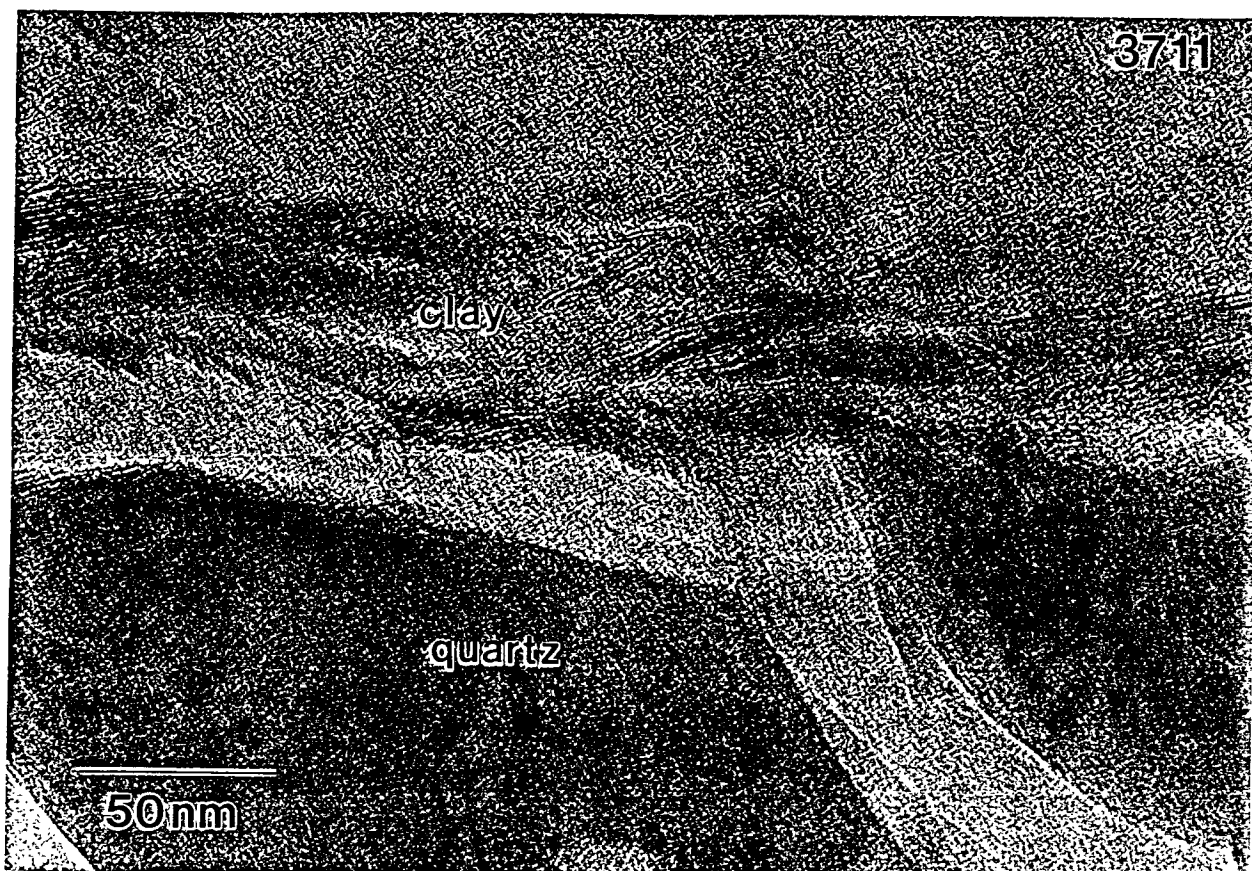


Figure 4:16. Brightfield electron micrograph of surface coating of clay on quartz grain in treated PECO soil (M2A).

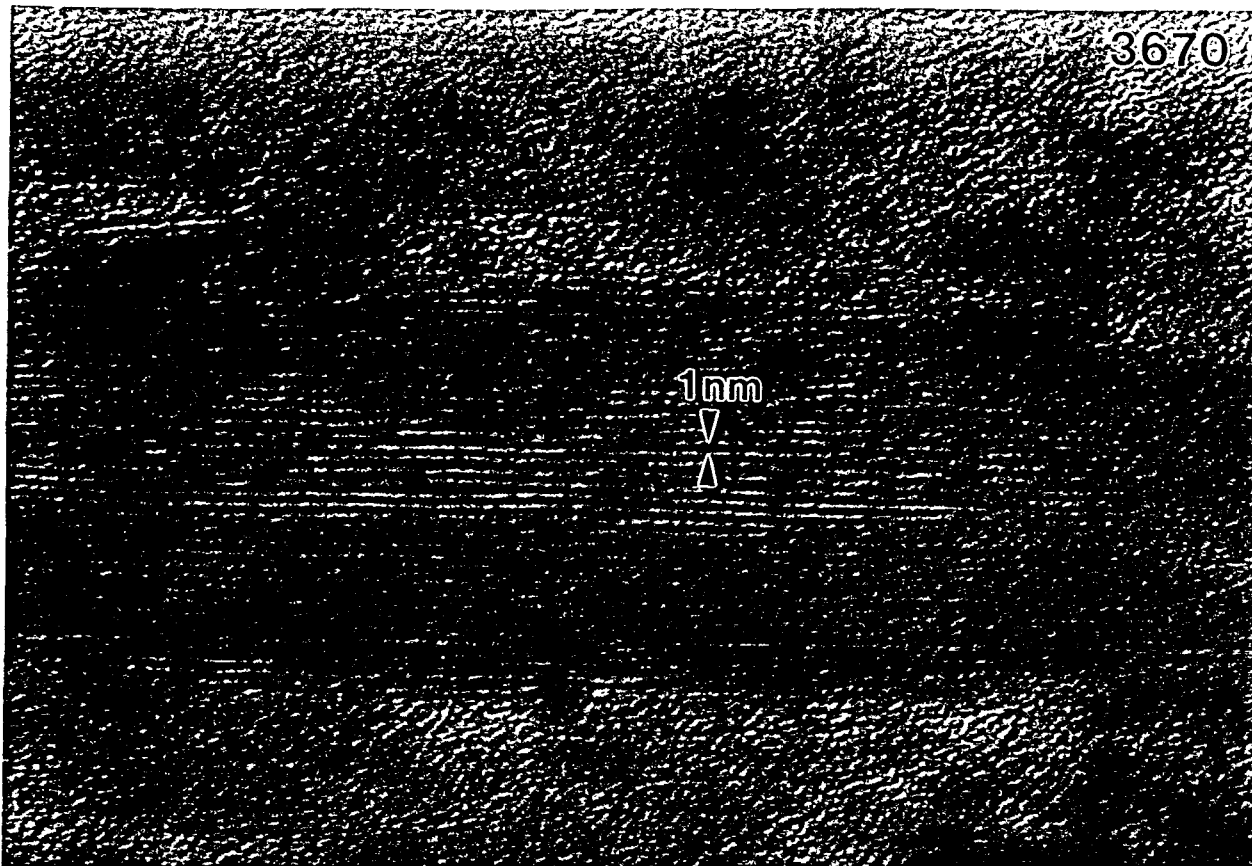


Figure 4:17. (a) High-resolution lattice fringe image and

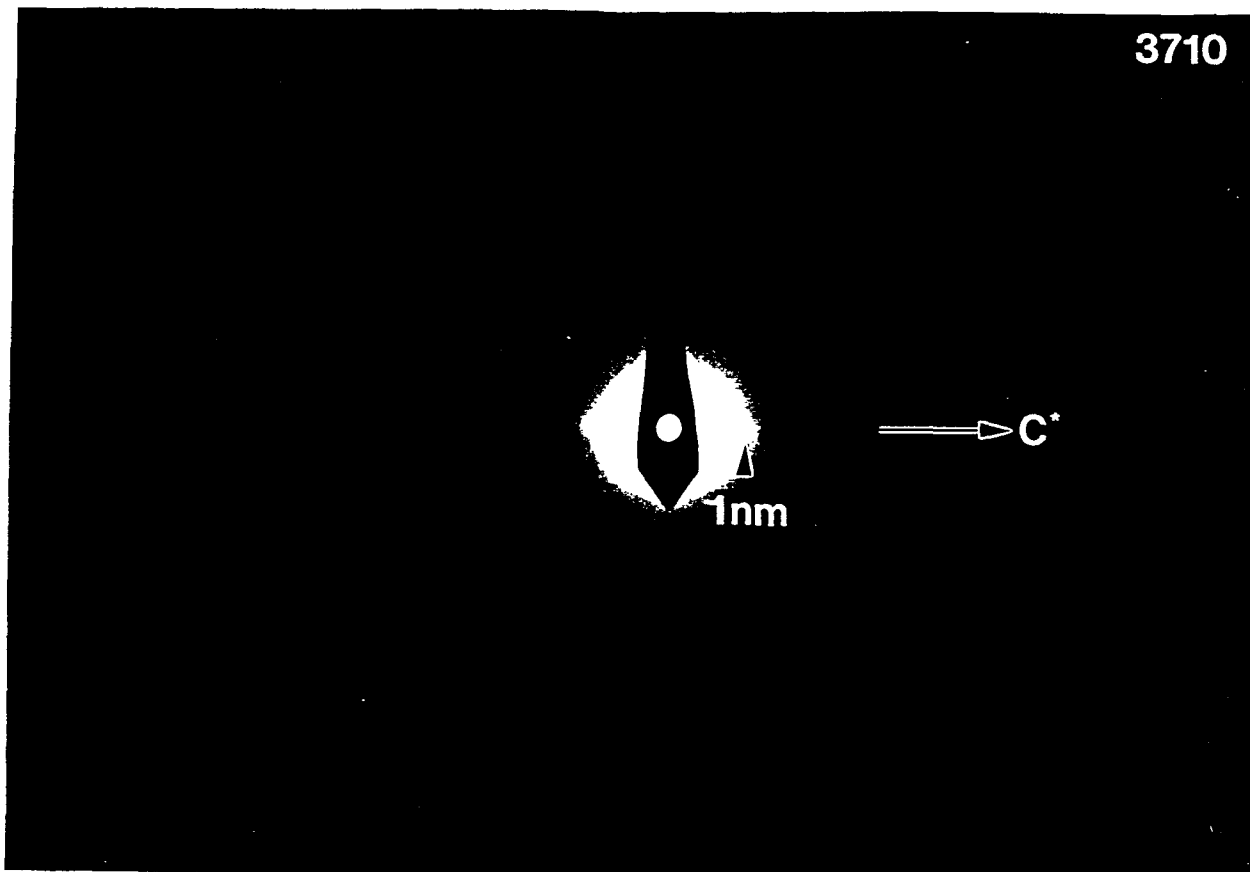
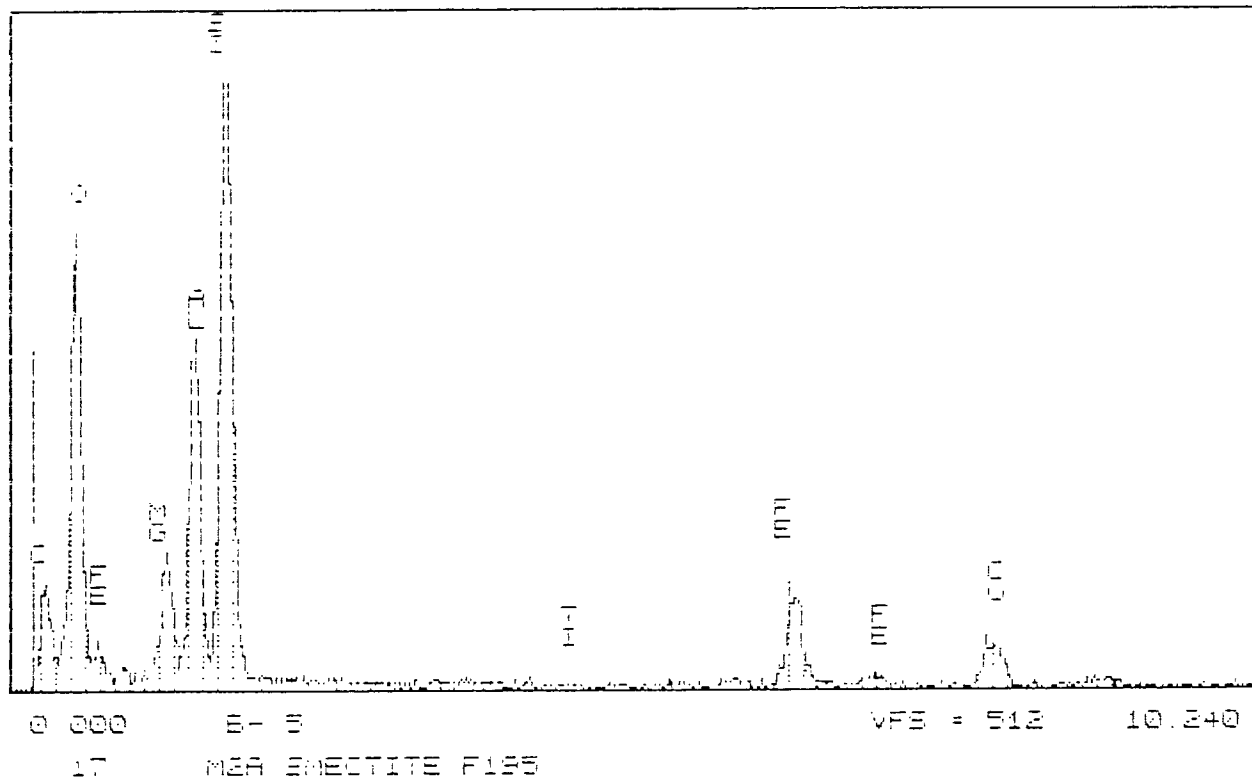


Figure 4:17. (b) Corresponding selected area electron diffraction pattern of feathery clay in PECO treated soil (M2A).

SERIES II

NOV 21-AUG-88 17:36

CURSOR: 0 000keV = 0



ERROR-AD 9999

**Figure 4:18.** Energy-dispersive x-ray spectrum from feathery clay in treated soil (M2A).

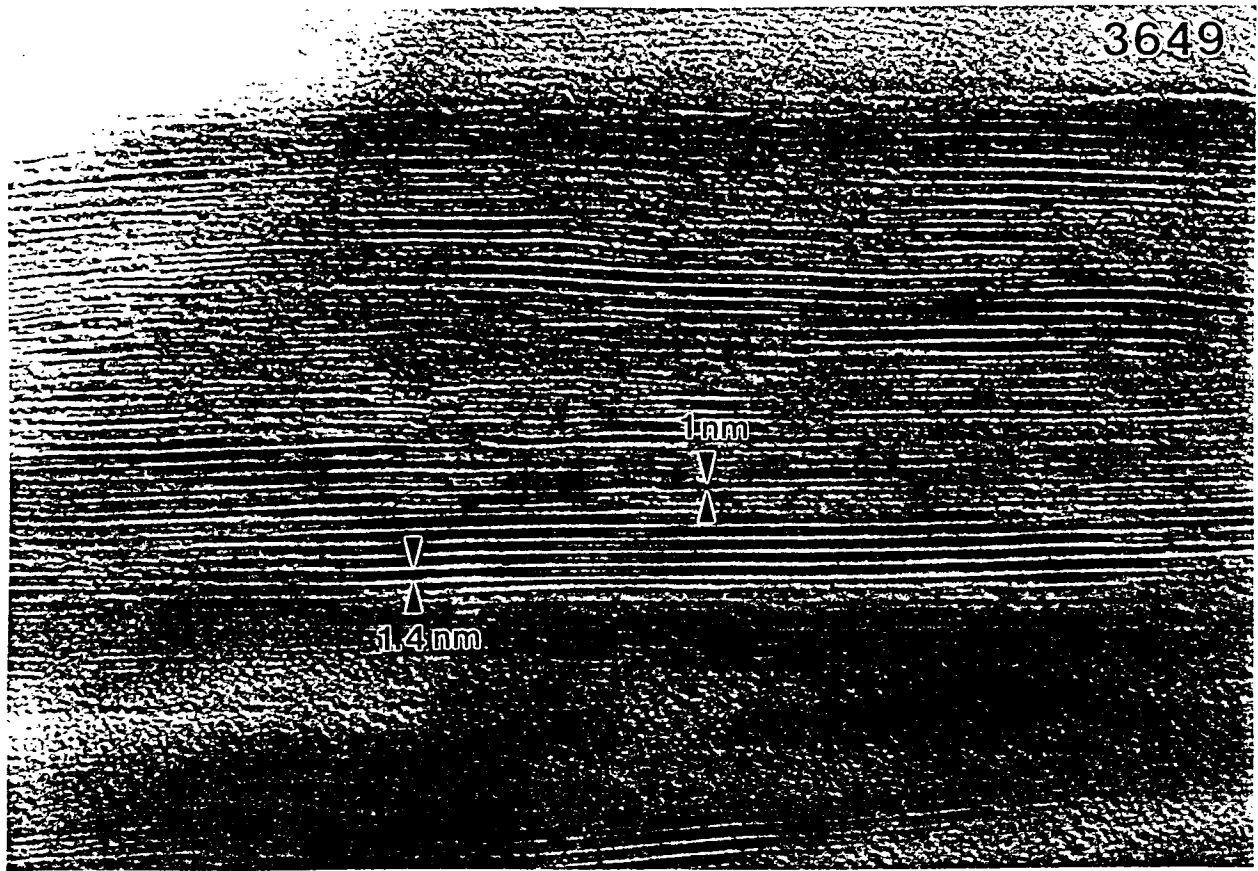


Figure 4:19. (a) High-resolution lattice fringe image, and

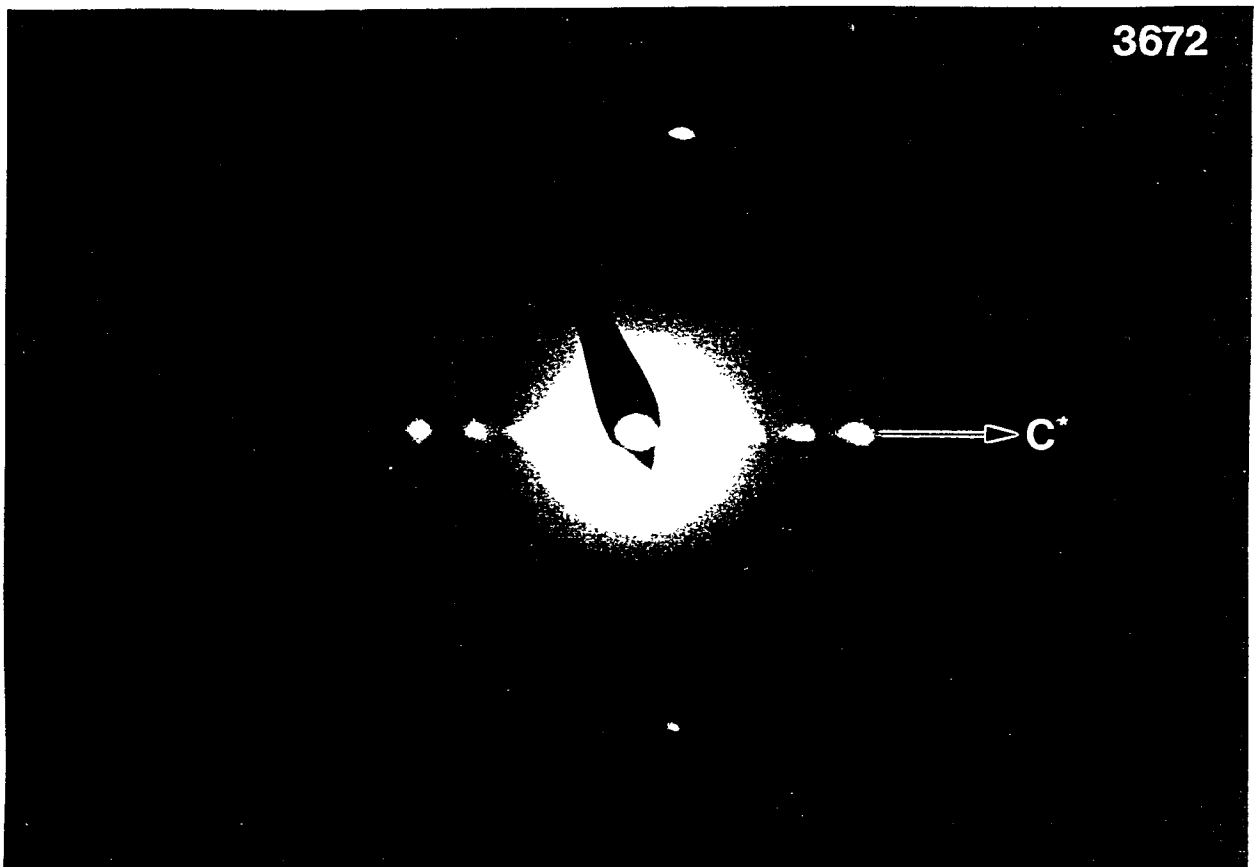


Figure 4:19. (b) Selected area electron diffraction pattern of mixed layer clay in treated soil (M2A).

SERIES II  
Cursor: 0.000keV = 0

MON 21-AUG-85 17:18

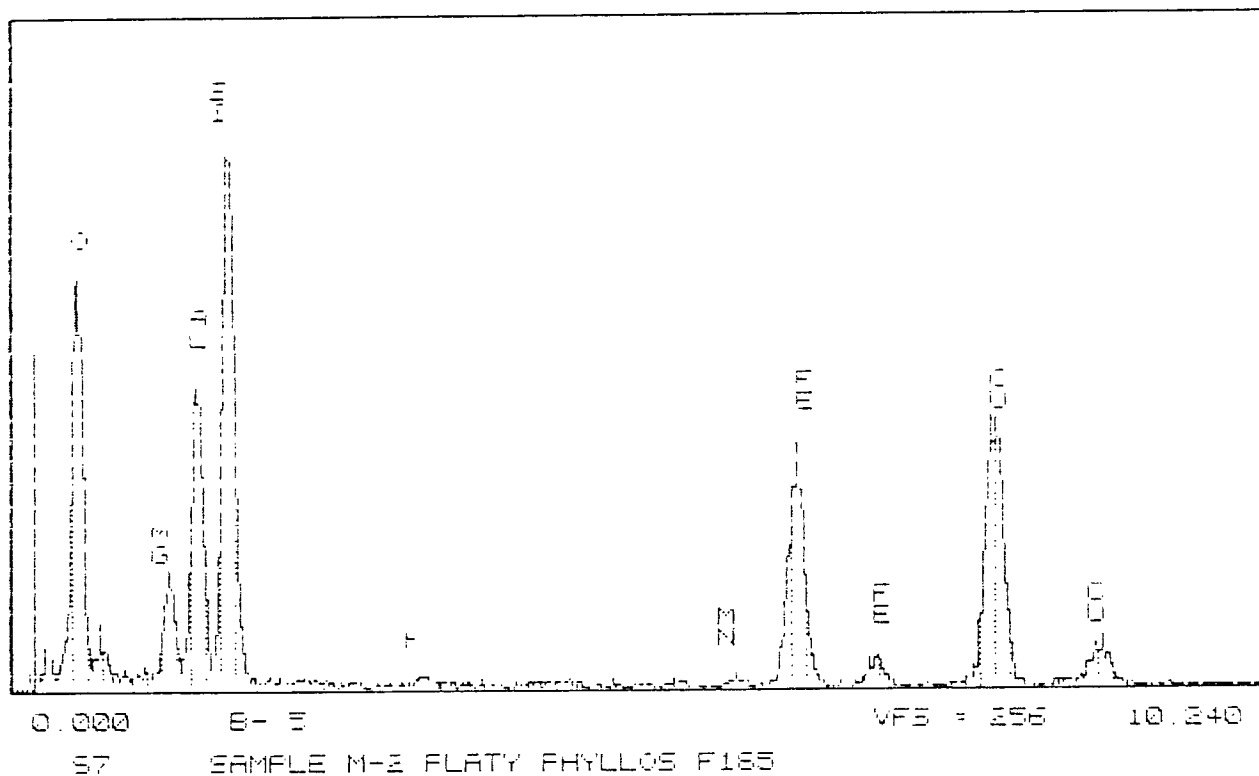


Figure 4:20. Energy-dispersive x-ray spectrum of mixed layer clay (see Fig. 4:19) in treated soil (M2A).

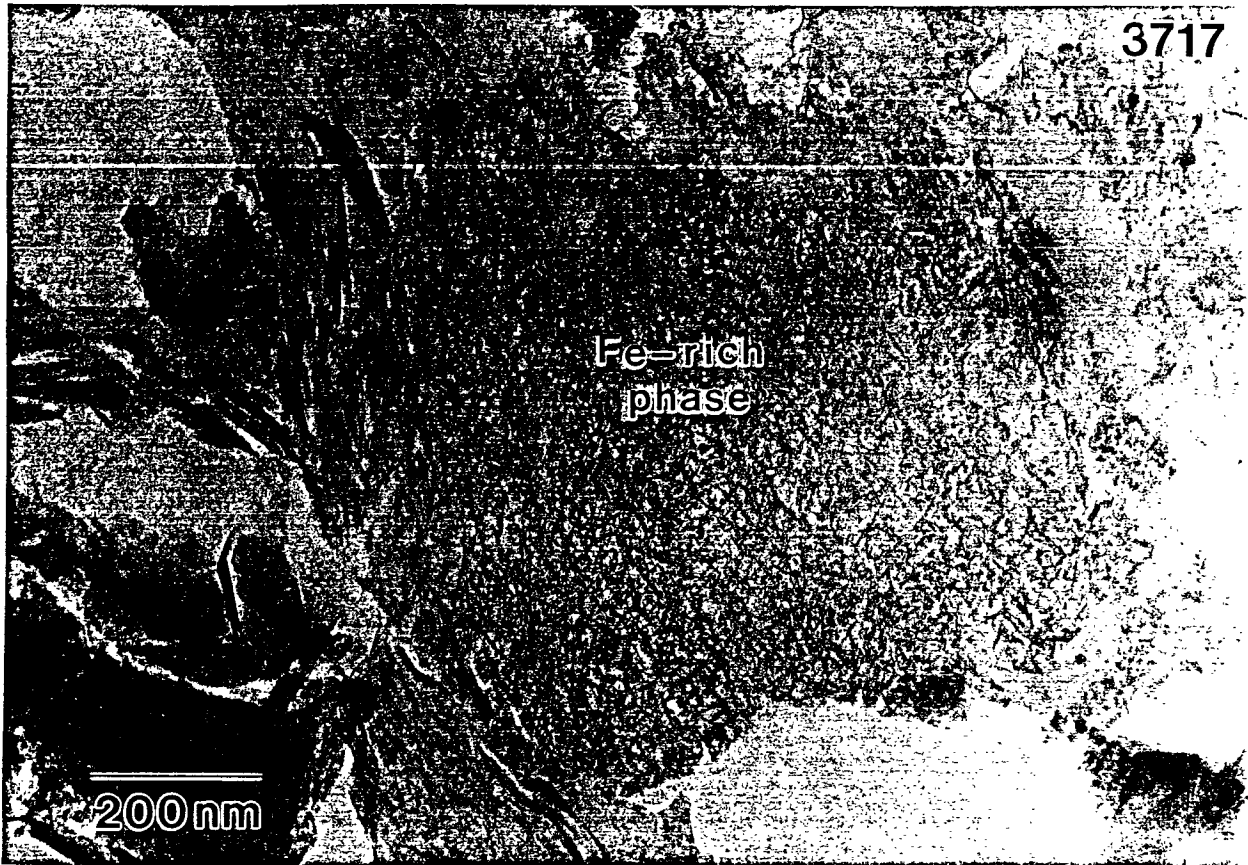


Figure 4:21. Brightfield electron micrograph of poorly-crystalline Fe-rich phase (Fe-oxide or hydroxide) in treated soil (M2A).

SERIES II

MON 21-AUG-95 17:32

Cursor: 0.000keV = 0

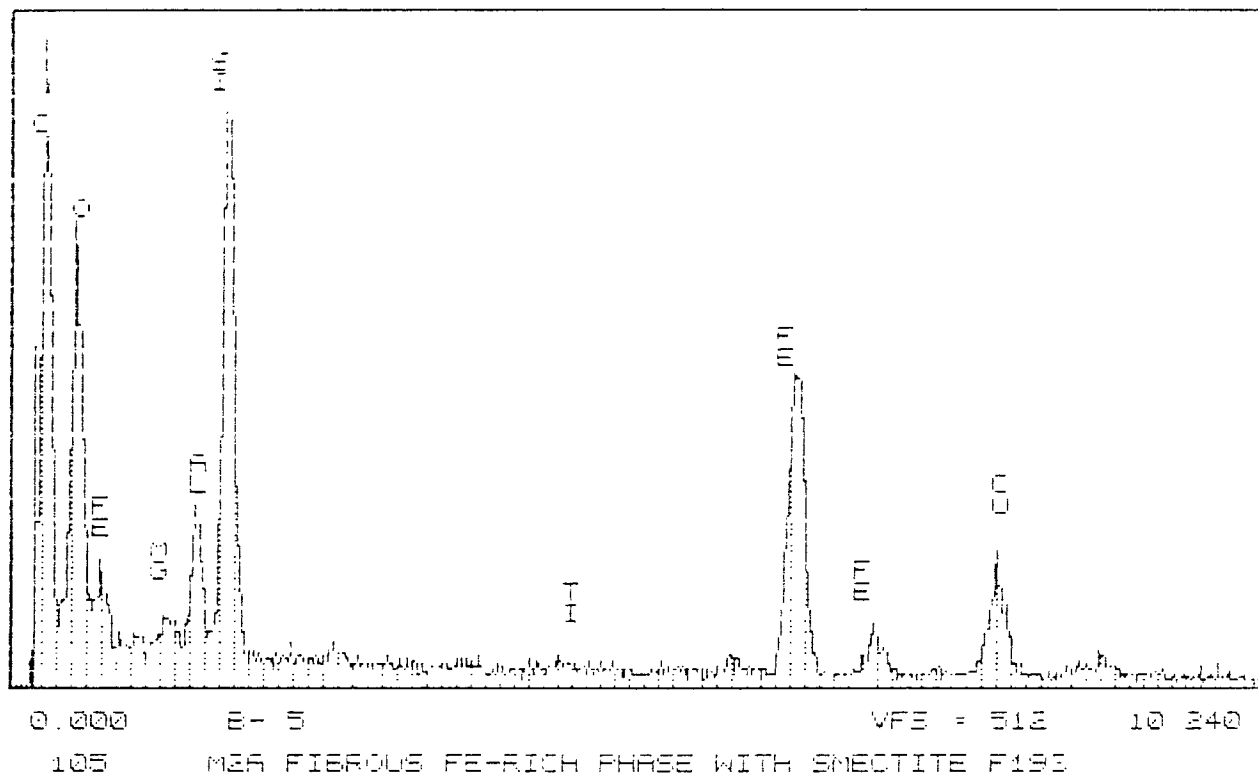


Figure 4:22. Energy-dispersive x-ray spectrum of Fe-rich phase (see Fig. 4:21) in treated soil (M2A).



Figure 4:23. Low-magnification brightfield electron micrograph of fine-grained smectite in HWT27.

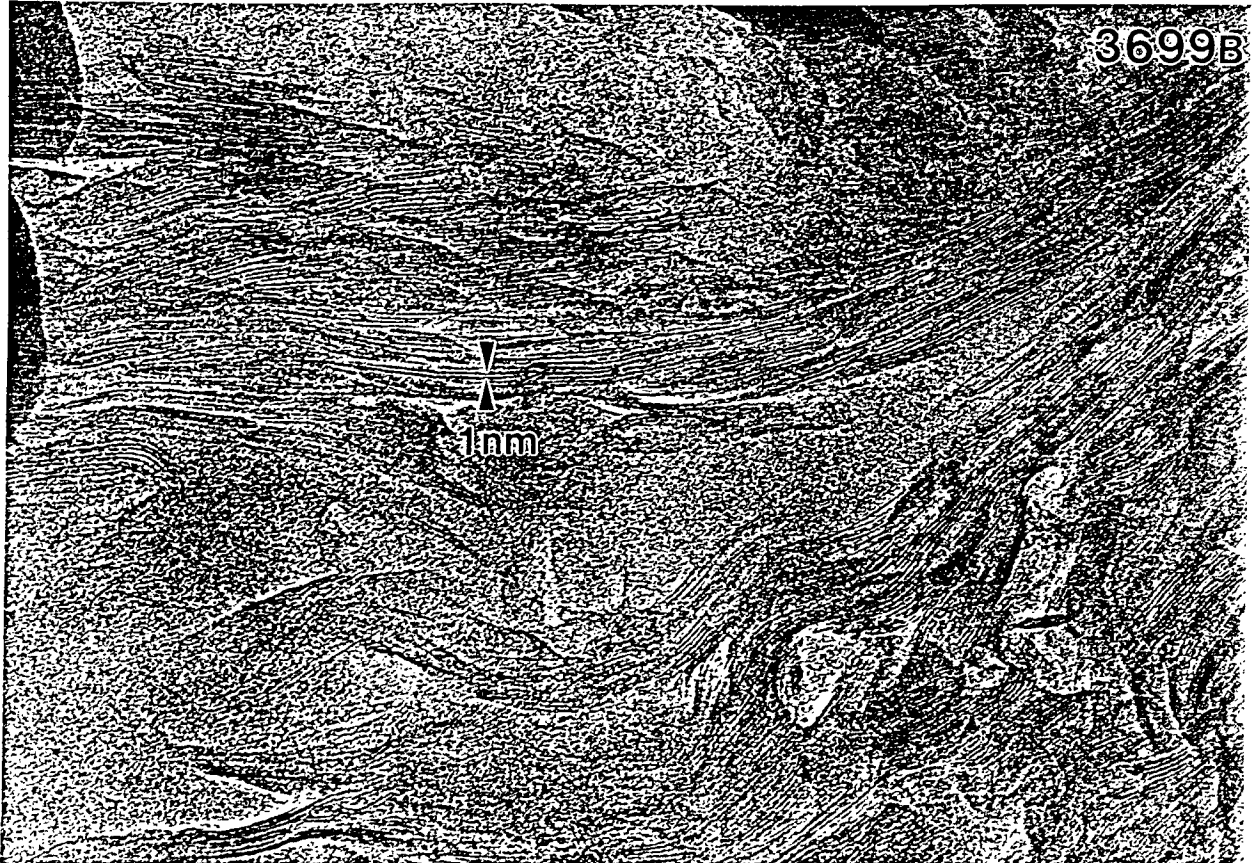


Figure 4:24. Higher magnification brightfield electron micrograph of clay in HWT27.

SERIES II

MON 21-AUG-85 17:23

Cursor: 0.000keV = 0

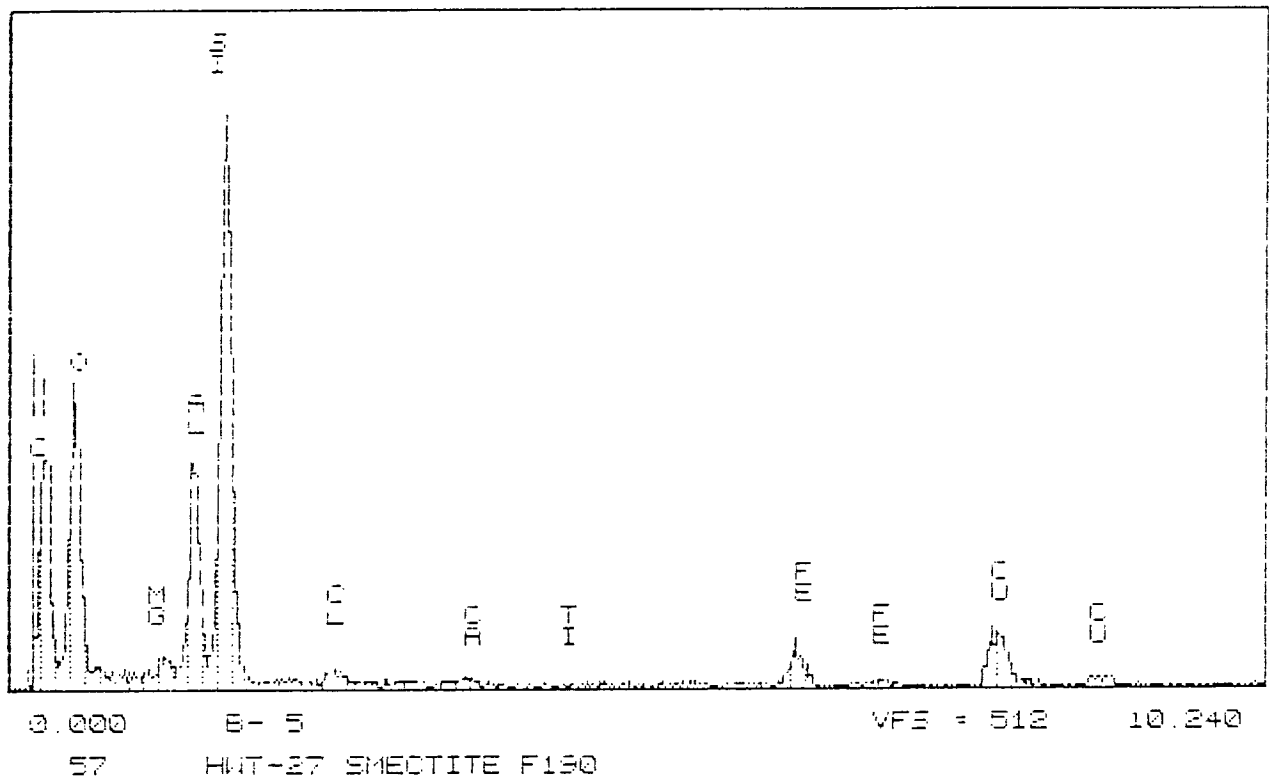


Figure 4:25. Energy-dispersive x-ray spectrum from clay in HWT27.

## Chapter 5

### Infrared (IR) microspectroscopy

**The primary purpose of IR microspectroscopy was to obtain an overall picture of the organic makeup of the untreated and treated soil and sludge. A second goal was to monitor the abundances of carbonates.**

In our original study, we observed fundamental differences between IR spectra of rapid solvent extracts from the untreated and treated soils (Appendix I). In the untreated soil, we observed band structure consistent with a mixture of aromatic and aliphatic compounds, whereas in the treated soil we observed intense carbonyl band structure and other features consistent with a relatively pure mixture of esters (Fig. 5:1).

#### Organics

In this study, we performed a more extensive and more aggressive series of solvent extractions. We found that differences between IR spectra of the untreated and treated soils became less pronounced as solvent extraction procedures were intensified. As in the original study (Fig. 5:1), we observed some differences in the spectra obtained following quick, non aggressive extractions. For example, the spectrum of a short extraction (5 minutes) of **untreated soil** (M1) suggests that the material is aromatic, but with a long aliphatic chain (Fig. 5:2). Note the C-H stretching at 3.4  $\mu\text{m}$  and wagging at 13.4  $\mu\text{m}$ . The material also shows some evidence of carbonyl functionality at  $\sim 5.8 \mu\text{m}$  (Fig. 5:2), although not nearly as dramatic as in our original study ( Fig. 5:1). Analysis of a residue obtained following a longer extraction time shows more hydrocarbon character (Fig. 5:3). Note the ratio of the carbonyl band at 5.8  $\mu\text{m}$  to that of the C-H band at 6.9  $\mu\text{m}$ . Extraction of the **treated soil** (M2) followed by IR analysis of the residue remaining following solvent evaporation, reveals significantly more carbonyl of ester character (see Fig. 5:4). The spectrum in Figure 5:4 actually resembles IR spectra of phthalates, diesters of phthalic acid. the above results indicate that carbonyl compounds are important products of the ACT treatment, and some of them (e.g. esters) appear to be highly accessible to solvent extraction.

#### Inorganics (carbonates)

IR microspectroscopy was also employed to investigate changes in the mineralogical makeup of the sludge. Figure 5:5 shows IR spectra of sludge samples before and after treatment. As expected, the dominant absorption feature in both spectra is broad Si-O stretching vibration center around 10  $\mu\text{m}$ . Additional bands at  $\sim 3$  and  $\sim 6 \mu\text{m}$  are due to H<sub>2</sub>O and a small peak at  $\sim 3.4 \mu\text{m}$  is the C-H stretch of organic C. The most significant difference between the two spectra is the appearance of intense carbonate bands in the treated sludge (Fig. 5:5).

Similar IR measurements were made on residues of ACT (HWT27) powder and a 16 PAH standard solution that had been reacted together in a highly controlled experiment. (The control experiment is described in Chapter 6, pp. 80-81). Figure 5:6 shows spectra of the HWT 27 powder before and after reaction with the PAHs. Note the appearance of intense carbonate band structure in the treated (reacted) sample.

IR microspectroscopy was also used to look at solvent extracts from the treated sludge. The purpose of the measurements was to determine whether there is any association between organic reaction products (e.g. carbonyl compounds) and a particular inorganic constituent of the HWT27 formulation (e.g. clay). Such an association could implicate a catalytically active inorganic species. Figure 5:7 shows an IR spectrum from the extract. In addition to organic C-H and C=O features, a clay-like Si-O band (peaked at ~9.8  $\mu\text{m}$ ) and carbonate bands are also present.

#### Summary of IR observations

IR spectroscopy shows that the untreated soil and sludge samples contain aromatic and aliphatic compounds. **After treatment with ACT, carbonyl compounds (e.g. esters and phthalates) and inorganic carbonates appear as major reaction byproducts** in both soils and sludges.

IR spectra from a control experiment using only the ACT formulation (HWT27) and a 16 PAH standard confirm that **a significant fraction of the PAHs in PECO soils and sludges were mineralized as carbonates.**

Spectra of solvent extracts (from the treated sludge) hint at an affinity between organic matter and clay-like silicates, which suggests that clays could be catalytically active in the ACT treatment process. However, the clay hypothesis definitely requires further investigation.

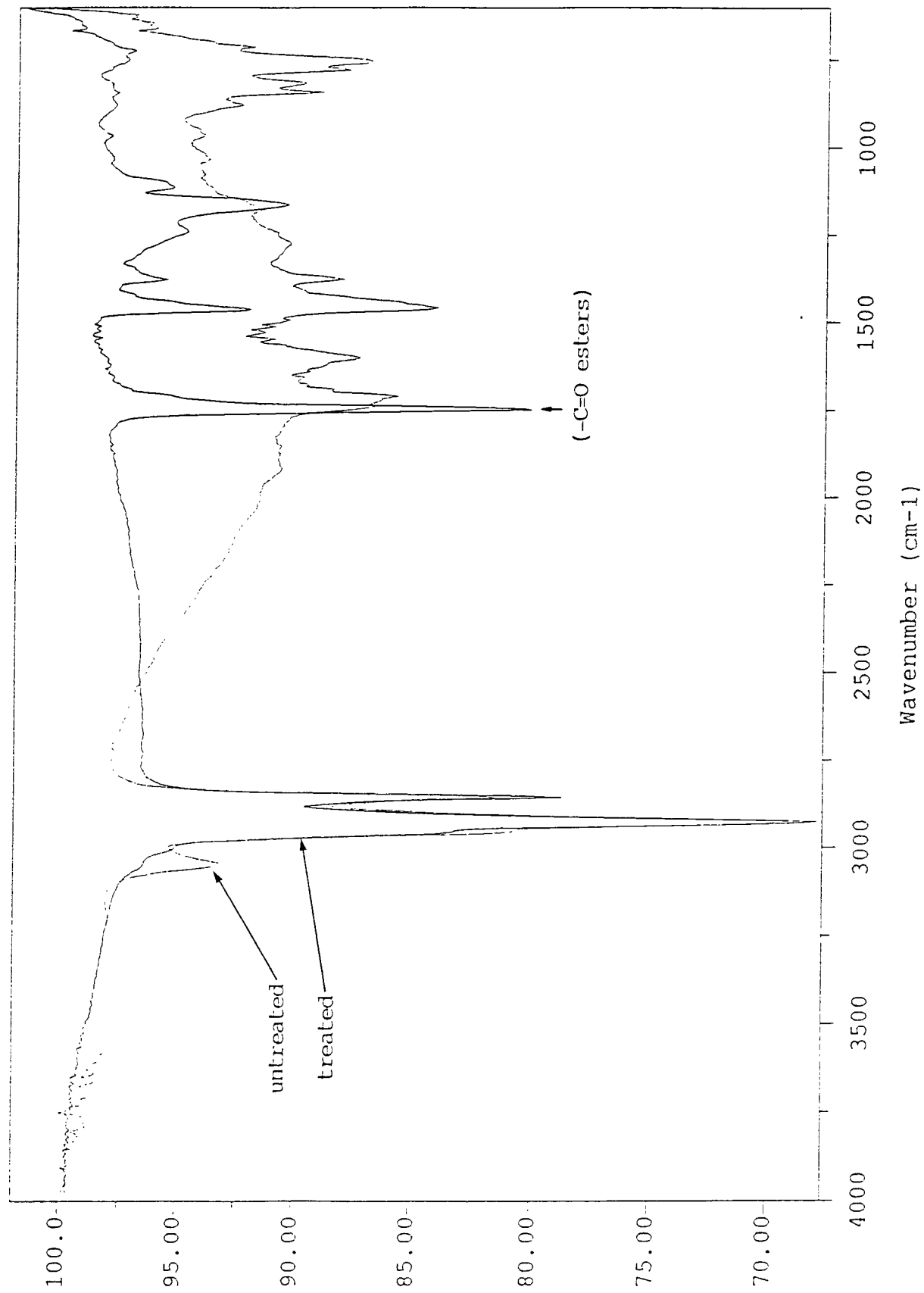


Figure 5:1. Comparison of infrared (IR) spectra from untreated and treated PECO soils after mild solvent extraction in chloroform.

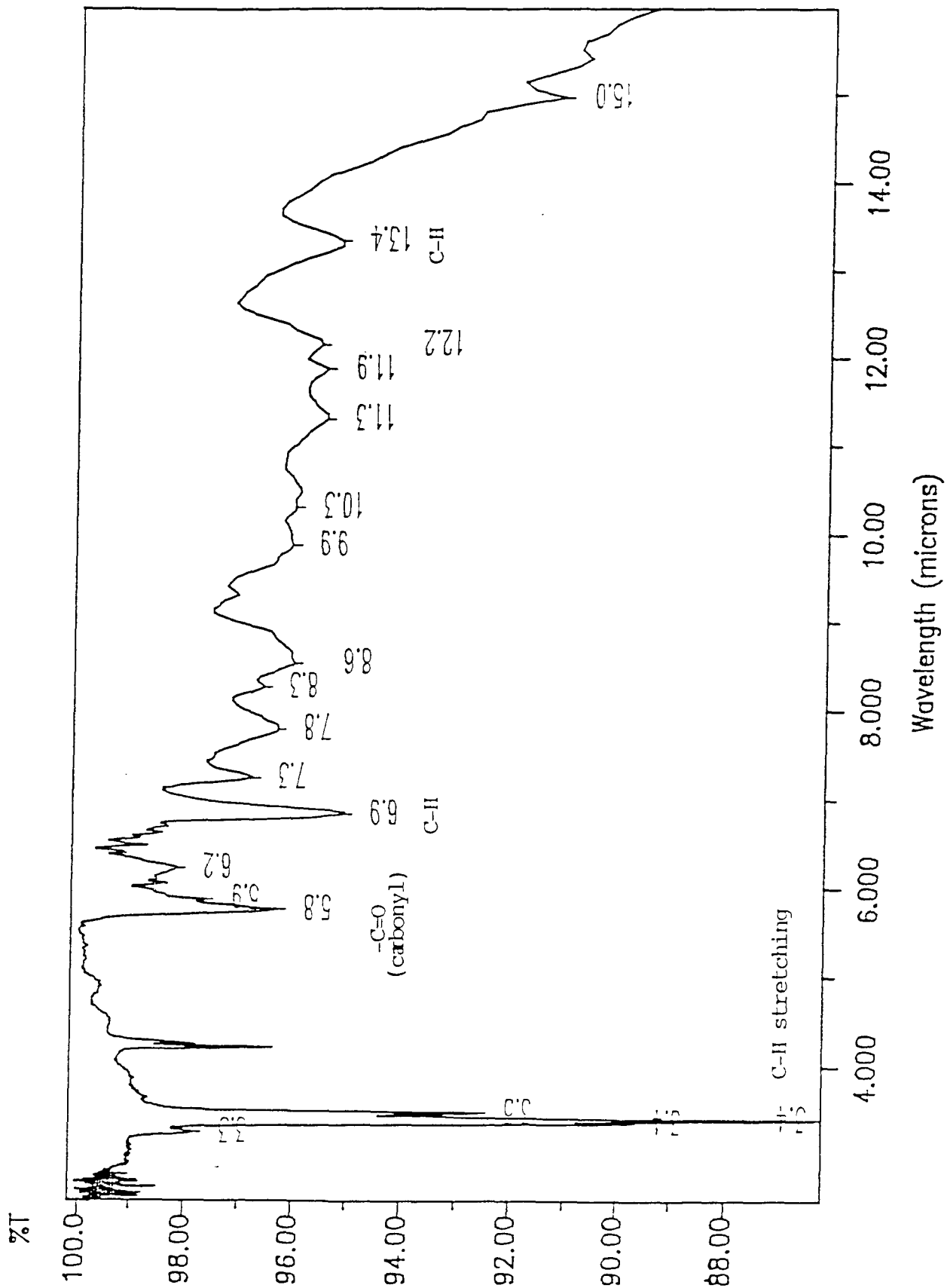


Figure 5:2. Infrared (IR) spectrum of chloroform extract from untreated PECO soil after short (~5 min) extraction interval.

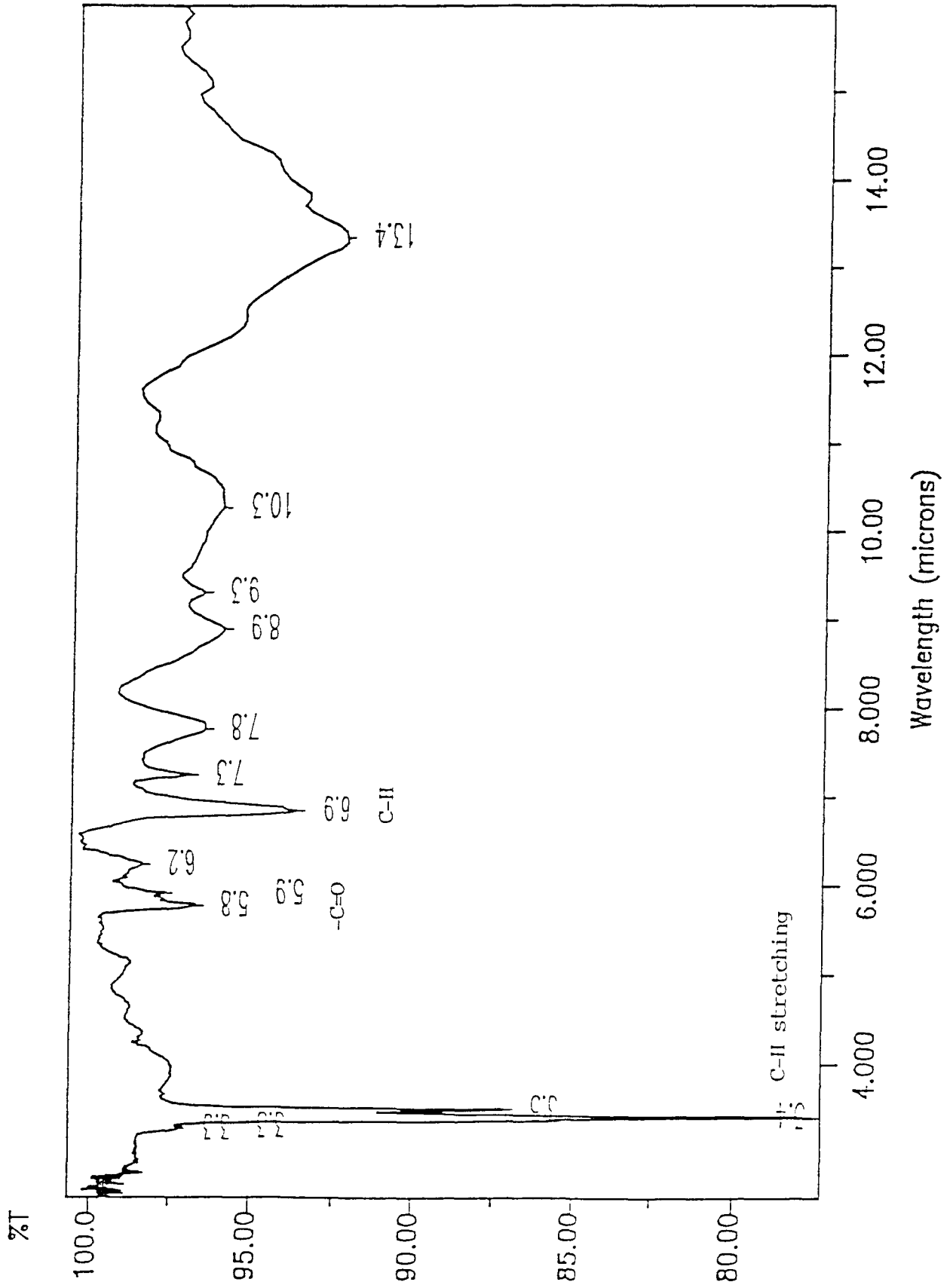
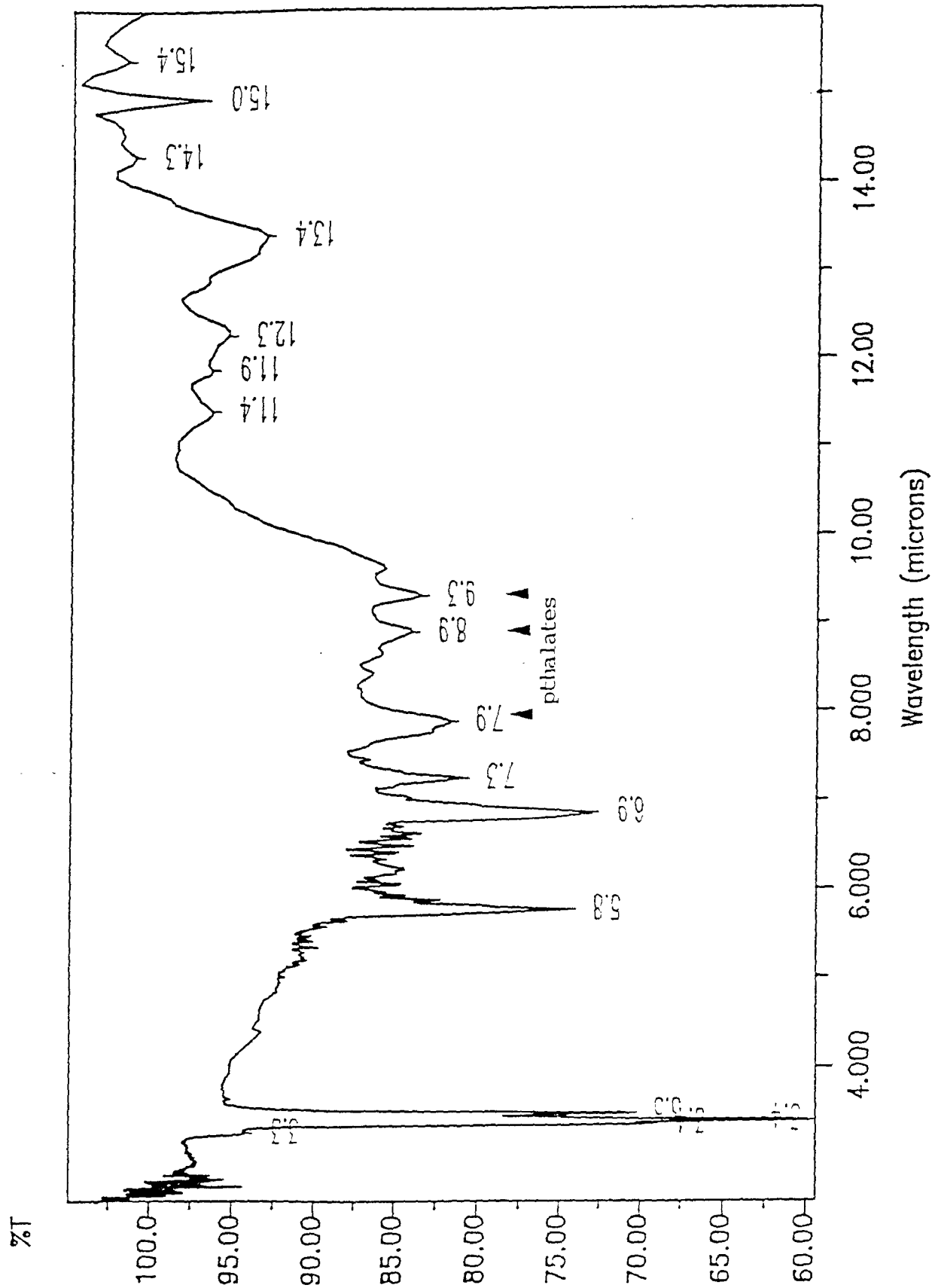


Figure 5:3. Infrared (IR) spectrum of chloroform extract from untreated PECO soil after long solvent extraction.



**Figure 5:4.** Infrared (IR) spectrum of chloroform extract from treated PECO soil. Note the relative strength of the carbonyl band at ~5.8  $\mu\text{m}$ . The 5.8  $\mu\text{m}$  band plus the bands at 7.9, 8.9, and 9.3  $\mu\text{m}$  are typical of phthalates (diesters of phthalic acid).

Infrared Spectroscopy shows that carbonates are formed during ACT treatment

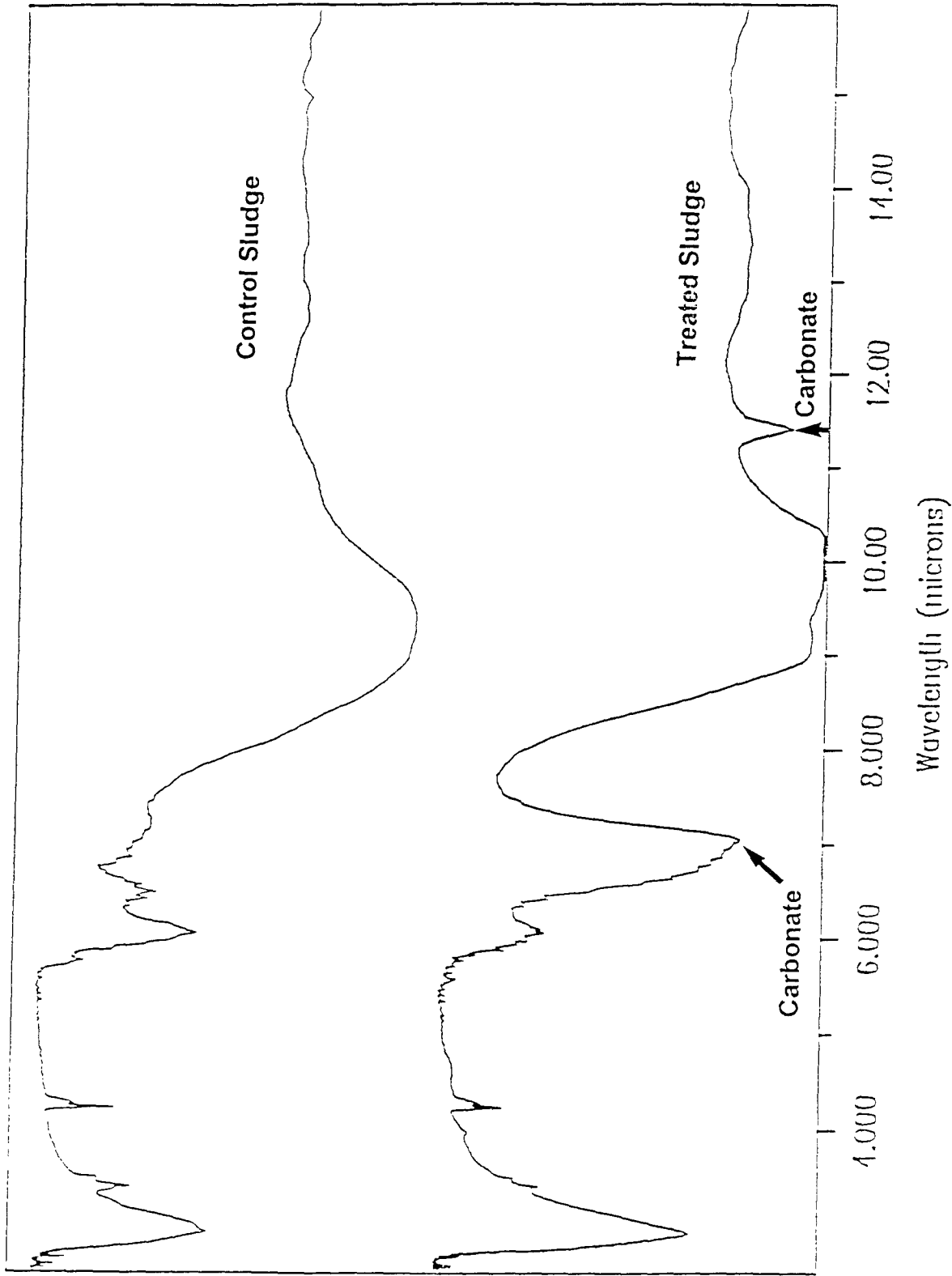


Figure 5:5. Comparison of infrared (IR) spectra of control (untreated) and treated sludges. Note the appearance of intense carbonate ( $\text{CO}_3^{2-}$ ) bands in the treated sludge.

# Infrared Spectroscopy shows that carbonates formed during HWT27/16PAH Reaction

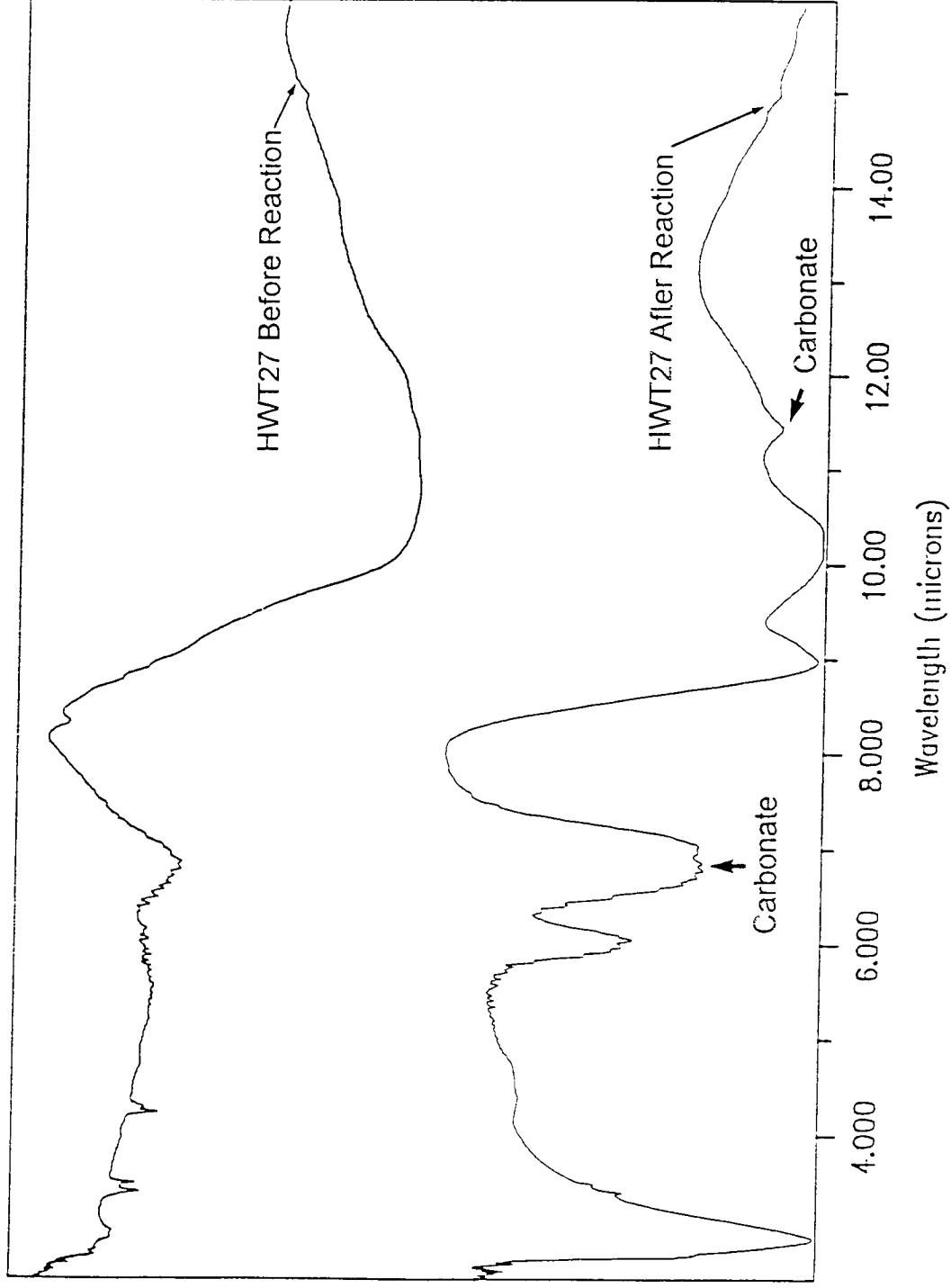


Figure 5:6. Comparison of infrared (IR) spectra of the ACT formulation (HWT27) before and after reaction with a 16 PAH standard solution (see pp. 80 and 81). Note the appearance of carbonate ( $\text{CO}_3^{2-}$ ) bands in the HWT27 after reaction with the PAHs.

Infrared spectrum of solvent extract from treated sample

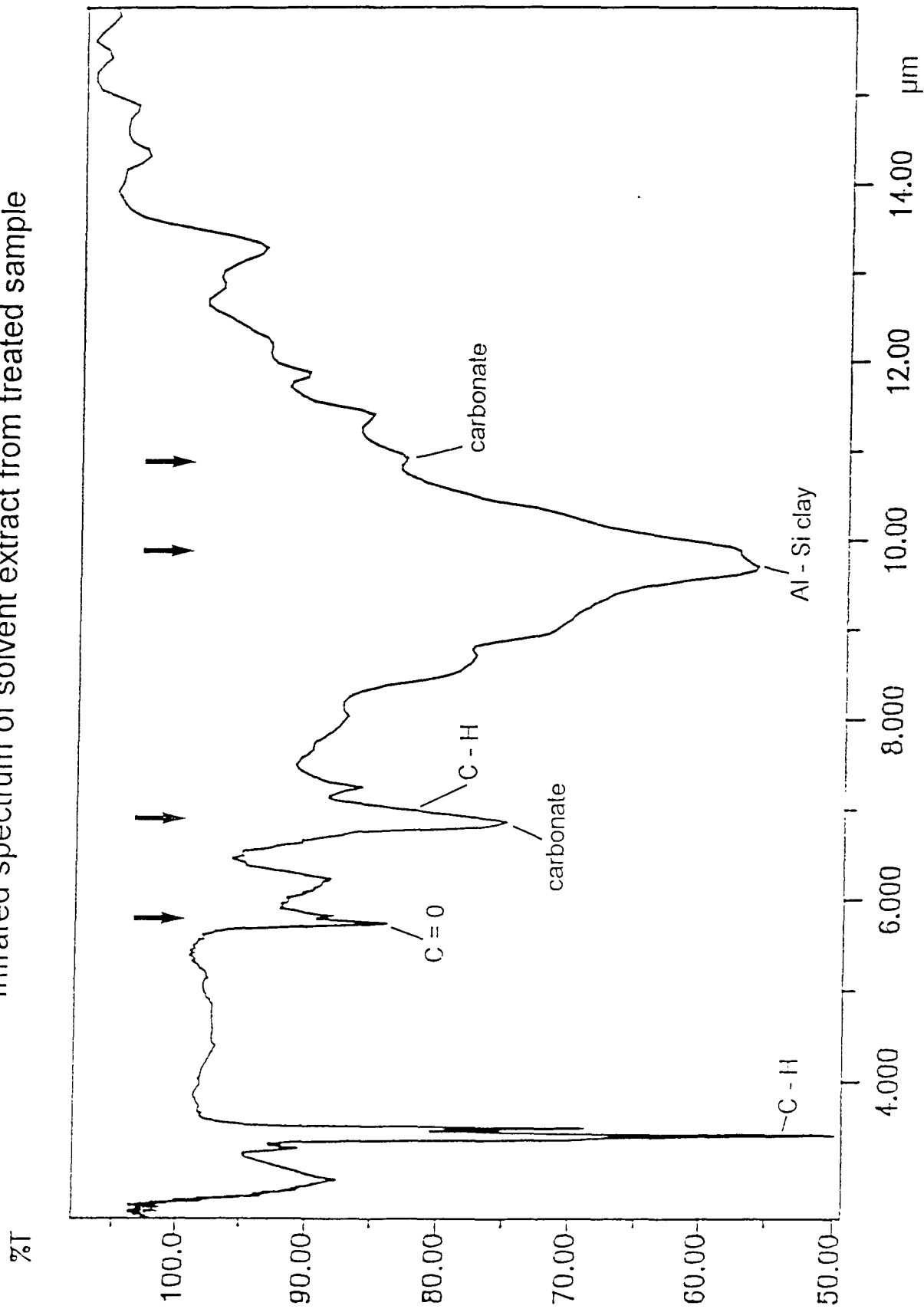


Figure 5:7. Infrared (IR) spectrum of solid residue remaining after evaporation of organic extract of treated soil sample (M2A). In addition to organic C-H and C=O bands, prominent carbonate and silicate features are present. The position of the silicate band at ~9.8 μm is consistent with clays.

## Chapter 6

### Microprobe Two-step Laser Desorption Mass Spectrometry

The purpose of laser desorption mass spectrometry was to determine the effect of ACT specifically on polyaromatic hydrocarbons (PAHs) in PECO soils and sludges. Both untreated and treated samples were analyzed for the presence of PAHs by two-step laser mass spectrometry ( $\mu\text{L}^2\text{MS}$ ) using two different preparation procedures, analysis of the "neat" powder samples and the solvent extract. For the purposes of quantitation a standard mixture of sixteen PAHs was used as a calibration for comparison with the solvent extract samples.

Two control experiments were also performed. In the first experiment, the ACT formulation (HWT27) was allowed to react with the 16 PAHs under controlled conditions. In a second experiment, (unrelated to the PECO soils and sludges), HWT27 was allowed to react with polychlorobiphenyls (PCBs).

#### 6:1 Analysis of PECO soils and sludges

##### Sample Preparation and Experimental Procedure

*Neat Powder Samples:* Approximately 0.1 gms of each sample was dry pressed into a pellet with a mean thickness of  $\sim 0.5$  mm. In the case of untreated soil (M1) and treated soil (M2), the samples were first precrushed to a uniform particle size of approximately 150  $\mu\text{m}$ . Pellets were then analyzed directly by the  $\mu\text{L}^2\text{MS}$  instrument.

*Solvent Extract Samples:* Solvent extractions were carried out with a methylene chloride ( $\text{CH}_2\text{Cl}_2$ ): benzene ( $\text{C}_6\text{H}_6$ ) (50:50) solvent mix. The extraction procedure involved the addition of 0.312 gms of sample to 2 ml of solvent mix while stirring the solution with a nickel-chrome spatula. Extractions were performed in 5 ml Pyrex sample vials which were immediately sealed after mixing using a Teflon sealing disc held tight with a Bakelite screw cap. The samples were then transferred to a hot water bath ( $35^\circ\text{C}$ ) and ultrasonicated for 5 hours. During this period the samples were periodically removed from the water bath and vigorously shaken to facilitate the extraction process. At the end of the extraction period, 0.3 ml of solvent was decanted from each vial and added to 2 gms of a standardized powder matrix containing aluminum oxide ( $\text{Al}_2\text{O}_3$ ) and glucose (50:50) in a 10 ml Pyrex beaker. A cleaned copper stirring wire was used to mix the solvent into the matrix after which time the powder was allowed to dry. Approximately 0.1 gms of this standard matrix was then pressed into a pellet using the same procedure as for the neat powder samples, and this was analyzed directly by  $\mu\text{L}^2\text{MS}$ .

*PAH Standard Sample:* For preparation of a standard PAH sample a commercial mixture (Supelco 4-8905M) of sixteen PAHs dissolved in methylene chloride:benzene (50:50) was used. The solution was diluted down to a concentration of 20 ppm per PAH and 0.3 ml added to 2 gms of standardized powder matrix and a sample pellet pressed.

*$\mu\text{L}^2\text{MS}$  Analysis:* All samples were analyzed within six minutes of introduction into the  $\mu\text{L}^2\text{MS}$  vacuum chamber. Analysis was carried out primarily at a fixed photoionization wavelength of 266 nm, however for isomer resolution of photoionization wavelength of 212 nm was also utilized. Laser desorption was in all cases achieved with a carbon

dioxide laser operating at a wavelength of 10.6  $\mu\text{m}$ , giving sample analysis area of approximately 40  $\mu\text{m}$  in diameter. For the neat powder samples 2000-shot moving averages were taken to minimize the effects of spatial inhomogenities in the samples, while 1000-shot moving averages were taken for the solvent extract samples on the standardized matrix. For all the samples identical laser desorption and ionization conditions were used. For the standard PAH sample the laser powder densities used produced almost no fragmentation of parent molecular species, giving essentially parent ion molecular spectra.

## Results

### *Total Extractable Organics:*

A 0.5 ml solvent extract was decanted from each of the solvent extract vials and allowed to evaporate to dryness on a glass Petri dishes. The involatile residue that remained after evaporation was weighed and the total concentration of extractable organic matter calculated, as shown below:

<u>Sample</u>	<u>Extractable Organic Matter (ppm)</u>
M1 (untreated)	29,500
M2 (treated)	>15,000
M4 (untreated)	98,200
M3 (treated)	34,500

### *Qualitative Observations for Neat and Solvent Extract Samples:*

Since all spectra were obtained under identical experimental conditions direct comparison between spectra is possible. In all the samples a rich distribution of aromatic species, with extensive alkylation, is observed with mass envelopes extending from 100 amu to beyond 450 amu.

The solvent extract spectra for untreated and treated sludges and soils all show a large decrease in the concentration of aromatic species between treated and untreated samples, this decrease typically ranging between 25-75% (Figs. 6:1 and 6:2). Interestingly when the difference spectra are obtained it appears that there is no introduction of new aromatic species into the treated samples. Thus while the concentration of aromatic species has been decreased in the solvent extract samples, the spectra provide no clue as to possible breakdown products or breakdown pathways.

The neat powder samples of the untreated soil and sludge show a one to one correspondence with their respective solvent extract spectra indicating the extraction process for the untreated samples faithfully represents the true distribution of PAHs in the original sample (Figs. 6:3 and 6:4). This however is not the case for the treated samples, where it appears that a substantial concentration of low mass PAHs (100 amu - 178 amu) are observed in the treated neat samples but not the treated solvent extract samples. The implication is that there is an organic component within the treated samples that is highly resistive to exhaustive solvent extraction. Since these low mass PAHs also show a large enrichment in concentration relative to the untreated samples, they presumably must of been formed as a consequence the chemical treatment process. This argument is further supported by the observation that this effect is most

apparent between the untreated sludge (M4) and treated sludge (M3) samples, which also appear to show the most dramatic reduction in the concentration of the middle to higher molecular weight PAHs (>200 amu).

#### *Quantitative Observations for Neat and Solvent Extract Samples:*

Since the intensity of a peak observed in the spectra obtained by  $\mu\text{L}^2\text{MS}$  depends both on the concentration of the species present and its photoionization cross-section, exact quantitation requires careful comparison with standards. Fortunately, relative comparisons between samples at the same photoionization wavelength depends only on concentration, Table 6:1 summarizes the percentage change in the main aromatic species as a result of treatment for both neat and solvent extract samples.

Exact quantitation was attempted for several PAH species in the sludge samples M3 and M4. Calibration of the instrument was achieved by comparison of the solvent extract signals with the standard sample. The mass spectra of the three calibrated species, fluorene, phenanthrene and pyrene, are shown in Figure 6:5(a). All the PAH concentrations in the standard are identical and the variation in peak intensities reflects the differing photoionization cross-sections of these PAHs. For phenanthrene and pyrene there are possible isomeric interferences from anthracene and fluoranthene respectively. Even though phenanthrene and pyrene are both the thermodynamically favored isomers it was necessary to establish whether these isomeric interferences would be significant. Isomeric resolution can be achieved by using two photoionization laser wavelengths and taking advantage of the fact that each isomer has a different wavelength dependent photoionization cross-section. Preliminary measurements using 266 nm and 212 nm established that phenanthrene is approximately three times more abundant in concentration than anthracene and similarly pyrene is approximately three times more abundant than fluoranthene, for the untreated sludge sample M4. Further accuracy is unnecessary since at 266 nm the photoionization cross-section for phenanthrene is 19.1 times greater than that of anthracene, and pyrene is 23.0 times greater than that of fluoranthene. Thus at 266 nm isomeric interferences from anthracene and fluoranthene are essentially negligible. The results of the quantitative analysis are illustrated in Figure 6:5(b).

### **6:2 Control Experiment A: *Effect of ACT on Polycyclic Aromatic Hydrocarbons (PAHs).***

#### **Outline:**

This experiment was aimed at evaluating the effect of ACT (HWT27) on a standard mixture of sixteen polycyclic aromatic hydrocarbons (PAHs) classified by the Environmental Protection Agency (EPA) as priority pollutants (Supelco 4-8905M) (see Figure 6:6).

#### **Experimental Details:**

Two samples mixtures were prepared, one containing HWT-27 powder, and the other an equivalent volume of aluminum oxide ( $\text{Al}_2\text{O}_3$ ) powder (99.5%) with similar mean particle size and thus a similar effective surface area. Each sample was mixed into a fine slurry with the addition of water and a methylene chloride ( $\text{CH}_2\text{Cl}_2$ ): benzene ( $\text{C}_6\text{H}_6$ ) mixture containing the EPA standards.

### Slurry 1 (HWT-27)

### Slurry 2 (Al<sub>2</sub>O<sub>3</sub>)

1 ml nanopure (2x distilled) H<sub>2</sub>O

1 ml nanopure (2x distilled) H<sub>2</sub>O

1 ml CH<sub>2</sub>Cl<sub>2</sub>:C<sub>6</sub>H<sub>6</sub> mix with 16 PAHs each at 20 ppm concentration

1 ml CH<sub>2</sub>Cl<sub>2</sub>:C<sub>6</sub>H<sub>6</sub> mix with 16 PAHs each at 20 ppm concentration.

1 ml (vol.) HWT-27 powder

1 ml (vol.) Al<sub>2</sub>O<sub>3</sub> powder

Two 5 ml Pyrex glass sample vials were used to contain each slurry. After each sample had been mixed thoroughly using a cleaned nickel-chrome spatula, the samples vials were sealed from the atmosphere using a Teflon sealing disc held tight with a Bakelite screw cap. Both samples were then simultaneously placed in a hot water bath (~ 35°C) and ultrasonicated for 24 hours. During this time each of the samples vials were periodically removed from the water bath and vigorously shaken to minimize settling of the slurry.

At the completion of the experiment each sample vial was opened and a further 2 ml of benzene added and the slurry agitated before the benzene solution was allowed to separate out over the course of 15 minutes. During this time the sample vials were resealed. Since the density of benzene (d=0.8787) is lower than that of water and benzene is not miscible with water, the benzene layer separated out at the top of the slurry. Next, 0.3 ml of this benzene solution was decanted from the top of each slurry and added to 2 gms of a standardized powder matrix containing aluminum oxide and glucose (50:50) in a 10 ml Pyrex beaker. A cleaned copper stirring wire was used to mix the benzene into the standard matrix after which time the powder was allowed to dry. Approximately 0.1 gm of the standard matrix was then pressed into a pellet ~ 0.5 mm thick and analyzed immediately by microprobe two-step laser mass spectrometry (μL<sup>2</sup>MS). Additionally the HWT-27 and aluminum oxide were recovered from both sample vials, dried and pellets ~ 0.5 mm thick made from each and these were also analyzed by μL<sup>2</sup>MS.

### Results:

Figure 6:7 illustrates the salient features of the analysis. In the benzene extracts, a decrease in the concentration of the sixteen standard PAHs of approximately 75% is observed in the sample containing the HWT-27 powder relative to that of the inert aluminum oxide sample. It is interesting to note that while the HWT-27 appears to have "destroyed" the PAHs there is no evidence of intermediate breakdown products of an *aromatic nature* in the benzene extracts (see Fig. 6:7). However, subsequent analysis of the recovered HWT-27 powder does show, in addition to the peaks assignable to the initially introduced PAHs, further peaks that would appear to represent intermediate breakdown products from the destruction of the standard PAHs (Figs. 6:8 & 6:9). These new PAH species include phenol (C<sub>6</sub>H<sub>6</sub>OH) and styrene (C<sub>6</sub>H<sub>6</sub>-CH<sub>2</sub>=CH<sub>2</sub>) and their alkylated homologues. Why these PAHs are not observed in the benzene extract is unclear, though it presumably has something to do with the mechanism by which HWT-27 effects PAHs breakdown. Perhaps carbonate formation effectively encapsulates or otherwise traps PAH breakdown products (see Chapters 3 & 4). At this point it should also be noted that a similar effect is now observed with soil and sludge samples that have been treated with ACT (Figs. 6:1 through 6:4). No such new PAH species are observed from the aluminum oxide pellet which is the anticipated result since this should be incapable of effecting PAH degradation.

### 6:3 Control Experiment B: *Effect of ACT on polychlorobiphenyls (PCBs).*

#### Outline:

To assess the effect of the treatment of HWT27 powder on the polychlorinated biphenyl Aroclor 1242 dissolved in isooctane under both anhydrous and hydrous reaction conditions.

#### Experimental Procedure:

Two anhydrous sample mixtures were prepared, one containing HWT-27 powder, and the other the control using equivalent volume of aluminum oxide ( $\text{Al}_2\text{O}_3$ ) powder (99.5%). The aluminum oxide was selected as a control since under the given reaction conditions it is inert and it had a similar mean particle size to the HWT-27 powder and thus a similar effective surface area. The samples were slurried with an equal volume of isooctane ( $\text{C}_8\text{H}_{18}$ ) solution, containing the polychlorinated biphenyl (PCB) Aroclor 1242 ( $\approx\text{C}_{12}\text{H}_{6.9}\text{Cl}_{3.1}$ ), in a 0.3 ml Pyrex glass vial.

Hydrous Slurry 1 (HWT027)	Hydrous Slurry 2 ( $\text{Al}_2\text{O}_3$ )
0.07 ml (vol.) (0.0484 g) HWT-27 powder	0.07 ml (vol.) (0.0957 g) $\text{Al}_2\text{O}_3$ powder
0.1 ml isooctane with Aroclor 1242 at 1000 ppm	0.1 ml isooctane with Aroclor 1242 at 1000 ppm
0.1 ml nanopure (2x distilled) $\text{H}_2\text{O}$	0.1 ml nanopure (2x distilled) $\text{H}_2\text{O}$

After the additional twenty four hours the sample mixtures in each vial were allowed to separate out. Since the density of isooctane is lower than that of water and isooctane is not miscible with water the organic phase separates out to the top of the reaction mixture and a 0.05 ml aliquot was extracted and evaporated on to a cleaned quartz disc which was then subsequently analyzed by  $\mu\text{L}^2\text{MS}$ .

#### Results:

Figures 6:10 through 6:12 illustrate the salient features of the analysis. Figure 6:10 is a mass spectrum of the Aroclor "as received". Under anhydrous conditions there is no observable degradation of the PCBs within experimental error, in that the mass spectra of the recovered Aroclor 1242 solution from both the control ( $\text{Al}_2\text{O}_3$ ) and the HWT-27 reaction vials show identical spectral distributions characteristic of neat Aroclor 1242 (cf. Figs. 6:10 & 6:11). There is no evidence of degradation of any of the chlorinated biphenyl structures or the generation of any aromatic decomposition products. This is consistent with visual observation of the reaction mixtures which showed no evidence of reaction, for example evolved gases, color changes and so on. Under hydrous conditions, however, there is clear evidence of chemical degradation, both in the mass spectra and by visual observation. Visually the hydrous HWT-27 slurry developed a gelatinous phase appearing at the water-isooctane interface, while the HWT-27 powder seemed to darken noticeably in color. The mass spectra while showing peaks characteristic of Aroclor 1242 also show numerous other peaks of similar intensity, many of which represent organic chlorinated species with at least partial aromatic character as evidenced by their isotopomer distributions (Fig. 6:12). The presence of chlorinated dibenzofurans appears likely although peak complexity makes unambiguous assignment difficult. The observation of simple non-chlorinated

aromatic hydrocarbons, most notably phenanthrene (C<sub>14</sub>H<sub>10</sub>) and pyrene (C<sub>16</sub>H<sub>10</sub>) maybe due to the trace impurities present within the neat Aroclor 1242 solution although there intensity would not rule out these species as possible decomposition products. The hydrous Al<sub>2</sub>O<sub>3</sub> control showed no evidence of reaction with a mass spectrum identical to neat Aroclor 1242, which is the anticipated result since Al<sub>2</sub>O<sub>3</sub> should be incapable of effecting PAH degradation.

$\mu\text{L}^2\text{MS}$  Analysis of Soil Samples M1 and M2, and Sludge Samples M3 and M4

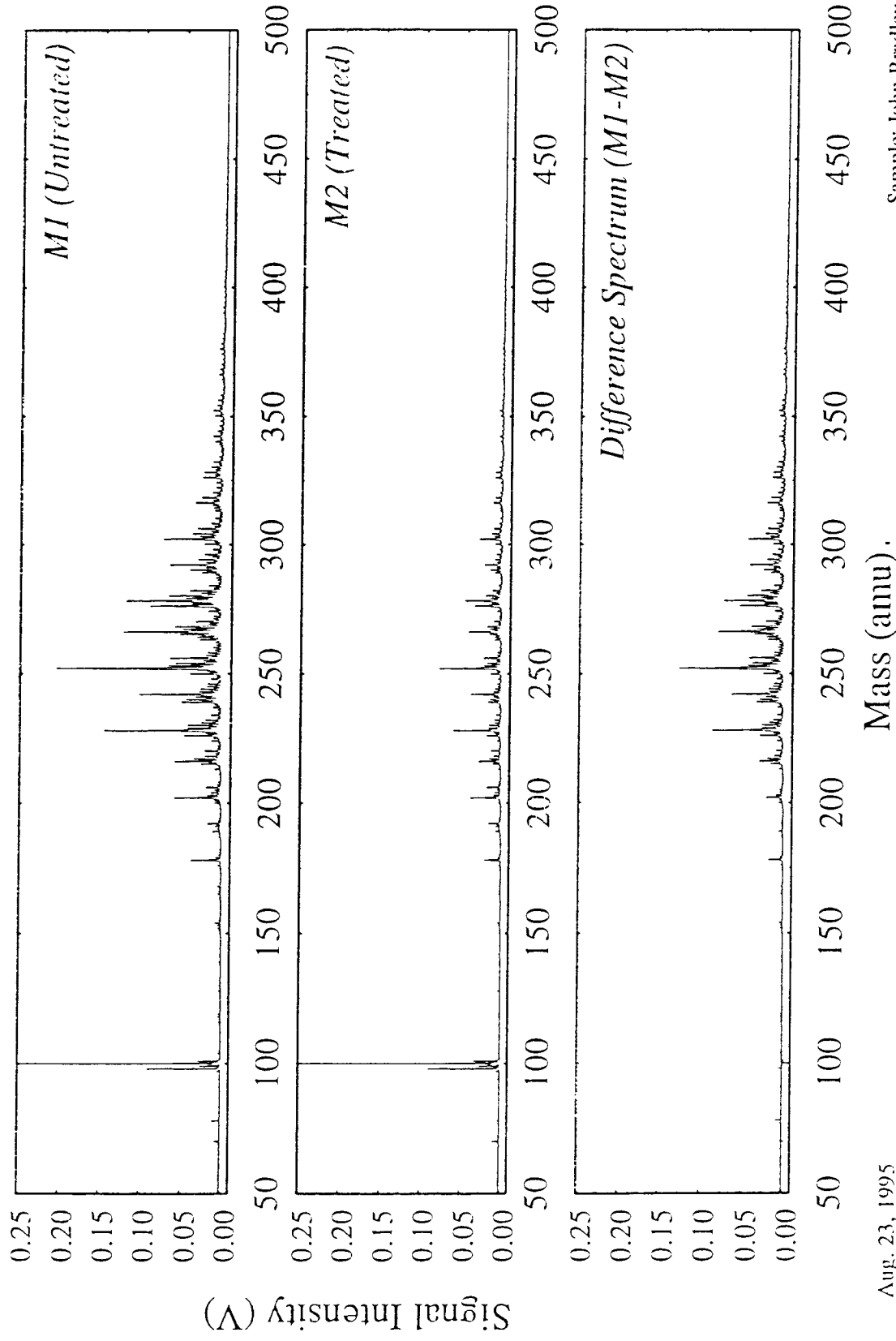
Table 6:1

Aromatic Species (amu)	$\Delta(\text{M1},\text{M2})_{\text{Extract}} (\%)$	$\Delta(\text{M1},\text{M2})_{\text{Nent}} (\%)$	$\Delta(\text{M4},\text{M3})_{\text{Extract}} (\%)$	$\Delta(\text{M4},\text{M3})_{\text{Nent}} (\%)$
Naphthalene (128)	4	75	55	-620
1-Alkyl Naphthalene (142)	3	37	63	-970
Acenaphthene (154)	55	50	80	-121
Fluorene (166)	50	34	81	-4
Acenaphthylene (168)	55	40	80	-51
Phenanthrene (178)	46	-32	80	-34
1-Alkyl Phenanthrene (192)	13	-34	82	-32
Pyrene (202)	35	28	75	8
2-Alkyl Phenanthrene (206)	9	26	75	-21
1-Alkyl Pyrene (216)	51	60	74	48
3-Alkyl Phenanthrene (220)	43	46	74	1
Chrysene (228)	59	74	63	56
Benzo(a)anthracene (228)				
2-Alkyl Pyrene (230)	62	72	76	55
4-Alkyl Phenanthrene (234)	50	62	71	38
1-Alkyl Chrysene (242)	62	73	63	57
+ Parent Isomers				
Benzo(b)fluoranthene (252)	61	76	61	65
Benzo(k)fluoranthene (252)				
Benzo(a)pyrene (252)				
1-Alkyl Benzo(a)pyrene (266)	65	80	67	69
+ Parent Isomers				
Benzo(ghi)perylene (276)	60	76	57	64
Indeno(1,2,3-cd)pyrene (276)				
Dibenzo(a,h)anthracene (278)	61	74	54	61

# Solvent Extracts: Samples M1 (Untreated) and M2 (Treated)

Extraction Procedure: 0.312 gms sample to 2 ml  $\text{CH}_2\text{Cl}_2:\text{C}_6\text{H}_6$  (50:50), 5 hrs at 35C

10.6  $\mu\text{m}$  Desorbition / 266 nm Photoionization, 1000-Shot Moving Average



Aug. 23, 1995

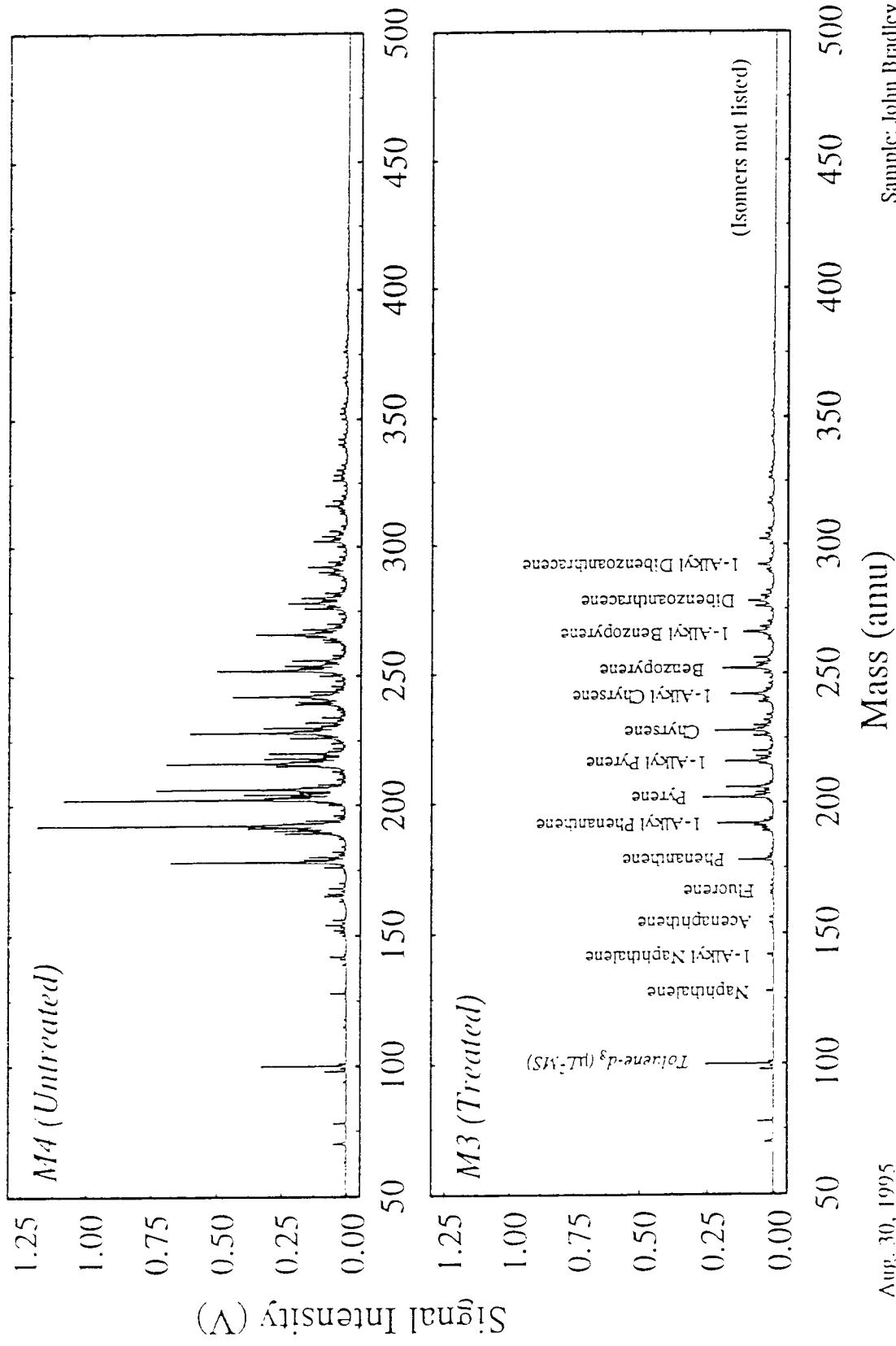
Sample: John Bradley

**Figure 6:1.** Comparison of laser desorption mass spectra of solvent extracts from untreated (M1) and treated (M2) PECO soil. Lower difference spectrum illustrates the mass reduction of PAHs in PECO soil (solvent extracts) resulting from the ACT treatment.

# Solvent Extracts: Samples M4(Untreated) and M3 (Treated)

Extraction Procedure: 0.312 gms sample to 2 ml  $\text{CH}_2\text{Cl}_2:\text{C}_6\text{H}_6$  (50:50), 5 hrs at 35C

10.6  $\mu\text{m}$  Desorbion / 266 nm Photoionization, 1000-Shot Moving Average



Aug. 30, 1995

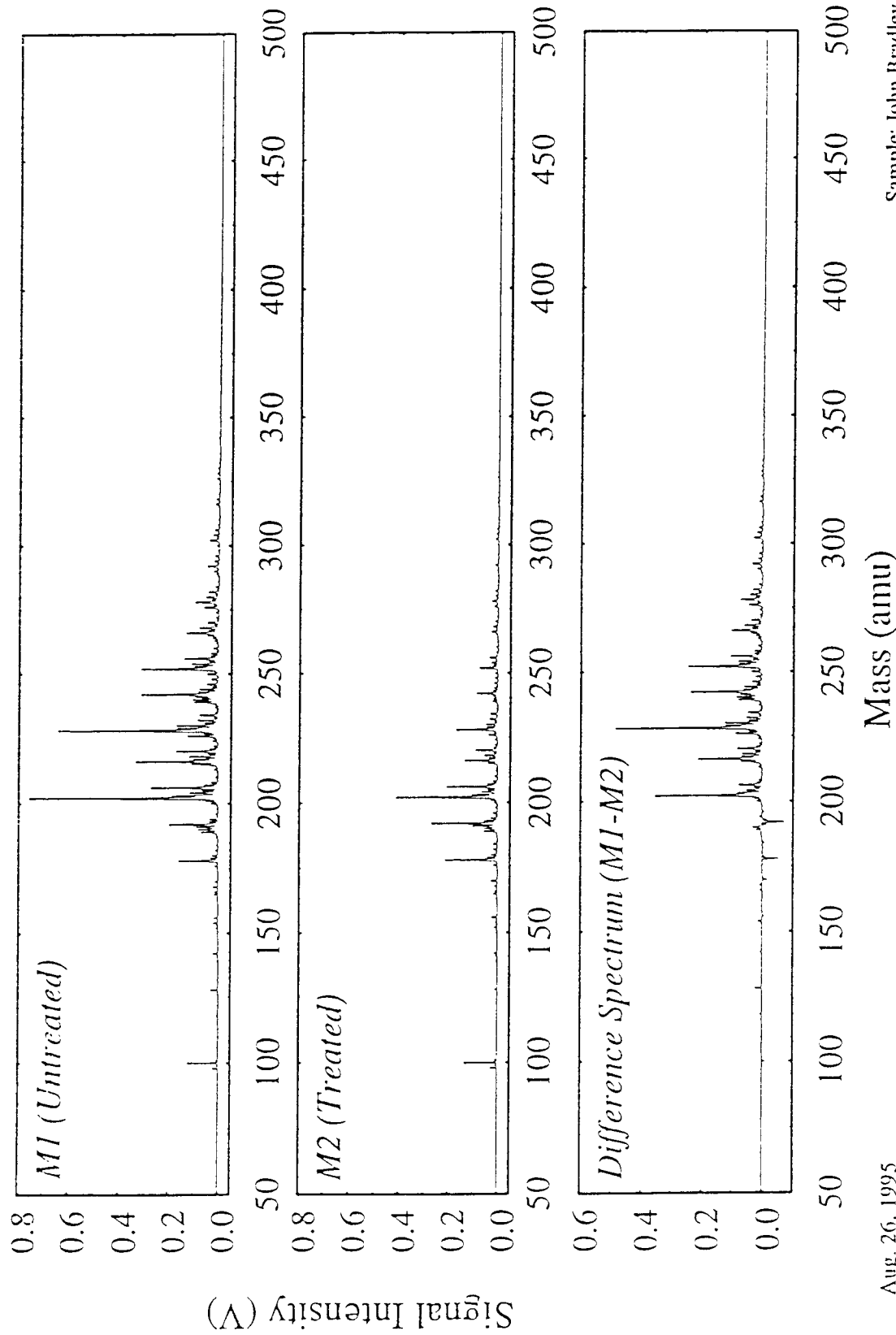
Sample: John Bradley

Figure 6:2. Comparison of laser desorption mass spectra of solvent extracts from untreated (M4) and treated (M3) PECO sludges.

# Neat Powder: Samples M1 (Untreated) and M2 (Treated)

Sample Preparation: Approx. 0.1 gms sample pressed into pellet 0.5 mm thick

10.6  $\mu\text{m}$  Desorbition / 266 nm Photoionization, 2000-Shot Moving Average



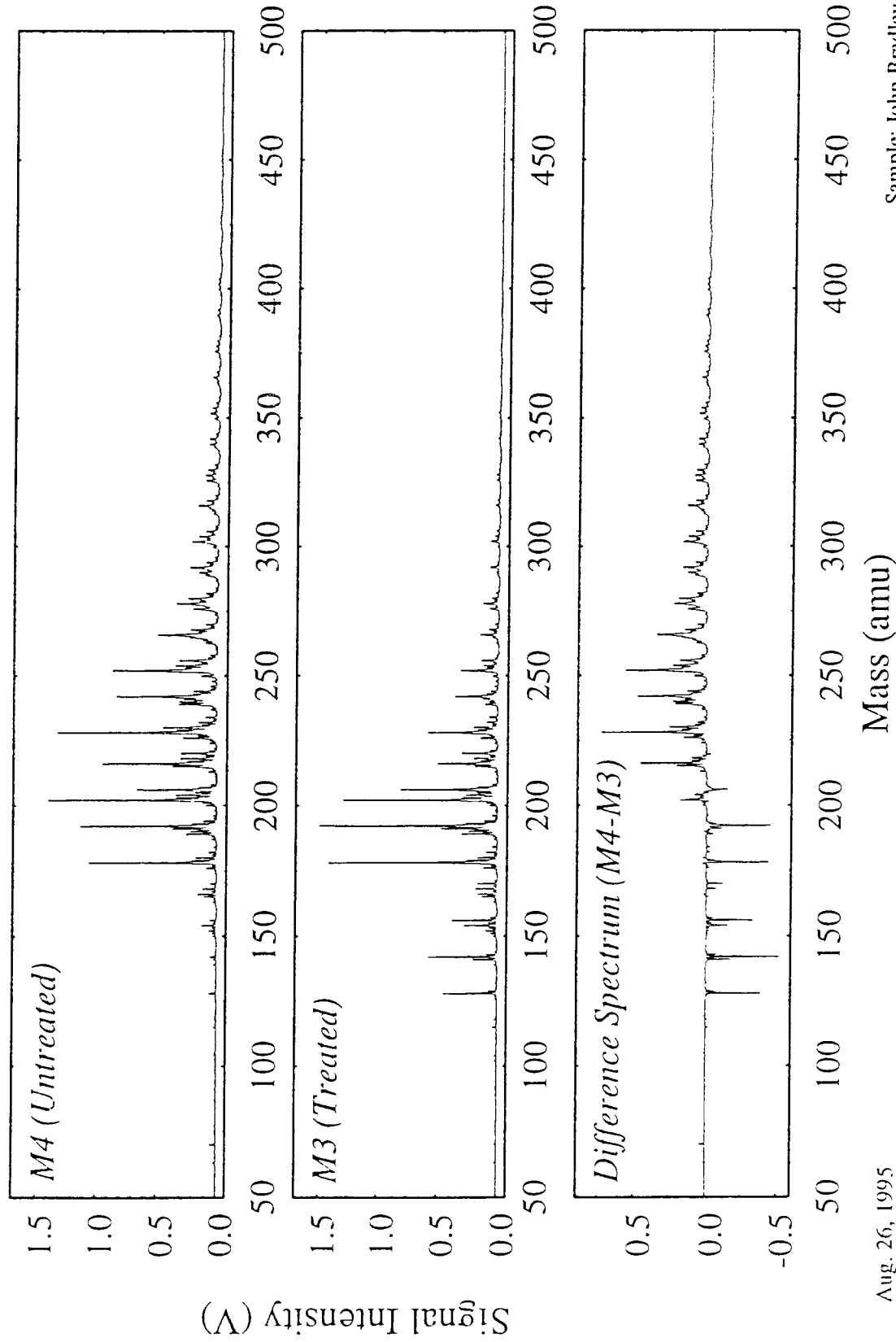
Aug. 26, 1995

Sample: John Bradley

**Figure 6:3.** Comparison of laser desorption mass spectra of neat powders of untreated (M1) and treated (M2) PECO soil. Lower difference spectrum illustrates the mass reduction of PAHs in PECO soil resulting from ACT treatment. The negative trace of several PAHs (at < 200 amu) in the difference spectrum indicates that their abundance has actually increased as a result of the ACT treatment.

# Neat Powder: Samples M4 (Untreated) and M3 (Treated)

Sample Preparation: Approx. 0.1 gms sample pressed into pellet 0.5 mm thick  
10.6  $\mu\text{m}$  Desorbion / 266 nm Photoionization, 2000-Shot Moving Average



Aug. 26, 1995

Sample: John Bradley

**Figure 6:4.** Comparison of laser desorption mass spectra of neat powders of untreated (M4) and treated (M3) PECO sludge. Lower difference spectrum illustrates the mass reduction of PAHs in PECO sludge resulting from ACT treatment. The negative trace of several PAHs (at < 225 amu) in the difference spectrum indicates that their abundance has actually increased as a result of the ACT treatment.

## Mass Spectra of Calibration Species in Standard Sample

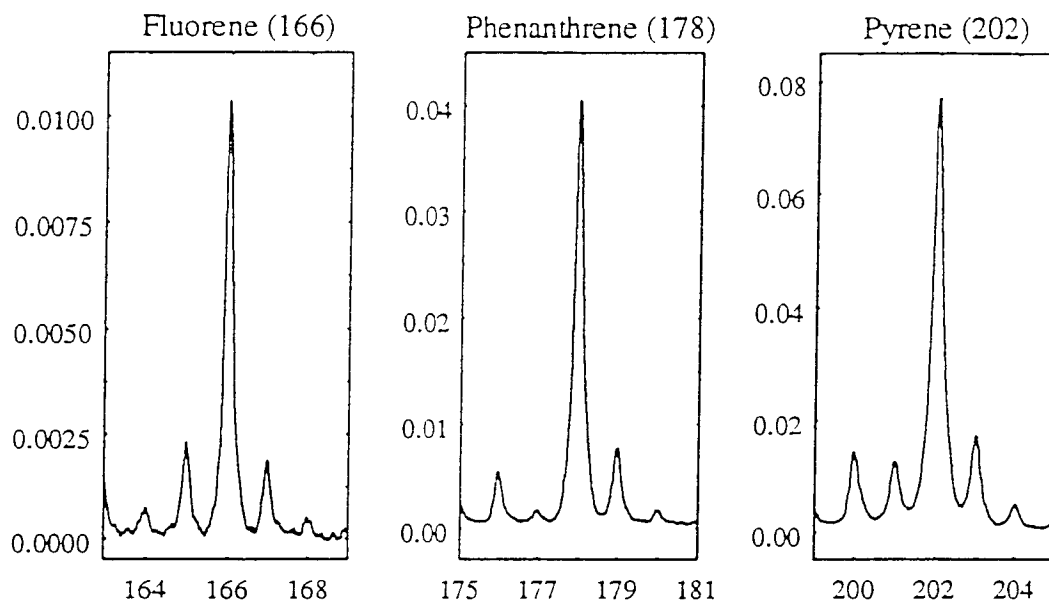


Figure 6.5. (a) Mass spectra of calibration species in standard PAH sample.

## Quantitative Analysis of Samples M3 and M4

Aromatic Species (amu)	M4 (Solv. Extract) (ppm)	M3 (Solv. Extract) (ppm)	% Change
Fluorene (166)	610	120	81
Phenanthrene (178)	2,500	500	80
Methyl Phenanthrene (192)	4,400	790	82
Pyrene (202)	1,150	290	75
Methyl Pyrene (216)	730	190	74

Figure 6.5. (b) Quantitative analysis of selected PAHs in untreated (M4) and treated (M3) PECO sludge.

# Polynuclear Aromatic Hydrocarbon Mixture

EPA Priority Pollutants (Supelco 4-8905M)

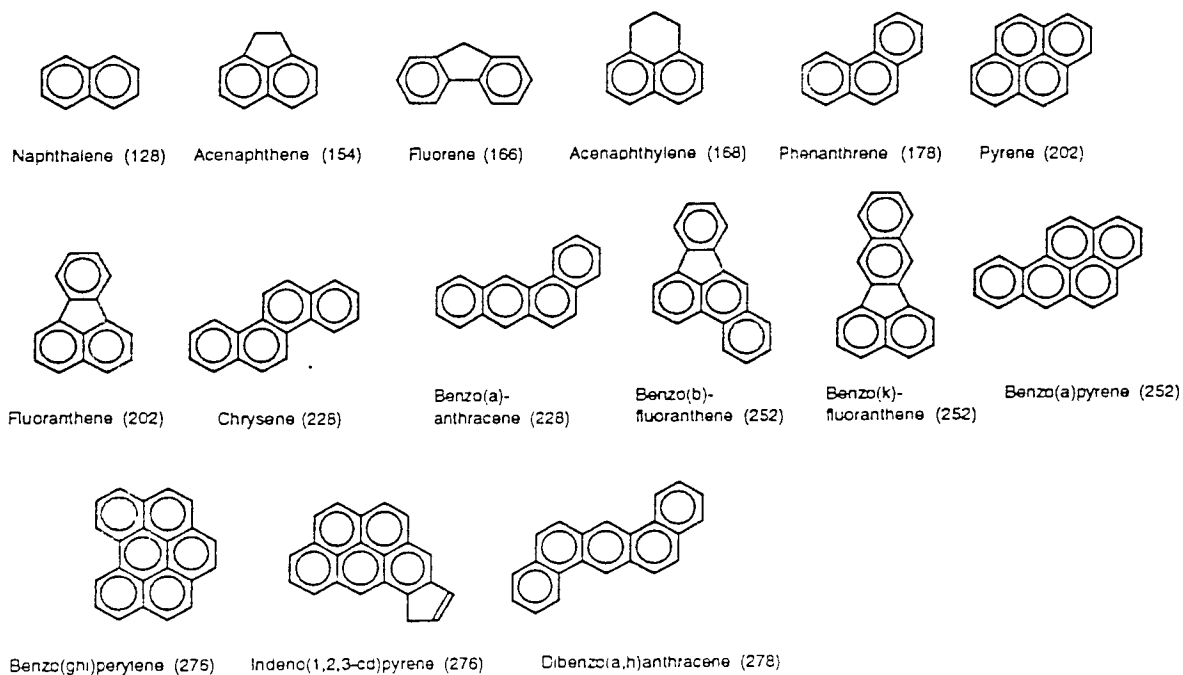
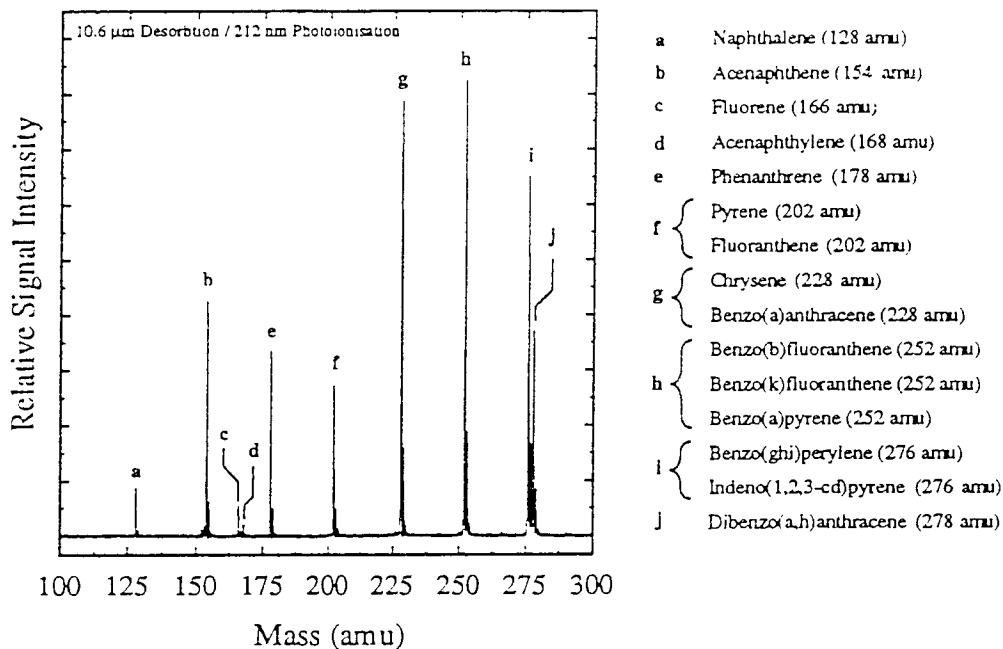
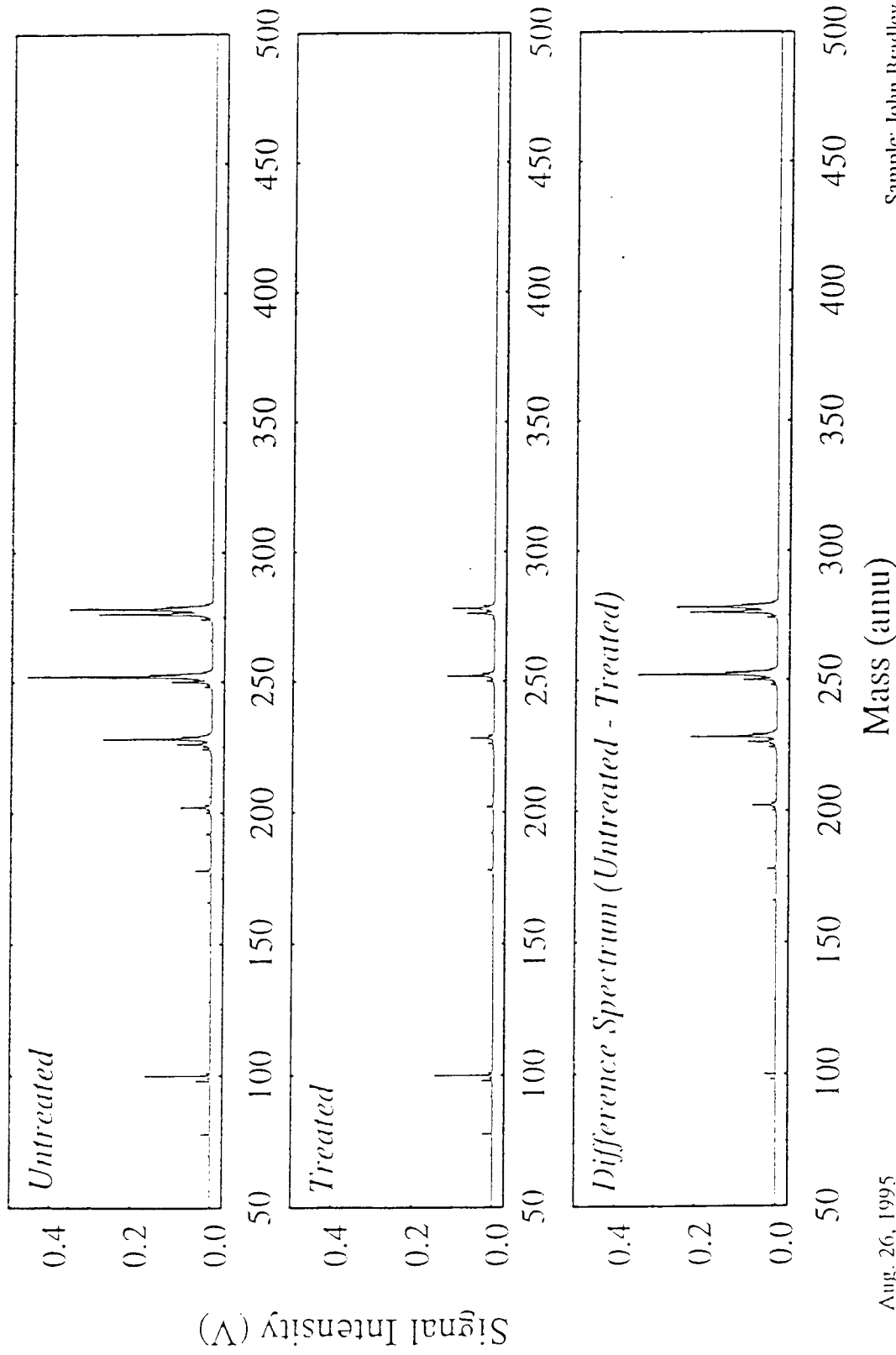


Figure 6:6. The sixteen PAHs present in Supelco 4-8905M standard.

## Control Experiment: Samples $Al_2O_3$ (Untreated) and IWT-27 (Treated)

Untreated: 1 ml Standard PAH Soln. added to 1 ml  $H_2O$  & 1ml (vol.)  $Al_2O_3$

Treated: 1 ml Standard PAH Soln. added to 1 ml  $H_2O$  & 1ml (vol.) IWT-27  
10.6  $\mu m$  Desorbion / 266 nm Photoionization, 2000-Shot Moving Average



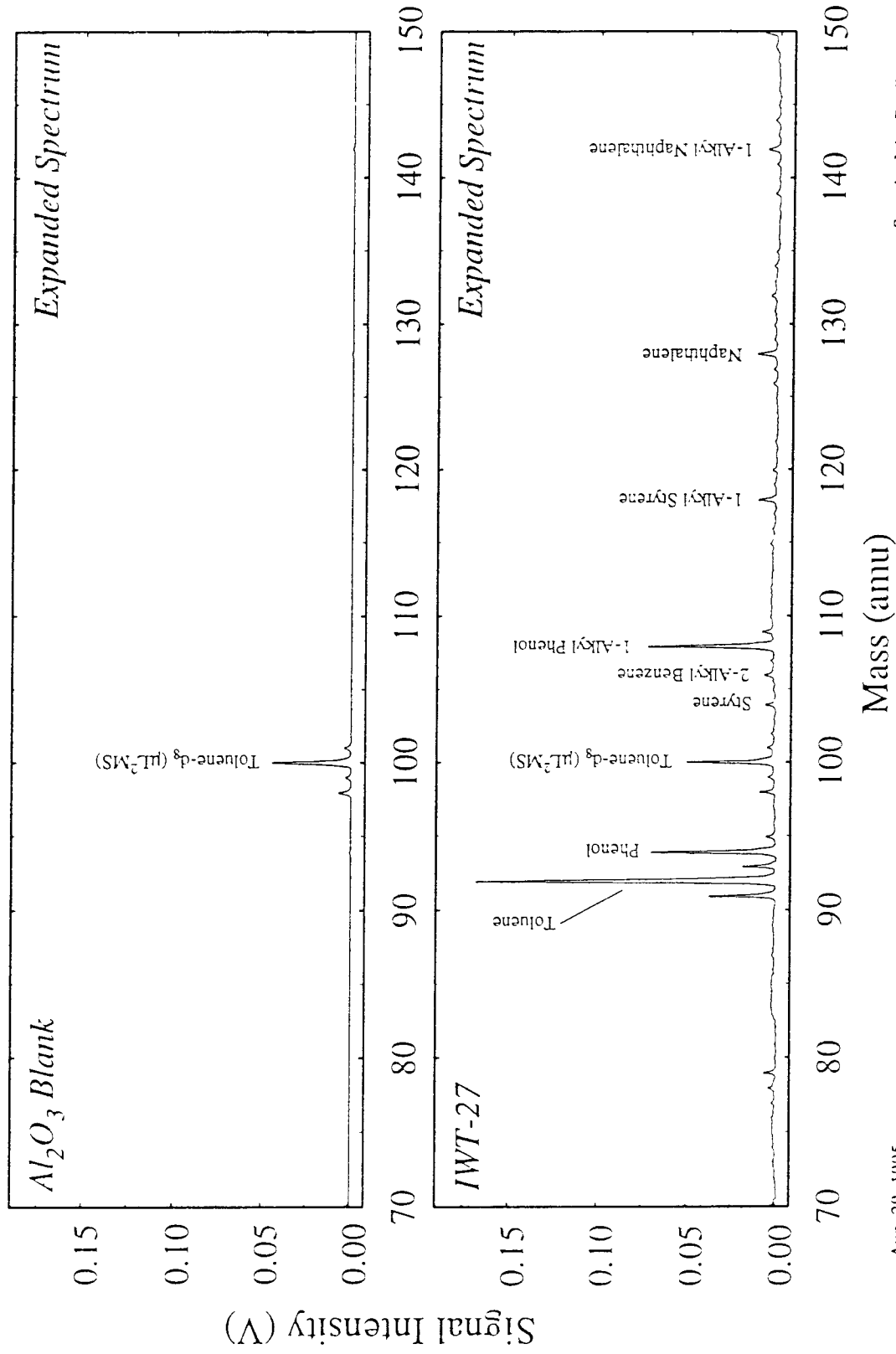
Aug. 26, 1995

Sample: John Bradley

**Figure 6:7.** Comparison of laser desorption mass spectra of solvent extracts from control experiment (16 standard PAHs plus HWT27 powder) in alumina blank ("untreated) and HWT27 ("treated"). Lower difference spectrum illustrates the mass reduction of PAHs in the HWT27 reaction vessel. Note there is no evidence of PAH breakdown products in the solvent extracts.

# Neat Powder Samples: IWT-27 and Al<sub>2</sub>O<sub>3</sub> Recovered from Control Experiment

Sample Preparation: Approx. 0.1 gms sample pressed into pellet 0.5 mm thick  
10.6 μm Desorbtion / 266 nm Photoionization, 1000-Shot Moving Average



Aug. 29, 1995

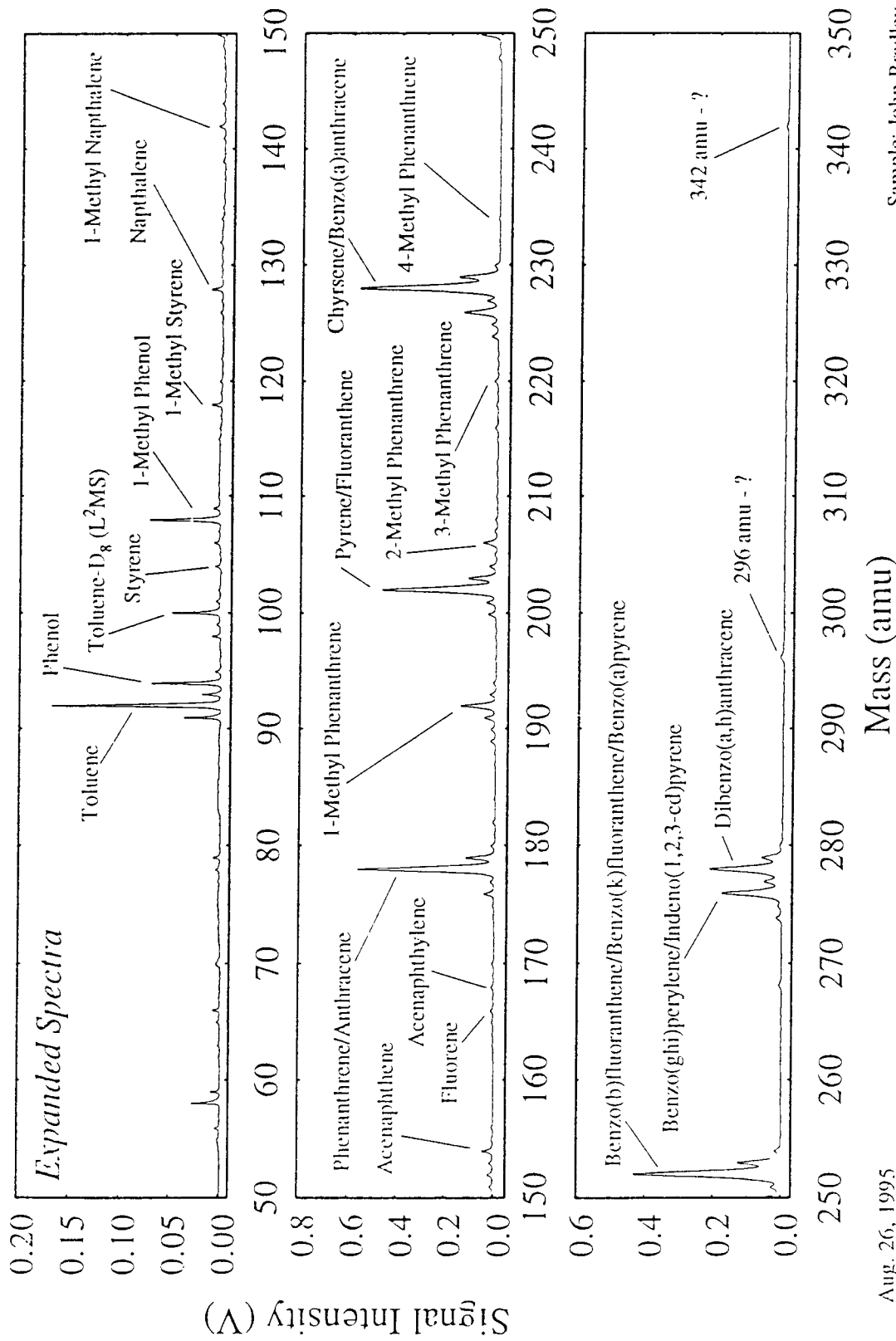
Sample: John Bradley

**Figure 6:8.** Comparison of laser desorption mass spectra of neat powders from control experiment (16 PAHs plus HWT27 powder) in alumina blank and HWT27. Note a variety of PAH breakdown products in the HWT27 spectrum that are not present in the spectrum from the alumina blank.

# Neat Powder: Sample IWT-27 Recovered from Control Experiment

Sample Preparation: Approx. 0.1 gms sample pressed into pellet 0.5 mm thick

10.6  $\mu\text{m}$  Desorbtion / 266 nm Photoionization, 2000-Shot Moving Average



Aug. 26, 1995

Sample: John Bradley

Figure 6:9. Expanded spectrum (from 50-350 amu) of neat powder of HWT27 after reaction with 16 PAH standard. Note that in addition to the original PAHs, the powder residue contains a variety of PAH breakdown products.

# PCB Analysis - Aroclor 1242 in Isooctane

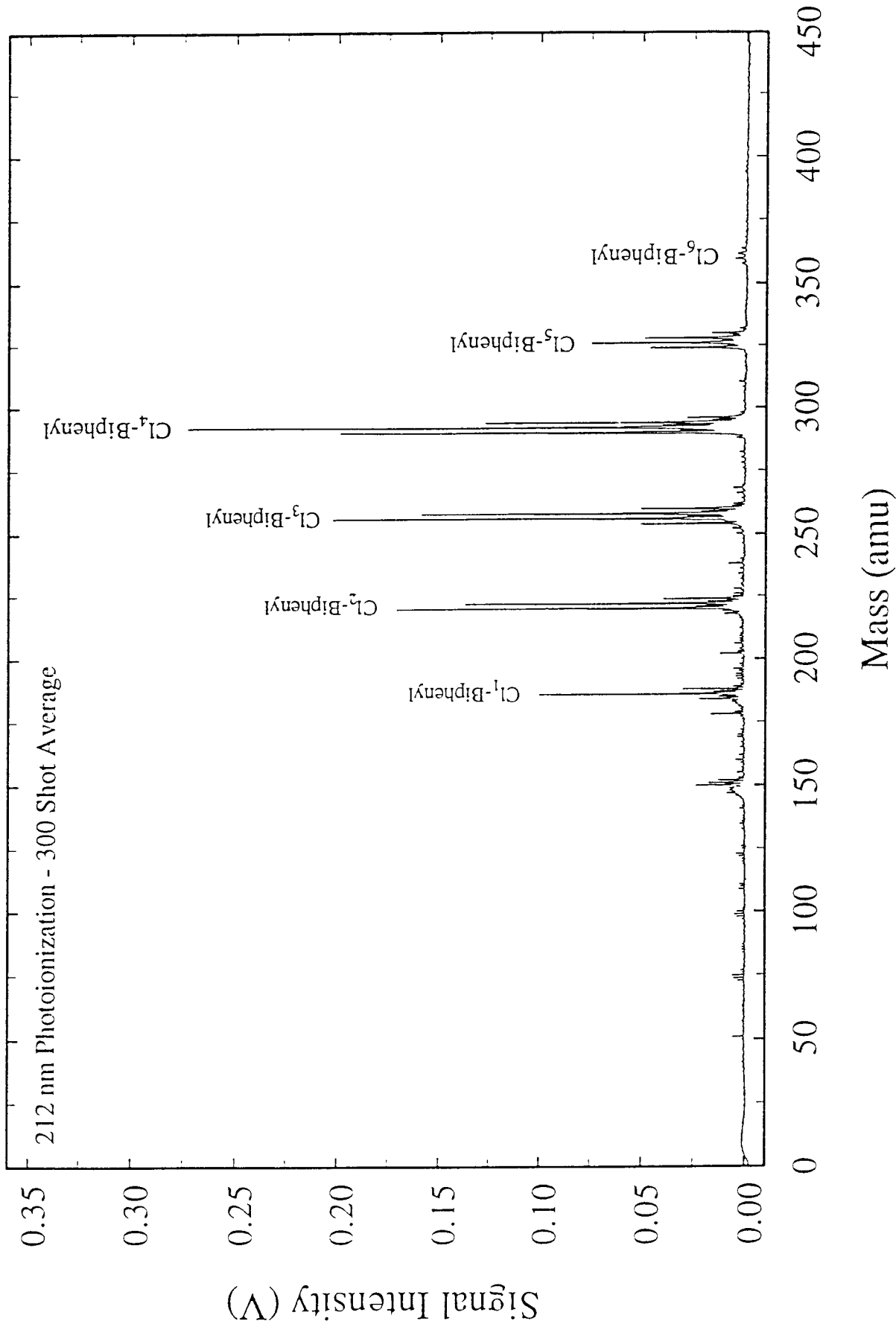
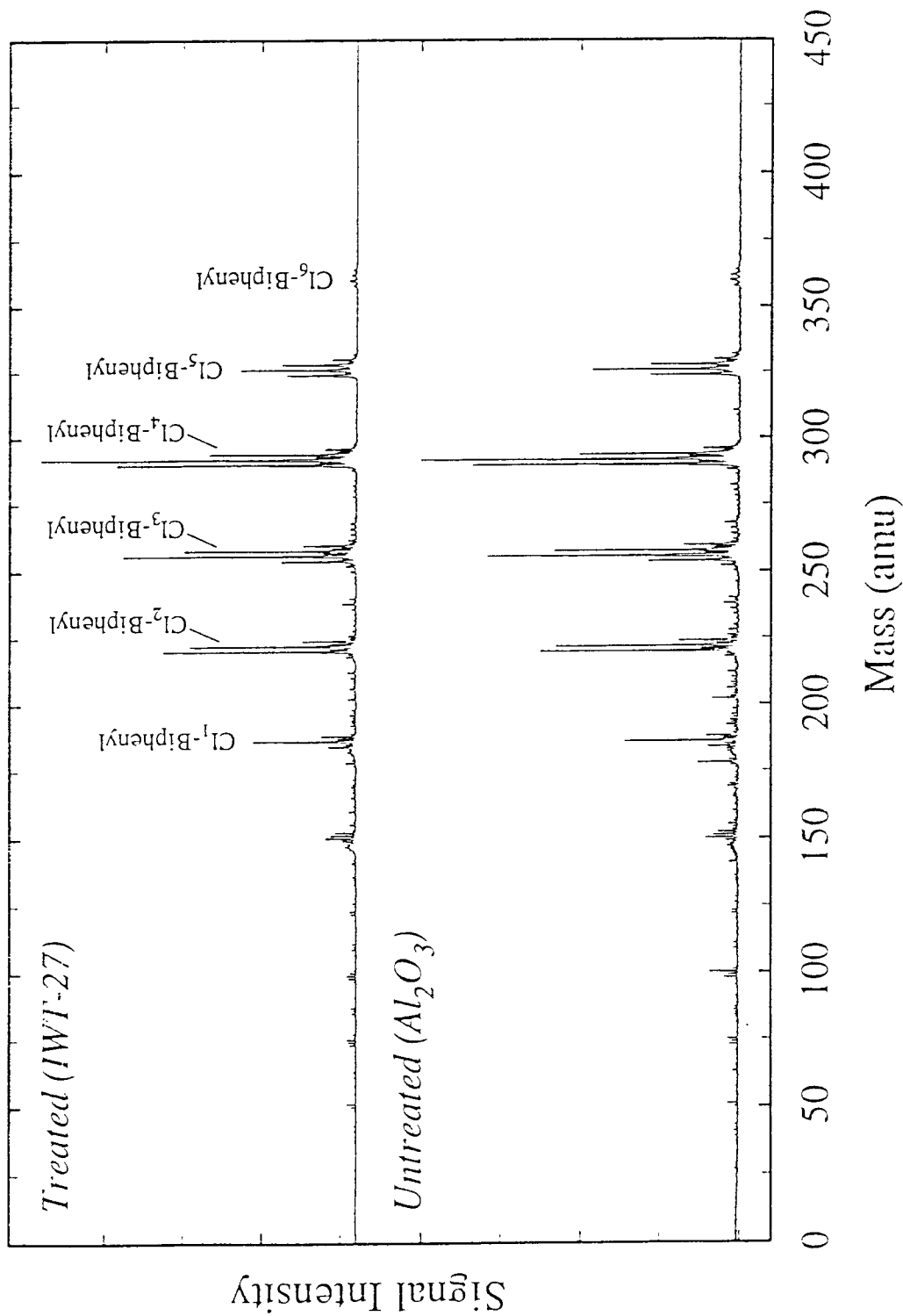


Figure 6:10. Laser desorption mass spectrum from Aroclor 1242 in isooctane.

## Control Experiment (Anhydrous): Sample $Al_2O_3$ (Untreated) and IWT-27 (Treated)

Untreated: 0.2 ml Aroclor 1242 soln. added to 0.07 ml (vol.)  $Al_2O_3$ , no  $H_2O$

Treated: 0.2 ml Aroclor 1242 soln. added to 0.07 ml (vol.) IWT-27, no  $H_2O$



Oct. 15, 1995

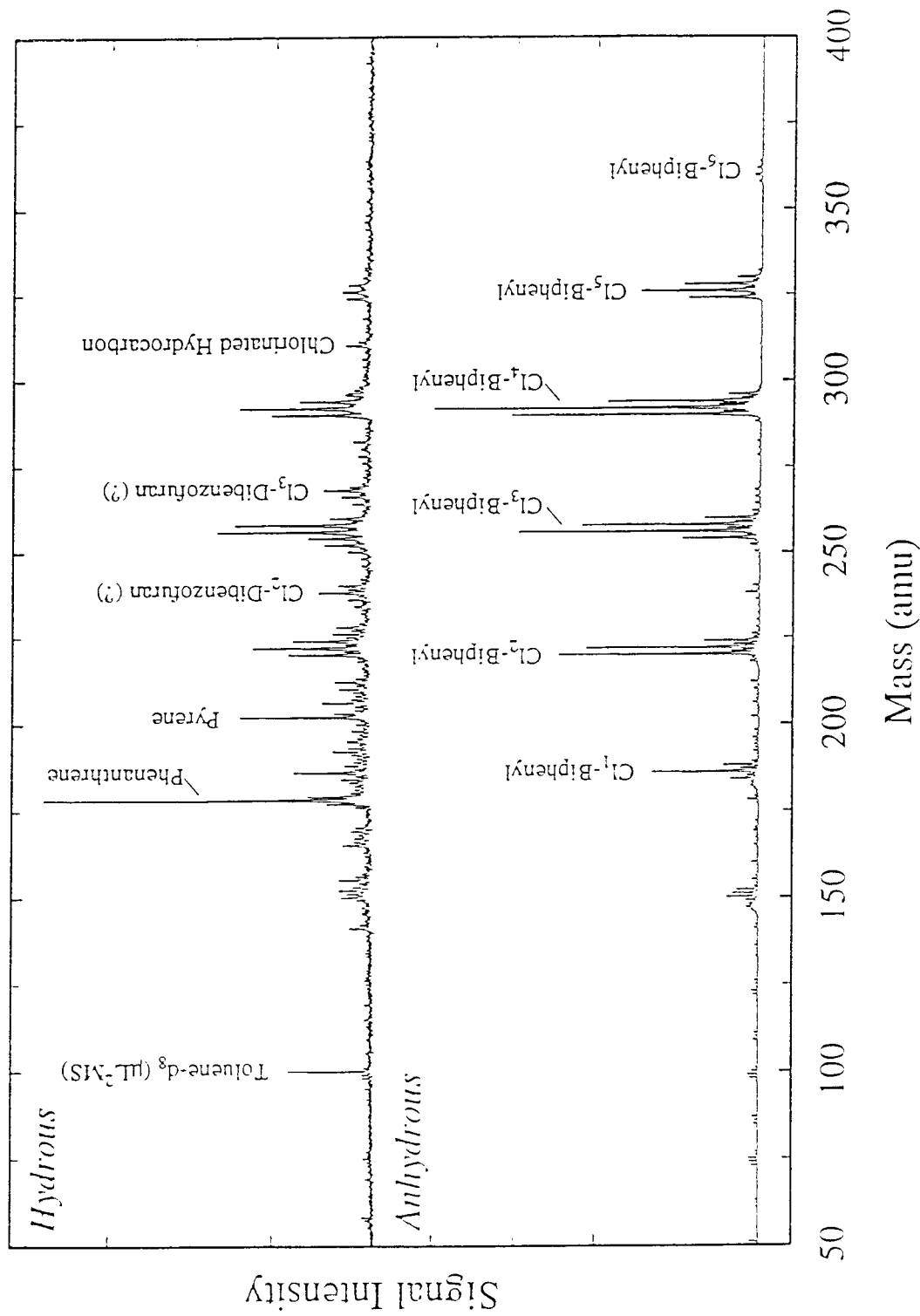
Sample: John Bradley

**Figure 6:11.** Comparison of laser desorption mass spectra of HWT27 and alumina powders after reaction with Aroclor 1242 under anhydrous conditions.

# Control Experiment: IWT-27 Anhydrous & Hydrous Treatments

Anhydrous: 0.2 ml Aroclor 1242 soln. added to 0.07 ml (vol.) IWT-27

Anhydrous: 0.1 ml Aroclor 1242 soln. & 0.1 ml H<sub>2</sub>O added to 0.07 ml (vol.) IWT-27



Oct. 17, 1995

Sample: John Bradley

**Figure 6:12.** Comparison of laser desorption mass spectra of HWT27 residue powders after reaction with Aroclor 1242 under hydrous and anhydrous conditions.

## Chapter 7

### Gas Chromatography

**The purpose of gas chromatography (GC) was to monitor changes in the abundances of all organics (aliphatic and aromatic) resulting from ACT treatment of untreated and treated PECO soils and sludges.**

Without systematically running standards, GC lacks the specificity of laser desorption mass spectroscopy ( $\mu\text{L}^2\text{MS}$ ) for aromatics compounds in general and PAHs in particular, but it offers the advantage (over  $\mu\text{L}^2\text{MS}$ ) of being able to detect both aliphatic and aromatic compounds. [Under the conditions employed for this study,  $\mu\text{L}^2\text{MS}$  laser wavelengths were optimized specifically for aromatics PAHs (see Chapter 6)]. If non-aromatic compounds are important breakdown products during the ACT treatment process, GC offers the means of detecting these products.

For this study, we first performed a series of solvent extractions and examined and weighed the extracts. Then we ran a standard PAH mixture through the GC column to establish the retention times (RT's) for specific PAH's of interest. Finally, we ran the "unknown" PECO soil and sludge samples over several different temperature ranges. Only selected chromatograms are presented in this Chapter, but chromatograms of all (standard and unknown) samples together with integrated peak areas have been archived for future reference.

#### Solvent extractions for gas chromatography

While preparing solvent extracts for GC, significant differences in the colors of extracts were seen from one sample to another. In order to quantify this effect, 1.45-1.46 gram samples of untreated and treated soils and sludges were extracted with 3 ml of chloroform by ultrasonication for 30 minutes at room temperature. It was noted (following sonication) that the centrifuge tubes were quite warm to the touch. The solids were allowed to settle. (The color of the chloroform solution was noted immediately after addition of the chloroform, and following sonication). Observed colors were as follows:

Untreated PECO soil (M1)	pale yellow to amber
Treated PECO soil (M2A) (aged 125 days)	yellow to amber
Untreated PECO sludge (M4)	dark amber to black
Treated PECO sludge (M3)	amber to dark brown

Following the sonication and settling steps, 1 ml aliquots of each were removed for GC analyses. The remainder of the chloroform extracts (2 ml) were transferred to preweighed aluminum evaporating pans. The solvent was evaporated at room temperature and the residues in the pans were weighed. Residue/sample weights were calculated as % chloroform extractables (as residues). Of course, only two thirds of the total was evaporated, but the weight percentages are relative. The actual weights of the residues and the corresponding sample weights were as follows:

**Table 7:1**

Sample	Sample weight	Residue from CHCl <sub>3</sub>	% Residual Extracts
M4	1.450 g	0.0024 g	0.165%
M3	1.459 g	0.0012 g	0.082%
M2A	1.439 g	0.0050 g	0.347%
M1	1.446 g	0.0100 g	0.691%

Table 6:1 indicates that there is ~50% decrease in the mass of solvent extractable organics as a result of the HWT 27 treatment. These results are of similar magnitude to those obtained in Chapter 6 (p. 78).

### GC Analysis of standard PAH mixture at 100-250 C

A PAH standard mixture (#525) containing 13 PAH's and 4 individual PAHs were analyzed (Fig. 7:1). The mixture includes the following compounds; the retention times of these compounds under the same conditions as the PECO sludge analyses below (100-250°C, increased at 5°C/minute) were as follows. The retention times reported for the standards below in minutes, are the average of two runs. Due to manual techniques, it is normal to experience some minor deviation and variation in the retention times. A list of the compounds follows:

Compound	RT (minutes)
acenaphthalene	9.44
fluorene	12.51
phenanthrene	16.92
anthracene	17.3
pyrene	23.69
benzanthracene	29.73
chrysene	29.92
benzo(b)fluorathene	31.09
benzko(k)fluoranthene	31.30
benzo(a)pyrene	31.45
indeno(1.2.3.-C.D)pyrene	35.22
1.2:5.6-dibenzanthracene	35.38
1.12-benzoperylene	37.20

A typical chromatogram of the PAH mix is provided (Fig. 7:1). Also, though not part of the standard PAH mixture, naphthalene was analyzed under these conditions; it eluted at 4.24 minutes.

### GC Analyses of CHCl<sub>3</sub> extracts of PECO sludge and soil samples at 100-250°C

Three (3) microliter (μL) volumes of soil and sludge solvent extracts were injected. The GC parameters were as follows:

Detector (FID):	290°C
Injector:	275°C
Initial Temp:	100°C, held for 2 minutes
Final Tem:	250°C, held for 5 minutes
Rate:	5°C /minute
Column:	30 meter, DB-5

The sample concentrations were as follows:

M3 and M4: 0.5 mL chloroform extract/5 mL CHCL3  
M2A and M1: concentrated CHC13 extract

(It was noted that a 0.5 mL chloroform extract of M2A (treated soil) in 2 mL of chloroform, about half the concentration of the sludge extracts was too dilute). Accordingly, the chloroform extracts were injected directly.

Figure 7:2 compares GC profiles of extracts of untreated "control" sludge M4 and treated sludge (M3). The following trends are evident:

- there is a loss or decrease in volatile components which elute between 1.5 and 4 minutes in the treated sludge
- no change in naphthalene concentration (4.2 minutes)
- significant loss or decrease is observed in these PAH's

Acenaphthalene (9.5 min): M4 (1821) to M3 (716)  
Fluorene (12.6 min): M4 (1413) to M3 (362)  
Phenanthrene (16.99 min): M4 (4432) to M3 (1833)  
Anthracene (17.20 min): M4 (1183) to M3 (335)  
Pyrene (23.7 min): M4 (2498) to M3 (1244)

Unidentified #1 (6.2 min): M4 (4503) to M3 (2542)  
Unidentified #2 (6.5 min): M4 (3308) to M3 (1506)  
Unidentified #3 (22.7 min): M4 (1045) to M3 (468)

The numbers within the parenthesis for M4 and M3 represent the area of the peaks for those eluting components. Since the sample weight/solution volume and all other analytical parameters were held constant, the difference in areas correspond to concentration of that eluting component. These values are, of course, semi-quantitative, since we have not established a linear relationship between the area and concentration of each component

The untreated (M1) and treated (M2A) soil samples were treated identically to the sludges. Although the chromatograms are not presented in this report, they but can be made available at any time. The soil results indicate:

- More peaks (i.e., additional components) in M2A between 1.5 and 4 minutes
- a slight increase in the signal from naphthalene in the extract of M2A
- an additional peak at 6.88 minutes in M2A
- decrease/loss of PAH in the following components:

Acenaphthalene (9.5 min): M1 (1122) to M2A (847)  
Fluorene (12.60): M1 (912) to M2A (<300)  
Phenanthrene (16.99 min): M1 (4854) to M2A (862)  
Anthracene (17.2 min): M1 (1620) to M2A (754)  
Benzanthracene (29.7 min): M1 (2546) to M2A (1785)  
Chrysene (29.9 min): M1 (3018) to M2A (2200)

Unidentified #1 (22.76 min): M1 (6168) to M2A (3781)

- Note there is essentially no change in the signal/area of pyrene at 23.76 minutes- M1 (6342) M2A (6394).

### GC Analyses of CHCL3 extracts of untreated and treated sludge at 40-250°C

The purpose of running the sludge samples for a second time at a much lower temperature (40°C) was to look for volatile compounds that elute very early. In fact, there was a significant increase in at least two components which elute very early in the chromatographic run in the extract of the treated sludge. These peaks are observed in 3.01 and 3.4 minutes (cf. Figs. 7:3 & 7:4). These two peaks are clearly reduced in that of the untreated extract. PAHs identified in Figures 7:3 and 7:4 include the following:

Compound	RT (minutes)
acenaphthalene	13.5
fluorene	15.3
phenanthrene	17.7
anthracene	17.8
pyrene	21.2
benzanthracene	24.5
chrysene	24.7

Also, toluene was analyzed under these conditions and was determined to have a retention time of 2.36 minutes

### Headspace GC of untreated and treated sludge at 40-250°C

The sludges were also analyzed by headspace GC, in an attempt to determine if we could see any additional peaks in the GC of the treated sludge. Portions of the sludges were weighed and gently heated in closed containers for a few minutes. The vapors above the solid phase of the sludge were injected into the GC. The GC profiles are shown in Figures 7:5 and 7:6. The headspace analyses showed some differences in the untreated/treated sludges, especially at the lower or early part of the GC runs between 2 and 6 minutes. Presumably, these peaks are due to aromatic and/or aliphatic compounds with lower boiling points. In the GC of the treated sludge, we do see a component eluting at 2.38 minutes, which is consistent with toluene (Fig. 7:6). The GC runs from 40-250 clearly indicate the need for improved separation/identification techniques such as GC/MS.

### Summary of gas chromatography analyses

There is ~50% reduction in solvent extractable organics in both soils and sludges after treatment with ACT. Although most (non-PAH) peaks in the chromatograms remain unidentified, **GC analyses clearly indicate a fundamental shift in the total organic content of the PECO soils and sludges as a result of the ACT treatment. Higher mass PAHs are reduced by >50% on average**, at least under the GC conditions used for this study. However, a slight increase in naphthalene was observed in the treated soil and no change in naphthalene in the sludge. Clearly, different PAHs respond differently to the ACT treatment with the higher mass PAHs selectively reduced. GC headspace analyses of the sludge suggest higher concentrations of lower boiling point compounds in vapors from the treated sludge.

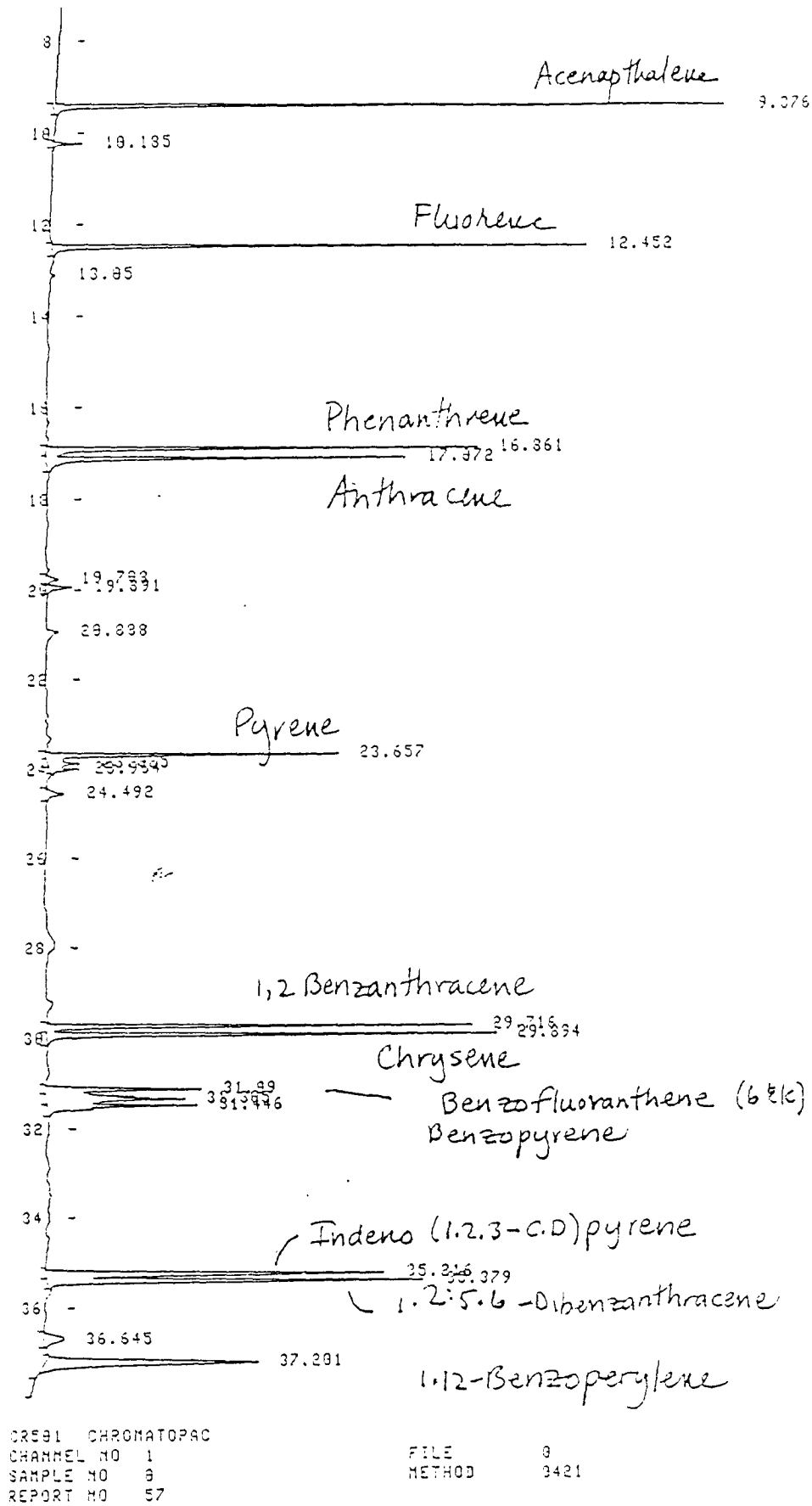


Figure 7:1. Gas chromatogram of a thirteen (13) PAH standard mixture (#525) collected at 100 - 250°C.

100 - 250° C

5° C/Min

Control Sludge

Treated Sludge

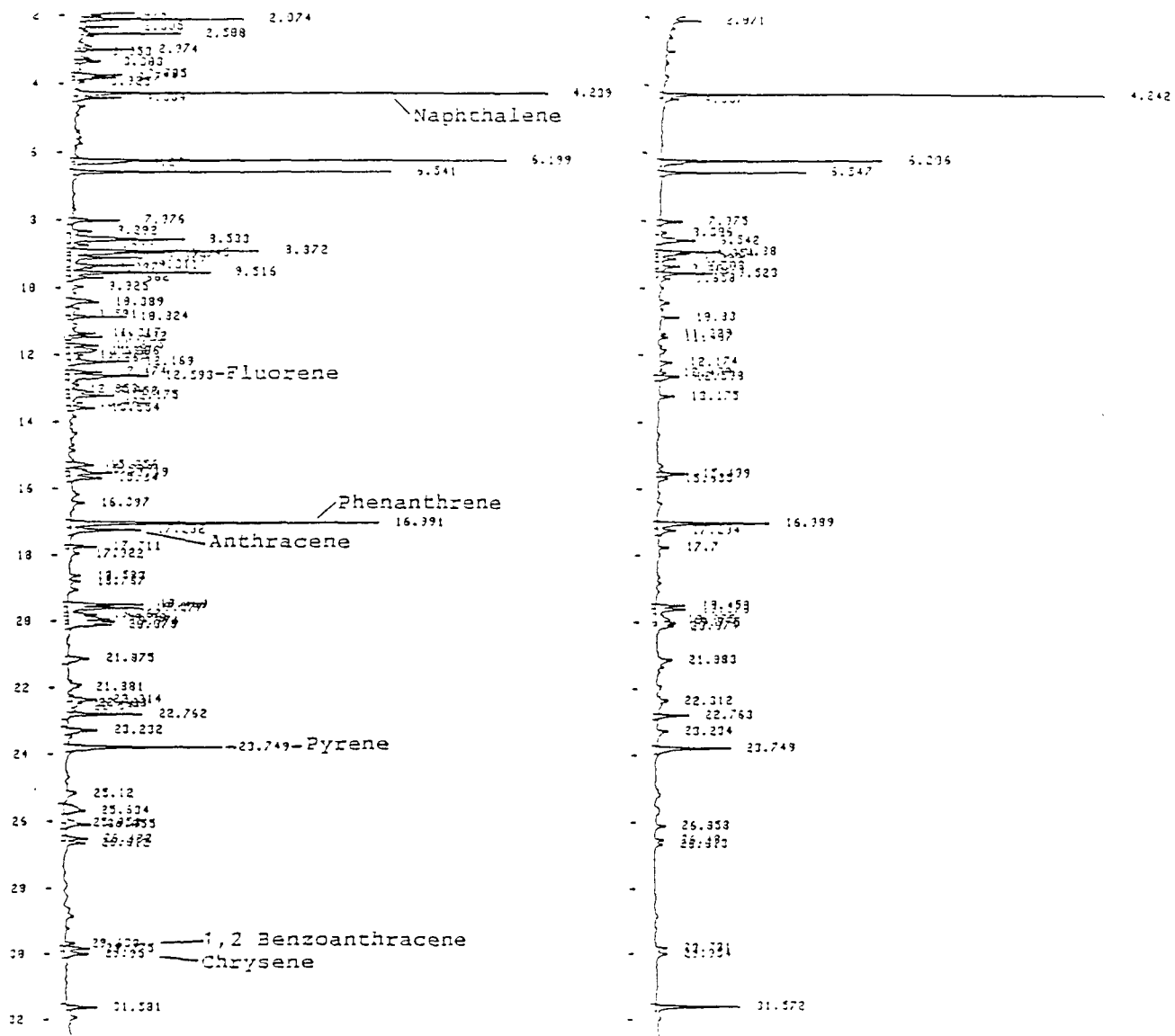


**Figure 7:2.** Comparison of GC profiles of untreated "control" and treated sludge samples run under the same conditions as those of the standard PAH mixture (Fig. 7:1). Note the selective decrease in higher mass PAHs (e.g. pyrene and chrysene) and little change in naphthalene concentration.

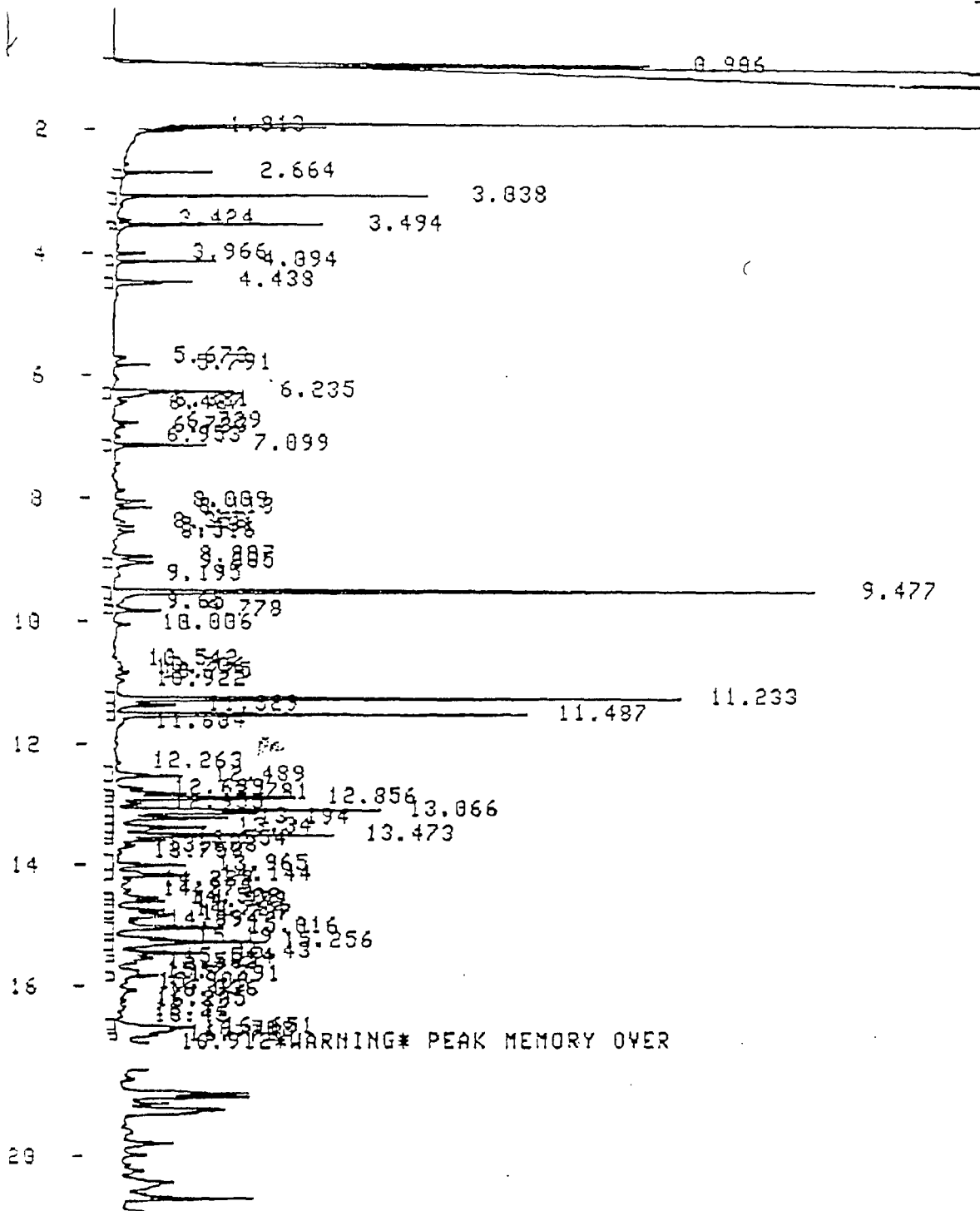


Figure 7:3. Gas chromatogram of untreated 'control' sludge collected at 40 - 250°C.

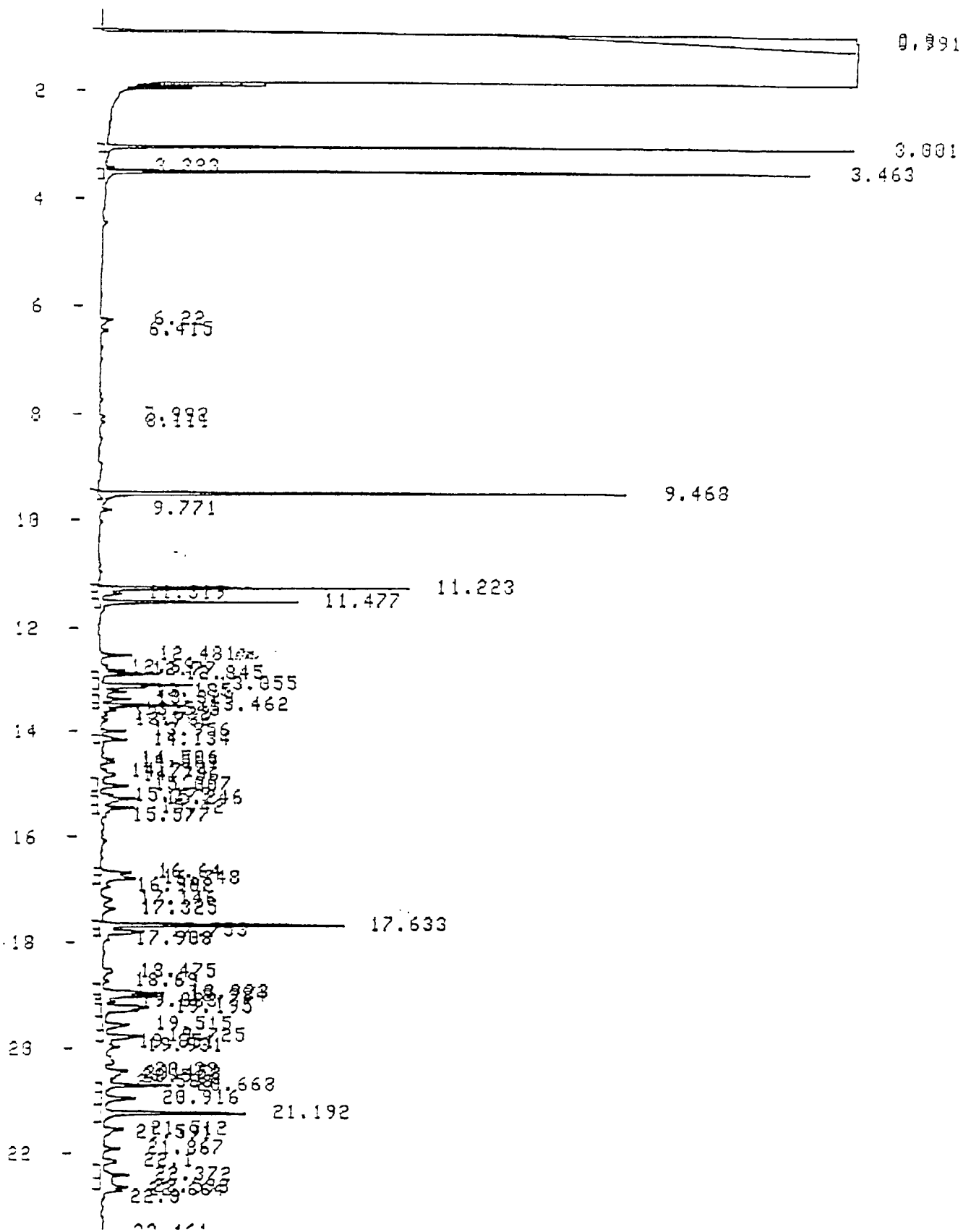


Figure 7:4. Gas chromatogram of treated sludge collected at 40 - 250°C.

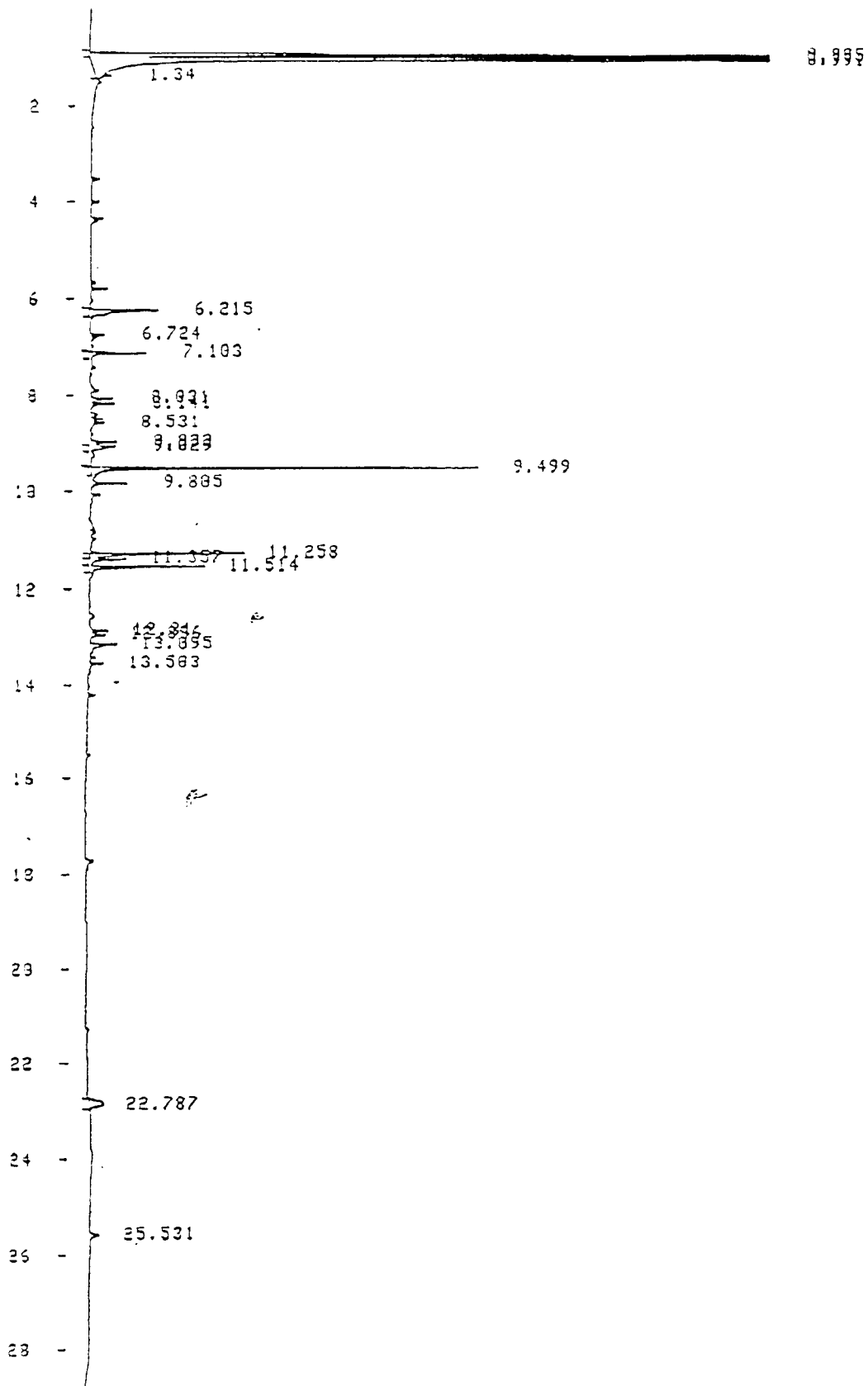


Figure 7:5. Headspace gas chromatogram of vapors (collected at 40-250°C) from untreated sludge.

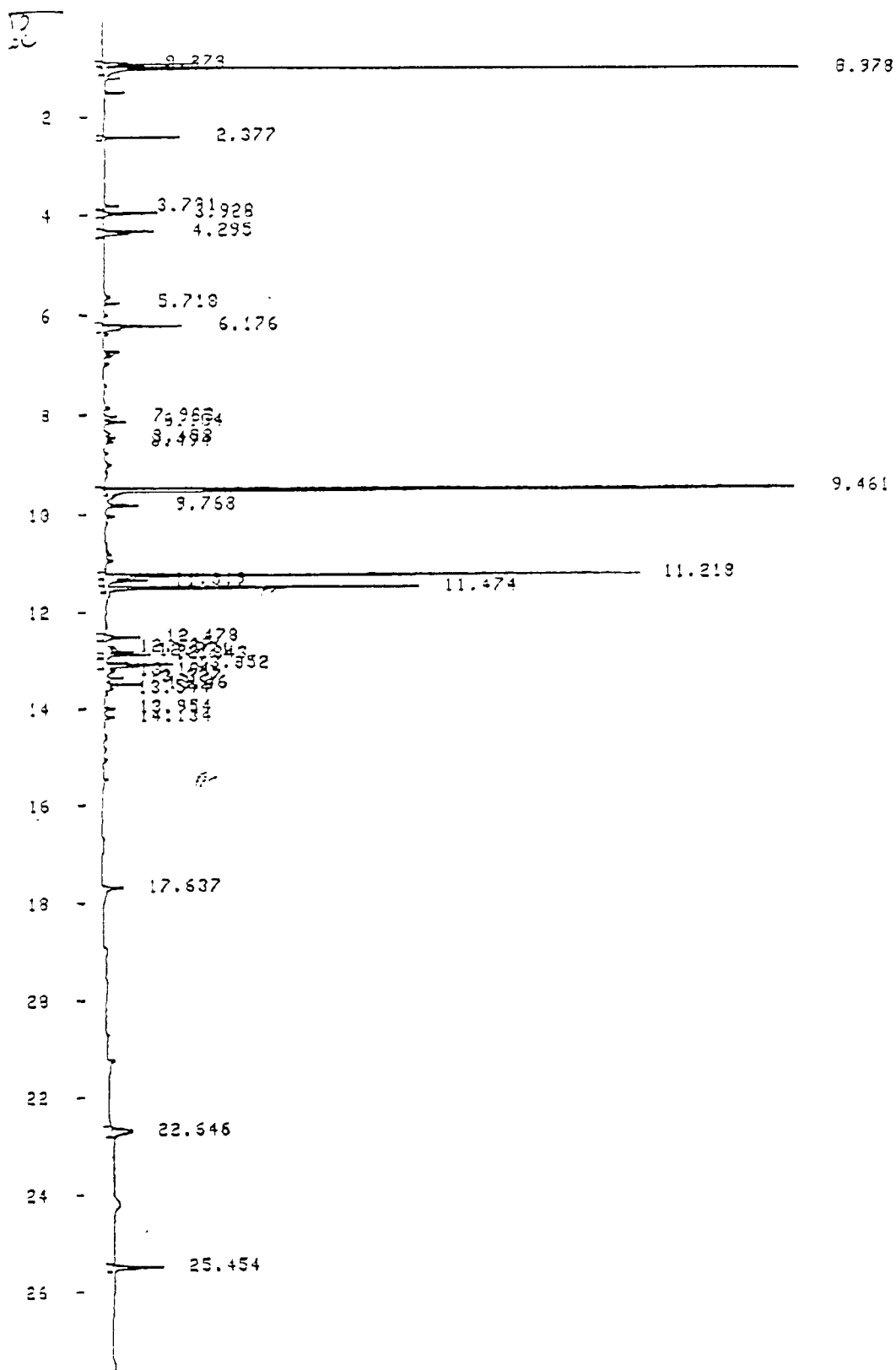


Figure 7:6. Headspace gas chromatogram of vapors (collected from 40 - 250°C) from treated sludge

APPENDIX I

Report of Results: MVA1342

Job No. EV-00701-002

Prepared for:

Ms. Karen Hartley  
Marcor of Pennsylvania, Inc.  
540 Trestle Place  
Downington, PA 19335

Prepared by:

John P. Bradley  
MVA, Inc.  
5500 Oakbrook Parkway, Suite 200  
Norcross, GA 30093

31 May 1995

D:\PROJECTS 1342\RP053195



MVA, Inc.  
Excellence in  
Microanalysis

5500 Oakbrook Parkway #200  
Norcross, Georgia 30093  
404-662-8509

## Report of Results: MVA1342

Job No. EV-00701-002

### Introduction

This report describes MVA's characterization of two (2) hydrocarbon contaminated soil samples that were received on May 5, 1995. The samples identified as from the PECO pilot demonstration were labelled "Control Soil" and SM1 respectively. The purpose of our characterization was to investigate the overall compositions of the organic fractions and, if possible, provide an explanation for the significantly different leach test results obtained from the samples. We employed a combination of infrared (IR) microspectroscopy and two step laser desorption mass spectroscopy ( $\mu\text{L}^2\text{MS}$ ) to analyze the samples.

### Experimental Procedures

The samples were in the form of a grey-black granular soil mix. For IR microspectroscopy, approximately 0.5 gm of each sample was placed in a test tube along with 5 mls of chloroform. The mixture was agitated, then 5 ml of water was added, and the mixture was vigorously agitated again. When the chloroform layer had settled out, a micro pipette was used to remove about 0.1 ml from the chloroform layer. The aliquot was dispersed onto a silver chloride substrate and allowed to dry, leaving an organic residue. This residue was analyzed by transmission IR microspectroscopy over the wavelength range 800 - 4000  $\text{m}^{-1}$ .

Both "neat" (as received) and chloroform extracted samples were prepared for  $\mu\text{L}^2\text{MS}$  analyses. For the neat powder samples preparation involved grinding each of the powders until the mean grain size was  $<150 \mu\text{m}$ . This fine powder was then dried and pressed onto a roughened aluminum sample mount. The purpose of grinding is to produce samples with approximately equivalent surface areas when analyzed by the laser microprobe, and so allow the most accurate comparison of the relative concentrations of the organic phase between the samples. Solvent extracts were made by taking  $\sim 0.085 \text{ mg}$  each of the finely powdered samples and adding 0.4 ml of chloroform solvent. The solvent was evaporated onto a clean quartz sample mount heated to  $70^\circ\text{C}$ . On evaporation of the solvent a dark yellow-brown residue was left.

For all samples a  $10.6 \mu\text{m}$   $\text{CO}_2$  laser beam was used to desorb material from the sample in a spot  $40 \mu\text{m}$  in diameter, the resulting plume of desorbed material was then photoionized at 266 nm by a frequency quadrupled Nd:YAG laser beam. To compensate for spatial inhomogeneities in the samples, 300 shot moving averages were taken. The laser photoionization energy was  $\sim 500 \mu\text{J/pulse}$  in an unfocused beam of cross sectional area  $1 \text{ mm}^2$ . Under these conditions the peaks observed in the spectra represent the parent ion molecular species present in the sample, i.e., there is little to no fragmentation associated with the ionization process.

### Results

Figure 1 shows an IR spectrum of the chloroform extracted organic fraction of the control soil. The absorption band structure is consistent with a mixture of aromatic and aliphatic compounds. Although aliphatic C-H stretching at  $\sim 2850 \text{ cm}^{-1}$  is the dominant feature of the spectrum, aliphatic compounds are not necessarily more abundant than aromatics. Figure 2 shows an IR spectrum from treated sample. Note the almost complete loss of aromatic absorption features together with the appearance

of an intense carbonyl (-C=O) absorption band at  $\sim 1750 \text{ cm}^{-1}$ . For comparison, IR spectra from both samples are plotted together in Figure 3.

The spectrum from the treated sample was compared via computer with a data base containing IR spectra of over 50,000 organic compounds. The treated sample was spectrally matched with a reference spectrum for palm oil, which consists mainly of the esters palmitin ( $\text{C}_5$ ,  $\text{H}_{98}$ ,  $\text{O}_6$ ), stearin, and lanolin.

Laser desorption mass spectra of both samples are compared in Figure 5. The untreated sample shows a very strong distribution of polycyclic aromatic hydrocarbons (PAHs) with a mass range extending from 100 amu to beyond 450 amu (Fig. 5a). The most prominent PAHs observed include pyrene (202 amu;  $\text{C}_{16}\text{H}_{10}$ ), chrysene (228 amu;  $\text{C}_{18}\text{H}_{12}$ ) and dibenzopyrene (252 amu;  $\text{C}_{20}\text{H}_{12}$ ). Extensive alkylation of all parent PAH skeletons is observed, with alkylation series extending beyond 6-alkyl observed for nearly all the prominent PAH skeletons. The treated sample, a similar distribution of PAH species is observed although at a greatly reduced concentration (Figs. 5b, 7-9). The decrease of the signal varies between individual PAHs as can be observed from the expanded spectra, (Figs. 7-9) with the total integrated signal being  $\sim 0.6$  times that of the untreated sample.

## Discussion

Infrared (IR) microspectroscopy demonstrates that there is a fundamental difference in the molecular composition of the treated and untreated samples. Whereas the concentrated sample is clearly dominated by aliphatic and aromatic compounds, the treated sample displays intense carbonyl (-C=O) absorption and an overall spectra features consistent with esters. The spectral match to that of palm oil supports the notion that esters are the dominant organic phases in the treated sample. Since the strength of the aromatic absorption bands has decreased in proportion to the increase in carbonyl band intensity, it appears that much of the aromatic material in the untreated sample was oxidized to esters.

The  $\mu\text{L}^2\text{MS}$  results support the above interpretation of the IR spectra. The overall concentration of polyaromatics has been decreased  $\sim 17$  times (Fig. 5). Though the mass envelopes are similar for both samples, there are several notable differences. In the treated sample, the lower mass PAHs (below 230 amu) appear to be more prominent whilst at the higher mass PAHs (greater than 300 amu) appear depleted. Additionally the alkylated/unalkylated PAH ratio in the treated sample is lower on average than that of the untreated sample, with 1-alkyl and 2-alkyl substituents being the most abundant in the treated sample as compared to 3-alkyl and 4-alkyl substituents for the untreated sample. There are no prominent odd mass peaks observed in either sample and there appear to be species that are unique to either sample.

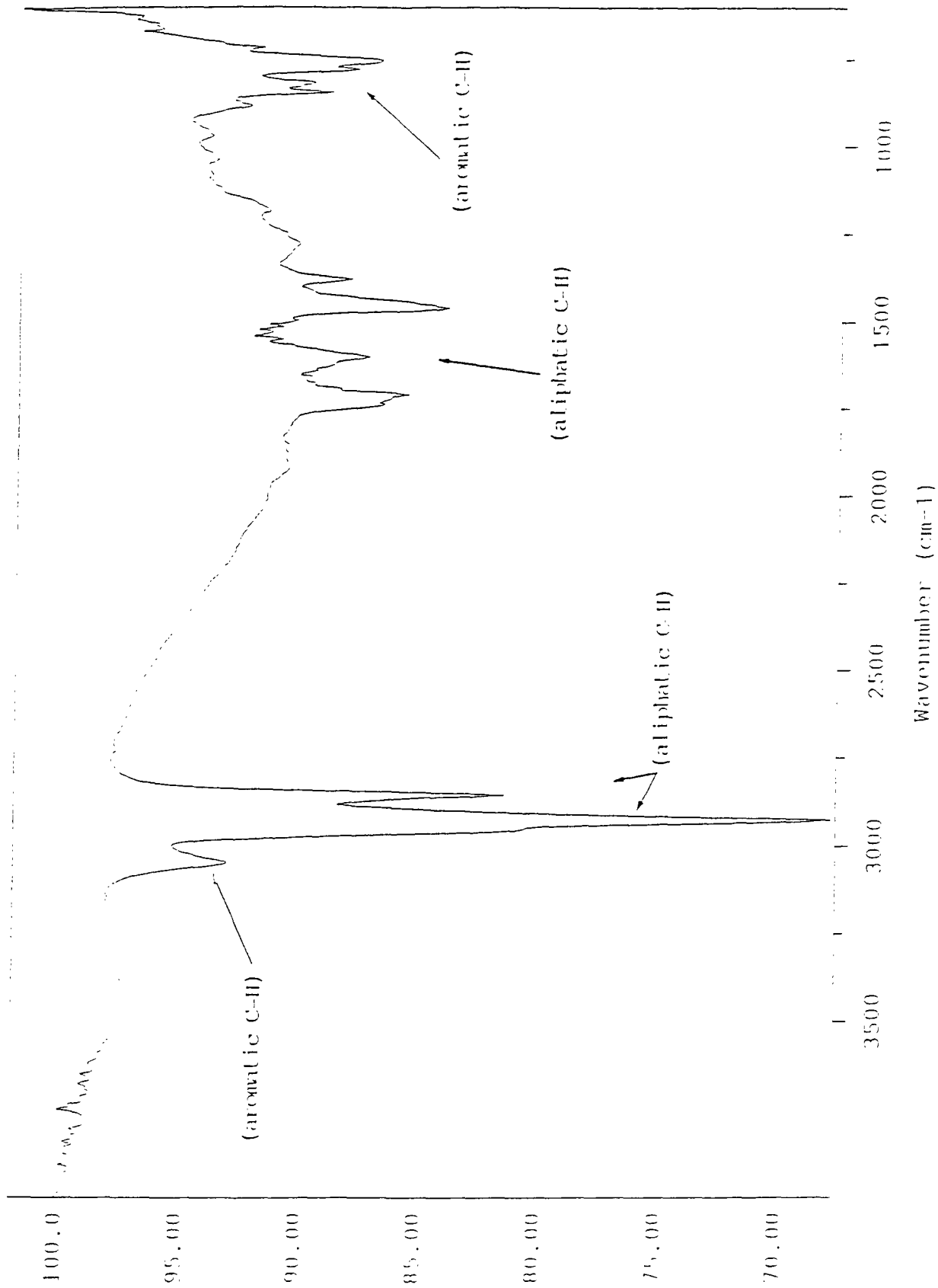


Figure 1. IR spectrum of chloroform extract from untreated PECO control soil.

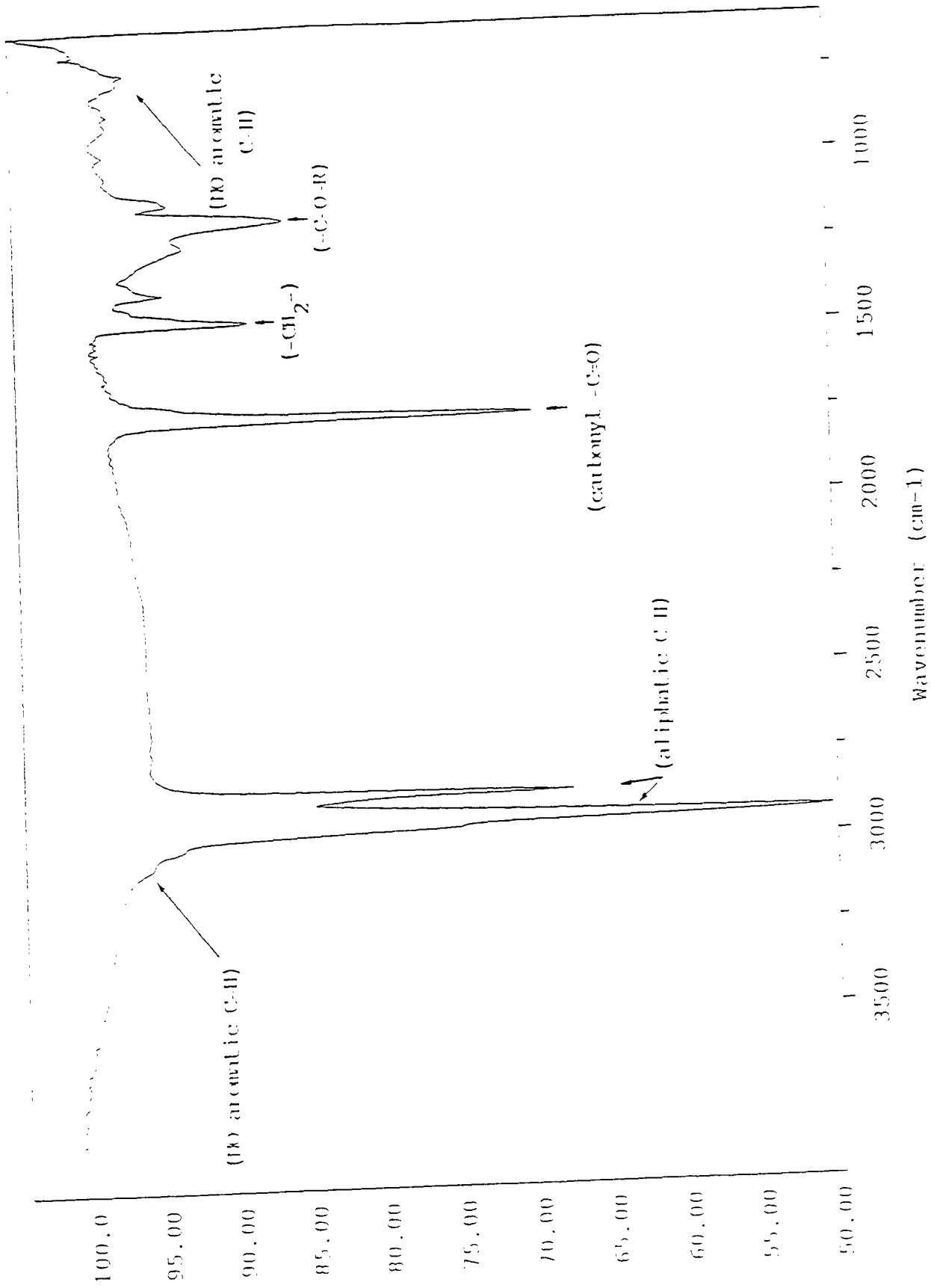


Figure 2. IR spectrum of chloroform extract from treated PECO soil mix, design 1.

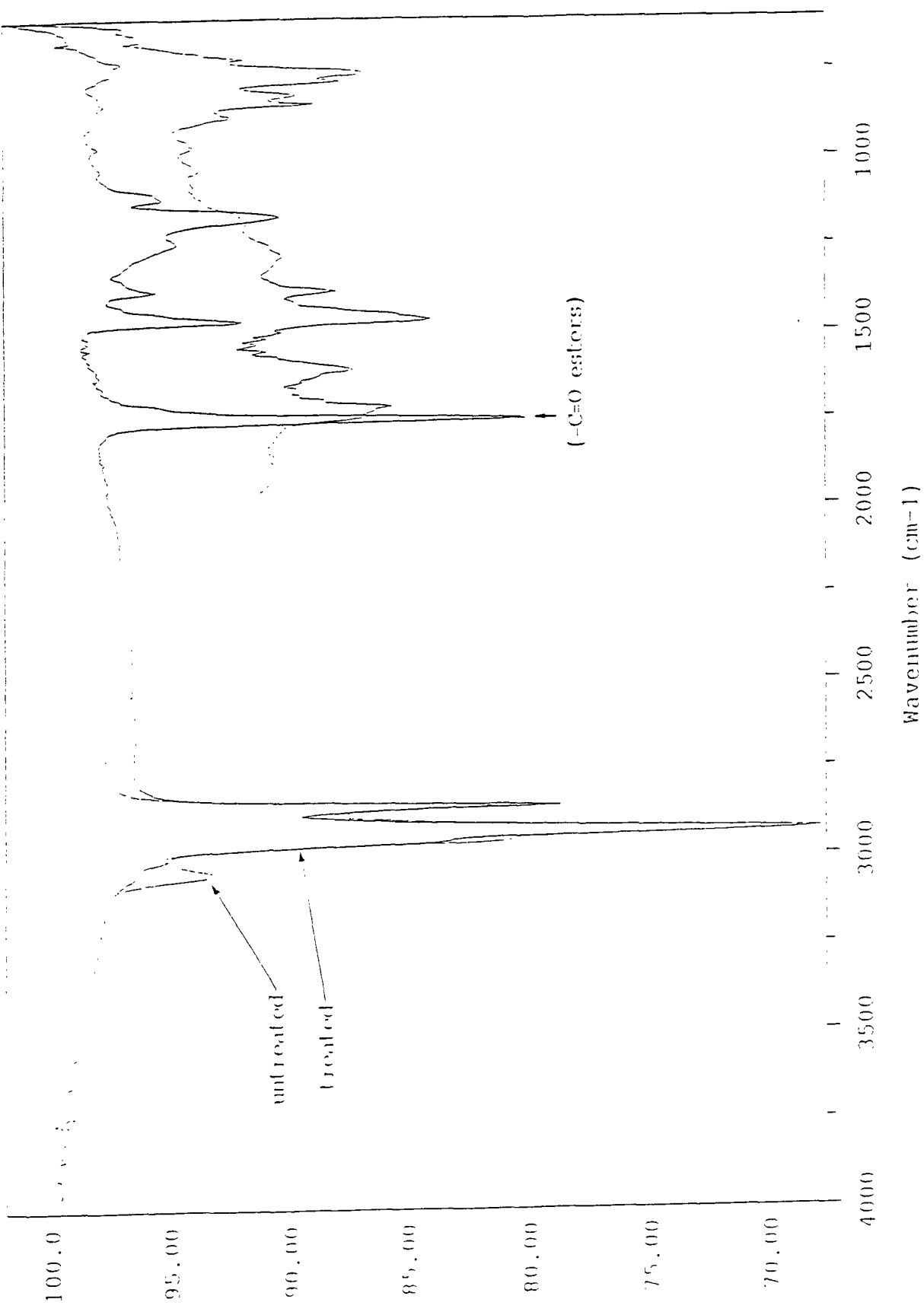


Figure 3. IR spectra of untreated and treated soils.

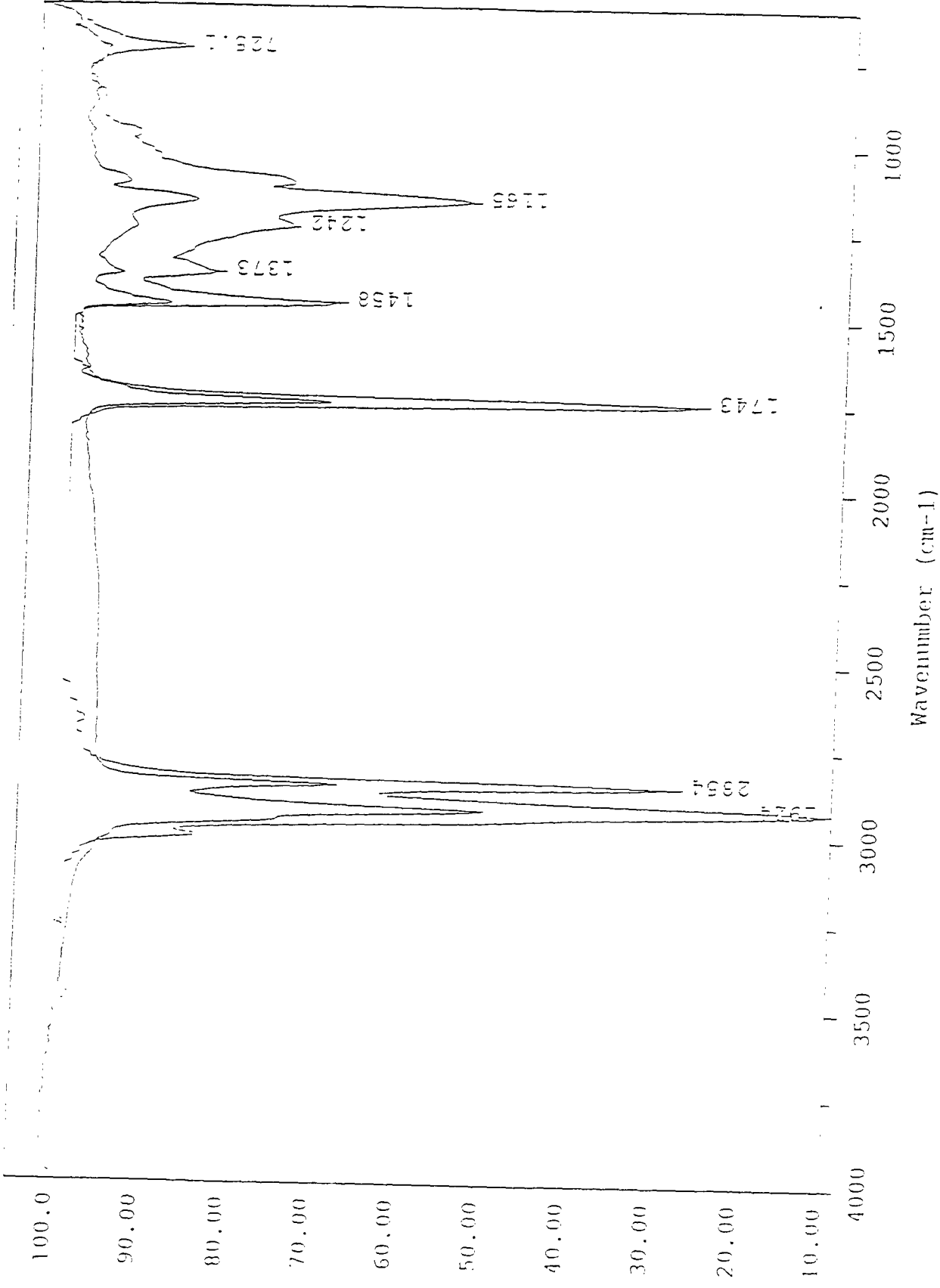


Figure 4. IR spectrum of treated PECO soil mix compare with spectrum of palm oil.

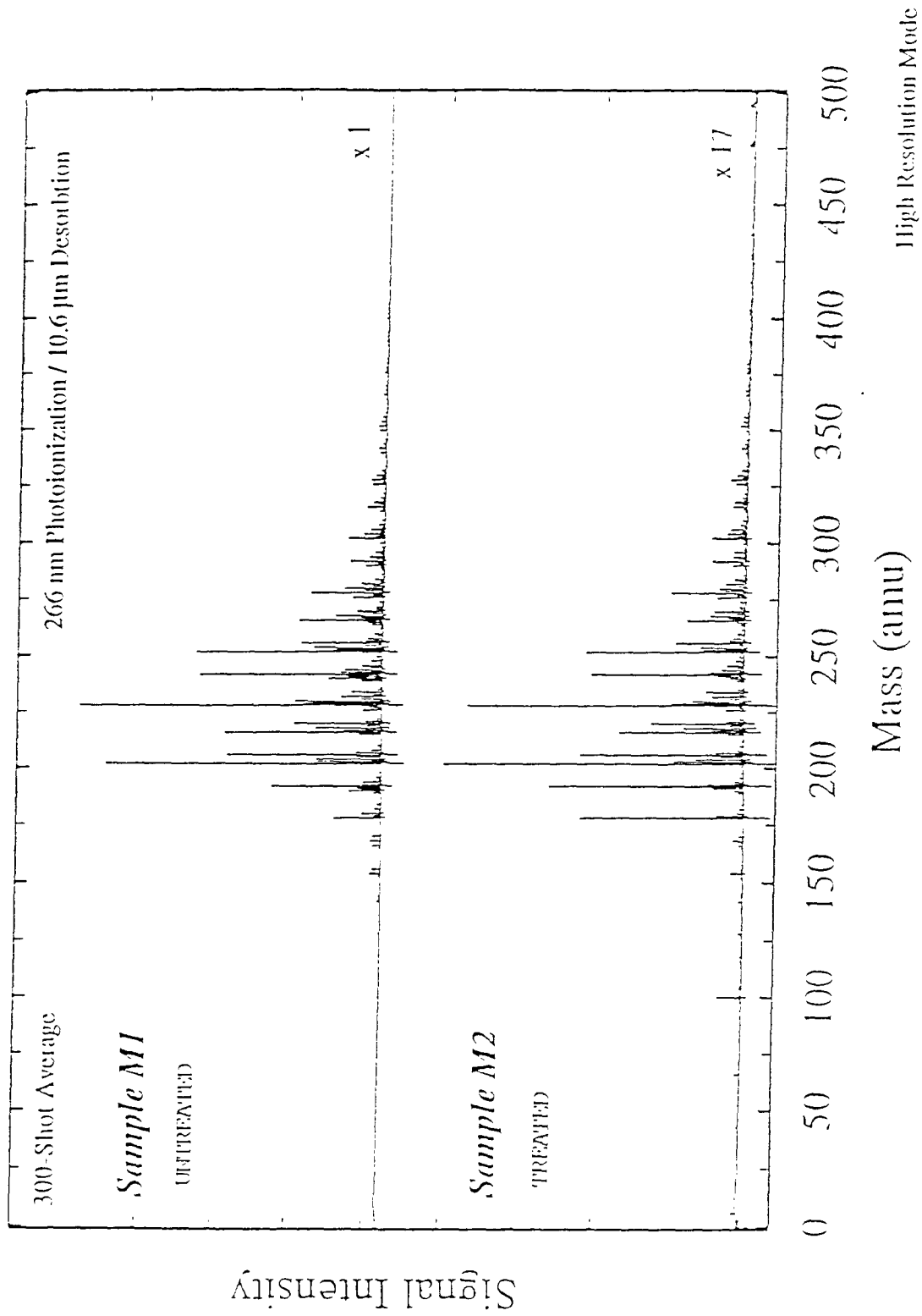


Figure 5.  $\mu\text{L}^2\text{MS}$  spectra of untreated control soil (upper) and treated soil (lower).

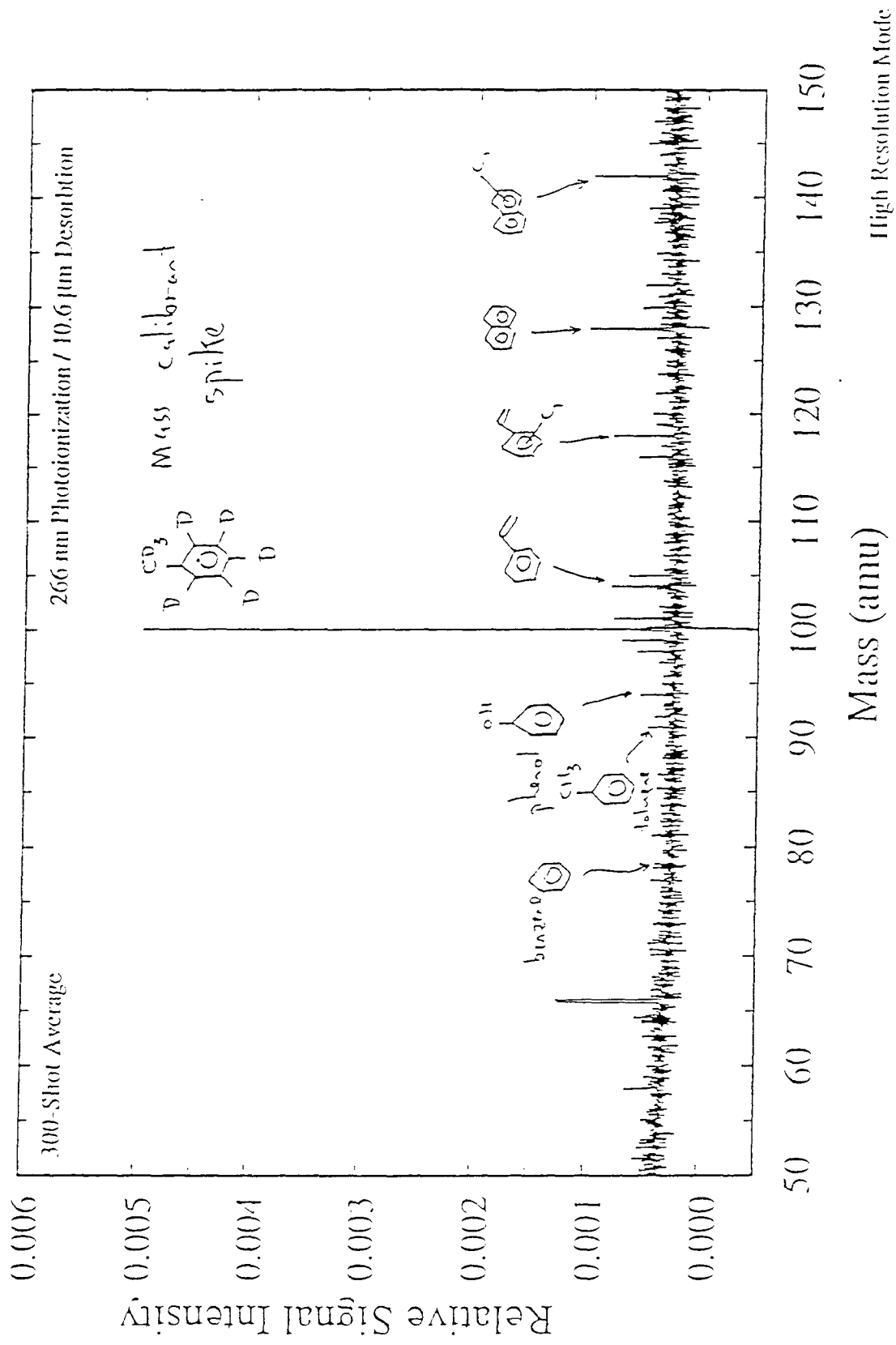


Figure 6.  $\mu\text{L}^2\text{MS}$  spectrum (expanded 8 trace) of 50-150 amu region.

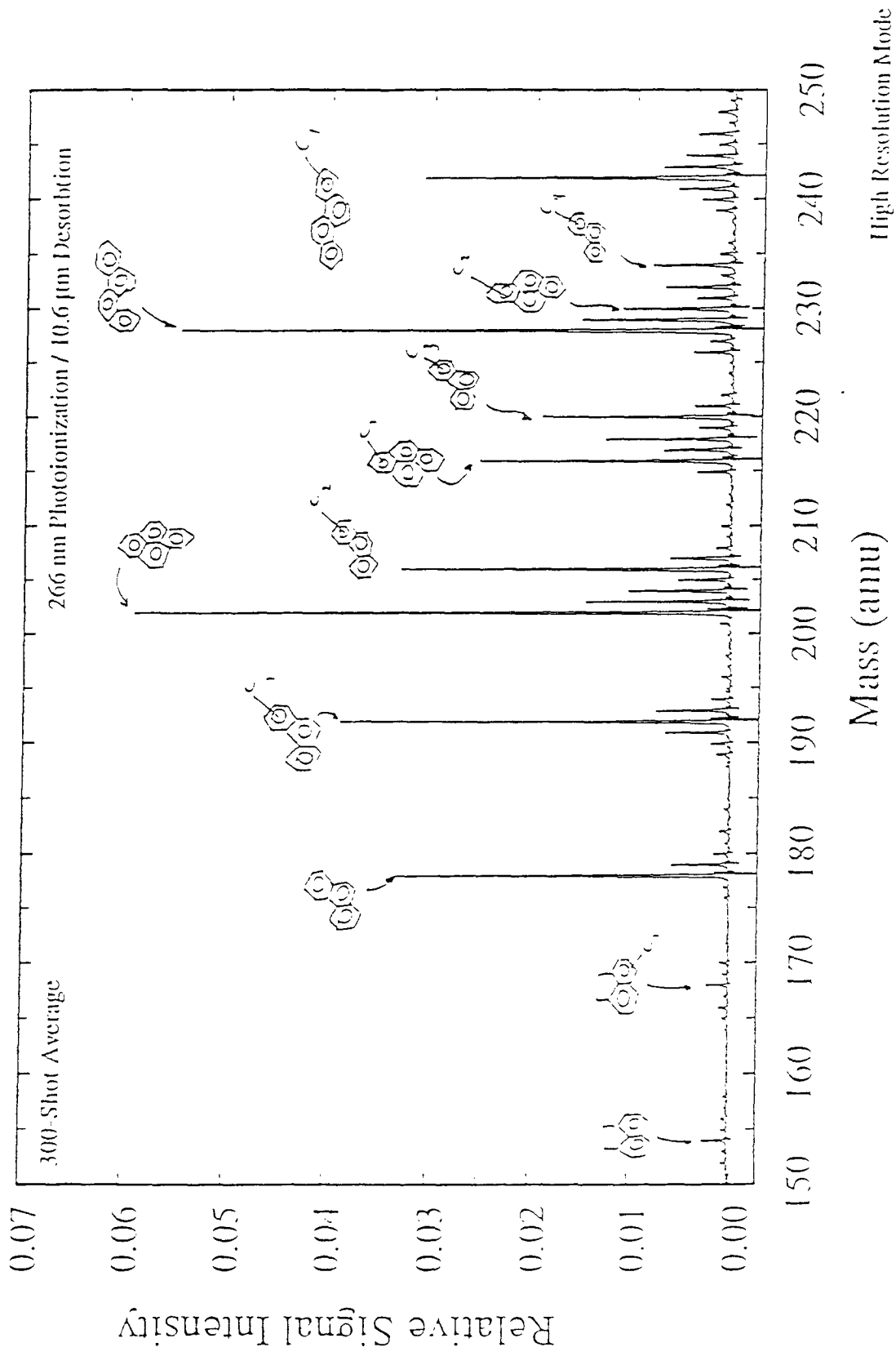


Figure 7.  $\mu$ L<sup>2</sup>MS spectrum (expanded trace) of 150-250 amu region.

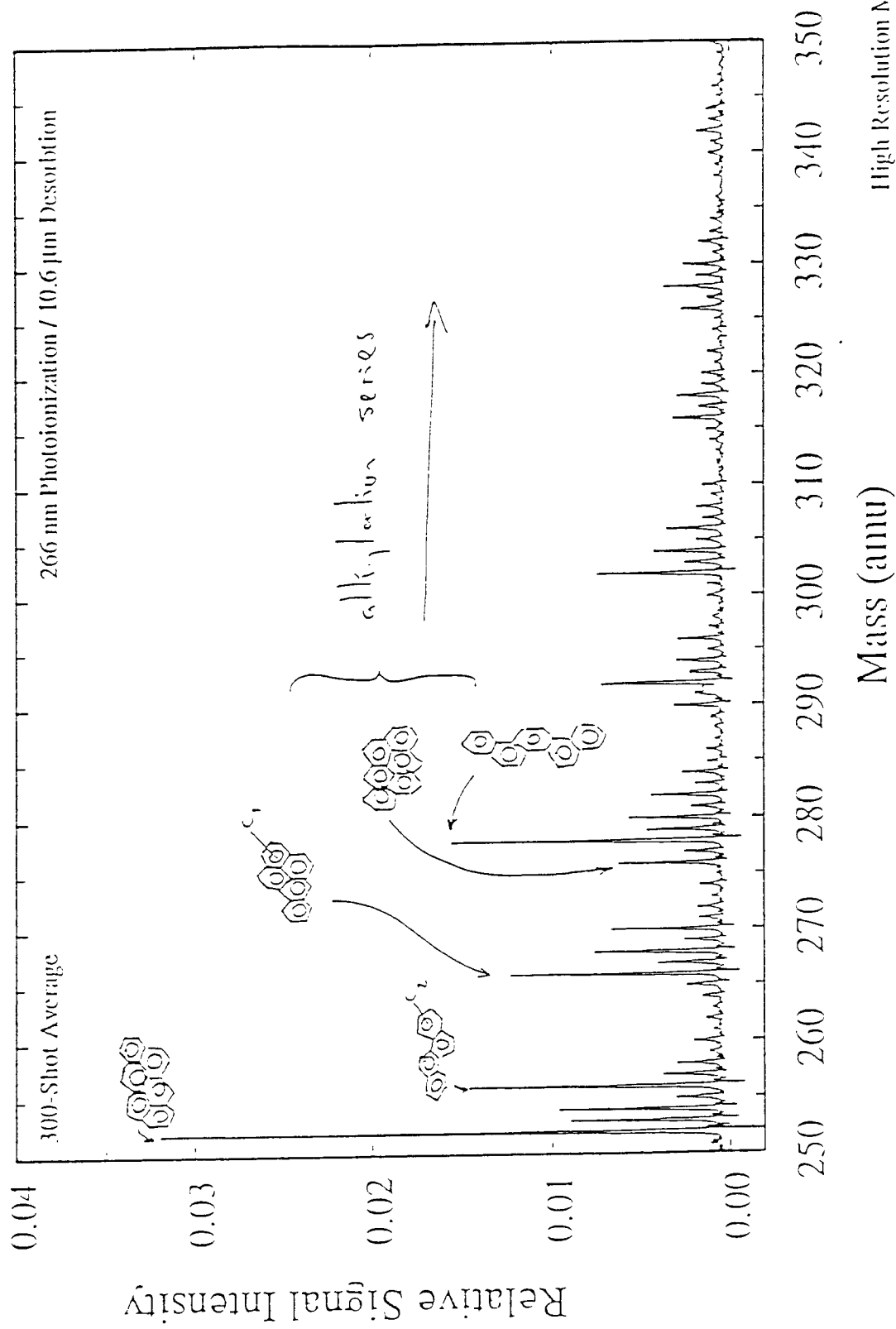


Figure 8.  $\mu\text{L}^2\text{MS}$  spectrum (expanded trace) of 250-350 amu region.

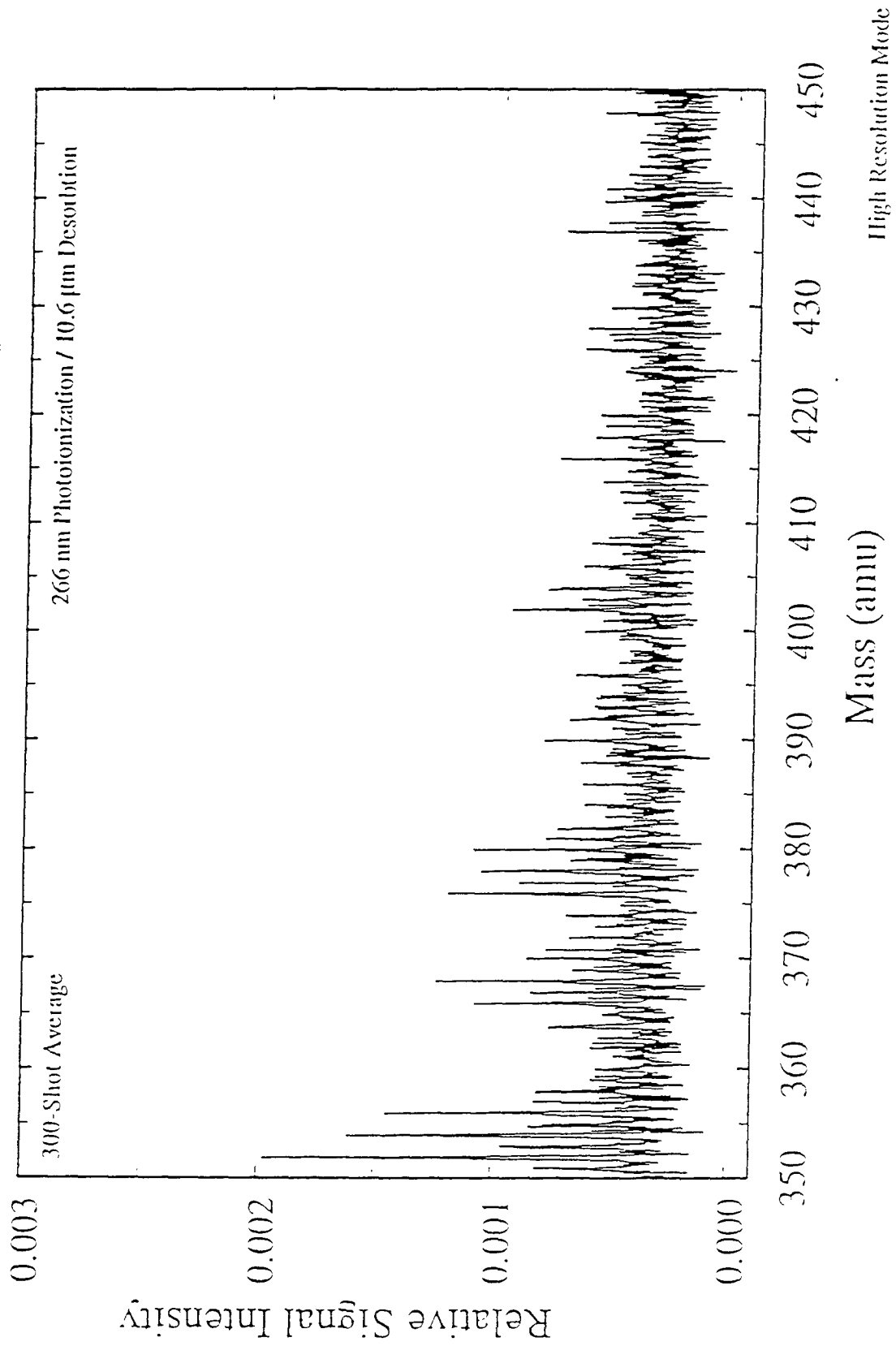


Figure 9.  $\mu\text{L}^2\text{MS}$  spectrum (expanded trace) of 350-450 amu region.

**Report of Results: MVA1646**  
**Investigation of Chemical Degradation of Dioxins and Furans**

**Prepared for:**

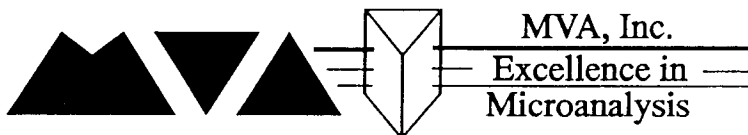
**Ms. Karen Hartley  
Marcor of Pennsylvania  
540 Trestle Place  
Downingtown, PA 19335**

**Prepared by:**

**John P. Bradley, Ph.D.  
MVA, Inc.  
5500 Oakbrook Parkway, Suite 200  
Norcross, GA 30093**

**13 February 1996**

D:PROJECTS:1646:PROJ1646



**5500 Oakbrook Parkway #200  
Norcross, GA 30093  
770-662-8509 • FAX 770-662-8532**

## Report of Results - MVA Project No. 1646

### Investigation of Chemical Degradation of Dioxins and Furans

#### INTRODUCTION

This report describes our investigation of the effectiveness of the ACT formulation SWT-25 on dioxins and furans. Two controlled experiments were performed. In the first experiment, SWT-25 was mixed with a single compound 2,4,8-trichlorodibenzo furan. In the second experiment, SWT-25 was mixed with a dioxin/furan mixture. Both experiments were carried out in sealed reaction vessels. At the completion of each mixing experiment the recovered liquids and solid residues were analyzed by microprobe two-step laser desorption mass spectroscopy ( $\mu\text{L}^2\text{MS}$ ).

#### EXPERIMENTAL PROCEDURES

We purchased a standard solution of seventeen (17) dioxins and furans from Cambridge Isotope Laboratories. The solution is identified as Cat. # EDF-7999 standard for EPA Method 1613. Because of the high cost, low volume (200  $\mu\text{L}$ ), and extreme toxicity of this solution, we also purchased eight (8) grams of a single furan 2,4,8-TCDF dissolved in methylene chloride (Aldrich Chemicals, 38,051-2; 98%). This compound is inexpensive and considerably less toxic than the EDF-7999 solution. Unfortunately, we were unable to locate a single dioxin compound in significant quantities.

In the first experiment, two 2,4,8-TCDF sample mixtures were prepared, one serving as a "control" and the other containing the reagent mixture SWT-25, to be evaluated. The "control" was made using aluminum oxide ( $\text{Al}_2\text{O}_3$ ) (>99.5% purity) as an inert substrate mixed into a fine slurry with doubly distilled water, while the "reactive mixture" was an SWT-25 substrate mixed with an equivalent volume of doubly-distilled water. To each slurry a methylene chloride ( $\text{CH}_2\text{Cl}_2$ ) solution was added with 2,4,8-TCDF dissolved at a concentration of 1000 ppm as shown below.

<u>CONTROL MIXTURE</u>	<u>SWT-25 MIXTURE</u>
~0.3 ml vol (0.5390 gms) $\text{Al}_2\text{O}_3$	~0.3 ml vol. (0.3721 gms) SWT-25
500 $\mu\text{l}$ 2x Distilled $\text{H}_2\text{O}$	500 $\mu\text{l}$ 2x Distilled $\text{H}_2\text{O}$
1000 $\mu\text{l}$ $\text{CH}_2\text{Cl}_2$ with 1000 ppm TCDF	1000 $\mu\text{l}$ $\text{CH}_2\text{Cl}_2$ with 1000 ppm TCDF

Two 5 ml Pyrex reaction vials were used to hold each slurry, and after each sample had been thoroughly mixed with a nickel-chrome spatula, the samples were sealed closed for the duration of the experiment with a Teflon sealing disk held tight with a Bakelite screw cap. To facilitate chemical processing both vials were maintained at ~35°C in a water bath and periodically ultrasonicated and thoroughly shaken to minimize settling of the slurry. Both mixtures were processed in this way for a period of thirty-six hours prior to analysis.

At the thirty-six hour period, both vials were allowed to stand undisturbed for one hour to allow settling before being opened. A glass microsyringe was used to withdraw 25 µl of the methylene chloride solution (immiscible with water) from each vial, which was then injected on to a hot (~80°C) aluminum sample platter in a fumehood. The methylene chloride was allowed to evaporate leaving a solid residue which was then analyzed directly by microprobe two-step laser mass spectrometry (µL<sup>2</sup>MS).

Additionally, a cleaned copper wire was used to scrape a small quantity of the substrate/methylene chloride/water slurry from each vial, and this was “painted” onto small sections of aluminum foil. This was then allowed to dry in a fumehood and the residue, encrusted onto the aluminum foil, was mounted on to a sample platter and also analyzed by µL<sup>2</sup>MS.

In the second experiment, two dioxin/furan mixtures were made up, one serving as a aluminum oxide “control” and the other containing the reagent mixture (SWT-25) to be evaluated. The samples were mixed as slurries in microvials (see table below) and reacted for 24 hours at ~30°C. At the completion of the 24 hour period, both samples were analyzed using the same procedures employed for the first experiment.

CONTROL MIXTURE	SWT-25 MIXTURE
0.0463 gms Al <sub>2</sub> O <sub>3</sub>	0.0264 gms SWT-25
10-15 µL 2x Distilled H <sub>2</sub> O	10-15 µL 2X Distilled H <sub>2</sub> O
10-15 µl dioxin/furan soln.	10-15 µL dioxin/furan soln.

Solid residues in all reaction vessels were tested for the presence of carbonates. Normally, infrared (IR) spectroscopy is used for carbonate identification but, because of the toxicity of dioxins and furans, we opted instead for a microchemical test. The test consists of adding of microdroplets of an aqueous solution of 10% HCl and observation of bubbles of (CO<sub>2</sub>) gas.

## **RESULTS**

The sample mixture containing the SWT-25 substrate appeared visually to undergo a reaction within a few hours of mixing with the methylene chloride/TCDF solution, with the color of the substrate darkening from a lightish grey to a dark grey/brown. At the same time, the substrate appeared to increase in volume encapsulating much of the methylene chloride phase. Upon addition of 10% HCl, the SWT-25 substrate gave off bubbles of gas (presumably CO<sub>2</sub>) suggesting that carbonates formed as a byproduct of the reaction. (The alumina "control" residue produced no observable reaction with 10% HCl).

Figures 1 through 5 are  $\mu\text{L}^2\text{MS}$  spectra from the 2,4,9-TCDF experiment. Figure 1 is a parent ion spectrum of the neat methylene chloride/TCDF solution. For comparison purposes, a theoretical spectrum calculated on the assumption of no molecular fragmentation of 2,4,8-TCDF is also shown in Figure 1. This figure establishes that the  $\mu\text{L}^2\text{MS}$  instrument is able to provide a "clean" isotopically resolved parent ion spectrum of 2,4,8-TCDF with no fragmentation peaks.

Figure 2 shows a spectrum from the dried aluminum oxide "control" substrate. Since the only aromatic species present in the original sample mixture was the TCDF, this should be the only peak present in the  $\mu\text{L}^2\text{MS}$  spectrum. This is observed to be the case, with the exception of a small peak at 207 amu, which is assigned as impurity present within the original sample. Analysis of the isotopomer distribution shows that species contains only two chloride atoms. Figure 3 shows a spectrum from the analysis of the dried SWT-25 substrate. Since 2,4,8-TCDF was initially the only aromatic species present in the mixture, any aromatic degradation products will show up as additional peaks in the  $\mu\text{L}^2\text{MS}$  spectrum. This is found to be the case with a substantial

growth in the 207 “impurity” peak relative to the parent TCDF peak as well as additional dominant peaks at 137 and 178 amu. The 178 amu peak can be reasonably inferred to be due to phenanthrene ( $C_{14}H_{10}$ ). Further, careful analysis of the spectra indicates a plethora of additionally low intensity peaks both above and below the TCDF parent peak. Figure 4 illustrates this by subtracting the  $Al_2O_3$  and SWT-25 substrate spectra to yield a difference spectrum, whilst Figure 5 provides a vertical scale expanded trace of this difference spectrum. Due to the peak complexity, assignments are difficult. However, it appears that these low intensity peaks represent contributions from both non-chlorinated polycyclic aromatic hydrocarbons (peaks labelled in italics) and chlorinated aromatic species. The isotopomer distributions of the chlorinated species suggest a range of chlorine numbers both below and above tri-substitution.

Spectra from the dioxin/furan control experiment are shown in Figure 6. Only the 330-440 amu mass envelopes are shown because signal below 300 amu is essentially swamped out by PAH contaminants (from the solvents, etc.) and above 435 amu no peaks are observed. (Both the control and SWT-25 sample spectra are plotted on the same intensity scale in Figure 6). About equal quantities ( $\pm 20\%$ ) of the dioxins and furans are observed in both cases. However, due to spectral crowding and overlying contaminant peaks in the 100-300 amu region, it is difficult to conclude whether any breakdown products are being observed in the SWT-25 sample. (For help in peak identification, simulated spectra for the dioxin/furan mixture in the mass window are also plotted in Figure 6). It is assumed that intensities between species are proportional to their absolute concentration, which is an approximation in the case of  $\mu L^2 MS$  since photoionization cross-sections also need to be factored in. The solid residue from the SWT-25/dioxin/furan reaction vessel gave a positive test for carbonates but the alumina “control” residue did not.

## **DISCUSSION AND SUMMARY**

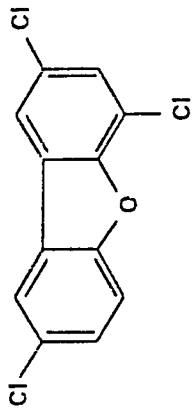
The 2,4,8-TCDF experiment clearly indicate that the SWT-25 reagent has effected the chemical degradation of a least a fraction of the original 2,4,8-TCDF (Figs. 1-5). However, the absolute reduction in the signal is difficult to quantify since the SWT-25 powder expanded into a hard grey solid residue which encapsulates the organic phase

making it difficult to get a clean extract. Nonetheless, **the reduction in concentration of the 2,4,8-TCDF must be larger than 40% and it may well be very much more than this.** Additionally, a few other peaks appear in the treated sample, though their combined intensity is less than 10% that of the parent TCDF (primary mass 270 amu) (Figures 3-5). These peaks are at 178 (phenathrene), 207 (? but chlorinated) and 296 (? but unchlorinated). This implies that any breakdown products are not primarily aromatic in nature. However, since some of the degradation products are also chlorinated aromatics, it is not clear whether these are less toxic than the original starting material. Toxicity of the breakdown products is an issue that needs to be explored further. The positive reaction for carbonates suggests that a significant fraction of the TCDF was “mineralized”.

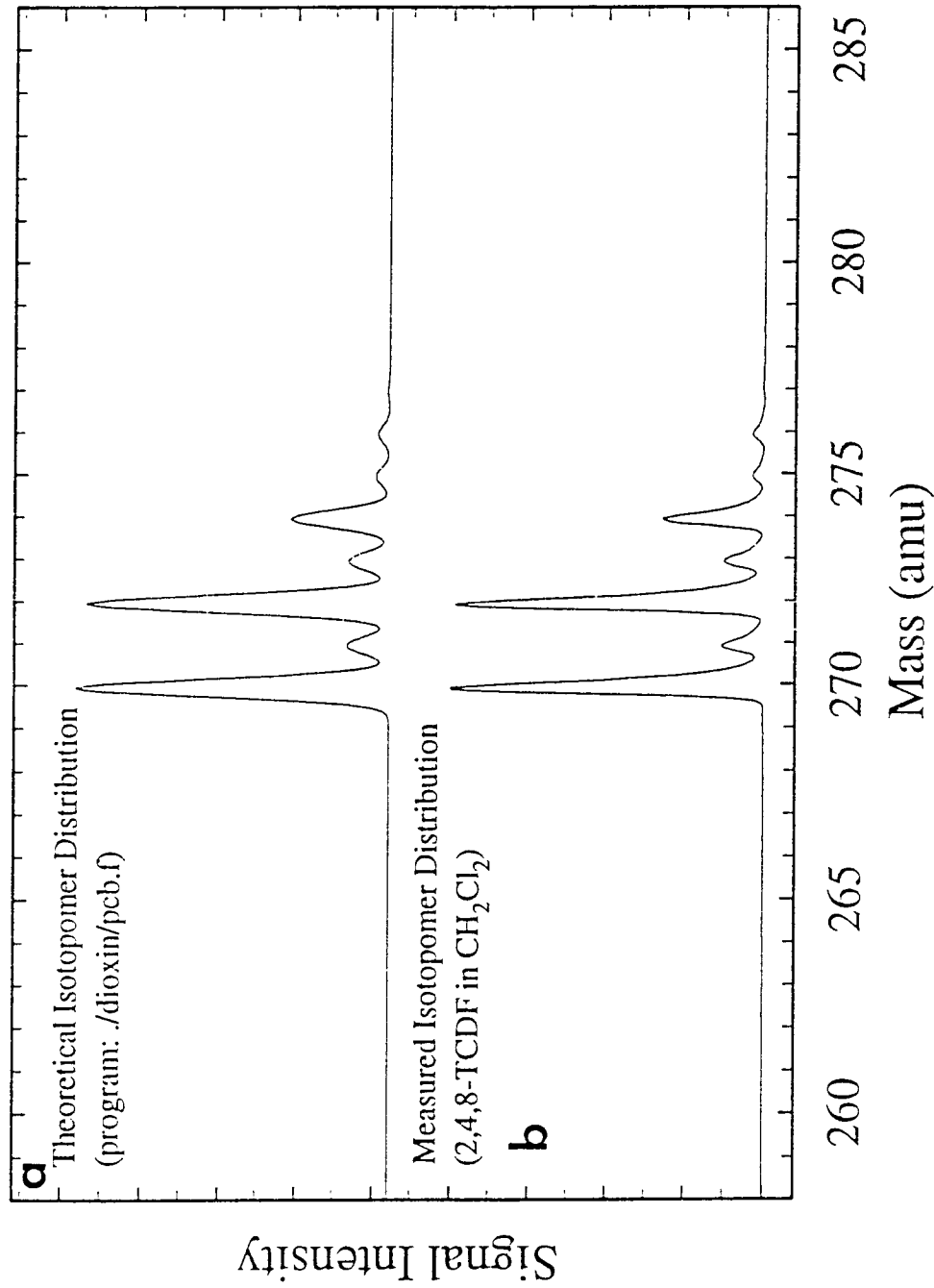
The results of the dioxin/furan experiment are more difficult to interpret (Figure 6). Using only 10-15  $\mu$ L volumes for the experiment was clearly a limitation but, considering the toxicological properties of the mixture, larger volumes are to be avoided. The complexity of the EDF-7999 mixture (17 dioxins and furans) was also a complication. As a result the degree of spectral complexity in Figure 6 is simply too great to really evaluate whether SWT-25 is having a significant effect although. Nonetheless, the dioxin/furan residue tested positive for carbonates, an indication that **the furans and dioxins in the EDF-7999 mixture *may have been chemically degraded and mineralized.*** If a single dioxin standard can be found, another control experiment like that performed using the 2,4,8-TCDF could clarify the effect of SWT-25 on dioxins.

Jan. 29, 1996

# 2,4,8-Trichlorodibenzofuran



**a**



Sample: John Bradley

Figure 1. Mass spectrum of 2,4,8-trichlorodibenzofuran. (a) Simulated spectrum. (b) Measured spectrum.

Jan. 29, 1996

# Control Result; Inert Substrate (powdered $\text{Al}_2\text{O}_3$ )

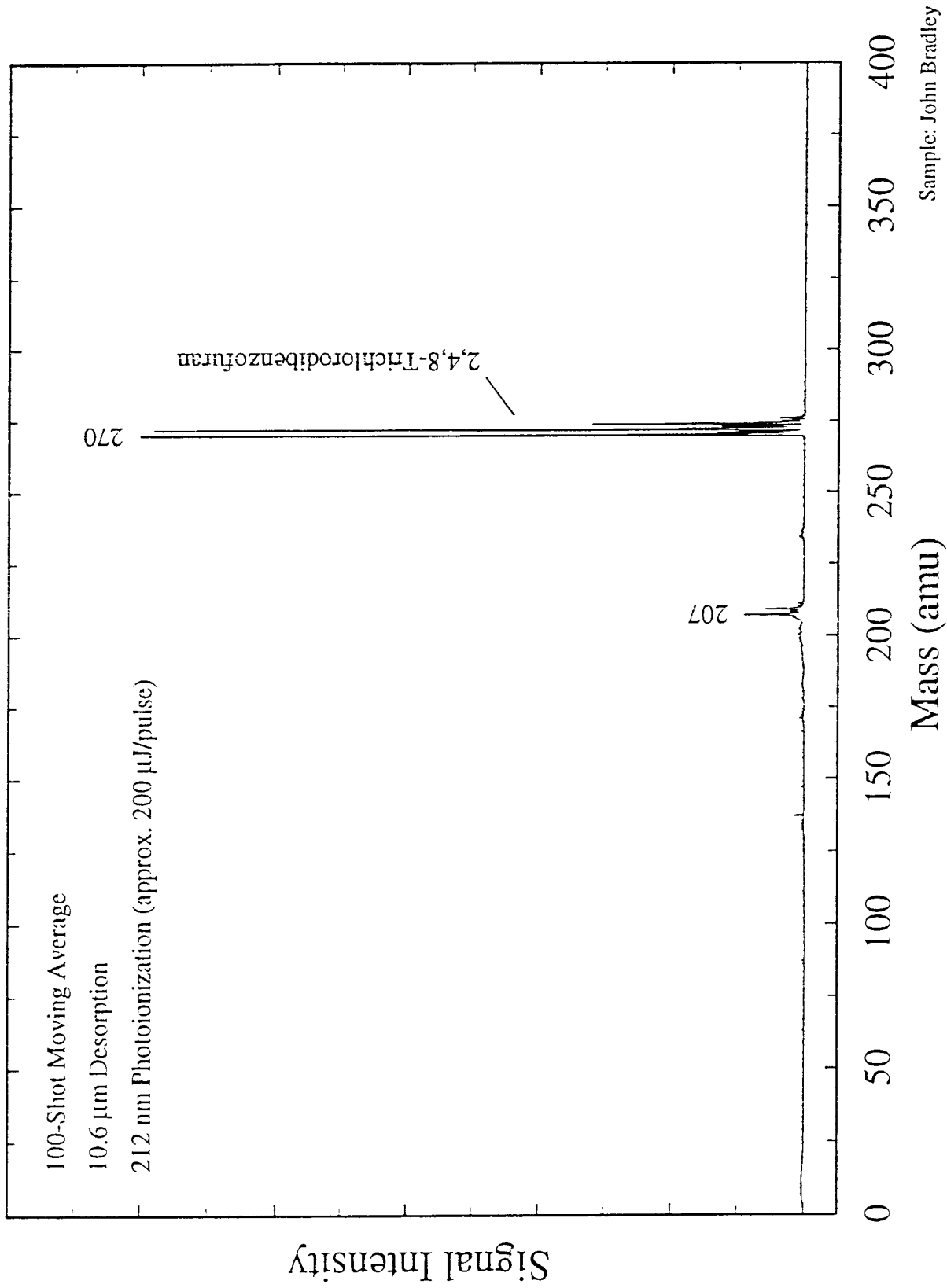


Figure 2. Mass spectrum of control substrate after experiment.

Jan. 29, 1996

# Treatment Result; Active Substrate (SWT-25)

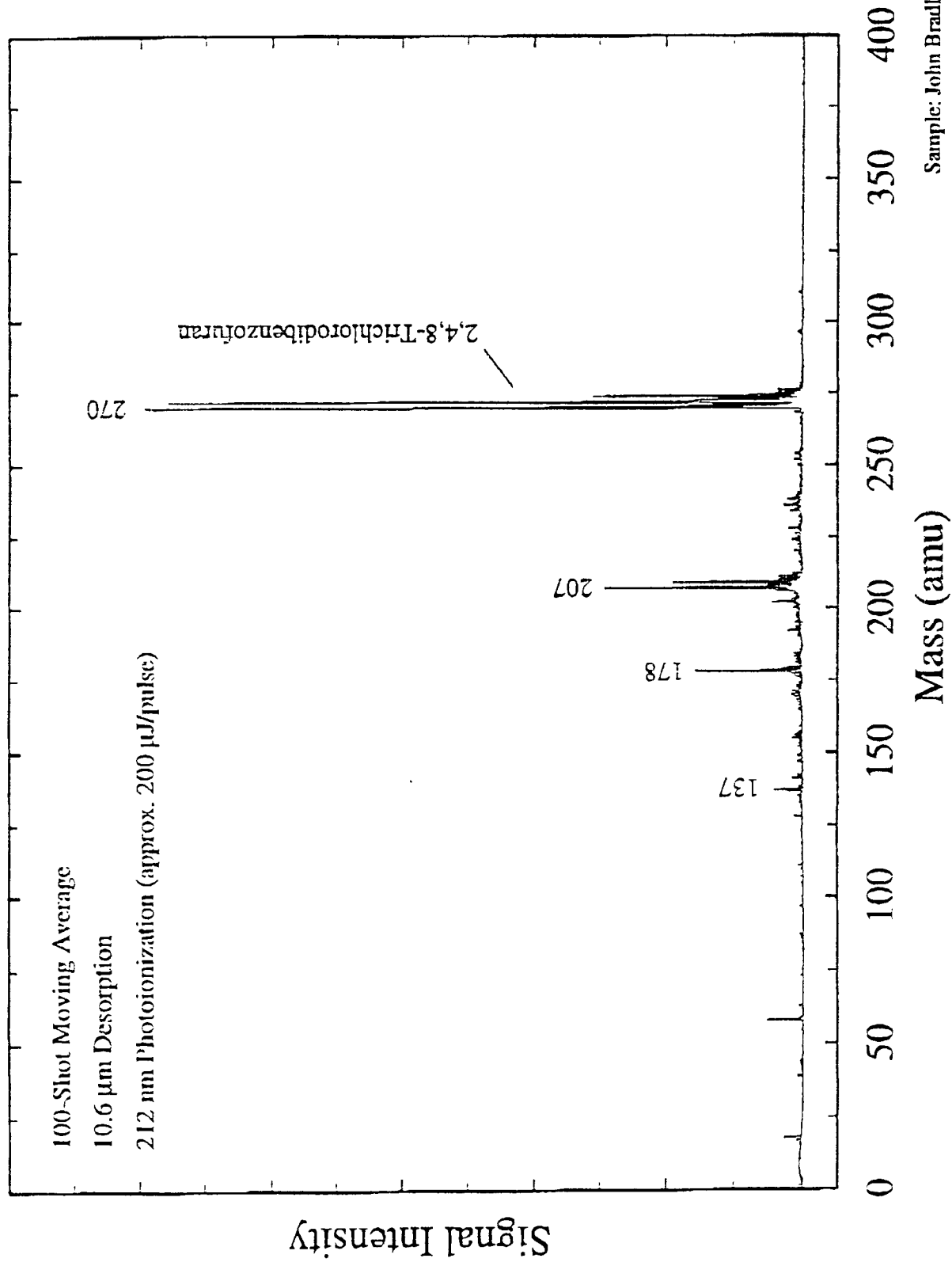


Figure 3. Mass spectrum of active (SWT-25) substrate after experiment.

Jan. 29, 1996

## Control and Treatment Results

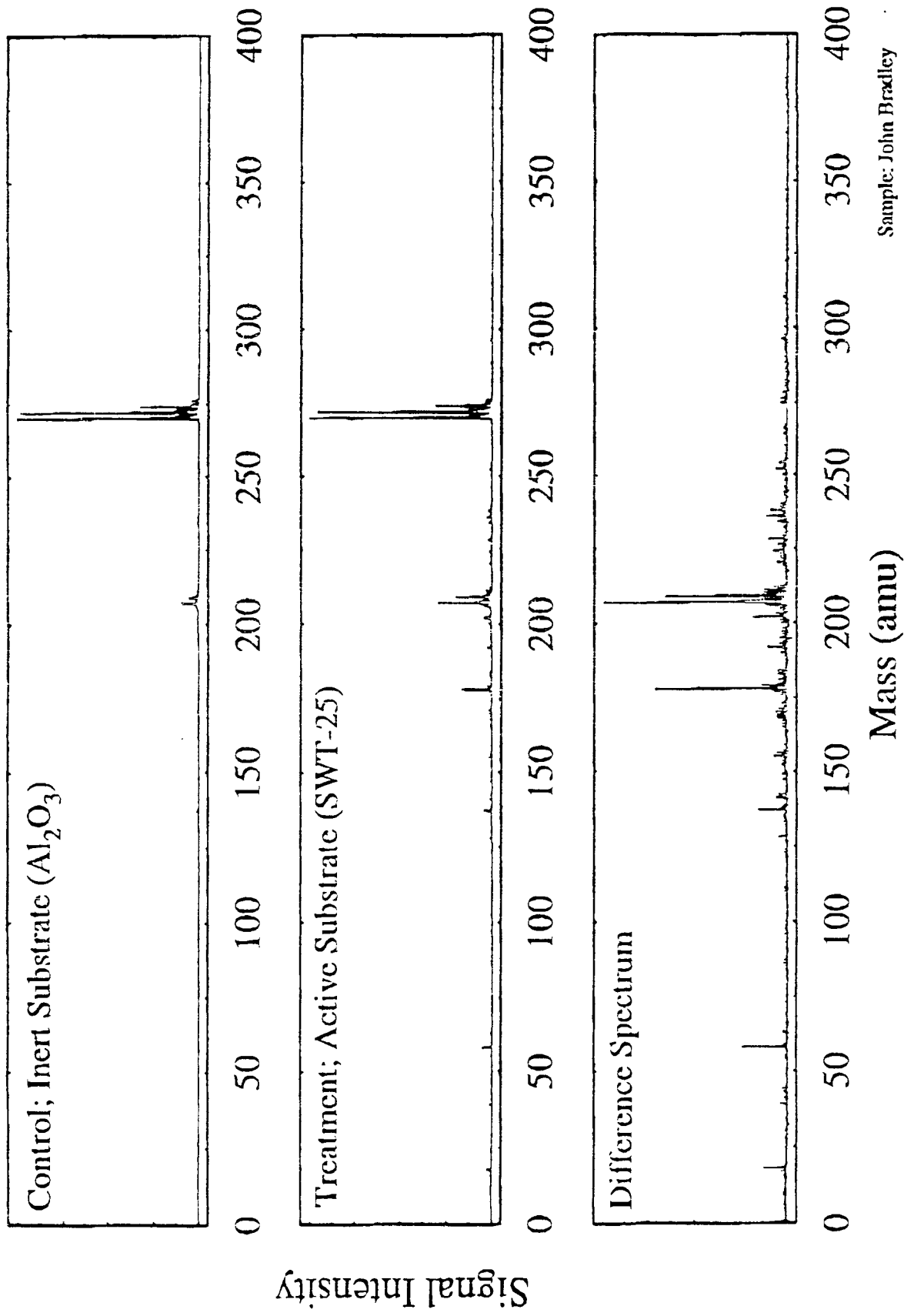
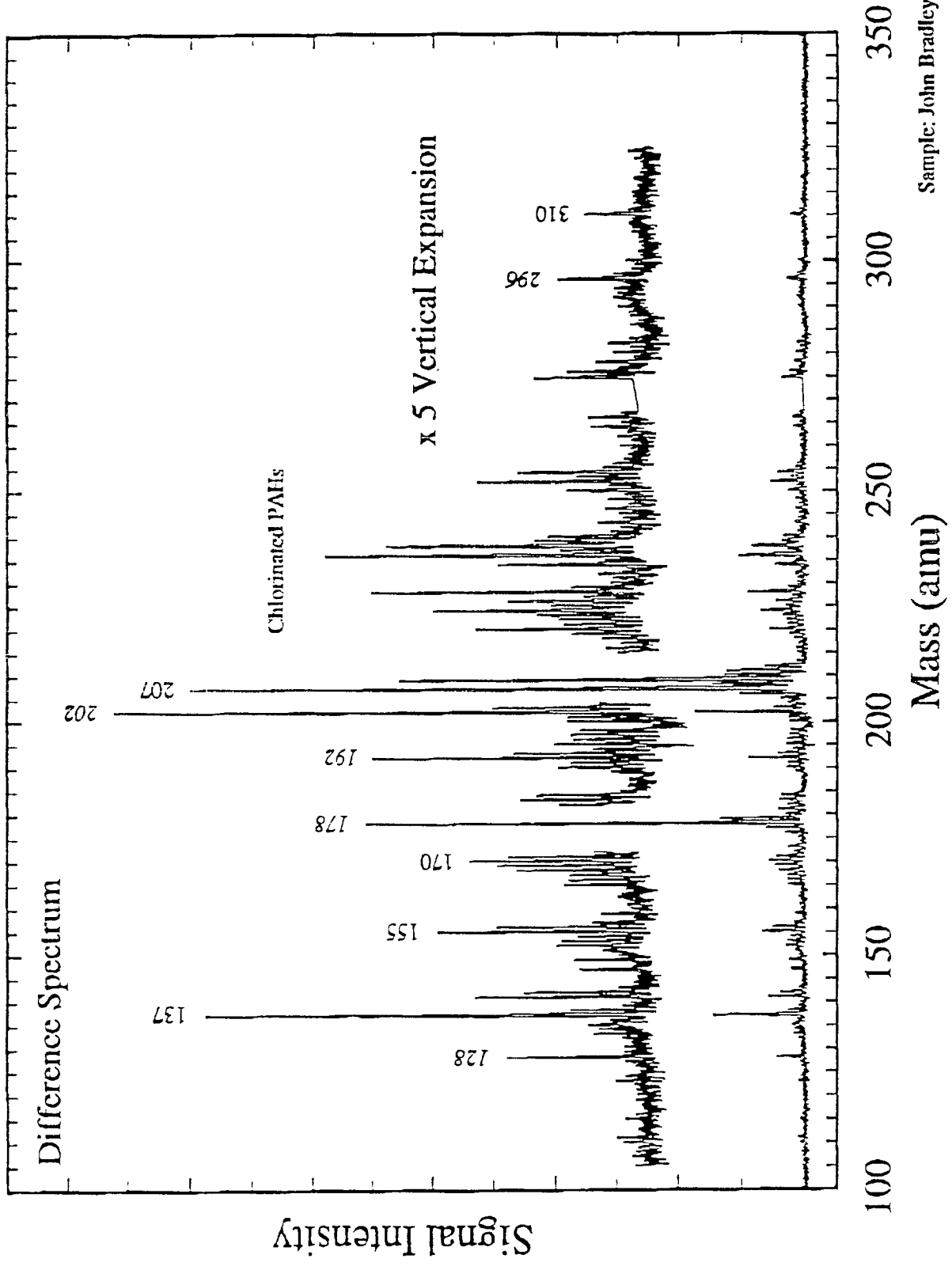


Figure 4. Mass spectra of Control substrate (upper), active (SWT-25) substrate (middle), and difference spectrum (lower). See also Figure 5.

Jan. 29, 1996

# Expanded Trace; Difference Spectrum

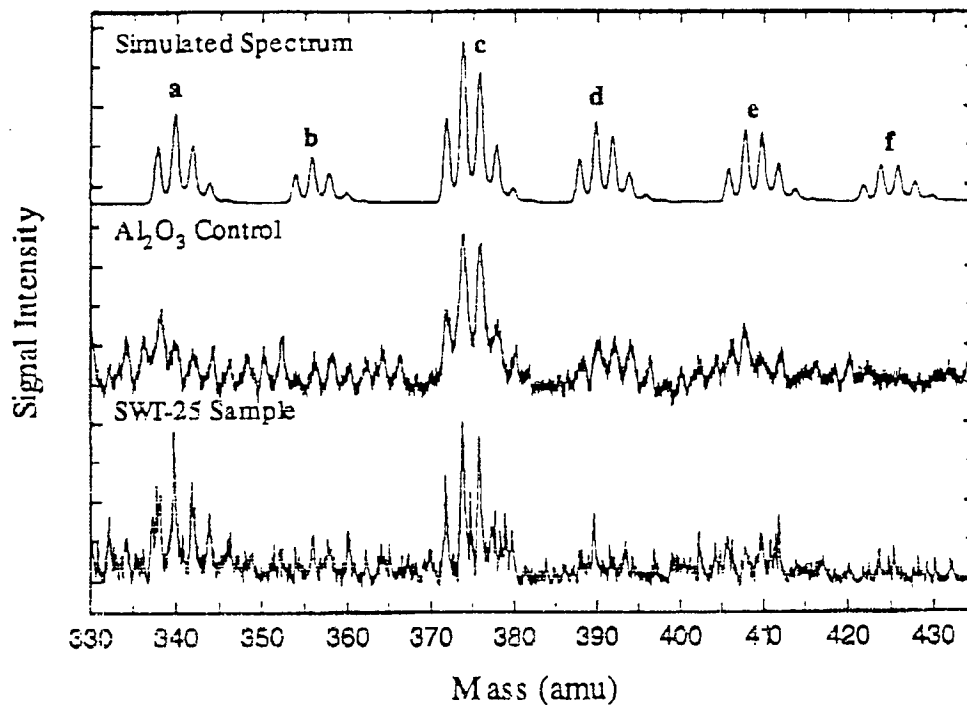


Sample: John Bradley

Figure 5. Expanded trace of difference spectrum (in Figure 4).

## Cambridge Isotopes Dioxin / Furan Standard (10-15 $\mu$ l Samples)

(500-Shot Averages; 10.6  $\mu$ m Desorption; 212 nm Photoionization)



Feb. 8, 1996

Sample: John Bradlov

Peak	Molecular Species	Formula	Conc. (ppm)
a)	1,2,3,7,8-Pentachlorodibenzofuran	$C_{12}H_3Cl_5O$	200
	2,3,4,7,8-Pentachlorodibenzofuran	$C_{12}H_3Cl_5O$	200
b)	1,2,3,7,8-Pentachlorodibenzo-p-dioxin	$C_{12}H_3Cl_5O_2$	40
c)	1,2,3,4,7,8-Hexachlorodibenzofuran	$C_{12}H_2Cl_6O$	200
	1,2,3,6,7,8-Hexachlorodibenzofuran	$C_{12}H_2Cl_6O$	200
	1,2,3,7,8,9-Hexachlorodibenzofuran	$C_{12}H_2Cl_6O$	200
	2,3,4,6,7,8-Hexachlorodibenzofuran	$C_{12}H_2Cl_6O$	200
d)	1,2,3,4,7,8-Hexachlorodibenzo-p-dioxin	$C_{12}H_2Cl_6O_2$	200
	1,2,3,6,7,8-Hexachlorodibenzo-p-dioxin	$C_{12}H_2Cl_6O_2$	200
e)	1,2,3,4,6,7,8-Heptachlorodibenzofuran	$C_{12}HCl_7O$	200
	1,2,3,4,7,8,9-Heptachlorodibenzofuran	$C_{12}HCl_7O$	200
f)	1,2,3,4,6,7,8-Heptachlorodibenzo-p-dioxin	$C_{12}HCl_7O_2$	200

Figure 6. Mass spectra of dioxin/furan mixtures (EDF-7999). Simulated spectrum (upper trace), control substrate after experiment (middle trace), active (SWT-25) substrate after experiment (lower trace). Peaks labelled (a) through (f) are identified in table.